Recognising two planar objects under a projective transformation

A thesis presented for the Degree of
Doctor of Philosophy in Mathematics
at the
University of Canterbury
by

Christopher Eric Hann

University of Canterbury
Christchurch, New Zealand
February 8, 2001

Abstract

This thesis involves solving problems associated with **object recognition** for two dimensional images under a projective transformation.

In order to recognise an object under any viewing angle requires invariant features to be identified. These invariant features can be used to match two images arising from two different views of a single object.

One invariant is the **projective curvature** which characterises all curves up to a projective transformation. However the projective curvature depends on seventh order derivatives so is very sensitive to noise in the discretisation of the images and is of little practical use.

Using links between the projective group and its subgroups, invariant points are found which depend on much lower order derivatives so are less sensitive to noise. They can be located on the images using a smoothing process then used to match the curves. However the smoothing process introduces error into the invariant points so that there will be error in the matching. This will not cause a problem if the two images have significantly different image features as then they can be detected within the wider tolerances of error. But this will cause a problem in distinguishing two images which are similar but different as it will not be known whether the error in the matching is due to error in the identification of the invariant points or not.

A method, called the canonical form method, is developed incorporating an error analysis which corrects the error in the matchings of the images. This enables two similar but different two dimensional objects to be distinguished. It also provides the background knowledge to solve new problems as they arise.

In addition to this practical method for two dimensional object recognition, a new characterisation of curves under the projective group and two of its subgroups is done using potentials and an alternative method for deriving and representing the projective curvature is given.

Acknowledgements

I would like to thank my supervisor Mark Hickman for all his assistance.

Thanks to Mum for her support but a special thanks to Dad for encouraging me to study mathematics from an early age.

Contents

Abstract **i**

Acknowledgements **iii**

1 Introduction **1**

1.1 Derivation of differential invariants on $\mathbf{R}^2$. 1

1.1.1 Notation and framework 1

1.1.2 Regularization 4

1.1.3 Moving coframes 5

1.1.4 Curvatures of the projective group and subgroups . . 8

1.2 Signature curves and vector field curvatures 10

1.2.1 Euclidean group $\big(E(2)\big)$ 10

1.2.2 Problem with finding discrete signature curves 11

1.2.3 Interpolation using vector fields 12

2 Invariants and curve matching **27**

2.1 Invariants 27

2.1.1 Links between groups 28

2.1.2 Locating and identifying invariant points between two curves 37

2.2 Smoothing and curve matching using links between groups . . 43

2.2.1 Moving of inflection points 45

2.2.2 Moving of special affine curvature turning points . . . 47

2.2.3 Matching curves 49

2.3 Overshooting, undershooting method 55

2.3.1 Example 1 56

2.3.2 Example 2 65

2.3.3 Example 3 70

3 Canonical form **77**

3.1 Euclidean canonical form 77

3.2 Discussion of the following sections 78
3.3 Utilising the Euclidean canonical form 79
3.4 Geometric interpretation. 104
3.5 Global method 105

4 Error correction **111**
4.1 Correcting error and rejecting curves 112
4.1.1 Left-ventricle 115
4.1.2 Different curves 123
4.2 Analytic error analysis 127
4.3 Error bound for rejecting curves 132
4.4 Simpler method for error correction 139
4.5 Curves that are close to symmetric 145

5 Integral invariants and projective curvature **147**
5.1 Integral Invariants 147
5.2 Alternative derivation of projective curvature 158
5.2.1 First approach 158
5.2.2 Second approach 159

Bibliography **163**

A Error correction and strategy **165**
A.1 Example compared with Taylor series 166
A.2 Potentially fast convergent method 168
A.3 General strategy of planar object recognition 171

Chapter 1

Introduction

1.1 Derivation of differential invariants on $\mathbf{R}^2$.

1.1.1 Notation and framework

Note, all the following definitions can be generalized to any manifold.

Lie group

An *r-parameter Lie group* is a group G which also carries the structure of an r-dimensional smooth manifold in such a way that both the group operation

$$m : G \times G \mapsto G, \quad m(g,h) = g \cdot h, \quad g,h \in G,$$

and the inversion

$$i : G \mapsto G, \quad i(g) = g^{-1}, \quad g \in G,$$

are smooth maps between manifolds.

Lie group action on $\mathbf{R}^2$

A *Lie group action* on $\mathbf{R}^2$ is given by a Lie group G with identity element e, an open subset $\mathcal{U}$, with

$$\{e\} \times \mathbf{R}^2 \subseteq \mathcal{U} \subseteq G \times \mathbf{R}^2,$$

which is the domain of definition of the group action, and a smooth map $\Psi : \mathcal{U} \mapsto \mathbf{R}^2$ with the following properties:
(a) If $(h,z) \in \mathcal{U}$, $(g, \Psi(h,z)) \in \mathcal{U}$, and also $(g \cdot h, z) \in \mathcal{U}$, then

$$\Psi(g, \Psi(h,z)) = \Psi(g \cdot h, z).$$

(b) For all $z \in \mathbf{R}^2$,

$$\Psi(e, z) = z.$$

(c) If $(g, z) \in \mathcal{U}$, then $(g^{-1}, \Psi(g, z)) \in \mathcal{U}$ and

$$\Psi(g^{-1}, \Psi(g, z)) = z.$$

For $(x, u) \in \mathbf{R^2}$, $\Psi(g, (x, u))$ is denoted by $g \cdot (x, u)$ whenever it is defined. Here $x \in X$, the space of the independent variable, and $u \in U$, the space of the dependent variable.

Given a smooth function $u = f(x)$, it induces a function $u^{(n)} = \mathrm{pr}^{(n)} f(x)$, called the nth prolongation of f, where $\mathrm{pr}^{(n)} f : \mathbf{R} \mapsto \mathbf{R}^{n+1}$ is the vector consisting of all the derivatives of $u = f(x)$ of orders from 0 to n. This $n+1$ dimensional space is denoted by $U^{(n)}$. For example, the second prolongation $u^{(2)} = \mathrm{pr}^{(2)} f(x)$ is given by

$$(u\,;\, u_x,\ u_{xx}) = (f\,;\, \frac{\mathrm{d}f}{\mathrm{d}x},\ \frac{\mathrm{d}^2 f}{\mathrm{d}x^2})$$

all evaluated at x. The total space $X \times U^{(n)} \subseteq \mathbf{R}^{n+1}$, whose coordinates represent the independent variable, dependent variable and the derivatives of u up to order n is called the ***n*th order jet space** of the underlying space $X \times U$.

Prolongation of group actions

Suppose G is a Lie group action defined on some open subset $M \subseteq X \times U$. A given transformation $g \in G$ transforms a function $u = f(x)$ in the following way. Identify $u = f(x)$ with its graph,

$$\Gamma_f = \{(x, f(x)) : x \in \Omega\} \subseteq X \times U,$$

where $\Omega \subseteq X$ is the domain of definition of f. If $\Gamma_f \subseteq M_g$, the domain of definition of the group transformation g, then the transform of Γ_f by g is,

$$g \cdot \Gamma_f = \{(\tilde{x}, \tilde{u}) = g \cdot (x, u) : (x, u) \in \Gamma_f\}.$$

By suitably shrinking the domain of definition Ω of f, for elements g near the identity, the transform $g \cdot \Gamma_f = \Gamma_{\tilde{f}}$ is the graph of some single-valued smooth function $\tilde{u} = \tilde{f}(\tilde{x})$. The function $\tilde{f}$ is denoted by $\tilde{f} = g \cdot f$ and is called the transform of f by g.

Now there is an induced action of G on the n-jet space $X \times U^{(n)}$ called

the ***n*th prolongation** of G and is denoted $\mathrm{pr}^{(n)}G$. This prolongation is defined so that it transforms the derivatives of the function $u = f(x)$ into the corresponding derivatives of the transformed function $\tilde{u} = \tilde{f}(\tilde{x})$. Suppose $(x_0, u_0^{(n)})$ is a given point in $U^{(n)}$. Choose an arbitrary smooth function $u = f(x)$ defined in a neighbourhood of x_0 which has the given derivatives at x_0,

$$u_0^{(n)} = \mathrm{pr}^{(n)} f(x_0).$$

Let $\tilde{u} = \tilde{f}(\tilde{x})$ be the transformed function under $g \in G$. The action of the prolonged group transformation $\mathrm{pr}^{(n)}g$ on the point $(x_0, u_0^{(n)})$ is defined by

$$\mathrm{pr}^{(n)}g \cdot (x_0, u_0^{(n)}) = (\tilde{x}_0, \tilde{u}_0^{(n)}).$$

See section 1.1.2 for an example of this. Note by the chain rule this prolonged group action is independent of the function $f(x)$.

Maurer-Cartan forms

Let G be an r dimensional Lie group and $L_g : h \mapsto g \cdot h$ denote the standard left multiplication map.

Definition A one-form μ on G is called a (left-invariant) **Maurer-Cartan form** if it satisfies,

$$(L_g)^*\mu = \mu \quad \text{for all } g \in G,$$

where the symbol * is the standard notation for the **pull back**. An introduction to differential geometry can be found in [5].

A way of explicitly determining the Maurer-Cartan forms on a given Lie group is to realize the group $G \subset GL(n)$ as a matrix Lie group. Let $A = A(g^1, \ldots, g^r) \in G$ represent the general matrix in G, which is parametrized by local coordinates $(g^1, \ldots, g^r)$ near the identity. Then the independent entries of the $n \times n$ matrix of one-forms

$$\mu = A^{-1}dA$$

form a basis for the left-invariant Maurer-Cartan forms on G, where

$$dA = \sum_{i=1}^{r} \left(\frac{\partial A}{\partial g^i} \right) dg^i.$$

1.1.2 Regularization

A general method for deriving the differential invariants of Lie group actions on manifolds, together with a rigorous theoretical justification was developed in [3]. For the case of r dimensional Lie group actions on $\mathbf{R}^2$, the theory says that the fundamental differential invariant, called the **curvature**, which characterises all curves up to a Lie group transformation $g \in G$ can be derived in the following way.

Consider the $(r-1)$st prolonged group action $\mathrm{pr}^{(r-1)}g\cdot(x,u)$. Normalize the r parameters by setting

$$\mathrm{pr}^{(r-2)}g\cdot(x,u) = (\bar{x}_0, \bar{u}_0^{(r-2)})$$

for some point $(\bar{x}_0, \bar{u}_0^{(r-2)}) \in \bar{X}\times\bar{U}^{(n)}$ and solving for the parameters in terms of x, u and the derivatives of u up to order $r-2$. These are then substituted into the $(r+1)$th component of $\mathrm{pr}^{(r-1)}g\cdot(x,u)$. This gives the fundamental differential invariant. Note that higher order differential invariants can be found by substituting these parameters into the components of higher order prolongations of g. This method is applied on the following example.

Consider the group action $SL(2)$ on $\mathbf{R}^2$ given by,

$$(x,u) \longmapsto (\bar{x},\bar{u}) = (ax+bu, dx+eu), \quad \det\begin{pmatrix} a & b \\ d & e \end{pmatrix} = 1$$

so that $r=3$. The second prolonged group action is given by,

$$\mathrm{pr}^{(2)}g\cdot(x,u,u_x,u_{xx}) = (\bar{x},\bar{u},\bar{u}_{\bar{x}},\bar{u}_{\bar{x}\bar{x}})$$

where,

$$\bar{u}_{\bar{x}} = \frac{d+eu_x}{a+bu_x}, \quad \bar{u}_{\bar{x}\bar{x}} = (ae-bd)\frac{u_{xx}}{a+bu_x}.$$

Now using the normalization $\bar{x}=0$, $\bar{u}=1$, $\bar{u}_{\bar{x}}=0$ and the condition $ae-bd=1$, the equations

$$ax+bu=0, \quad dx+eu-1=0, \quad d+eu_x=0, \quad ae-bd-1=0$$

are solved for a, b, d and e. This gives

$$a=u, \quad b=-x, \quad d=-\frac{u_x}{u-xu_x}, \quad e=\frac{1}{u-xu_x}$$

These are then substituted into $\bar{u}_{\bar{x}\bar{x}}$ which yields

$$\kappa = \frac{u_{xx}}{(u - xu_x)^3}.$$

This is the fundamental differential invariant for this Lie group action.

The curvatures presented in later sections of other Lie group actions on $\mathbf{R}^2$ can all be derived in a way similar to the above example.

Note, in the final chapter, it is shown that certain subgroups of the projective group can be prolonged to a group action involving integrals. The group $GL(2)$ (with $\det \begin{pmatrix} a & b \\ d & e \end{pmatrix} \neq 0$ above) is one such group. Thus, using the regularization method, the fundamental invariants can be derived which depend on x, u and integrals involving x and u.

1.1.3 Moving coframes

The following method is an alternative method to regularization for calculating the differential invariants of Lie group actions on $\mathbf{R}^2$, as well as the group invariant arclength element which was developed in the paper [2]. For a rigorous theoretical justification of this method see [3]. This method will be explained using the Lie group action of a subgroup of the projective group on $\mathbf{R}^2$.

Consider the group action G on $\mathbf{R}^2$ given by,

$$(x, u) \longmapsto (\frac{x}{\rho x + \sigma u + \tau}, \frac{\lambda x + \mu u + \nu}{\rho x + \sigma u + \tau}), \quad \det \begin{pmatrix} \mu & \nu \\ \sigma & \tau \end{pmatrix} = 1,$$

where an element $A \in G$ is given by,

$$A = \begin{pmatrix} 1 & 0 & 0 \\ \lambda & \mu & \nu \\ \rho & \sigma & \tau \end{pmatrix}.$$

The six independent Maurer-Cartan forms are components of the matrix

$$\mu = \begin{pmatrix} 0 & 0 & 0 \\ \mu_1 & \mu_2 & \mu_3 \\ \mu_4 & \mu_5 & \mu_6 \end{pmatrix} = A^{-1}dA.$$

These are given by,

$$\mu_1 = \tau d\lambda - \nu d\rho, \quad \mu_2 = \sigma d\nu - \frac{1+\nu\sigma}{\tau} d\tau, \quad \mu_3 = \tau d\nu - \nu d\tau,$$
$$\mu_4 = -\sigma d\lambda + \frac{1+\nu\sigma}{\tau} d\rho, \quad \mu_5 = -\frac{\sigma^2}{\tau} d\nu + \frac{1}{\tau} d\sigma + \frac{\nu\sigma^2+\sigma}{\tau^2} d\tau,$$
$$\mu_6 = -\sigma d\nu + \frac{1+\nu\sigma}{\tau} d\tau.$$

Consider the smooth map $\gamma_0 : \mathbf{R}^2 \longrightarrow G$ given by

$$\gamma_0(x,u) \cdot (x_0, u_0) = (x,u)$$

for some $(x_0, u_0) \in \mathbf{R}^2$. This map will be called the moving frame of order zero. For this example, if (x_0, u_0) is chosen to be $(1,0)$ then the moving frame of order 0 is,

$$\gamma_0 = \begin{pmatrix} 1 & 0 & 0 \\ \frac{u-\nu x}{x} & \frac{(1+\nu\sigma)x}{1-\rho x} & \nu \\ \rho & \sigma & \frac{1-\rho x}{x} \end{pmatrix} \tag{1.1}$$

where $\nu = \nu(x,u)$, $\rho = \rho(x,u)$ and $\sigma = \sigma(x,u)$ are arbitrary functions.

Let $\tilde{H}$ be the three dimensional group with $\tilde{h} = (\nu, \rho, \sigma) \in \tilde{H}$. Then there is an induced action, $\Psi : \mathbf{R}^2 \times \tilde{H} \longrightarrow \mathbf{R}^2 \times \tilde{H}$ given by,

$$\gamma_0 \longrightarrow \bar{\gamma}_0 = \begin{pmatrix} 1 & 0 & 0 \\ d & \frac{1+fh}{i} & f \\ g & h & i \end{pmatrix} \gamma_0.$$

The next step is to pull back the Maurer-Cartan forms using γ_0^*. This gives,

$$\xi_1 = \frac{x^2(\rho x-1)d\nu - \nu x^3 d\rho + u(\rho x-1)dx - x(\rho x-1)du}{x^3}$$
$$\xi_2 = \frac{\sigma x(\rho x-1)d\nu - x^2(\nu\sigma+1)d\rho - (\nu\sigma+1)dx}{x(\rho x-1)}$$
$$\xi_3 = \frac{-x(\rho x-1)d\nu + \nu x^2 d\rho + \nu dx}{x^2}$$
$$\xi_4 = \frac{\sigma x^2(\rho x-1)d\nu - x^3(\nu\sigma+1)d\rho + \sigma u(\rho x-1)dx - \sigma x(\rho x-1)du}{x^2(\rho x-1)}$$
$$\xi_5 = \frac{\sigma^2 x(\rho x-1)d\nu - \sigma x^2(\nu\sigma+1)d\rho - x(\rho x-1)d\sigma - \sigma(\nu\sigma+1)dx}{(\rho x-1)^2}$$
$$\xi_6 = \frac{-\sigma x(\rho x-1)d\nu + x^2(\nu\sigma+1)d\rho + (\nu\sigma+1)dx}{x(\rho x-1)}$$

which spans the space of one-forms on $\mathbf{R}^2 \times \tilde{H}$. These one-forms are invariant

under Ψ, that is

$$\Psi^*\xi_i = \xi_i, \quad i = 1, \ldots, 6$$

and they completely characterise the group action given by Ψ above. They will be called the moving coframe of order zero.

These forms are pulled back to $J^1\mathbf{R}^2 \times \tilde{H}$ by putting $du = u_x\, dx$, where $J^1\mathbf{R}^2$ is the first jet space of curves in $\mathbf{R}^2$. The resulting one-forms are called the restricted moving coframe forms, denoted by θ_1, θ_2, θ_3, θ_4, θ_5 and θ_6.

These coframe forms have a linear dependency,

$$\theta_1 + J(\theta_2 - \theta_4) + \theta_3 = 0$$

where

$$J = \frac{2\rho x u - u + u_{xx} - \rho^2 x^2 u + \nu x - \nu\rho x^2 - 2\rho x^2 u_x + \rho^2 x^3 u_x}{x(-\sigma\rho x u + \sigma\rho x^2 u_x + \sigma u - \sigma u_{xx} - x\nu\sigma - x)}$$

Since the coframe forms are invariant, J can be used to normalize one of the group parameters. Thus J may be set equal to any convenient constant. Here J is set to be 0 and ν is solved for to give,

$$\nu = \frac{\rho x^2 u_x - \rho x u - x u_x + u}{x}.$$

Substituting this into (1.1) produces the first order moving frame

$$\gamma_1(x, u, u_x, \rho, \sigma) = \begin{pmatrix} 1 & 0 & 0 \\ -\rho x u_x + \rho u + u_x & \frac{\rho\sigma x^2 u_x - \rho\sigma x u - \sigma x u_x + \sigma u + x}{1 - \rho x} & \frac{(1-\rho x)(u - x u_x)}{x} \\ \rho & \sigma & \frac{1-\rho x}{x} \end{pmatrix}$$

This has a corresponding first order moving coframe. The same procedure above can be applied to this coframe which leads to a chain of successive normalizations and reductions. This will eventually eliminate all the undetermined parameters. In this example the final restricted coframe is given by,

$$\theta_1 = \frac{u_{xx}^{\frac{1}{3}}}{x} dx, \quad \theta_2 = 0, \quad \theta_3 = -\theta_1, \quad \theta_4 = \theta_1$$
$$\theta_5 = \frac{1}{9} \frac{x^2(3u_{xx}u_{xxxx} - 5u_{xxx}^2) - 3u_{xx}(2x u_{xxx} + 3u_{xx})}{x u_{xx}^{\frac{7}{3}}} dx, \quad \theta_6 = 0$$

The final linear dependency $\theta_5 = \kappa\theta_1$, where

$$\kappa = \frac{1}{9}\frac{x^2(3u_{xx}u_{xxxx} - 5u_{xxx}^2) - 3u_{xx}(2xu_{xxx} + 3u_{xx})}{u_{xx}^{\frac{8}{3}}}$$

is the fundamental differential invariant of the transformation group. The remaining one-form θ_1 forms the group invariant arclength,

$$ds = \frac{u_{xx}^{\frac{1}{3}}}{x}dx.$$

All higher order differential invariants can be found by differentiating κ with respect to ds, for instance

$$\frac{d\kappa}{ds} = \frac{1}{27}\frac{x^3(9u_{xx}^2u_5 - 45u_{xx}u_3u_4 + 40u_3^3)}{u_{xx}^4}.$$

1.1.4 Curvatures of the projective group and subgroups

The Lie group action which describes all possible viewing transformations on $\mathbf{R}^2$ is the projective group. There are three important subgroups of the projective group which are Euclidean, special affine and affine groups. Their group action, curvature and arclength element plus the projective group action, projective curvature and projective arclength element are shown below (see [2] for derivations of these). Note that the nth derivative of u where $n > 2$ is denoted by u_n.

EUCLIDEAN GROUP:

$$(x, u) \longmapsto (x\cos\theta + u\sin\theta + a, -x\sin\theta + u\cos\theta + b)$$

$$\kappa^{\mathbf{E}} = \frac{u_{xx}}{(1 + u_x^2)^{\frac{3}{2}}}$$

$$\mathrm{d}s_{\mathbf{E}} = \sqrt{1 + u_x^2}\,\mathrm{d}x$$

SPECIAL AFFINE GROUP:

$$(x, u) \longmapsto (ax + bu + e, cx + du + f), \quad \det\begin{pmatrix} a & b \\ c & d \end{pmatrix} = 1$$

$$\kappa^{\mathbf{SA}} = \frac{3u_{xx}u_4 - 5u_3^2}{(u_{xx})^{\frac{8}{3}}}$$

$$\mathrm{d}s_{\mathbf{SA}} = (u_{xx})^{\frac{1}{3}}\ \mathrm{d}x$$

AFFINE GROUP:

$$(x,u) \longmapsto (ax+bu+e, cx+du+f), \quad \det\begin{pmatrix} a & b \\ c & d \end{pmatrix} \neq 0$$

$$\kappa^{\mathbf{A}} = \frac{9u_{xx}^2u_5 - 45u_{xx}u_3u_4 + 40u_3^3}{(3u_{xx}u_4 - 5u_3^2)^{\frac{3}{2}}}$$

$$\mathrm{d}s_{\mathbf{A}} = \frac{(3u_{xx}u_4 - 5u_3^2)^{\frac{1}{2}}}{u_{xx}}\ \mathrm{d}x$$

PROJECTIVE GROUP:

$$(x,u) \longmapsto (\tfrac{ax+bu+c}{gx+hu+i}, \tfrac{dx+eu+f}{gx+hu+i}), \quad \det\begin{pmatrix} a & b & c \\ d & e & f \\ g & h & i \end{pmatrix} = 1$$

$$\begin{aligned}\kappa^{\mathbf{PROJ}} = \Big(&-33600u_{xx}u_3^6u_4 - 756u_{xx}^4u_5^2u_3^2 - 2835u_{xx}^5u_5^2u_4 \\ &+ 162u_{xx}^6u_5u_6 + 31500u_{xx}^2u_3^4u_4^2 - 7875u_{xx}^3u_3^2u_4^3 \\ &+ 6720u_3^5u_{xx}^2u_5 + 720u_3^3u_{xx}^4u_7 + 1890u_{xx}^5u_6u_4^2 \\ &+ 1134u_{xx}^5u_5u_6u_3 - 12600u_{xx}^3u_5u_3^3u_4 \\ &+ 13230u_{xx}^4u_5u_3u_4^2 - 3150u_{xx}^4u_3^2u_4u_6 \\ &- 810u_{xx}^5u_3u_4u_7 + 11200u_3^8 - 189u_{xx}^6u_6^2 \\ &- 4725u_{xx}^4u_4^4\Big) \Big/ \ \Big(9u_{xx}^2u_5 - 45u_{xx}u_3u_4 + 40u_3^3\Big)^{\frac{8}{3}}\end{aligned} \tag{1.2}$$

$$\mathrm{d}s_{\mathbf{PROJ}} = \frac{(9u_{xx}^2u_5 - 45u_{xx}u_3u_4 + 40u_3^3)^{\frac{1}{3}}}{u_{xx}}\ \mathrm{d}x$$

1.2 Signature curves and vector field curvatures

Definition. The *signature curve* associated with a parametrized curve $C = \{(x(t),\ y(t))\} \subset \mathbf{R^2}$ is the parametrised curve $S = \{(\kappa(t),\ \kappa_s(t))\} \subset \mathbf{R^2}$ where κ is the curvature and κ_s is the rate of change of curvature with respect to invariant arclength.

Theorem. Two curves $C = \{(x(t),\ y(t))\}$ and $\bar{C} = \{(\bar{x}(\bar{t}),\ \bar{y}(\bar{t}))\}$ are equivalent under a group transformation if and only if their signature curves are identical, i.e. $\bar{S} = S$.

In [1], the signature curve was introduced which avoids the parametrisation problem. For example $\{(\kappa(\frac{1}{2}t), t)\}$ stretches graph out by a factor of two. The theorem above is a special case of the general theorem of Cartan.

1.2.1 Euclidean group $\big(E(2)\big)$

The Euclidean group $E(2)$ is the group of rotations and translations of the plane. For a curve $C = \{(x(t),\ y(t))\}$, the formulas for κ and κ_s are,

$$\kappa = \frac{x_t u_{tt} - u_t x_{tt}}{(x_t^2 + u_t^2)^{\frac{3}{2}}} \tag{1.3}$$

$$\kappa_s = \frac{(x_t^2 + u_t^2)(u_{ttt}x_t - u_t x_{ttt}) + 3(u_t^2 - x_t^2)u_{tt}x_{tt} + 3x_t u_t(x_{tt}^2 - u_{tt}^2)}{(x_t^2 + u_t^2)^3}$$

In practical cases C does not have a formula but is a discretised curve. As was developed in [1], a discrete invariant numerical approximation to the Euclidean signature curve can be given by the following method.

Take three points P_0, P_1 and $P_2 \in C$ and consider the unique circle of radius r_1 passing through them (a straight line is considered a degenerate circle). Then the curvature $\kappa^{(1)} = \frac{1}{r_1}$ of this circle approximates the curvature at P_1 of C (see section 2.1.2 for the formula and Taylor series expansion showing how close this approximation is). Similarly an approximation to the curvature at the next point P_3 is given by $\kappa^{(2)} = \frac{1}{r_2}$.

The value for κ_s at P_1 can be approximated by $\kappa_s^{(1)} \simeq \frac{\kappa^{(2)} - \kappa^{(1)}}{s_1}$, where s_1 is the arclength of the circle through P_0, P_1 and P_2 from P_1 to P_2. In practice the Euclidean distance d_1 between the points P_1 and P_2 can be used to approximate s_1. By doing this for every point around the discretised curve, the discrete Euclidean signature curve can be built up.

Note that the circle is the unique constant Euclidean curvature curve going through 3 points and can be found by integrating the following equa-

tions which are called the infinitesimal generators of the Euclidean group action.

$$x_t = a - cu(t)$$
$$u_t = b + cx(t)$$

1.2.2 Problem with finding discrete signature curves

For the **projective group** which is the group,

$$(x,u) \longmapsto \left(\frac{\alpha x+\beta u+\gamma}{\rho x+\sigma u+\tau}, \frac{\lambda x+\mu u+\nu}{\rho x+\sigma u+\tau}\right), \quad \det\begin{pmatrix} \alpha & \beta & \gamma \\ \lambda & \mu & \nu \\ \rho & \sigma & \tau \end{pmatrix} = 1$$

the infinitesimal generators are,

$$x_t = au(t) + b + dx(t) + fx(t)^2 + gx(t)u(t)$$
$$u_t = cx(t) + e + fx(t)u(t) + gu(t)^2 + u(t).$$

These cannot be integrated in terms of elementary functions.

The **similarity group**

$$(x,u) \longmapsto \left(\alpha x + a, \alpha^k u + b\right), \quad k \text{ fixed integer},$$

and the **full affine group**

$$(x,u) \longmapsto (ax+bu+e, cx+du+f), \text{ where } \det\begin{pmatrix} a & b \\ c & d \end{pmatrix} \neq 0$$

have interpolation equations (equations that are required to fit the unique constant curvature curve through required number of points) which are non-linear. So this method will **not** generalise. Note that in the case of the circle, the interpolation equations are linear.

1.2.3 Interpolation using vector fields

Euclidean group

Motivation

Take three points (P_0, P_1, P_2) and consider unique circle passing through them. This corresponds to an integral curve of the vector field (up to scale factor),

$$\mathbf{v} = (a - u)\partial_x + (b + x)\partial_u$$

with initial condition $(x_0, u_0) = P_0$. Thus $\mathbf{v}$ can be specified uniquely by giving the tangent vectors at two points, P_0 and P_1 say.

An arbitrary integral curve of $\mathbf{v}$ is the solution to the following equations,

$$x_t = a - u(t)$$
$$u_t = b + x(t)$$

Then substituting these into the curvature (1.3) and setting $t = 0$ gives the curvature of the integral curve of $\mathbf{v}$ through $(x(0), u(0))$,

$$\kappa = \frac{1}{\sqrt{a^2 - 2au_0 + u_0^2 + b^2 + 2bx_0 + x_0^2}}, \tag{1.4}$$

where $x_0 = x(0)$, $u_0 = u(0)$. Thus the following definition can be made,

Definition: The curvature of vector field $\mathbf{v}$ at (x_0, u_0) is the curvature at (x_0, u_0) of the integral curve of $\mathbf{v}$ passing through (x_0, u_0).

In general, the tangent vectors of a constant curvature curve through a set of points are not known, but they can be approximated by joining the points with straight lines.

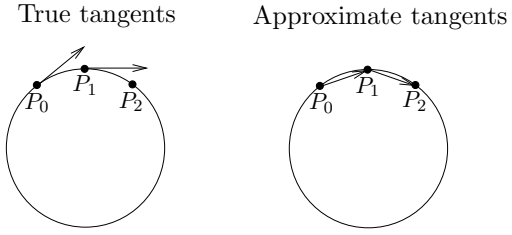

With $P_0 = (x_0, u_0), P_1 = (x_1, u_1), P_2 = (x_2, u_2)$ an approximate tangent vector at P_0 has the form

$$\mathbf{v}_1 = \alpha((x_1 - x_0)\partial_x + (u_1 - u_0)\partial_u)$$

for some constant α and an approximate tangent vector at P_1 has the form

$$\mathbf{v}_2 = \beta((x_2 - x_1)\partial_x + (u_2 - u_1)\partial_u)$$

for some constant β.

Setting $\mathbf{v}|_{(x_0,u_0)} = \mathbf{v}_1$ implies

$$\begin{aligned} a - u_0 &= \alpha(x_1 - x_0) \\ b + x_0 &= \alpha(u_1 - u_0). \end{aligned}$$

Eliminating α gives

$$(x_1 - x_0)(b + x_0) - (u_1 - u_0)(a - u_0) = 0.$$

Similarly setting $\mathbf{v}|_{(x_1,u_1)} = \mathbf{v}_2$ and eliminating β gives

$$(x_2 - x_1)(b + x_1) - (u_2 - u_1)(a - u_1) = 0.$$

This gives two equations in two unknowns which can be solved for a and b to get a new vector field $\tilde{\mathbf{v}}$ say. (1.4) gives the curvature of $\tilde{\mathbf{v}}$ at (x_0, u_0), call this $\kappa_{\tilde{\mathbf{v}}}$. Now it is shown that $\kappa_{\tilde{\mathbf{v}}}$ is invariant under the Euclidean group.

Consider the unique integral curve C_0 through (x_0, u_0) corresponding to $\tilde{\mathbf{v}}$, with curvature $\kappa_{\tilde{\mathbf{v}}}$ and tangent vector $\tilde{\mathbf{v}}|_{(x_0,u_0)}$ at (x_0, u_0). If a Euclidean transformation is done on C_0 then, by the uniqueness of the integral curve, $\overline{C}_0$ will coincide with the integral curve through $(\bar{x}_0, \bar{u}_0)$ corresponding to $\bar{\tilde{\mathbf{v}}}$. Here $\bar{\tilde{\mathbf{v}}}$ is determined from joining the points $(\bar{x}_0, \bar{u}_0)$, $(\bar{x}_1, \bar{u}_1)$ and $(\bar{x}_2, \bar{u}_2)$ by straight lines. Thus $\bar{\kappa}_{\bar{\tilde{\mathbf{v}}}} = \kappa_{\tilde{\mathbf{v}}}$ as required.

In order to see how good an approximation $\kappa_{\tilde{\mathbf{v}}}$ is, a Taylor series for $\kappa_{\tilde{\mathbf{v}}}$ is computed. Take three points P_0, P_1, P_2 on curve and apply a Euclidean transformation so the points become $P_0 = (-h, u(-h)), P_1 = (0, 0), P_2 = (k, u(k))$ and for P_0 and P_2 sufficiently close to P_1 the curve is the graph of a function $y = u(x)$ with $u(0) = 0$, $u_x(0) = 0$.

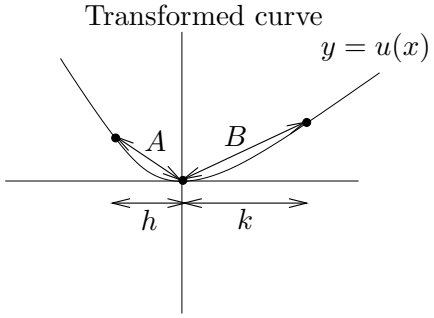

The values of the curvature and its arclength derivatives at $x = 0$ are $\kappa(0) = u_{xx}$, $\kappa_s(0) = u_{xxx}$, and $\kappa_{ss}(0) = u_{xxxx} - 3u_{xx}^3$ where the derivatives

are evaluated at 0. Now expand in a Taylor series,

$$\begin{aligned} u(-h) &= \frac{1}{2}u_2h^2 - \frac{1}{6}u_3h^3 + \frac{1}{24}u_4h^4 - \cdots \\ u(k) &= \frac{1}{2}u_2k^2 + \frac{1}{6}u_3k^3 + \frac{1}{24}u_4k^4 + \cdots \end{aligned}$$

where $u_2 = u_{xx}(0)$, $u_3 = u_{xxx}(0)$, $u_4 = u_{xxxx}(0)$, $\cdots$.

The distances A and B have expansions,

$$\begin{aligned} A &= \sqrt{h^2 + u(-h)^2} = h + \frac{1}{8}u_2^2h^3 - \frac{1}{12}u_2u_3h^4 + \cdots \\ B &= \sqrt{k^2 + u(k)^2} = k + \frac{1}{8}u_2^2k^3 + \frac{1}{12}u_2u_3k^4 + \cdots \end{aligned}$$

Inverting this series gives

$$\begin{aligned} h &= A + o(A^3) \\ k &= B + o(B^3). \end{aligned}$$

Substituting $h = A$ and $k = B$ into Taylor series for $u(-h)$ and $u(k)$ $\kappa_{\tilde{\mathbf{v}}}$ becomes

$$\begin{aligned} \kappa_{\tilde{\mathbf{v}}} &= \frac{1}{2}\frac{(A+B)}{A}\kappa + \frac{1}{6}\frac{(B-A)(A+B)}{A}\kappa_s + \frac{1}{48}(2\kappa_{ss} + 3\kappa^3)A^2 \\ &\quad -\frac{3}{16}\kappa^3AB - \frac{1}{8}\kappa^3B^2 + \text{higher order terms} \end{aligned}$$

For equally spaced points where $A = B$, $\kappa_{\tilde{\mathbf{v}}}$ is a second order approximation to κ.

Now consider four points,

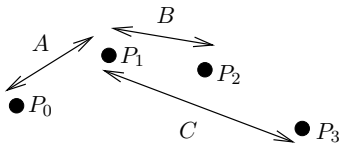

It is required to find κ and κ_s at P_1. P_0, P_1, P_2 are used to get $\kappa_{\tilde{\mathbf{v}}_1}$ and P_0, P_1, P_3 are used to get $\kappa_{\tilde{\mathbf{v}}_2}$. Thus

$$\begin{aligned} \kappa_{\tilde{\mathbf{v}}_1} &\simeq \frac{1}{2}\frac{(A+B)}{A}\kappa + \frac{1}{6}\frac{(B-A)(A+B)}{A}\kappa_s \\ \kappa_{\tilde{\mathbf{v}}_2} &\simeq \frac{1}{2}\frac{(A+C)}{A}\kappa + \frac{1}{6}\frac{(C-A)(A+C)}{A}\kappa_s \end{aligned}$$

and so

$$\kappa \simeq \frac{2(A^2-C^2)A\kappa_{\tilde{\mathbf{v}}_1} + 2(B^2-A^2)A\kappa_{\tilde{\mathbf{v}}_2}}{(A+C)(A+B)(B-C)}$$

$$\kappa_s \simeq \frac{6A(A+C)\kappa_{\tilde{\mathbf{v}}_1} - 6(A+B)A\kappa_{\tilde{\mathbf{v}}_2}}{(A+C)(A+B)(B-C)}$$

Since $\kappa_{\tilde{\mathbf{v}}_1}$ and $\kappa_{\tilde{\mathbf{v}}_2}$ are unaffected by Euclidean transformation of the points P_0, P_1, P_2, P_3, and A, B, C are joint-invariants, this gives an **invariant numerical approximation** to κ and κ_s at P_1.

The following figures show an example to demonstrate that the discrete approximation is in agreement with the true signature curve. Figure 1.5 illustrates the invariance of the numerical approximation. Note the deviation in the approximate signature curve in figure 1.3. This occurs where there is a high rate of change of curvature and is due to a κ^3 term in the Taylor series. However this may be reduced by plotting more points on regions of the curve where the rate of change of curvature is large. This effect is magnified when using large spacing, see figure 1.7.

Finally notice that in Figure 1.9, there is a small loop in the approximate signature curve which clearly distinguishes the original curve with the curve related by an affine transformation.

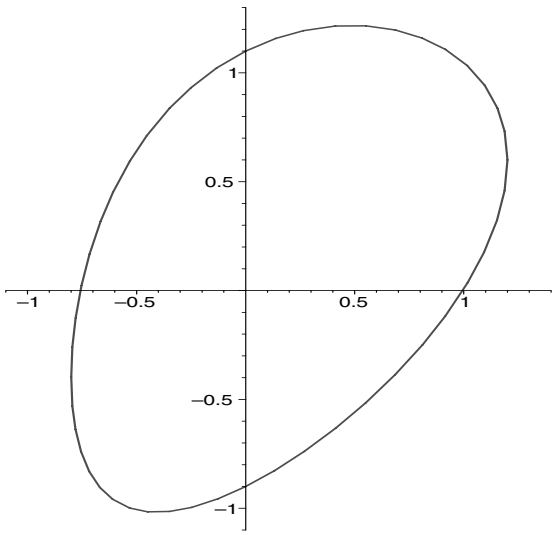

Figure 1.1: $\{x = \cos(t) + \frac{1}{5}\cos(t)^2, y = \frac{1}{2}x + \sin(t) + \frac{1}{10}\sin(t)^2\}$

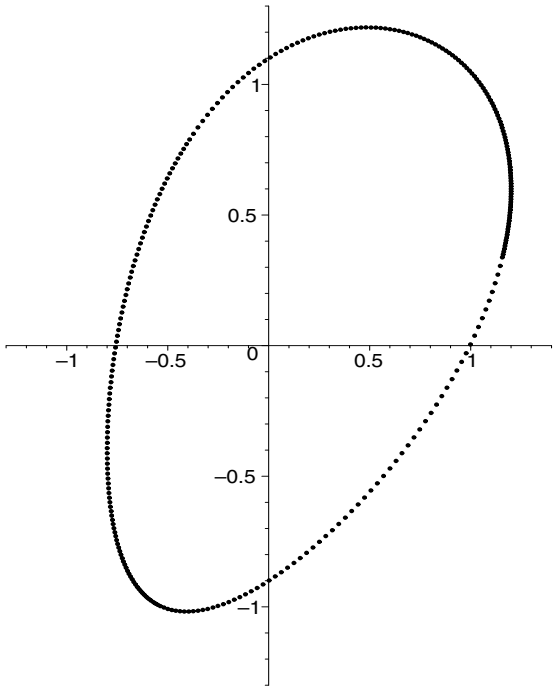

Figure 1.2: Discrete version (294 points)

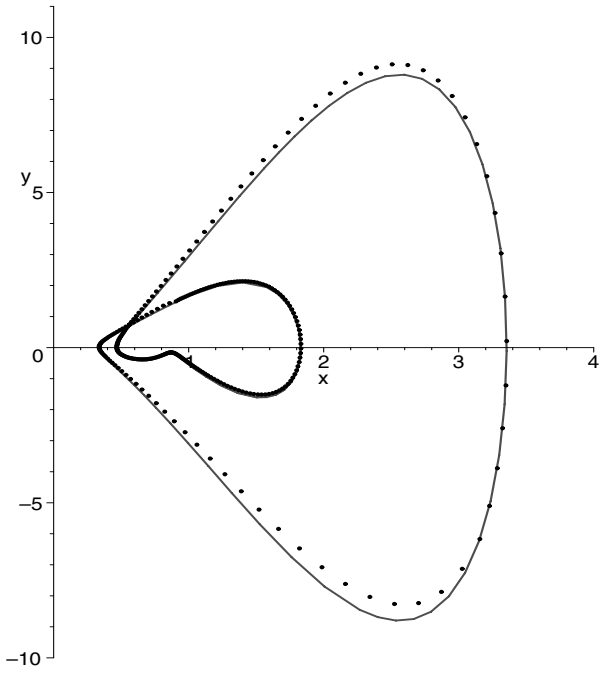

Figure 1.3: True signature curve vs approximate signature curve (294 points)

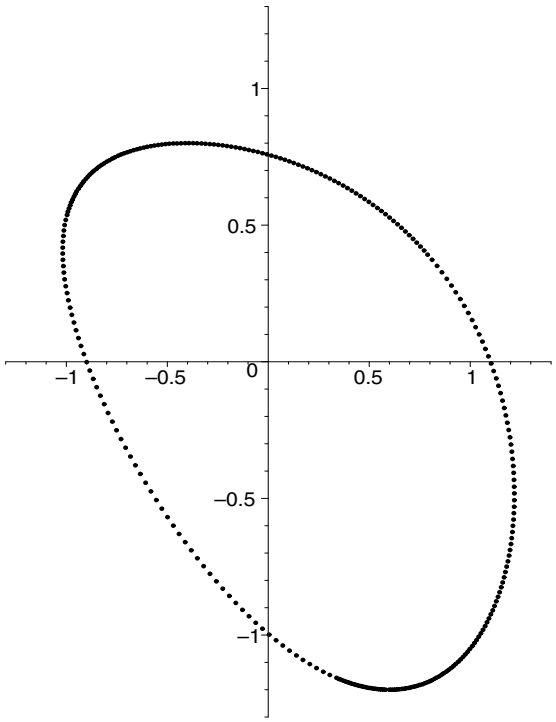

Figure 1.4: Rotate discrete curve by 90 degrees.

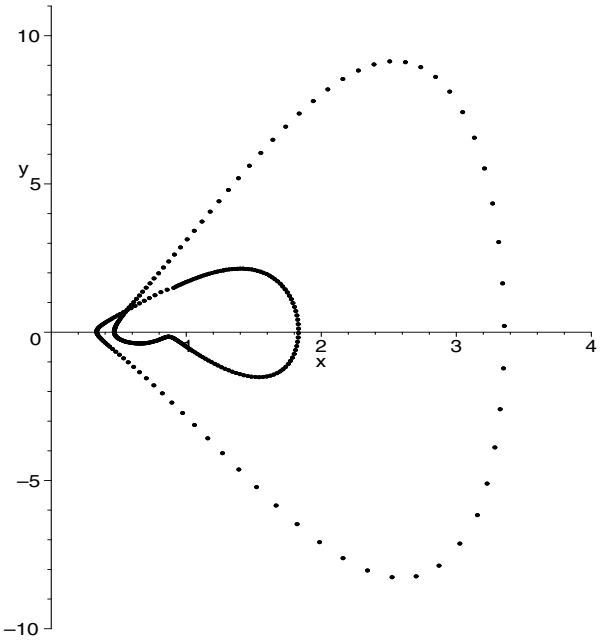

Figure 1.5: Approximate signature curves for original curve and rotated discrete curve with 294 points, plotted on same axes (note they are identical).

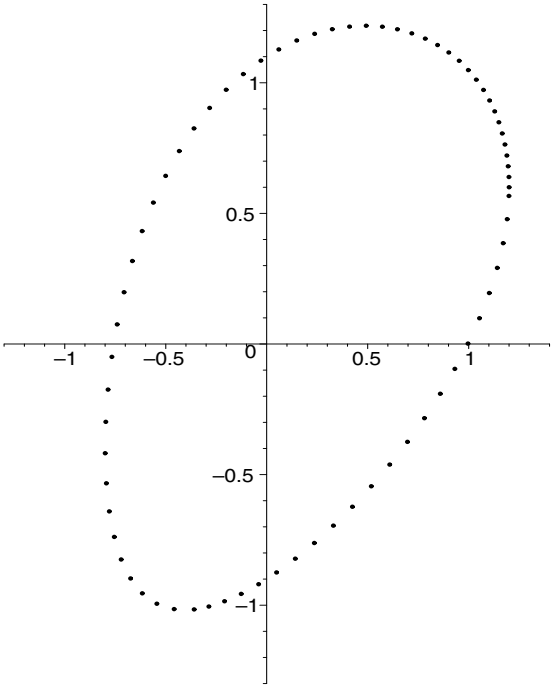

Figure 1.6: Original curve with large spacing (72 points).

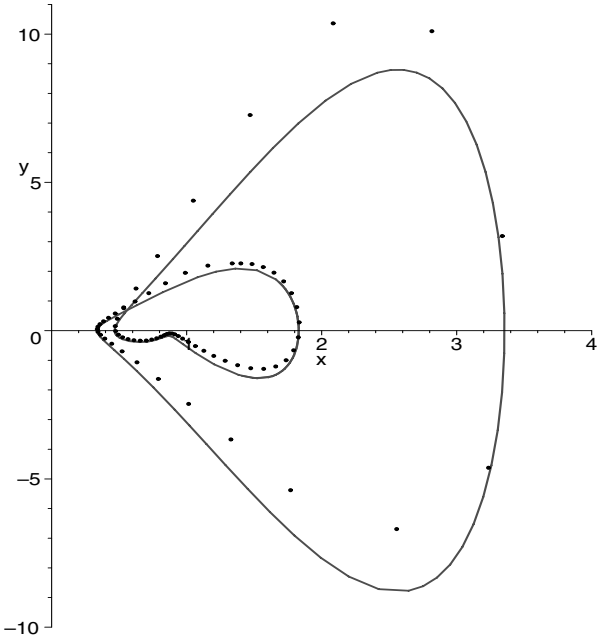

Figure 1.7: Signature curve of the curve with large spacing plotted against the true signature curve.

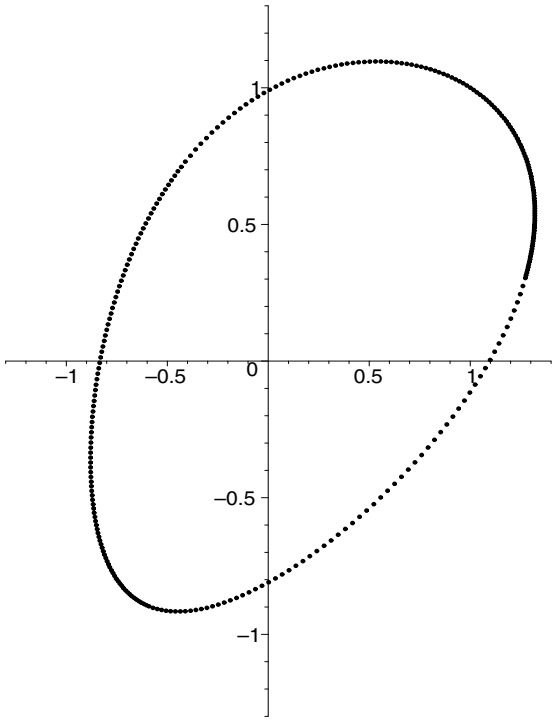

Figure 1.8: Applying the affine transformation $(x, y) \longmapsto (1.1x, 0.9y)$ to the curve

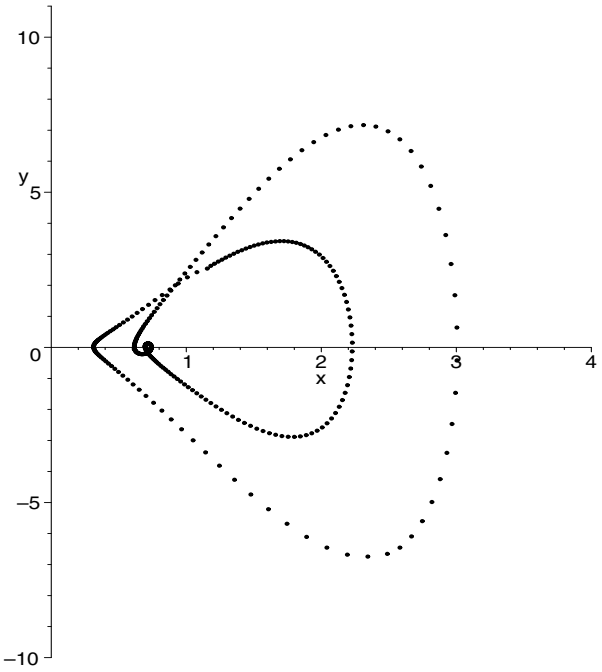

Figure 1.9: Approximate signature curve of transformed curve (294 points).

Special affine group

The special affine transformation is given by,

$$(x,u) \longmapsto (\alpha x + \beta u + \gamma, \lambda x + \mu u + \nu), \quad \det \begin{pmatrix} \alpha & \beta \\ \lambda & \mu \end{pmatrix} = 1,$$

the infinitesimal generators are,

$$\begin{aligned} x_t &= ax(t) + bu(t) + d \\ u_t &= -au(t) + cx(t) + e. \end{aligned}$$

Substituting $u_x = \frac{u_t}{x_t}$, $u_{xx} = \frac{(u_{tt}x_t - u_t x_{tt})}{x_t^2 x_{tt}}$, $\cdots$, into $\kappa^{\mathbf{SA}}$ (see section 1.1.4) and setting $t = 0$ gives,

$$\kappa^{\mathbf{SA}}_{\tilde{\mathbf{v}}} = -3(a^2+bc) \Big/ \Big(2a^3x_0u_0 + a^2bu_0^2 + 2a^2du_0 - 2a^2ex_0 - 2aed + 2abcx_0u_0 + b^2cu_0^2 + 2bcdu_0 + cd^2 - a^2cx_0^2 - bc^2x_0^2 - 2bcex_0 - be^2\Big)^{\frac{2}{3}}$$

The vector field $\tilde{\mathbf{v}}$ is obtained by joining five points $\big\{(x_1,u_1),(x_2,u_2),(x_3,u_3),(x_4,u_4),(x_5,u_5)\big\}$ with straight lines. This gives the equations,

$$\begin{aligned} (u_2-u_1)(ax_1+u_1b+d) - (x_2-x_1)(-au_1+cx_1+e) &= 0 \\ (u_3-u_2)(ax_2+u_2b+d) - (x_3-x_2)(-au_2+cx_2+e) &= 0 \\ (u_4-u_3)(ax_3+u_3b+d) - (x_4-x_3)(-au_3+cx_3+e) &= 0 \\ (u_5-u_4)(ax_4+u_4b+d) - (x_5-x_4)(-au_4+cx_4+e) &= 0 \end{aligned}$$

which can be solved for a, b, c, d, e. This yields the approximation $\kappa^{\mathbf{SA}}_{\tilde{\mathbf{v}}}$ to $\kappa^{\mathbf{SA}}$.

Now by a similar proof to the Euclidean case above, $\kappa^{\mathbf{SA}}_{\tilde{\mathbf{v}}}$ is invariant under a special affine transformation of the five points. Thus $\kappa^{\mathbf{SA}}_{\tilde{\mathbf{v}}}$ can be written in terms of the joint-invariants of the special affine group.

Given three points (x_i,u_i), (x_j,u_j), (x_k,u_k), the joint-invariant of the special affine group is the bracket value

$$[ijk] = \det \begin{pmatrix} x_i & u_i & 1 \\ x_j & u_j & 1 \\ x_k & u_k & 1 \end{pmatrix}.$$

(See [2] for the theory behind joint-invariants). However, the numerator and denominator of $\kappa^{\mathbf{SA}}_{\tilde{\mathbf{v}}}$ are very large multinomials in $\{x_i, u_i, i = 1,\ldots,5\}$ so an algorithm is required for writing these in terms of the bracket values.

There is a general theory in [9] which deals with a similar problem but this theory applies to bracket values defined differently from the above, they are given by

$$[ijk]_2 = \det \begin{pmatrix} x_{11} & x_{12} & x_{13} \\ x_{21} & x_{22} & x_{23} \\ x_{31} & x_{32} & x_{33} \end{pmatrix}$$

The algorithm developed in [9] can be reformulated. The following example shows how this is done.

Given five points $(x_{11}, x_{12}), \ldots, (x_{51}, x_{52})$ consider the multinomial,

$$F = \text{expand}\Big([124]^2 - 2[345] + [125][245][134]\Big).$$

where expand refers to evaluating the determinant in the bracket values and expanding in terms of monomials. Compute the leading term l_F say of F using the ordering $x_{11} < x_{12} < \cdots < x_{51} < x_{52}$ and rearrange the factors of l_F in the form

$$\prod_{k=1}^{n} (x_{i_k 1} x_{j_k 2})^N$$

for some positive integers n, N, i_k and j_k where $i_k < j_k$, $i_1 \leq \cdots \leq i_n$ and $j_1 \leq \cdots \leq j_n$. This corresponds to the leading term of all the combinations of multinomials $P_1 = [12\,i][13j][24k]$ where $i = 3, 4, 5$, $j = 4, 5$ and $k = 5$.

Choose i, j and k such that they are one digit more than the previous digit which gives

$$P_1 = [123][134][245].$$

Now define a new polynomial $F_1 = F - P_1$ and apply the above procedure to F_1. This gives

$$\begin{aligned} l_{F_1} &= (x_{11}x_{32})^2 x_{21}x_{42} \\ P_2 &= [134]^2[245] \\ F_2 &= F_1 - P_2 \end{aligned}$$

Continuing this process will eventually remove all coefficients of x_{11} then x_{21} and so on until for some $m \geq 1$, $F_m = 0$, so that F can be written in

terms of the bracket values by,

$$F = \sum_{k=1}^{m} P_k.$$

The 12th iteration gives

$$\begin{aligned} l_{F_{11}} &= -2x_{31}x_{42} \\ P_{12} &= -2[345] \\ F_{12} &= F_{11} - P_{12} = 0 \end{aligned}$$

so that

$$\begin{aligned} F = {} & [123][134][245] + [134]^2[245] + [134][145][245] + [123]^2 + 2[123][134] \\ & + [134]^2 - [134][234][245] - [134][245]^2 - 2[123][234] - 2[134][234] \\ & + [234]^2 - 2[345] \end{aligned}$$

Now the above method is applied on $\kappa_{\hat{\mathbf{v}}}^{\mathbf{SA}}$ which produces after a large computation in **MAPLE** (see [11]),

$$\begin{aligned} \kappa_{\hat{\mathbf{v}}}^{\mathbf{SA}} = 3\Big(& -4[123]^2[134][234][345]^2 - 3[123][234][345]^2[134]^2 \\ & + 4[134]^2[234]^2[245][345] + 2[123][134]^3[245][345] - [123][234]^3[245][345] \\ & + 4[123][134][234]^2[345]^2 - [123]^4[345]^2 - [234]^4[345]^2 - [234]^4[245]^2 \\ & - [134]^4[345]^2 - [123]^2[234]^2[245][345] + 2[134]^4[245][345] \\ & - 2[123][134]^3[345]^2 + [123][234]^3[345]^2 + 4[234]^3[134][145]^2 \\ & + [123]^3[234][345]^2 + 4[123][134][234]^2[245][345] + 4[134][234]^3[245]^2 \\ & + 2[234]^4[245][345] - 8[134][234]^3[245][345] + 2[134]^2[234]^2[345]^2 \\ & - 6[134]^2[234]^2[245]^2 + 2[123]^2[234][134][145][345] \\ & + 3[123][134]^2[234][245][345] - [134]^4[245]^2 \\ & - [123]^2[134]^2[345]^2\Big) \Big/ \Big(- [123]\Big([234]^2[345] - [234]^2[245] - [123]^2[345] \\ & - 2[134][234][345] + 2[134][234][245] + [134]^2[345] \\ & - [134]^2[245]\Big)\Big([234][123][345] - [123]^2[345] + [134][234][345] \\ & - [134][234][245] - [123][134][345] - [134]^2[345] + [134]^2[245]\Big)^2\Big)^{\frac{2}{3}}. \end{aligned}$$

A Taylor series of $\kappa_{\hat{\mathbf{v}}}^{\mathbf{SA}}$ is computed with equally spaced points in the x coordinate. First a special affine transformation is done so that $u(0) = 0$, $u_x(0) = 0$, $u_{xx}(0) = 1$ and $u_{xxx}(0) = 0$ (see section 2.1.1). Then two points P_1, P_2 and two points P_4, P_5 are equally spaced each side of P_3, so that

$P_1 = (-2h, u(-2h))$, $P_2 = (-h, u(-h))$, $P_3 = (0,0)$, $P_4 = (h, u(h))$ and $P_5 = (2h, u(2h))$, with $h > 0$. The values of the curvature and its arclength derivatives at $x = 0$ are $\kappa^{\mathbf{SA}}(0) = u_4$, $\kappa_s^{\mathbf{SA}}(0) = u_5$, and $\kappa_{ss}^{\mathbf{SA}}(0) = u_6 - 5u_4$. Now expand in a Taylor series,

$$\begin{aligned}
u(-2h) &= 2h^2 + \frac{2}{3}u_4h^4 - \frac{4}{15}u_5h^5 + \frac{4}{45}u_6h^6 - \frac{8}{315}u_7h^7 + \cdots \\
u(-h) &= \frac{1}{2}h^2 + \frac{1}{24}u_4h^4 - \frac{1}{120}u_5h^5 + \frac{1}{720}u_6h^6 - \frac{1}{5040}u_7h^7 + \cdots \\
u(h) &= \frac{1}{2}h^2 + \frac{1}{24}u_4h^4 + \frac{1}{120}u_5h^5 + \frac{1}{720}u_6h^6 + \frac{1}{5040}u_7h^7 - \cdots \\
u(2h) &= 2h^2 + \frac{2}{3}u_4h^4 + \frac{4}{15}u_5h^5 + \frac{4}{45}u_6h^6 + \frac{8}{315}u_7h^7 - \cdots
\end{aligned}$$

where $u_4 = u_{xxxx}(0)$, $u_5 = u_{xxxxx}(0)$, $\cdots$. Substituting into $\kappa_{\tilde{\mathbf{v}}}^{\mathbf{SA}}$ yields

$$\kappa_{\tilde{\mathbf{v}}}^{\mathbf{SA}} = \kappa^{\mathbf{SA}} + \frac{1}{54}(23(\kappa^{\mathbf{SA}})^2 + 9\kappa_{ss}^{\mathbf{SA}})h^2 + \frac{5}{36}\kappa^{\mathbf{SA}}\kappa_s^{\mathbf{SA}}h^3 + O(h^4)$$

The discrete approximation to the special affine signature curve for unequally spaced points could be obtained by a similar method to the Euclidean case. That is given five points $(-m, u(-m))$, $(-k, u(-k))$, $(0,0)$, $(h, u(h))$ and $(l, u(l))$, the Taylor series for these can be computed and substituted into $\kappa_{\tilde{\mathbf{v}}}^{\mathbf{SA}}$. The coefficients are written in terms of the bracket values $[ijk]$ by inverting the Taylor series. The first two terms can be used to get the special affine invariant approximation to the special affine signature curve. This calculation has not been done.

Projective group

The projective transformation is given by,

$$(x,u) \longmapsto \left(\frac{\alpha x + \beta u + \gamma}{\rho x + \sigma u + \tau}, \frac{\lambda x + \mu u + \nu}{\rho x + \sigma u + \tau}\right), \quad \det\begin{pmatrix} \alpha & \beta & \gamma \\ \lambda & \mu & \nu \\ \rho & \sigma & \tau \end{pmatrix} = 1,$$

the infinitesimal generators are,

$$\begin{aligned}
x_t &= au(t) + b + dx(t) + fx(t)^2 + gx(t)u(t) \\
u_t &= cx(t) + e + fx(t)u(t) + gu(t)^2 + u(t)
\end{aligned}$$

Substituting $u_x = \frac{u_t}{x_t}$, $u_{xx} = \frac{(u_{tt}x_t - u_tx_{tt})}{x_t^2x_{tt}}$, $\cdots$ into $\kappa^{\mathbf{proj}}$ and setting $t = 0$ yields, after a large computation in **MAPLE**,

$$\begin{aligned}
\kappa_{\tilde{\mathbf{v}}}^{\mathbf{proj}} \;=\; & (3ac - d + 1 - 3fb + d^2 - 3ge)\Big/(-54eaf + 18ac + 18cda + 36fb \\
& + 4d^3 - 6d - 6d^2 + 4 - 54cgb + 36dge - 18ge - 18dfb)^{\frac{2}{3}}
\end{aligned}$$

Note that $\kappa^{\mathbf{proj}}_{\tilde{\mathbf{v}}}$ does not depend on the initial point.

The vector field $\tilde{\mathbf{v}}$, is obtained by joining eight points $\{(x_1,u_1),(x_2,u_2),(x_3,u_3),(x_4,u_4),(x_5,u_5),(x_6,u_6),(x_7,u_7),(x_8,u_8)\}$ with straight lines. This gives

$$\begin{aligned}
&(u_2-u_1)(au_1+b+dx_1+fx_1^2+gx_1u_1)-(x_2-x_1)(cx_1+e+fx_1u_1+gu_1^2+u_1)=0\\
&(u_3-u_2)(au_2+b+dx_2+fx_2^2+gx_2u_2)-(x_3-x_2)(cx_2+e+fx_2u_2+gu_2^2+u_2)=0\\
&(u_4-u_3)(au_3+b+dx_3+fx_3^2+gx_3u_3)-(x_4-x_3)(cx_3+e+fx_3u_3+gu_3^2+u_3)=0\\
&(u_5-u_4)(au_4+b+dx_4+fx_4^2+gx_4u_4)-(x_5-x_4)(cx_4+e+fx_4u_4+gu_4^2+u_4)=0\\
&(u_6-u_5)(au_5+b+dx_5+fx_5^2+gx_5u_5)-(x_6-x_5)(cx_5+e+fx_5u_5+gu_5^2+u_5)=0\\
&(u_7-u_6)(au_6+b+dx_6+fx_6^2+gx_6u_6)-(x_7-x_6)(cx_6+e+fx_6u_6+gu_6^2+u_6)=0\\
&(u_8-u_7)(au_7+b+dx_7+fx_7^2+gx_7u_7)-(x_8-x_7)(cx_7+e+fx_7u_7+gu_7^2+u_7)=0
\end{aligned}$$

which can be solved for a, b, c, d, e, f, g. Thus an approximation $\kappa^{\mathbf{proj}}_{\tilde{\mathbf{v}}}$ to $\kappa^{\mathbf{proj}}$ is obtained.

Now by a similar proof to the Euclidean case above, $\kappa^{\mathbf{proj}}_{\tilde{\mathbf{v}}}$ is invariant under a projective transformation of the eight points. Thus $\kappa^{\mathbf{proj}}_{\tilde{\mathbf{v}}}$ can be written in terms of the joint-invariants of the projective group.

The projective joint-invariants depend on five points, $\{(x_1,u_1),(x_2,u_2),(x_3,u_3),(x_4,u_4),(x_5,u_5)\}$ and are given by,

$$J_1=\frac{[134][125]}{[135][124]}$$
$$J_2=\frac{[123][245]}{[125][234]}$$

The explicit expression for $\kappa^{\mathbf{proj}}_{\tilde{\mathbf{v}}}$ has not been calculated but could be done by using the algorithm from special affine group above to write the expression in terms of the bracket values $[ijk]$ then rearranging the expression in terms of J_1 and J_2.

A Taylor series of $\kappa^{\mathbf{proj}}_{\tilde{\mathbf{v}}}$ is computed with equally spaced points in the x coordinate. A projective transformation is done so that at the point $P_4\in u(x)$, $u(0)=0$, $u_x(0)=0$, $u_{xx}(0)=1$, $u_3=0$, $u_4=0$, $u_5=1$ and $u_6=0$. This is done by first doing a special affine transformation such that $u(0)=0$, $u_x(0)=0$, $u_{xx}=1$, $u_3=0$ and then applying the projective transformation,

$$c=0,\quad f=0,\quad d=0,\quad e=a^2,\quad b=ag,\quad h=\frac{1}{2}g^2-\frac{1}{6}u_4,\quad a=u_5^{\frac{1}{3}}$$
$$g=\frac{1}{3}\frac{5u_4^2-u_6}{u_5}.$$

The points P_1, P_2, P_3 and P_5, P_6, P_7, P_8 are equally spaced in the x coordinate both sides of P_4, so that $P_1 = (-3h, u(-3h))$, $P_2 = (-2h, u(-2h))$, $P_3 = (-h, u(-h))$, $P_4 = (0, 0)$ and $P_5 = (h, u(h))$, $P_6 = (2h, u(2h))$, $P_7 = (3h, u(3h))$, $P_8 = (4h, u(4h))$ with $h > 0$. The values of the curvature and its arclength derivatives at $x = 0$ are $\kappa^{\mathbf{proj}}(0) = u_7$, $\kappa_s^{\mathbf{proj}}(0) = 2u_8 - 35$ and $\kappa_{ss}^{\mathbf{proj}}(0) = \frac{1}{4}u_9 - u_7$ where $u_7 = u_{xxxxxxx}(0)$, $u_8 = u_{xxxxxxxx}(0)$, $u_9 = u_{xxxxxxxxx}(0)$. Now expand in a Taylor series,

$$\begin{aligned}
u(-3h) &= \frac{9}{2}h^2 - \frac{81}{40}h^5 - \frac{243}{560}u_7h^7 + \frac{729}{4480}u_8h^8 - \cdots \\
u(-2h) &= 2h^2 - \frac{4}{15}h^5 - \frac{8}{315}u_7h^7 + \frac{2}{315}u_8h^8 - \cdots \\
u(-h) &= \frac{1}{2}h^2 - \frac{1}{120}h^5 - \frac{1}{5040}u_7h^7 + \frac{1}{40320}u_8h^8 - \cdots \\
u(h) &= \frac{1}{2}h^2 + \frac{1}{120}h^5 + \frac{1}{5040}u_7h^7 + \frac{1}{40320}u_8h^8 + \cdots \\
u(2h) &= 2h^2 + \frac{4}{15}h^5 + \frac{8}{315}u_7h^7 + \frac{2}{315}u_8h^8 + \cdots \\
u(3h) &= \frac{9}{2}h^2 + \frac{81}{40}h^5 + \frac{243}{560}u_7h^7 + \frac{729}{4480}u_8h^8 + \cdots \\
u(4h) &= 8h^2 + \frac{128}{15}h^5 + \frac{1024}{315}u_7h^7 + \frac{512}{315}u_8h^8 + \cdots .
\end{aligned}$$

Substituting into $\kappa_{\tilde{\mathbf{v}}}^{\mathbf{proj}}$ yields

$$\begin{aligned}
\kappa_{\tilde{\mathbf{v}}}^{\mathbf{proj}} &= \kappa^{\mathbf{proj}} - \frac{1}{108}(32(\kappa^{\mathbf{proj}})^3 - 162 - 27\kappa_s^{\mathbf{proj}})h \\
&\quad + \frac{1}{1458}\left(-999(\kappa^{\mathbf{proj}})^2 - 324(\kappa^{\mathbf{proj}})^2\kappa_s^{\mathbf{proj}} + 2430\kappa_{ss}^{\mathbf{proj}} + 160(\kappa^{\mathbf{proj}})^5\right)h^2.
\end{aligned}$$

The discrete approximation to the projective signature curve could be obtained by a similar method to the Euclidean case.

Now this method is demonstrated by plotting the true curvature versus the approximate discrete curvature with equally spaced points for the curve $u = \tan(x)$ (200 points are used), see figures 1.10 and 1.11.

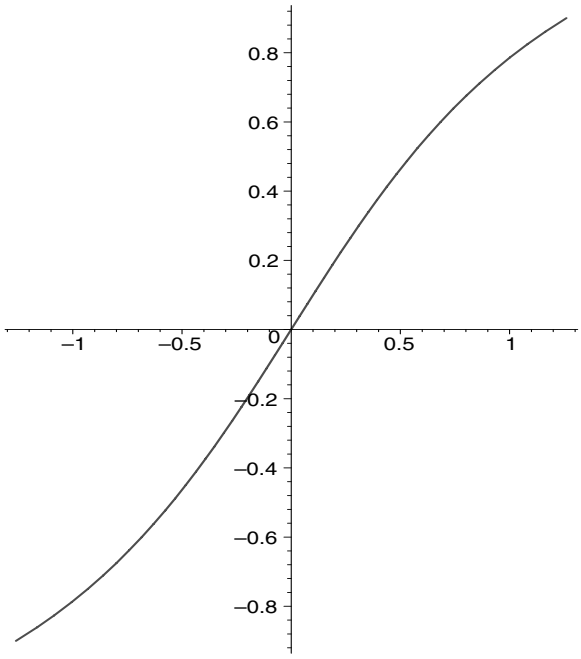

Figure 1.10: $u = \tan(x)$

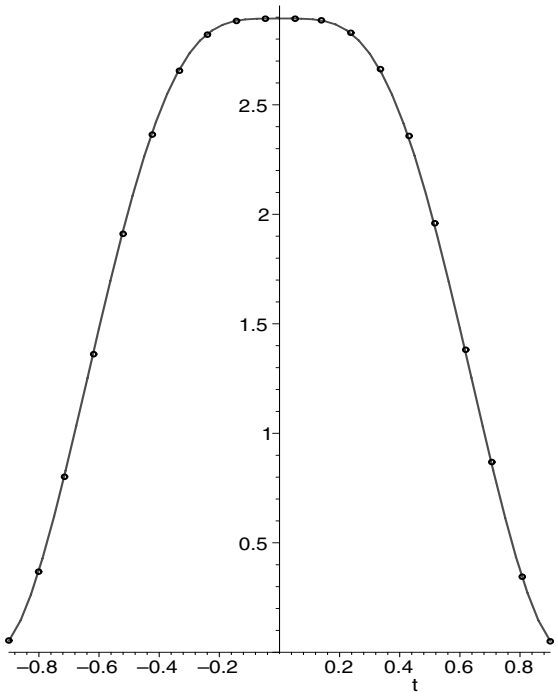

Figure 1.11: true curvature versus approximate curvature for equally spaced points, 20 points (out of 200) are plotted.

Chapter 2

Invariants and curve matching

2.1 Invariants

In chapter 3, a method is described for matching two curves related by a projective transformation. In this method it is required to find and identify common points in the two curves. Thus properties of the curves must be found which are invariant under a projective transformation.

One such property is the projective curvature which is a global invariant and characterises all curves up to a projective transformation. However, the projective curvature depends on up to seventh order derivatives and so is very sensitive to noise and is of no practice use. Thus invariants depending on much lower order derivatives are required.

In the following section 2.1.1, it is shown there are links between the curvatures of the Euclidean, special affine, affine and projective groups. These provide lower order invariants. One such lower order invariant is the special affine curvature turning points. It is shown that these points characterise all the singularities in the projective curvature.

In section 2.1.2 a way of locating the invariant points in practice is given. The property that tangency is preserved under a projective transformation is shown. For concave curves, two further invariant points called bi-tangents can be used. The projective joint-invariants are given which depend on five points and it is shown how these can be used to identify the invariant points between two curves. Also it is shown that if n points in one curve have their corresponding joint-invariants equal to n points in another curve, then the n points in both curves must be related by a projective transformation.

2.1.1 Links between groups

The curvatures of the projective group, special affine group and Euclidean goup are all related. The links (see section 5.2 for a derivation of $\kappa^{\mathbf{A}}$ and $\kappa^{\mathbf{PROJ}}$) are as follows,

$$\kappa^{\mathbf{SA}} = \frac{3(\kappa^{\mathbf{E}})^{\frac{5}{3}}\kappa^{\mathbf{E}}_{ss} + 9(\kappa^{\mathbf{E}})^{\frac{2}{3}}(\kappa^{\mathbf{E}}_s)^2 - (\kappa^{\mathbf{E}}_s)^2 - 9(\kappa^{\mathbf{E}})^6}{(\kappa^{\mathbf{E}})^{\frac{14}{3}}}, \quad \text{s} \equiv \text{Euclidean arclength}$$

$$\kappa^{\mathbf{A}} = \frac{\kappa^{\mathbf{SA}}_s}{(\kappa^{\mathbf{SA}})^{\frac{3}{2}}}, \quad \text{s} \equiv \text{special affine arclength}$$

$$\kappa^{\mathbf{PROJ}} = \frac{2\kappa^{\mathbf{A}}_{ss}}{(\kappa^{\mathbf{A}})^{\frac{5}{3}}} - \frac{7}{3}\frac{(\kappa^{\mathbf{A}}_s)^2}{(\kappa^{\mathbf{A}})^{\frac{8}{3}}} + \frac{\kappa^{\mathbf{A}}_s}{(\kappa^{\mathbf{A}})^{\frac{2}{3}}} - \frac{1}{3(\kappa^{\mathbf{A}})^{\frac{2}{3}}} + \frac{1}{12}(\kappa^{\mathbf{A}})^{\frac{4}{3}}, \quad \text{s} \equiv \text{affine arclength}$$

The expression for $\kappa^{\mathbf{SA}}_s$ is given by

$$\kappa^{\mathbf{SA}}_s = \frac{1}{3}\frac{9u^2_{xx}u_5 - 45u_{xx}u_3u_4 + 40u^3_3}{u^4_{xx}}$$

where it is assumed that $u \in C^\infty$.

Notice that the numerator of $\kappa^{\mathbf{SA}}_s$ is the denominator of $\kappa^{\mathbf{PROJ}}$ (see (1.2)). Assuming that $u_{xx} \neq 0$, the denominator of $\kappa^{\mathbf{PROJ}}$ will vanish at a critical point of the special affine curvature ($\kappa^{\mathbf{SA}}_s = 0$). This is equivalent to,

$$u_5 = \frac{5}{9}\frac{u_3(9u_{xx}u_4 - 8u^2_3)}{u^2_{xx}} \tag{2.1}$$

at the critical point. Substituting (2.1) into the numerator of $\kappa^{\mathbf{PROJ}}$ gives

$$\text{numer}(\kappa^{\mathbf{PROJ}}) = -21(40u^4_3 - 20u_{xx}u_4u^2_3 - 15u^2_{xx}u^2_4 + 3u^3_{xx}u_6)^2 \tag{2.2}$$

Substituting (2.1) into $\kappa^{\mathbf{SA}}_{ss}$ gives,

$$\kappa^{\mathbf{SA}}_{ss} = \frac{40u^4_3 - 20u_{xx}u_4u^2_3 - 15u^2_{xx}u^2_4 + 3u^3_{xx}u_6}{u^{16/3}_{xx}}$$

So if $u_{xx} \neq 0$ then at a non-degenerate critical point of $\kappa^{\mathbf{SA}}_s$ ($\kappa^{\mathbf{SA}}_{ss} \neq 0$), the numerator of $\kappa^{\mathbf{PROJ}}$ will be non-zero, and so $\kappa^{\mathbf{PROJ}}$ will have a singularity. Note that if $\kappa^{\mathbf{SA}}_s \neq 0$, then since $u \in C^\infty$, the numerator of $\kappa^{\mathbf{PROJ}}$ will be bounded thus no singularity will occur in $\kappa^{\mathbf{PROJ}}$.

Also note, if there exists an interval I, such that for $x \in I$, $u = u(x)$ is

part of a conic section, then $\kappa_s^{\mathbf{SA}} = 0$ and $\kappa_{ss}^{\mathbf{SA}} = 0$ on I. Thus $\kappa^{\mathbf{PROJ}}$ will be undefined on I. It is assumed that this is not the case.

If $u_{xx} = 0$, then

$$\kappa^{\mathbf{PROJ}} = \frac{280u_3^8}{40^{\frac{8}{3}}u_3^8}.$$

Thus, if $u_3 \neq 0$ $\kappa^{\mathbf{PROJ}}$ does not have a singularity. For the case $u_3 = 0$ (assuming $u \in C^\infty$) then u can be represented by (after a possible translation)

$$u(x) = ax + \phi(x)x^n$$

for some $n > 4$ (since $u_{xx} = 0$ and $u_3 = 0$) and, $\phi \in C^\infty$ with $\phi(0) \neq 0$. Note that if no such n exists then $u(x)$ is a straight line and the projective curvature is undefined. The projective curvature of $u(x)$ is now

$$\kappa^{\mathbf{PROJ}} = \frac{1}{4}\frac{(n^2 - n + 1)^3}{\Big((n-2)(2n-1)(n+1)\Big)^2}$$

Hence if $u_{xx} = 0$ then $\kappa^{\mathbf{PROJ}}$ does not have a singularity. Note that $u_{xx} = 0$ corresponds to zero Euclidean curvature at $x = 0$. Conversely as long as the tangent line at this point is not vertical ($u_x = \infty$) then a point with zero Euclidean curvature corresponds to a point where $u_{xx} = 0$. Thus if $\kappa^{\mathbf{E}} = 0$ then $\kappa^{\mathbf{PROJ}}$ does not have a singularity.

Now it is shown that if $\kappa^{\mathbf{E}} = 0$ at a point on a curve $u \in C^\infty$, then under any projective transformation, $\bar{\kappa}^{\mathbf{E}} = 0$ at the transformed point. Note as is shown further below this is **not** the case if the point of interest occurs at a singularity of u. First a Euclidean transformation is done such that $x = 0$, $u(0) = 0$, $u_x(0) = 0$, this has no effect on the condition $\kappa^{\mathbf{E}} = 0$. The projective transformation of the first and second derivatives are,

$$\bar{u}_{\bar{x}} = \frac{fg - di}{cg - ai}$$
$$\bar{u}_{\bar{x}\bar{x}} = -\frac{u_{xx}(0)i^3}{(cg - ai)^3}$$

This gives,

$$\bar{\kappa}^{\mathbf{E}} = \frac{i^3 u_{xx}(0)}{((ai - cg)^2 + (fg - di)^2)^{\frac{3}{2}}} = \frac{i^3}{((ai - cg)^2 + (fg - di)^2)^{\frac{3}{2}}}\kappa^{\mathbf{E}}$$

If $i \neq 0$ then at least one of $ai - cg$, $fg - di$ must be non-zero otherwise it is not a projective transformation. Under a projective transformation,

$(0,0) \longmapsto (\frac{c}{i}, \frac{f}{i})$ therefore $i = 0$ implies at least one of x, u is mapped to ∞. Therefore as long as the image point is finite $\kappa^{\mathbf{E}}(x,u) = 0$ if and only if $\bar{\kappa}^{\mathbf{E}}(\bar{x},\bar{u}) = 0$.

If $i = 0$, $g \neq 0$ then $\bar{\kappa}^{\mathbf{E}} = 0$ independent of $\kappa^{\mathbf{E}}$. If $i = 0$, $g = 0$, since $u \in C^{\infty}$, $u(x)$ can be written in the form,

$$u(x) = Ax^2 + \phi(x)x^n \tag{2.3}$$

where $n \geq 3$, $\phi \in C^{\infty}$ and $\phi(0) \neq 0$. $A = 0$ corresponds to $\kappa^{\mathbf{E}} = 0$. This gives

$$\bar{\kappa}^{\mathbf{E}} = \frac{x^{n+1}F(x)}{(\phi(0)^2 n^2 (c^2+f^2) + G(x))^{\frac{3}{2}}},$$

where $G(0) = 0$ and one of c or f must be non-zero otherwise it is not a projective transformation. Thus $x = 0$ gives $\bar{\kappa}^{\mathbf{E}} = 0$.

Hence, $\bar{\kappa}^{\mathbf{E}}$ is well defined at the transformed point $(\bar{x},\bar{u})$ even though $(\bar{x},\bar{u})$ is a point at ∞. Thus, if curves having singularities are allowed they may have points where $\kappa^{\mathbf{E}} = 0$ which are not true inflection points. That is they arise from a projective transformation of a point on a C^{∞} curve which has $\kappa^{\mathbf{E}} \neq 0$.

Let P^{∞} be the space of curves as those that are generated by projective transformations of C^{∞} **closed** curves. For curves in P^{∞}, the following method gives a way of detecting when a point is a true inflection point or not. Note this restriction is to avoid analysing the points at infinity of C^{∞} **open** curves. This is discussed further below. Locally a closed curve can be represented by a function $u = u(x)$. Without loss of generality assume that the point of interest occurs at $x = 0$, $u(0) = 0$ and $u_x(0) = 0$. Since $u \in C^{\infty}$, $u(x)$ takes the form (2.3). A projective transformation is done on the curve $u = u(x)$. If $i \neq 0$ then $\kappa^{\mathbf{E}} \neq 0$ if and only if $\bar{\kappa}^{\mathbf{E}} \neq 0$. If $i = 0$ then $\bar{\kappa}^{\mathbf{E}} = 0$; even if $\kappa^{\mathbf{E}} \neq 0$.

Assume $i = 0$. Consider the radius $\bar{R} = \sqrt{(\bar{x}^2 + \bar{u}^2)} = \infty$ of the transformed point $(\bar{x},\bar{u})$. This is the curvature for the rotational group $SO(2)$. Now

$$(\bar{\kappa}^{\mathbf{E}})^2 \bar{R}^6 = 4\,\frac{A^2}{g^6}$$

at the transformed point. If $g \neq 0$ then $A = 0$ implies $(\bar{\kappa}^{\mathbf{E}})^2 \bar{R}^6 = 0$. Note that since $i = 0$ implies $\bar{\kappa}^{\mathbf{E}} = 0$ the following also holds (independent of A),

$$(\bar{\kappa}^{\mathbf{E}})^4 \bar{R}^6 = 0.$$

If $g = 0$ then $h \neq 0$ (otherwise this is not a projective transformation), so that the following holds

$$(\bar{\kappa}^{\mathbf{E}})^2\bar{R}^6 = \frac{(c^2+f^2+F_1(x))^3\Big(2A + x^{n-2}(\phi(0)n(n-1)+F_2(x))\Big)^2}{x^6h^4\Big(AG_1(x)x^{n-2} + A^2G_2(x) + x^{2n-4}G_3(x)\Big)^3}$$

where $F_1(0) = 0$, $F_2(0) = 0$, and $c^2 + f^2 \neq 0$. Hence at $x = 0$, $(\bar{\kappa}^{\mathbf{E}})^2\bar{R}^6 = \infty$, independent of A. Furthermore,

$$(\bar{\kappa}^{\mathbf{E}})^4\bar{R}^6 = \frac{1}{256A^2(c^2+f^2)^3h^2}.$$

So if $A \neq 0$, $(\bar{\kappa}^{\mathbf{E}})^4\bar{R}^6 \neq 0$ and if $A = 0$, $(\bar{\kappa}^{\mathbf{E}})^4\bar{R}^6 = \infty$.

These results can be summarized in the following table.

				Inflection point
1.	$\bar{\kappa}^{\mathbf{E}} = 0$	$(\bar{\kappa}^{\mathbf{E}})^2\bar{R}^6 = 0$	$(\bar{\kappa}^{\mathbf{E}})^4\bar{R}^6 = 0$	Yes
2.	$\bar{\kappa}^{\mathbf{E}} = 0$	$(\bar{\kappa}^{\mathbf{E}})^2\bar{R}^6 = \infty$	$(\bar{\kappa}^{\mathbf{E}})^4\bar{R}^6 = \infty$	Yes
3.	$\bar{\kappa}^{\mathbf{E}} = 0$	$(\bar{\kappa}^{\mathbf{E}})^2\bar{R}^6 \neq 0$	$(\bar{\kappa}^{\mathbf{E}})^4\bar{R}^6 = 0$	No
4.	$\bar{\kappa}^{\mathbf{E}} = 0$	$(\bar{\kappa}^{\mathbf{E}})^2\bar{R}^6 = \infty$	$(\bar{\kappa}^{\mathbf{E}})^4\bar{R}^6 \neq 0$	No
5.	$\bar{\kappa}^{\mathbf{E}} \neq 0$			No

An alternative method is to use $\kappa_s^{\mathbf{SA}}$. As above it is assumed that $u(x)$ is of the form (2.3). If $A = 0$ ($u_{xx}(0) = 0$) then

$$\kappa_s^{\mathbf{SA}} = \frac{2\phi(0)^3n^3(n-2)(2n-1)(n+1)(n-1)^3 + F(x)}{x^{n+1}G(x)} \tag{2.4}$$

where $F(0) = 0$. Hence at $x = 0$, $\kappa_s^{\mathbf{SA}} = \infty$. Also

$$\kappa_s^{\mathbf{SA}}(x^2+u(x)^2)^{\frac{3}{2}} = x^3\kappa_s^{\mathbf{SA}}(1+(\phi(x)x^{n-1})^2)^{\frac{3}{2}}$$

so that, at $x = 0$, $\kappa_s^{\mathbf{SA}}R^3 = \infty$.

If $A \neq 0$, then since $u \in C^\infty$, the numerator of $\kappa_s^{\mathbf{SA}}$ will be bounded and so $\kappa_s^{\mathbf{SA}} \neq \infty$. Thus $\kappa_s^{\mathbf{SA}} = \infty$ if and only if $A = 0$. Also $\kappa_s^{\mathbf{SA}}R^3 = \infty$ if and only if $A = 0$.

If a projective transformation is done on the curve $u = u(x)$ then $\kappa_s^{\mathbf{SA}}$ transforms to

$$\bar{\kappa}_{\bar{s}}^{\mathbf{SA}} = (gx + hu(x) + i)^3\kappa_s^{\mathbf{SA}} \tag{2.5}$$

Also note that if two curves were related by a projective transformation with either $a = 1,\ b = 0,\ c = 0$ or with $d = 0,\ e = 1,\ f = 0$ then $\bar{\kappa}_{\bar{s}}^{\mathbf{SA}}\bar{x}^3 = \kappa_s^{\mathbf{SA}}x^3$ and $\bar{\kappa}_{\bar{s}}^{\mathbf{SA}}\bar{u}^3 = \kappa_s^{\mathbf{SA}}u^3$ respectively. These give two subgroup actions of the projective group action. The invariants of these subgroup actions are

$a = 1,\ b = 0,\ c = 0$

(1) $$(x,u) \longmapsto (\frac{x}{gx+hu+i}, \frac{dx+eu+f}{gx+hu+i}), \quad \det\begin{pmatrix} e & f \\ h & i \end{pmatrix} = 1$$

$$\kappa = \frac{x^2(3u_{xx}u_4 - 5u_3^2) - 3u_{xx}(2xu_3 + 3u_{xx})}{u_{xx}^{\frac{8}{3}}}$$

OR $$\kappa = x^2\kappa^{\mathbf{SA}} - 2\int (x\kappa^{\mathbf{SA}})\,\mathrm{d}x$$

$$\kappa_{\tilde{s}} = x^3\kappa_s^{\mathbf{SA}}$$

$$\mathrm{d}\tilde{s} = \frac{u_{xx}^{\frac{1}{3}}}{x}\mathrm{d}x$$

$d = 0,\ e = 1,\ f = 0$

(2) $$(x,u) \longmapsto (\frac{ax+bu+c}{gx+hu+i}, \frac{u}{gx+hu+i}), \quad \det\begin{pmatrix} a & c \\ g & i \end{pmatrix} = 1$$

$$\kappa = \frac{u^2(3u_{xx}u_4 - 5u_3^2) - 3u_{xx}(3u_x^2u_{xx} + 2uu_xu_3 - 6uu_{xx}^2)}{u_{xx}^{\frac{8}{3}}}$$

OR $$\kappa = u^2\kappa^{\mathbf{SA}} - 2\int (u\kappa^{\mathbf{SA}})\,\mathrm{d}u$$

$$\kappa_{\tilde{s}} = u^3\kappa_s^{\mathbf{SA}}$$

$$\mathrm{d}\tilde{s} = \frac{u_{xx}^{\frac{1}{3}}}{u}\mathrm{d}x.$$

Note the links to the special affine group.

Now multiplying (2.5) by $\bar{R}^3$ gives

$$\bar{\kappa}_{\bar{s}}^{\mathbf{SA}}\bar{R}^3 = \kappa_s^{\mathbf{SA}}\big((ax+bu(x)+c)^2+(dx+eu(x)+f)^2\big)^{\frac{3}{2}} \tag{2.6}$$

Thus, $\bar{\kappa}_{\bar{s}}^{\mathbf{SA}}\bar{R}^3 = \infty$ implies $\kappa_s^{\mathbf{SA}} = \infty$. However $\kappa_s^{\mathbf{SA}} = \infty$ if and only if $A = 0$. If $A = 0$ and $i = 0$ then at least one of c or f must be non-zero otherwise it is not a projective transformation and so $\bar{\kappa}_{\bar{s}}^{\mathbf{SA}}\bar{R}^3 = \infty$. For $A = 0$ and $i \neq 0$, $c = 0$, $f = 0$ implies that at least one of a and b is non-zero. Thus (2.3) becomes $u(x) = \phi(x)x^n$ and so (2.6) is

$$\bar{\kappa}_{\bar{s}}^{\mathbf{SA}}\bar{R}^3 = x^3\kappa_s^{\mathbf{SA}}((a+b\phi(x)x^n)^2+(d+e\phi(x)x^n)^2)^{\frac{3}{2}},$$

where $\kappa_s^{\mathbf{SA}}$ is given by (2.4) and $n \geq 3$. Hence at $x = 0$, $x^3\kappa_s^{\mathbf{SA}} = \infty$ implies $\bar{\kappa}_{\bar{s}}^{\mathbf{SA}}\bar{R}^3 = \infty$. Thus for any projective transformation,

$$\bar{\kappa}_{\bar{s}}^{\mathbf{SA}}\bar{R}^3 = \infty \text{ if and only if } A = 0.$$

Note for the case $i \neq 0$ then

$$\bar{\kappa}_{\bar{s}}^{\mathbf{SA}} = \infty \text{ if and only if } A = 0.$$

In summary, given any $\bar{u} \in P^\infty$, then if $\bar{\kappa}_{\bar{s}}^{\mathbf{SA}}\bar{R}^3 = \infty$ at some point, the point corresponds to an inflection point in a closed curve $u \in C^\infty$. Furthermore this point does not correspond to a singularity in $\kappa^{\mathbf{PROJ}}$.

Now (2.5) shows that,

$$\bar{\kappa}_{\bar{s}}^{\mathbf{SA}} \neq 0 \text{ implies } i \neq 0 \text{ and } \kappa_s^{\mathbf{SA}} \neq 0$$

and for $i \neq 0$,

$$\bar{\kappa}_{\bar{s}}^{\mathbf{SA}} = 0 \text{ if and only if } \kappa_s^{\mathbf{SA}} = 0.$$

Also by (2.6), if $i = 0$ so that at least one of c or f is non-zero, then

$$\bar{\kappa}_{\bar{s}}^{\mathbf{SA}}\bar{R}^3 = 0 \text{ if and only if } \kappa_s^{\mathbf{SA}} = 0.$$

So a point on a curve $\bar{u} \in P^\infty$ corresponds to a point at which $\kappa_s^{\mathbf{SA}} = 0$ on a closed curve $u \in C^\infty$ if and only if both $\bar{\kappa}_{\bar{s}}^{\mathbf{SA}}$ and $\bar{\kappa}_{\bar{s}}^{\mathbf{SA}}\bar{R}^3$ vanish at that point.

Under a projective transformation, $\kappa_{ss}^{\mathbf{SA}}$ transforms

$$\bar{\kappa}_{\bar{s}\bar{s}}^{\mathbf{SA}} = (gx + hu(x) + i)^4 \kappa_{ss}^{\mathbf{SA}} + \frac{3(gx + hu(x) + i)^3 (u_x(x)h + g)\kappa_s^{\mathbf{SA}}}{u_{xx}(x)^{\frac{1}{3}}}$$

If $\kappa_s^{\mathbf{SA}} = 0$ and $i \neq 0$ then the sign of $\bar{\kappa}_{\bar{s}\bar{s}}^{\mathbf{SA}}$ is the same as the sign of $\kappa_{ss}^{\mathbf{SA}}$. Note also that $\bar{\kappa}_{\bar{s}\bar{s}}^{\mathbf{SA}} = 0$ if and only if $\kappa_{ss}^{\mathbf{SA}} = 0$.

If $i = 0$ then, at a critical point of $\kappa^{\mathbf{SA}}$

$$\bar{\kappa}_{\bar{s}\bar{s}}^{\mathbf{SA}} \bar{R}^4 = \kappa_{ss}^{\mathbf{SA}} ((ax + bu(x) + c)^2 + (dx + eu(x) + f)^2)^2$$

where at least one of c of f is non-zero. Thus the sign of $\bar{\kappa}_{\bar{s}\bar{s}}^{\mathbf{SA}} \bar{R}^4$ is the same as the sign of $\kappa_{ss}^{\mathbf{SA}}$.

Therefore, for any curve $\bar{u} \in P^\infty$, $\bar{\kappa}_{\bar{s}}^{\mathbf{SA}}$ and $\bar{R}$ can be used to detect whether a point in $\bar{u}$ arises from a critical point of $\kappa^{\mathbf{SA}}$ of some **closed** curve $u \in C^\infty$. Furthermore $\bar{\kappa}_{\bar{s}\bar{s}}^{\mathbf{SA}}$ and $\bar{R}$ can be used to classify the type of critical point.

It was shown earlier that for a curve $u \in C^\infty$ if $u_{xx} \neq 0$ then at a non-degenerate critical point of $\kappa^{\mathbf{SA}}$ ($\kappa_{ss}^{\mathbf{SA}} \neq 0$), $\kappa^{\mathbf{PROJ}}$ has a singularity. It is now shown that for the degenerate case ($\kappa_{ss}^{\mathbf{SA}} = 0$), $\kappa^{\mathbf{PROJ}}$ also has a singularity.

First a special affine transformation is performed on $u = u(x)$ so that the critical point of $\kappa_s^{\mathbf{SA}}$ occurs at $x = 0$, $u(0) = 0$, $u_x(0) = 0$, $u_{xx}(0) = 1$ and $u_3(0) = 0$. The special affine transformation is given by

$$a = -\frac{1}{3}\frac{u_3 u_x - 3u_{xx}^2}{u_{xx}^{\frac{5}{3}}}, \qquad b = \frac{1}{3}\frac{u_3}{u_{xx}^{\frac{5}{3}}},$$
$$c = \frac{1}{3}\frac{x u_3 u_x - 3x u_{xx}^2 - u_3 u}{u_{xx}^{\frac{5}{3}}}, \qquad d = \frac{1}{u_{xx}^{\frac{1}{3}}},$$
$$e = -\frac{u_x}{u_{xx}^{\frac{1}{3}}}, \qquad f = \frac{x u_x - u}{u_{xx}^{\frac{1}{3}}}.$$

where each derivative is evaluated at the critical point. Note that in the above, $ad - be = 1$.

A projective transformation can now be done such that, $\bar{x} = 0$, $\bar{u}(0) = 0$, and $\bar{u}_{\bar{x}}(0) = 0$, $\bar{u}_{\bar{x}\bar{x}}(0) = 1$, $\bar{u}_{\bar{3}}(0) = 0$, $\bar{u}_{\bar{4}}(0) = 0$, $\bar{u}_{\bar{5}}(0) = 0$, $\bar{u}_{\bar{6}}(0) = 0$, $\bar{u}_{\bar{7}}(0) = \frac{u_7(0)}{a^5}$. This transformation is given by $i = 1$, $c = 0$, $f = 0$, $d = 0$, $e = a^2$, $b = ag$ and $h = \frac{1}{2}g^2 - \frac{1}{6}u_4(0)$. Since $i \neq 0$, this will have no effect on the conditions $\kappa_s^{\mathbf{SA}} = 0$, $\kappa_{ss}^{\mathbf{SA}} = 0$.

If $u_7(0) \neq 0$, then setting $a = (u_7(0))^{\frac{1}{5}}$, will yield $\bar{u}_{\bar{7}}(0) = 1$. Thus, in a

neighbourhood of $x = 0$, $u(x)$ has the form

$$u(x) = x^2 + x^7 + \phi(x)x^8, \tag{2.7}$$

where $\phi \in C^\infty$. The projective curvature of $u(x)$ is

$$\kappa^{\mathbf{PROJ}} = \frac{-175575859200 + F(x)}{x^{\frac{10}{3}}G(x)}$$

where $F(0) = 0$, and $F, G \in C^\infty$. Hence, at $x = 0$, $\kappa^{\mathbf{PROJ}}$ has a singularity.

If $u_7(0) = 0$, there must exist an n such that the nth order derivative at 0 is not equal to zero. Otherwise $u(x) = x^2$ which is a conic section (see above). Thus $u(x)$ has the form,

$$u(x) = x^2 + \phi(x)x^n, \tag{2.8}$$

where $\phi \in C^\infty$, $\phi(0) \neq 0$ and $n > 7$. The projective curvature of $u(x)$ is

$$\kappa^{\mathbf{PROJ}} = \frac{-n^2(n+1)(n-5)(n-1)^2(n-3)^2(n-4)^2 + F(x)}{x^{\frac{2n-4}{3}}G(x)},$$

where $F(0) = 0$, and $F, G \in C^\infty$. Thus $\kappa^{\mathbf{PROJ}}$ has a singularity at $x = 0$. Hence, at any point where $\kappa_s^{\mathbf{SA}} = 0$ (non-degenerate or degenerate) on a curve $u \in C^\infty$, there is a singularity in the projective curvature. If $\kappa_s^{\mathbf{SA}} \neq 0$ then there is no singularity in the projective curvature.

It has been shown above that for any $\bar{u} \in P^\infty$, $\bar{\kappa}_{\bar{s}}^{\mathbf{SA}}$ and $\bar{R}$ can be used to detect whether a point in $\bar{u}$ arises from a critical point of $\kappa^{\mathbf{SA}}$ of some **closed** curve $u \in C^\infty$. Hence, $\bar{\kappa}_{\bar{s}}^{\mathbf{SA}}$ and $\bar{R}$, completely characterise the singularities in the projective curvature. Note that for any point on a **closed curve** $u \in C^\infty$, only $\kappa^{\mathbf{SA}}$ is required to detect whether there is a singularity in the projective curvature.

The restriction of curves to P^∞ was to avoid analysing the points at ∞ of C^∞ **open** curves that do not arise from the projective transformation $i = 0$. The following is an analysis of the points at ∞ of polynomials.

Consider the polynomial

$$u(x) = \sum_{j=0}^{n} a_j x^j$$

for some $n \geq 3$ (as for $n < 3$ the projective curvature is undefined). Then

$$\kappa_s^{\mathbf{SA}} = \frac{2(n+1)(2n-1)(n-2)}{n(n-1)Ax^{n+1}} + \frac{P_{4n-11}^{(1)}(x)}{P_{4n-8}^{(2)}(x)},$$

$$R^3 = x^3(1 + a_n^2 x^{2n-2} + P^{(3)}_{2n-4}(x))^{\frac{3}{2}}$$

where $P^{(1)}_{4n-11}(x)$, $P^{(2)}_{4n-8}(x)$ and $P^{(3)}_{2n-4}(x)$ are polynomials of orders $4n-11$, $4n-8$ and $2n-4$ respectively. Thus at $x=\infty$, $\kappa_s^{\mathbf{SA}} = 0$ and $\kappa_s^{\mathbf{SA}} R^3 = \infty$. Also

$$\kappa^{\mathbf{PROJ}} = \frac{n^2 - n + 1}{(2(n-2)(2n-1)(n+1))^{\frac{2}{3}}}.$$

Thus $\kappa^{\mathbf{PROJ}}$ does not have a singularity at $x=\infty$.

Under a projective transformation on $u(x)$

$$\bar{\kappa}_{\bar{s}}^{\mathbf{SA}} = \kappa_s^{\mathbf{SA}}(gx + h\sum_{j=0}^{n} a_j x^j + i)^3$$

So if $h \neq 0$, $\bar{\kappa}_{\bar{s}}^{\mathbf{SA}} = \infty$ at $x=\infty$.

If $h=0$ then $\bar{\kappa}_{\bar{s}}^{\mathbf{SA}} = 0$ at $x=\infty$. But

$$\bar{R}^3 = \left((b^2+e^2)A^2x^{2n} + F_{2n-2}(x)\right)^{\frac{3}{2}}$$

where $F_{2n-2}(x)$ is a polynomial of order $2n-2$ and at least one of b or e must be non-zero otherwise it is not a projective transformation. Hence since $3n > n+1$, $\bar{\kappa}_{\bar{s}}^{\mathbf{SA}} \bar{R}^3 = \infty$ at $x=\infty$.

Thus for the case of curves in P^∞ and all curves which are projective transformations of polynomials, a point is a singularity of $\kappa^{\mathbf{PROJ}}$ if and only if both $\kappa_s^{\mathbf{SA}} = 0$ and $\kappa_s^{\mathbf{SA}} R^3 = 0$. Hence for this class of curves, $\kappa_s^{\mathbf{SA}}$ and R completely characterise the singularities in the projective curvature.

So in summary the above demonstrates a link between the projective curvature and lower order curvatures. Note that if $g=0$, $h=0$, $i=1$ then the projective transformation reduces to a special affine transformation (as must have $ae-bd=1$) so that the equation (2.5) becomes

$$\bar{\kappa}_{\bar{s}}^{\mathbf{SA}} = \kappa_s^{\mathbf{SA}}.$$

This reflects the fact that $\kappa_s^{\mathbf{SA}}$ is invariant under a special affine transformation.

Note in the case of two closed curves related by a projective transformation then $gx + hu(x) + i \neq 0$ everywhere (since $i \neq 0$ in this case). Thus the inflection points can be detected using $\kappa^{\mathbf{E}}$ only and singularities in $\kappa^{\mathbf{PROJ}}$ can be detected using $\kappa^{\mathbf{SA}}$ only. Also the two closed curves will have the same number of inflection points and special affine curvature critical points as well as the same type of critical point.

2.1.2 Locating and identifying invariant points between two curves

In practice a curve is given as a discrete number of points. Thus a discrete approximation is required for the Euclidean and special affine curvatures so that the invariant points discussed above can be calculated. Note that an inflection point $u_{xx} = 0$ is a turning point of the derivative curve, $u_x = u_x(x)$, so that the calculation of inflection points involves the first order derivative.

Given three points, $(x_1, u_1), (x_2, u_2), (x_3, u_3)$ on a curve $u = u(x)$, the Euclidean curvature of the circle passing through these three points approximates the Euclidean curvature of the middle point. The curvature of this circle is given by

$$\tilde{\kappa}^{\mathbf{E}} = \frac{4A_{123}}{abc}$$

where A_{123} is the area of the triangle determined by the three points and is given by

$$A_{123} = \frac{1}{2}\det\begin{pmatrix} x_1 & u_1 & 1 \\ x_2 & u_2 & 1 \\ x_3 & u_3 & 1 \end{pmatrix}$$

and

$$\begin{aligned} a &= \sqrt{(x_2 - x_1)^2 + (u_2 - u_1)^2} \\ b &= \sqrt{(x_3 - x_2)^2 + (u_3 - u_2)^2} \\ c &= \sqrt{(x_3 - x_1)^2 + (u_3 - u_1)^2} \end{aligned}$$

The error in this approximation can be found in the following way (see [1]).

Do a Euclidean transformation (which will not affect $\tilde{\kappa}^{\mathbf{E}}$) on the three points such that $(x_1, u_1) = (-h, u(-h))$, $(x_2, u_2) = (0, 0)$, $(x_3, u_3) = (k, u(k))$, where $h > 0$, $k > 0$ and $u_x(0) = 0$ so that the values of the Euclidean curvature and its arclength derivatives at $x = 0$ are $\kappa(0) = u_{xx}$, $\kappa_s(0) = u_{xxx}$, $\kappa_{ss}(0) = u_{xxxx} - 3u_{xx}^3$. Then taking a Taylor series gives

$$\begin{aligned} u(-h) &= \frac{1}{2}u_2h^2 - \frac{1}{6}u_3h^3 + \frac{1}{24}u_4h^4 - \cdots \\ u(k) &= \frac{1}{2}u_2k^2 + \frac{1}{6}u_3k^3 + \frac{1}{24}u_4k^4 + \cdots \\ a &= h\sqrt{1 + h^2(\frac{1}{2}u_2 - \frac{1}{6}u_3h + \frac{1}{24}u_4h^2 - \cdots)^2} \\ b &= k\sqrt{1 + k^2(\frac{1}{2}u_2 + \frac{1}{6}u_3k + \frac{1}{24}u_4k^2 + \cdots)^2} \end{aligned}$$

$$c = (h+k)\sqrt{1 + \frac{1}{4}u_2^2(k-h)^2 + \frac{1}{6}u_3u_2(k-h)(h^2-kh+k^2) + \cdots}$$

Inverting the Taylor series of a and b gives

$$h = a + o(a^3)$$
$$k = b + o(b^3)$$

Then substituting $h = a$ and $k = b$ into the Taylor series for $\tilde{\kappa}^{\mathbf{E}}$ gives

$$\tilde{\kappa}^{\mathbf{E}} = \kappa^{\mathbf{E}} + \frac{1}{3}(b-a)\kappa_s^{\mathbf{E}} + \frac{1}{12}(b^2-ab+a^2)\kappa_{ss}^{\mathbf{E}} + \text{higher order terms}$$

where s is the Euclidean arclength, and $\kappa^{\mathbf{E}}$ (the true curvature), $\kappa_s^{\mathbf{E}}$ and $\kappa_{ss}^{\mathbf{E}}$ are evaluated at the middle point. Hence, as long as the points are sufficiently close, the two points where $\tilde{\kappa}^{\mathbf{E}}$ changes sign will be a good approximation to the points where the **true** curvature $\kappa^{\mathbf{E}}$ changes sign. Note that only the sign of A_{123} is required to locate these two points. The point that is chosen out of these two which will serve as the approximation to the inflection point is essentially arbitrary. In practice for consistency, the point chosen is the point which has A_{123} the closest to zero.

For the special affine curvature case, given five points on a curve $u = u(x)$, the special affine curvature of the unique conic section passing through those five points, approximates the special affine curvature of the middle point. The curvature of this conic section (see [1]) is given by

$$\tilde{\kappa}^{\mathbf{SA}} = \frac{S}{T^{\frac{2}{3}}} \tag{2.9}$$

where,

$$\begin{aligned} S &= \frac{1}{4}[124]^2[135]^2([235]-[234])^2 + \frac{1}{4}[123]^2[145]^2([245]+[234])^2 \\ &\quad - \frac{1}{2}[123][145][124][135]([234][345]+[235][245]) \\ T &= \frac{1}{4}[123][124][125][134][135][145][234][235][245][345] \\ [ijk] &= \det\begin{pmatrix} x_i & u_i & 1 \\ x_j & u_j & 1 \\ x_k & u_k & 1 \end{pmatrix}. \end{aligned}$$

Again a Taylor series can be computed to show the error in this approximation (see [1] for derivation). Given five points $P_{i-2}, P_{i-1}, P_i, P_{i+1}, P_{i+2}$

the result is

$$\tilde{\kappa}^{\mathbf{SA}} = \kappa^{\mathbf{SA}} + \frac{1}{5}\left(\sum_{j=i-2}^{i+2} L_j\right)\kappa_s^{\mathbf{SA}} + \text{higher order terms}$$

where

$$L_j = \int_{P_j}^{P_i} \mathrm{d}s_{\mathbf{SA}}, \quad j = i-2, ..., i+2$$

denotes the special affine arc length of the conic section from P_i to P_j (assumed to be small); in particular $L_i = 0$.

Now the following shows that tangency is preserved under a projective transformation so that other invariant points called bi-tangents can be found (see [7]).

Consider a point (x_1, u_1) on a curve C with derivative $u_x^{(1)}$. The equation of the line tangent to C at (x_1, u_1) is given by,

$$u = u_1 + u_x^{(1)}(x - x_1) \tag{2.10}$$

Under a projective transformation the derivative u_x transforms by

$$u_x \longmapsto \bar{u}_{\bar{x}} = \frac{dhu + di + eu_x gx + eu_x i - dxhu_x - eug - fg - fhu_x}{ahu + ai + bu_x gx + bu_x i - axhu_x - bug - cg - chu_x}$$

The line (2.10) transforms to the line

$$\bar{u} = \bar{u}_{\bar{x}}\bar{x} + \bar{\alpha} \tag{2.11}$$

where

$$\bar{\alpha} = \frac{-dc + af - dbu_1 - cu_x^{(1)} + u_1 a + bu_x^{(1)} f + dbu_x^{(1)} x_1 - u_x^{(1)} x_1 a}{ai + ibu_x^{(1)} + hu_1 a - hu_x^{(1)} x_1 a - cg - chu_x^{(1)} - bu_1 g + bu_x^{(1)} x_1 g} \tag{2.12}$$

Hence the derivative of the line (2.11) coincides with the derivative of the transformed curve $\bar{C}$ at $(\bar{x}_1, \bar{u}_1)$. Thus tangency is preserved under a projective transformation.

Now consider the curve in figure 2.1. The two points marked are called bi-tangents. These points are the unique points in the concavity which have the same tangent line. Since tangency is preserved, this property is projectively invariant and can be used to locate these points in any projective transform of the curve. Thus bi-tangents also provide invariant points.

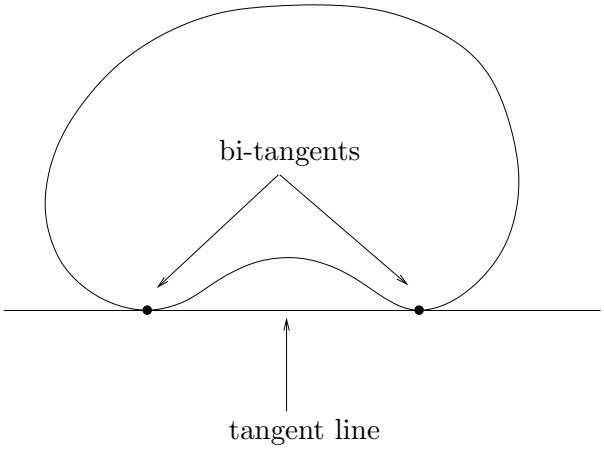

Figure 2.1: Concave curve showing two bi-tangents.

The invariant points in each curve can be identified by using the projective joint-invariants. The projective joint-invariants depend on five points $\{(x_1, u_1), (x_2, u_2), (x_3, u_3), (x_4, u_4), (x_5, u_5)\}$ and are given by

$$J_1 = \frac{[134][125]}{[135][124]} \tag{2.13}$$

$$J_2 = \frac{[123][245]}{[125][234]}. \tag{2.14}$$

If five points are identified correctly in each object they will have the same joint-invariants.

Consider two sets of five points $\{(x_1, u_1), (x_2, u_2), (x_3, u_3), (x_4, u_4), (x_5, u_5)\}$ and $\{(\bar{x}_1, \bar{u}_1), (\bar{x}_2, \bar{u}_2), (\bar{x}_3, \bar{u}_3), (\bar{x}_4, \bar{u}_4), (\bar{x}_5, \bar{u}_5)\}$ where

$$\bar{J}_1 = J_1, \quad \bar{J}_2 = J_2 \tag{2.15}$$

and

$$(\bar{x}_j, \bar{u}_j) = g_{\text{proj}} \cdot (x_j, u_j) = \left(\frac{ax_j + bu_j + c}{gx_j + hu_j + i}, \frac{dx_j + eu_j + f}{gx_j + hu_j + i} \right), \tag{2.16}$$

where $j = 1, \ldots, 4$. Substituting (2.16) into (2.15) gives two equations in the two unknowns $\bar{x}_5$ and $\bar{u}_5$. Using **MAPLE** these can be solved uniquely to yield

$$(\bar{x}_5, \bar{u}_5) = g_{\text{proj}} \cdot (x_5, u_5).$$

The following shows the **MAPLE** code.

```
> inv:=proc(x,u,i,j,k)
> linalg[det]([[x.i,u.i,1],[x.j,u.j,1],[x.k,u.k,1]]) end;
```

$$inv := \mathbf{proc}(x,\ u,\ i,\ j,\ k)\ linalg_{det}([[x.i,\ u.i,\ 1],\ [x.j,\ u.j,\ 1],\ [x.k,\ u.k,\ 1]])\ \mathbf{end}$$

```
> J1:=inv(x,u,1,3,4)*inv(x,u,1,2,5)/inv(x,u,1,3,5)/inv(x,u,
> 1,2,4);
```

$$J1 := ((x1\ u3 - x1\ u4 - x3\ u1 + x3\ u4 + x4\ u1 - x4\ u3)$$
$$(x1\ u2 - x1\ u5 - x2\ u1 + x2\ u5 + x5\ u1 - x5\ u2))/($$
$$(x1\ u3 - x1\ u5 - x3\ u1 + x3\ u5 + x5\ u1 - x5\ u3)$$
$$(x1\ u2 - x1\ u4 - x2\ u1 + x2\ u4 + x4\ u1 - x4\ u2))$$

```
> for k from 1 to 4 do
> xb.k:=(a*x.k+b*u.k+c)/(g*x.k+h*u.k+i);
> ub.k:=(d*x.k+e*u.k+f)/(g*x.k+h*u.k+i) od;
```

$$xb1 := \frac{a\,x1 + b\,u1 + c}{g\,x1 + h\,u1 + i}$$

$$ub1 := \frac{d\,x1 + e\,u1 + f}{g\,x1 + h\,u1 + i}$$

$$xb2 := \frac{a\,x2 + b\,u2 + c}{g\,x2 + h\,u2 + i}$$

$$ub2 := \frac{d\,x2 + e\,u2 + f}{g\,x2 + h\,u2 + i}$$

$$xb3 := \frac{a\,x3 + b\,u3 + c}{g\,x3 + h\,u3 + i}$$

$$ub3 := \frac{d\,x3 + e\,u3 + f}{g\,x3 + h\,u3 + i}$$

$$xb4 := \frac{a\,x4 + b\,u4 + c}{g\,x4 + h\,u4 + i}$$

$$ub4 := \frac{d\,x4 + e\,u4 + f}{g\,x4 + h\,u4 + i}$$

```
> J1b:=inv(xb,ub,1,3,4)*inv(xb,ub,1,2,5)/inv(xb,ub,1,3,5)
> /inv(xb,ub,1,2,4):
> J2:=inv(x,u,1,2,3)*inv(x,u,2,4,5)/inv(x,u,1,2,5)/inv(x,u,
> 2,3,4);
```

$$J2 := ((x1\ u2 - x1\ u3 - x2\ u1 + x2\ u3 + x3\ u1 - x3\ u2)$$
$$(x2\ u4 - x2\ u5 - x4\ u2 + x4\ u5 + x5\ u2 - x5\ u4))/($$
$$(x1\ u2 - x1\ u5 - x2\ u1 + x2\ u5 + x5\ u1 - x5\ u2)$$
$$(x2\ u3 - x2\ u4 - x3\ u2 + x3\ u4 + x4\ u2 - x4\ u3))$$

```
> J2b:=inv(xb,ub,1,2,3)*inv(xb,ub,2,4,5)/inv(xb,ub,1,2,5)
> /inv(xb,ub,2,3,4):
> #the following are polynomial equations:
> eq1:=numer(normal(J1-J1b)):
```

```
> eq2:=numer(normal(J2-J2b)):
> solve({eq1,eq2},{xb5,ub5});
```

$$\{ub5 = \frac{f + d\,x5 + u5\,e}{i + h\,u5 + x5\,g},\ xb5 = \frac{x5\,a + u5\,b + c}{i + h\,u5 + x5\,g}\}$$

That is, the fifth points are related by the same projective transformation as the first four points. Similarly, if there is a sixth point (x_6, u_6) and $(\bar{x}_6, \bar{u}_6)$, where (2.15) holds for the pair of five points (x_j, u_j) $j = 2, \ldots, 6$ and $(\bar{x}_j, \bar{u}_j)$ $j = 2, \ldots, 6$, then $(\bar{x}_6, \bar{u}_6) = g_{\text{proj}} \cdot (x_6, u_6)$. Continuing this process shows that if (2.15) is satisfied for all the consecutive groups of five points in a group of n points then the set of n points in each curve must be related by a projective transformation.

2.2 Smoothing and curve matching using links between groups

In section 2.1, a method for approximating the projectively invariant inflection points and special affine curvature turning points is given. This involves a discrete approximation to the Euclidean and special affine curvatures respectively.

The inflection points and special affine curvature turning points can be used to match the curves in the following way.

If two curves C and $\overline{C}$ are related by a projective transformation and four points are correctly identified in each curve, then the projective transformation that relate the curves can be found. Let $\{(x_1,u_1),(x_2,u_2),(x_3,u_3),(x_4,u_4)\}$ be four of these points in C and $\{(\bar{x}_1,\bar{u}_1),(\bar{x}_2,\bar{u}_2),(\bar{x}_3,\bar{u}_3),(\bar{x}_4,\bar{u}_4)\}$ be the corresponding four points in $\overline{C}$. Then the projective transformation mapping C to $\overline{C}$ is given by the solution to the following set of equations,

$$\begin{aligned}
\text{eq1} &= (ax_1+bu_1+c)-\overline{x}_1(gx_1+hu_1+i) = 0\\
\text{eq2} &= (dx_1+eu_1+f)-\overline{u}_1(gx_1+hu_1+i) = 0\\
\text{eq3} &= (ax_2+bu_2+c)-\overline{x}_2(gx_2+hu_2+i) = 0\\
\text{eq4} &= (dx_2+eu_2+f)-\overline{u}_2(gx_2+hu_2+i) = 0\\
\text{eq5} &= (ax_3+bu_3+c)-\overline{x}_3(gx_3+hu_3+i) = 0\\
\text{eq6} &= (dx_3+eu_3+f)-\overline{u}_3(gx_3+hu_3+i) = 0\\
\text{eq7} &= (ax_4+bu_4+c)-\overline{x}_4(gx_4+hu_4+i) = 0\\
\text{eq8} &= (dx_4+eu_4+f)-\overline{u}_4(gx_4+hu_4+i) = 0
\end{aligned}$$

After a large computation in **MAPLE**, the solution to the above equations is

$$\begin{aligned}
a = {} & \overline{x}_1\overline{x}_2Y_{34}\overline{Y}_{34}[123][124]-\overline{x}_1\overline{x}_3Y_{24}\overline{Y}_{24}[123][134]+\overline{x}_2\overline{x}_3\overline{Y}_{14}Y_{14}[123][234]\\
& +\overline{x}_1\overline{x}_4Y_{23}\overline{Y}_{23}[124][134]-\overline{x}_2\overline{x}_4\overline{Y}_{13}Y_{13}[124][234]+\overline{x}_4\overline{x}_3\overline{Y}_{12}Y_{12}[134][234]
\end{aligned}$$

$$\begin{aligned}
b = {} & -\overline{x}_1\overline{x}_2\overline{Y}_{34}X_{34}[123][124]+\overline{x}_1\overline{x}_3\overline{Y}_{24}X_{24}[123][134]-\overline{x}_2\overline{x}_3\overline{Y}_{14}X_{14}[123][234]\\
& -\overline{x}_1\overline{x}_4\overline{Y}_{23}X_{23}[124][134]+\overline{x}_4\overline{x}_2\overline{Y}_{13}X_{13}[124][234]-\overline{x}_4\overline{x}_3X_{12}\overline{Y}_{12}[134][234]
\end{aligned}$$

$$\begin{aligned}
c = {} & \overline{x}_1\overline{x}_2\overline{Y}_{34}D_{34}[123][124]-\overline{x}_1\overline{x}_3\overline{Y}_{24}D_{24}[123][134]+\overline{x}_2\overline{x}_3\overline{Y}_{14}D_{14}[123][234]\\
& +\overline{x}_1\overline{x}_4\overline{Y}_{23}D_{23}[124][134]-\overline{x}_2\overline{x}_4\overline{Y}_{13}D_{13}[124][234]+\overline{x}_4\overline{x}_3\overline{Y}_{12}D_{12}[134][234]
\end{aligned}$$

$$\begin{aligned}
d = {} & -\overline{u}_2\overline{u}_1\overline{X}_{34}Y_{34}[123][124]+\overline{u}_3\overline{u}_1\overline{X}_{24}Y_{24}[123][134]-\overline{u}_3\overline{u}_2\overline{X}_{14}Y_{14}[123][234]\\
& -\overline{u}_4\overline{u}_1\overline{X}_{23}Y_{23}[124][134]+\overline{u}_4\overline{u}_2\overline{X}_{13}Y_{13}[124][234]-\overline{u}_4\overline{u}_3\overline{X}_{12}Y_{12}[134][234]
\end{aligned}$$

$$
\begin{aligned}
e = {} & \overline{u}_2\overline{u}_1\overline{X}_{34}X_{34}[123][124] - \overline{u}_3\overline{u}_1\overline{X}_{24}X_{24}[123][134] + \overline{u}_2\overline{u}_3\overline{X}_{14}X_{14}[123][234] \\
& + \overline{u}_4\overline{u}_1\overline{X}_{23}X_{23}[124][134] - \overline{u}_4\overline{u}_2\overline{X}_{13}X_{13}[124][234] + \overline{u}_4\overline{u}_3X_{12}\overline{X}_{12}[134][234]
\end{aligned}
$$

$$
\begin{aligned}
f = {} & -\overline{u}_2\overline{u}_1\overline{X}_{34}D_{34}[123][124] + \overline{u}_3\overline{u}_2\overline{X}_{24}D_{24}[123][134] - \overline{u}_2\overline{u}_3\overline{X}_{14}D_{14}[123][234] \\
& - \overline{u}_4\overline{u}_1\overline{X}_{23}D_{23}[124][134] + \overline{u}_4\overline{u}_2\overline{X}_{13}D_{13}[124][234] - \overline{u}_4\overline{u}_3\overline{X}_{12}D_{12}[134][234]
\end{aligned}
$$

$$
\begin{aligned}
g = {} & Y_{34}\overline{D}_{34}[123][124] - Y_{24}\overline{D}_{24}[123][134] + \overline{D}_{14}Y_{14}[123][234] \\
& + Y_{23}\overline{D}_{23}[124][134] - \overline{D}_{13}Y_{13}[124][234] + \overline{D}_{12}Y_{12}[134][234]
\end{aligned}
$$

$$
\begin{aligned}
h = {} & -\overline{D}_{34}X_{34}[123][124] + \overline{D}_{24}X_{24}[123][134] - \overline{D}_{14}X_{14}[123][234] \\
& - \overline{D}_{23}X_{23}[124][134] + \overline{D}_{13}X_{13}[124][234] - X_{12}\overline{D}_{12}[134][234]
\end{aligned}
$$

$$
\begin{aligned}
i = {} & \overline{D}_{34}D_{34}[123][124] - \overline{D}_{24}D_{24}[123][134] + \overline{D}_{14}D_{14}[123][234] \\
& + \overline{D}_{23}D_{23}[124][134] - \overline{D}_{13}D_{13}[124][234] + \overline{D}_{12}D_{12}[134][234]
\end{aligned} \tag{2.17}
$$

where

$$
D_{ij} = \det\begin{pmatrix} x_i & u_i \\ x_j & u_j \end{pmatrix}, \quad \overline{D}_{ij} = \det\begin{pmatrix} \overline{x}_i & \overline{u}_i \\ \overline{x}_j & \overline{u}_j \end{pmatrix},
$$

$$
X_{ij} = \det\begin{pmatrix} x_i & 1 \\ x_j & 1 \end{pmatrix}, \quad \overline{X}_{ij} = \det\begin{pmatrix} \overline{x}_i & 1 \\ \overline{x}_j & 1 \end{pmatrix},
$$

$$
Y_{ij} = \det\begin{pmatrix} u_i & 1 \\ u_j & 1 \end{pmatrix}, \quad \overline{Y}_{ij} = \det\begin{pmatrix} \overline{u}_i & 1 \\ \overline{u}_j & 1 \end{pmatrix}.
$$

Note that more than four points in each curve can be used to match the curves by solving the resulting overdetermined system of linear equations by least squares.

Now the Euclidean and special affine curvatures depend on second and fourth order derivatives respectively, so are sensitive to noise. This noise can be smoothed out by the following averaging process.

Replace each point on curve by the average of itself and one point on each side (this number is essentially arbitrary) and repeat until the noise is smoothed out.

Under smoothing, inflection points (points where $u_{xx} = 0$) do not remain inflection points as over time they are smoothed out. But given a graph $u = u(x)$, if $u_{xx} = 0$ then this corresponds to a turning point of the graph of the derivative of $u(x)$, $u_x = u_x(x)$. Thus these points can be calculated

using first order derivatives so only a small number of smoothings will be required to locate them. Even so, as is shown in the section 2.2.1, an error can still develop when using the inflection points of the smoothed curve to locate the inflection points of the original (noisy) curve. This is also the case in the calculation of the special affine curvature turning points which is shown in section 2.2.2.

2.2.1 Moving of inflection points

Given six points $P_1, P_2, P_3, P_4, P_5, P_6$, define

$$\bar{P}_2 = \frac{P_1 + P_2 + P_3}{3},$$
$$\bar{P}_3 = \frac{P_2 + P_3 + P_4}{3},$$
$$\bar{P}_4 = \frac{P_3 + P_4 + P_5}{3},$$
$$\bar{P}_5 = \frac{P_4 + P_5 + P_6}{3},$$

The area of the triangle area determined by $\bar{P}_2, \bar{P}_3, \bar{P}_4$ is

$$\bar{A}_{234} = \frac{1}{9}\,(A_{124} + A_{145}).$$

Suppose that for the above six points that $A_{123} > 0, A_{234} < 0, A_{345} < 0, A_{456} < 0$ and also $A_{235} < 0, A_{256} < 0$. That is the two points between which the discrete curvature changes sign are P_2 and P_3. If $A_{124} + A_{145} > 0$ then $\bar{A}_{234} > 0$ and also $\bar{A}_{345} = \frac{1}{9}\,(A_{235} + A_{256}) < 0$. So the two points between which the discrete curvature changes sign on the **smoothed curve** after one smoothing is now $\bar{P}_3$ and $\bar{P}_4$. Figure 2.2 shows an example of this.

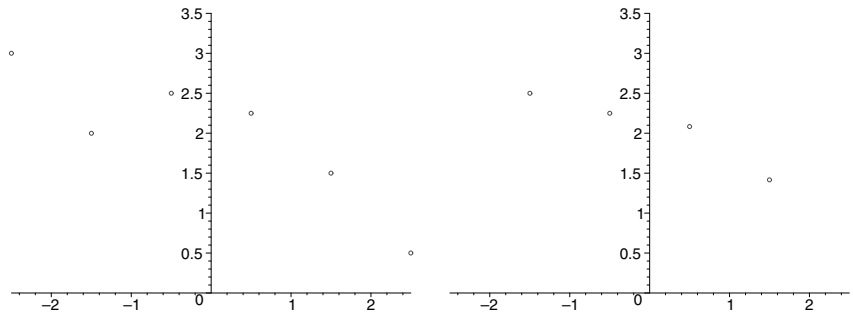

Figure 2.2: Graphs showing the six points $P_1, P_2, P_3, P_4, P_5, P_6$ with triangle areas $A_{123} = 1.5, A_{234} = -0.75, A_{345} = -0.5, A_{456} = -0.25$, $A_{124} + A_{145} = 0.75$, $A_{235} + A_{256} = -4.5$ and the four smoothed points $\bar{P}_2, \bar{P}_3, \bar{P}_4, \bar{P}_5$ with triangle areas $\bar{A}_{234} = 0.04, \bar{A}_{345} = -0.25$ (all values are to two decimal places)

The point chosen to approximate the inflection point on this **smoothed** curve is the point which has triangle area closest to zero. Suppose $\bar{P}_4$ is this point. Since it is the inflection point on **original** (noisy) curve that is required, the corresponding point P_4 is used as the approximation. Further smoothings may move the approximation to inflection point on original curve further but inflection points only depend on first order derivatives and so the noise is smoothed out quickly. Thus the inflection points will not move significantly after the first few smoothings. The error however, will still have an effect on the matching of curves, (see section 2.2.3).

The first graph in figure 2.3 shows a concavity of a discretised curve (points equally spaced) with the true inflection points denoted by a box. The two points corresponding to where the **discrete** curvature changes sign for each inflection point are denoted by a circle. Notice that the second (true) inflection point lies just outside the two circled points. This curve is smoothed five times and the points where the discrete curvature changes sign on **smoothed** curve are located. The second graph in figure 2.3 shows the corresponding points on the **original** curve, which have moved slightly away from the true inflection points.

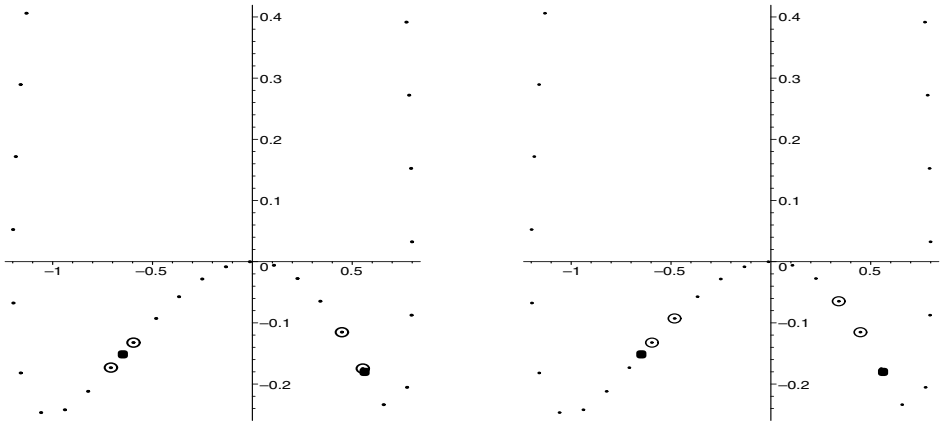

Figure 2.3: Approximations to true inflection points on discretised curve without smoothing and with smoothing.

In general, there can be no guarantee that the approximated inflection points in one curve match up precisely with the approximated inflection points in the transformed curve. However this is the case for two equally spaced curves (in Euclidean distance from a common point) C and $\overline{C}$ related either by a Euclidean transformation, $(x, u) \longmapsto (x\cos\theta + u\sin\theta, -x\sin\theta + u\cos\theta)$, or a similarity transformation, $(x, u) \longmapsto (\alpha x + a, \alpha u + b)$, $\alpha > 0$.

Let g be a Euclidean or similarity transformation which maps C to $\overline{C}$.

Euclidean distance is invariant under the Euclidean group and is scaled by a constant factor under the similarity group. Define $C = \{P_i\}$ where P_i are all equally spaced in Euclidean distance. Also define $\overline{C} = \{\bar{P}_i\}$ where

$$\bar{P}_i = g \cdot P_i. \tag{2.18}$$

Then $\bar{P}_i$ are also equally spaced in Euclidean distance.

Assume that an inflection point I_{true} in C has been identified correctly with an inflection point $\overline{I}_{\text{true}}$ in $\overline{C}$. Let $I^s = \frac{P_0+P_1+P_2}{3}$, be the discrete approximation to the inflection point in the **smoothed** curve of C so that P_1 will be the approximation to I_{true}. (I^s is chosen so that the absolute value of its associated triangle area is locally the closest to zero). Let

$$\overline{I}^s = g \cdot I^s = \frac{g \cdot P_0 + g \cdot P_1 + g \cdot P_2}{3} \tag{2.19}$$

since g is a linear transformation. Also, by (2.18), $\overline{I}^s = \frac{\bar{P}_0+\bar{P}_1+\bar{P}_2}{3}$.

Under the Euclidean group, the triangle areas are preserved and, under the similarity group, they are all scaled by a constant factor. So that $\overline{I}^s$ will have the same sign as I^s and its associated triangle area will be locally the closest to zero. Therefore, $\overline{I}^s$ will be the discrete approximation to the inflection point in the **smoothed** curve of $\overline{C}$ so that $\bar{P}_1 = g \cdot P_1$ will be the approximation to $\overline{I}_{\text{true}}$. This shows that the approximated inflection points of C match up **precisely** with those in $\overline{C}$ under this discretisation.

But if g was **not** a Euclidean transformation or similarity transformation, but was an affine transformation or projective transformation, equally spaced points are NOT preserved under g. Furthermore, if g was a projective transformation then (2.19) does not hold. So in general the approximated inflection points of C and $\overline{C}$ will not match up precisely.

Note that this construction also holds for special affine curvature turning points.

2.2.2 Moving of special affine curvature turning points

The mechanism behind how the special affine curvature turning points move under smoothing though is much more complicated to analyse as fourth order derivatives are involved. As yet an effective way of analysing this has not been found. Though the following example shows the behaviour.

Consider the convex curve $C = \{(X(t), U(t))\}$ where

$$X(t) = \cos t + \frac{1}{5}\cos^2 t$$
$$U(t) = \frac{1}{2}X(t) + \sin t + \frac{1}{10}\sin^2 t$$

This is equally spaced in Euclidean distance with 60 points, see figure 2.4, and the curve is then smoothed 10 times using five points each side of the middle point in the averaging process.

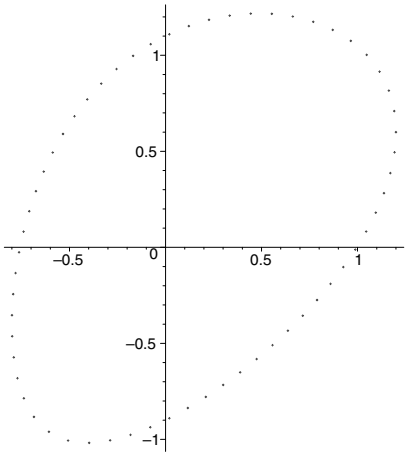

Figure 2.4: Discretised curve with 60 equally spaced points.

Using the discrete approximation $\tilde{\kappa}^{\mathbf{SA}}$ (given by (2.9)) to the special affine curvature of the curve C, the turning points are located and their position is compared with the positions of the turning points found from the smoothed curve. Figure 2.5 shows that some of the turning points have moved away from there initial position. Here $\tilde{\kappa}^{\mathbf{SA}}$is plotted against the parameter t and the points which correspond to the turning points of the original curve are denoted by a circle.

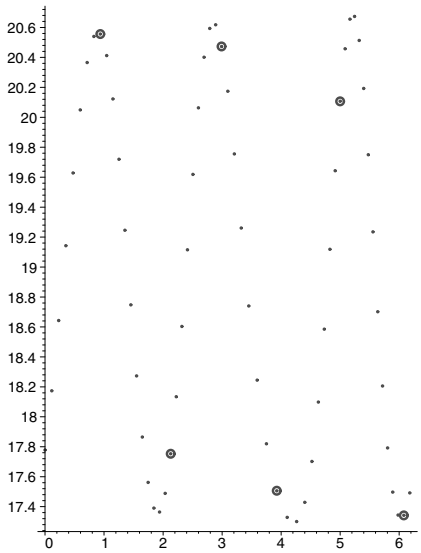

Figure 2.5: Comparing the positions of special affine curvature turning points of original curve with smoothed curve.

2.2.3 Matching curves

In general, there is never a precise matching of the objects because smoothing changes the positions of the invariant points. A method is now described for reducing some of this error which works well on the first example of a convex curve. However when it is applied to the second example of a concave curve, it gives no further improvement to the initial matching. But it led to an overshooting undershooting method which is described in the next section. This method works for both the convex curve and two examples of concave curves.

Consider two curves, related by a projective transformation very close to the identity which are sampled at equally spaced (in Euclidean arclength) points from a common point. Suppose each sampling has the same number of points and that the curves are both smoothed using this averaging process. Then their smoothed curves will remain close as well. Consider two curves C and $\overline{C}$ related by a projective transformation. Using the approximated inflection points and/or special affine curvature turning points, map $\overline{C}$ on to a curve $\hat{C}$. The two curves C and $\hat{C}$ represent the initial matching. It is assumed that $\hat{C}$ will be more closely matched to C than $\overline{C}$ so that if $\hat{C}$ is equally spaced in Euclidean distance and smoothed again the inflection points and/or special affine curvature turning points should move less relative to the corresponding points in C. Thus the next mapping will be closer.

If C and $\overline{C}$ are related by a Euclidean transformation or a similarity transformation and they are each equally spaced from a common point then the amount the invariant points move relative to each other will be exactly the same. In practice though, they will not be equally spaced from precisely a common point. But the error in the matching of the discretisations (due to not starting at precisely the same common point) will be within at least half the distance between the points. If two discretisations of $\overline{C}$ are used where their starting points differ by half the distance between the points then one of these discretisation's will have an error within at least one quarter of the distance between the points. (This error can be further reduced by using more discretisations all more points). So if both of these discretisations are used to match the curves, one of them will have a starting point which coincides very closely to the starting point of the discretisation of C. Thus the difference in the amount the invariant points move in each curve relative to each other will be small.

So the method is to first equally space C and $\overline{C}$, then map $\overline{C}$ to $\hat{C}$, equally space $\hat{C}$ and repeat the procedure. Note that equal spacing is used

as it is the simplest spacing that can be placed consistently on the curves.

Example 1

Consider the curve

$$X = \cos t + \frac{1}{5}\cos^2 t$$
$$Y = \frac{1}{2}X + \sin t + \frac{1}{10}\sin^2 t$$

Take a projective transformation of this curve, discretise both curves using 60 points, add random noise to both, then equally space each curve approximately in Euclidean arclength. This is done by joining every two points by a straight line, and summing up all the distances between points to get the approximate arclength of each curve, then dividing by 60 to get the required distance d between points. Then 60 points are placed on curve such that the distance between every two points is d, see figure 2.6.

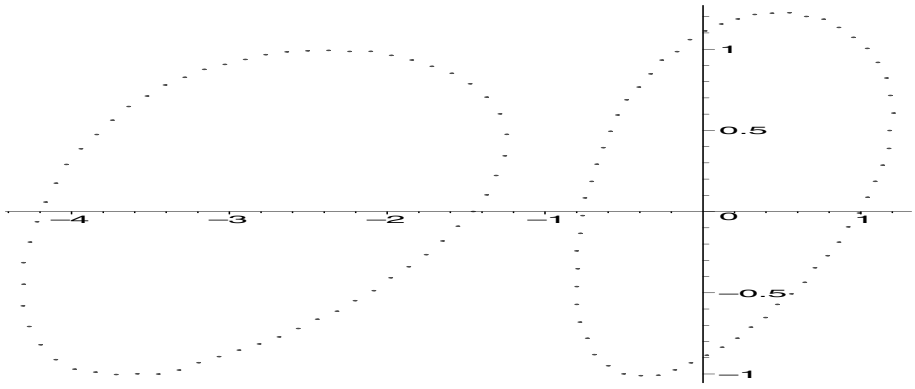

Figure 2.6: Two convex curves related by a projective transformation

Each curve is smoothed a number of times (until the noise is smoothed out, which is determined by when the number of turning points stays constant after further smoothings), and the discrete special affine curvature is computed for both curves. Both curves have six special affine curvature turning points, which are located on each curve. For each of the six possible combinations of five consecutive points in each curve, the joint-invariants are computed. The following table shows the six joint-invariants in each curve plus the corresponding combination of five points. For example [12345] refers to the joint-invariants involving the consecutive points (x_i, u_i), $i = 1, \ldots, 5$ in the first curve ($[\bar{1}\bar{2}\bar{3}\bar{4}\bar{5}]$ refers to the consecutive points $(\bar{x}_i, \bar{u}_i)$, $i = 1, \ldots, 5$ in second curve). The initial ordering of the points chosen in the second curve is such that the types of special affine curvature turning points coin-

cide with the same type in the ordering of the first curve. Note that they still do not match up.

Table of joint-invariants

Combination	$[J_1, J_2]$	Combination	$[\bar{J}_1, \bar{J}_2]$
$[12345]$	$[0.7313, 1.0025]$	$[\bar{1}\bar{2}\bar{3}\bar{4}\bar{5}]$	$[0.5618, 2.9282]$
$[23456]$	$[0.7050, 0.5765]$	$[\bar{2}\bar{3}\bar{4}\bar{5}\bar{6}]$	$[0.8483, 0.3188]$
$[34561]$	$[0.5355, 2.6568]$	$[\bar{3}\bar{4}\bar{5}\bar{6}\bar{1}]$	$[0.5334, 1.5098]$
$[45612]$	$[0.8075, 0.4835]$	$[\bar{4}\bar{5}\bar{6}\bar{1}\bar{2}]$	$[0.6730, 1.2167]$
$[56123]$	$[0.6382, 0.9766]$	$[\bar{5}\bar{6}\bar{1}\bar{2}\bar{3}]$	$[0.7348, 0.7575]$
$[61234]$	$[0.5918, 1.3794]$	$[\bar{6}\bar{1}\bar{2}\bar{3}\bar{4}]$	$[0.6430, 0.7700]$

The sequence of six points in the second curve which has the best matching of joint-invariants with the sequence of six points in first curve is found (because of noise and the fact that the parametrisations in each curve do not match up, the joint-invariants will not be exactly the same). This is done by first computing the square root of the sum of the distances squared between each joint-invariant pair in the above table. This corresponds to the sequence $[\bar{1}\bar{2}\bar{3}\bar{4}\bar{5}], \ldots, [\bar{6}\bar{1}\bar{2}\bar{3}\bar{4}]$ in the second curve. Then repeating this for the sequences $[\bar{3}\bar{4}\bar{5}\bar{6}\bar{1}], [\bar{4}\bar{5}\bar{6}\bar{1}\bar{2}], \ldots, [\bar{2}\bar{3}\bar{4}\bar{5}\bar{6}]$ and $[\bar{5}\bar{6}\bar{1}\bar{2}\bar{3}], [\bar{6}\bar{1}\bar{2}\bar{3}\bar{4}], \ldots, [\bar{4}\bar{5}\bar{6}\bar{1}\bar{2}]$ (these are the sequences which have the type of special affine curvature turning points coinciding between the curves). The result is 2.4752, 3.0772 and 0.7300 respectively. Thus the sequence $[\bar{5}\bar{6}\bar{1}\bar{2}\bar{3}], [\bar{6}\bar{1}\bar{2}\bar{3}\bar{4}], \ldots, [\bar{4}\bar{5}\bar{6}\bar{1}\bar{2}]$ in the second curve has the best matching with the sequence $[12345], \ldots, [61234]$ in the first curve.

Now since there are six points, the mapping back equations are solved by least squares and $\bar{C}$ is mapped back onto C. Call the resulting curve $\hat{C}$. Figure 2.7 shows the initial mapping is quite close but their is still error present.

The procedure is repeated on $\hat{C}$. That is, $\hat{C}$ is discretised by equally spacing and smoothing the same number of times as the previous curves. The six points are relocated then $\hat{C}$ is mapped onto C. Figure 2.8 shows that most of the initial error has been corrected.

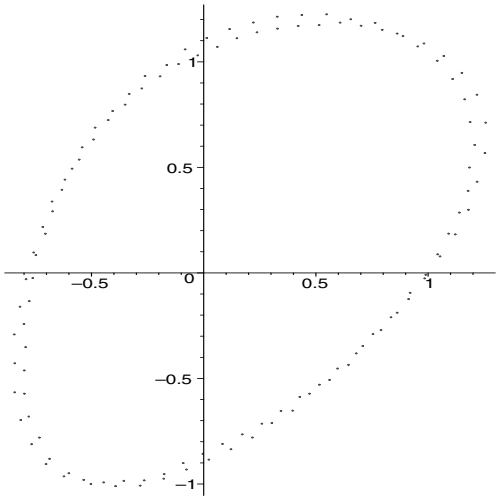

Figure 2.7: Initial mapping

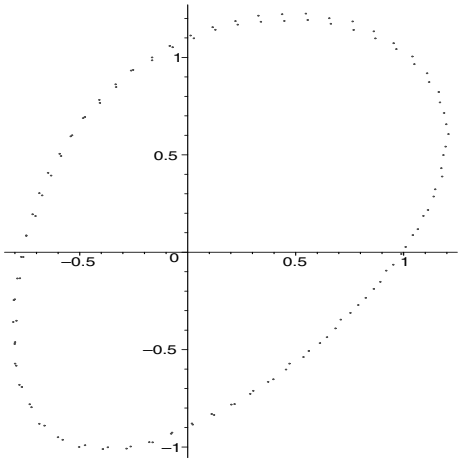

Figure 2.8: First iteration of method.

Example 2

Consider the following two images (figure 2.9 and figure 2.10) which are two digital photographs of a planar object taken from two different positions. The planar object used comes from a picture from the paper [1] where they take an image of a canine left ventricle and extract the boundary of it.

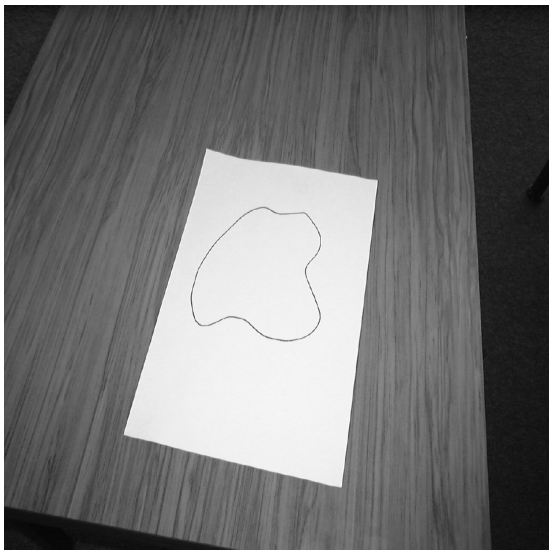

Figure 2.9: First camera angle

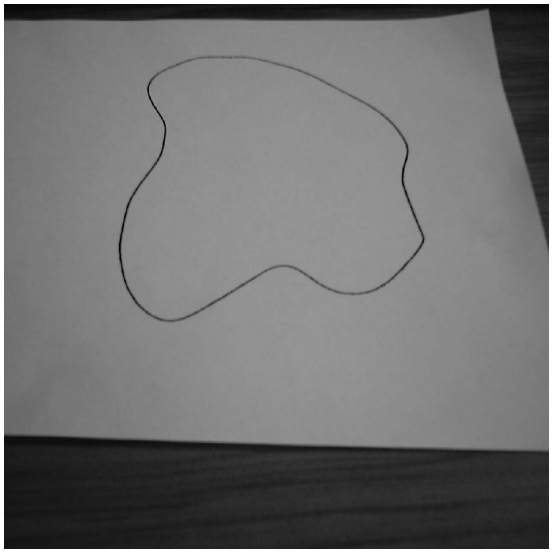

Figure 2.10: Second camera angle

The .jpg files are read into MATLAB (see [12]), and the curves are discretised, see figure 2.11.

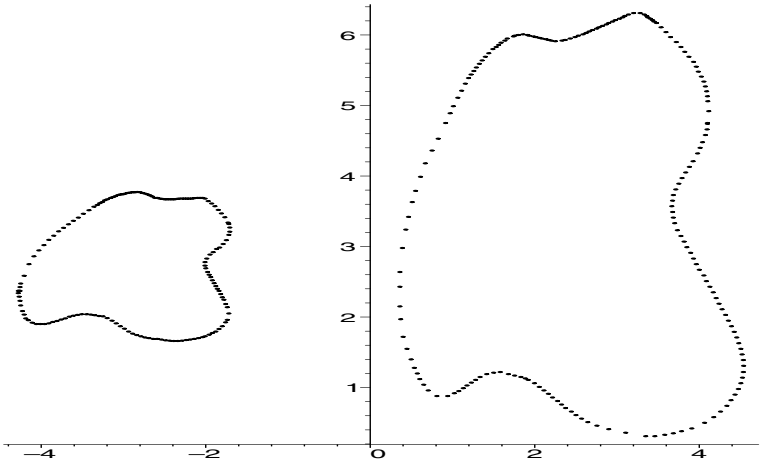

Figure 2.11: Discretised curves

193 points are equally spaced around each curve then the curves are smoothed six times. All the triangle areas are plotted on a graph, and the inflection points are located on each curve by finding where the triangle areas change sign. Figure 2.12 shows the triangle areas associated with the first curve.

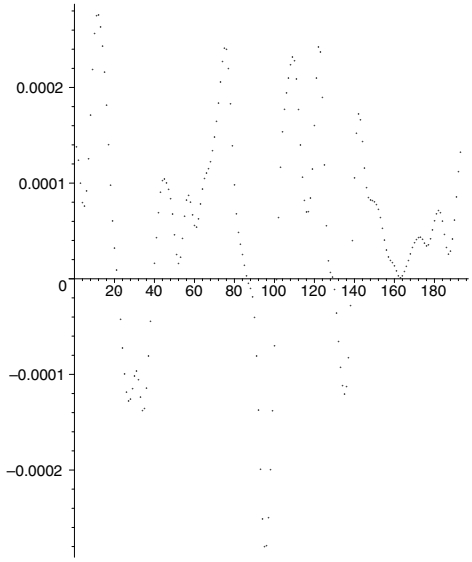

Figure 2.12: Triangle areas of the first curve after smoothing six times.

The second curve is then mapped back onto the first. Figure 2.13 shows the initial mapping is quite close.

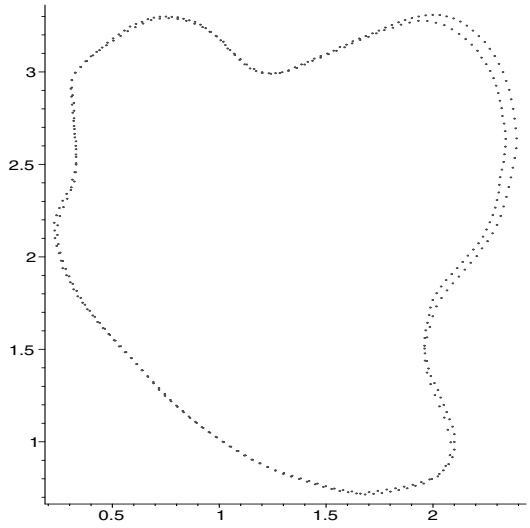

Figure 2.13: The initial mapping.

However applying the above method to this curve produces no further improvement. One possible reason for this is that all the inflection points in second curve are within one point of matching up precisely with those in the first curve and that the error in the initial mapping of second curve is enough so that smoothing this curve always shifts at least one of these inflection points one point away from the true position. This example led to the overshooting, undershooting method which is described in the following section.

2.3 Overshooting, undershooting method

In general, the first mapping back never gives a precise matching of the objects because smoothing changes the positions of the invariant points. A method for correcting the error in the initial matching will now be given which is demonstrated on three examples. This method is explained for the case of concave curves, but the example of convex curve below gives evidence that it can also be applied in the convex case.

Take two concave curves C and $\overline{C}$ related by projective transformation. Locate four approximate inflection points in C. Now assume the four points in $\overline{C}$ have been found that match up precisely with those in C. That is the exact projective transformation mapping $\overline{C}$ to C can be found.

Let $\mathcal{C}_1$ be a concavity of C with two of these inflection points I_1, I_2, say and $\bar{\mathcal{C}}_1$ be the corresponding concavity of $\overline{C}$ with the corresponding two inflection points $\bar{I}_1, \bar{I}_2$, see figure 2.14.

Figure 2.14: Two corresponding concavities in C and $\overline{C}$

Suppose $\bar{I}_1$ is mapped to a point on $\mathcal{C}_1$ to one side of I_1 and $\bar{\mathcal{C}}_1$ overshoots $\mathcal{C}_1$. On the other hand if $\bar{I}_1$ is mapped to a point on $\mathcal{C}_1$ to the **other** side of I_1, $\bar{\mathcal{C}}_1$ will undershoot $\mathcal{C}_1$, see figure 2.15. Note, the solid line is part of $\mathcal{C}_1$, the dashed line is the corresponding part of $\bar{\mathcal{C}}_1$.

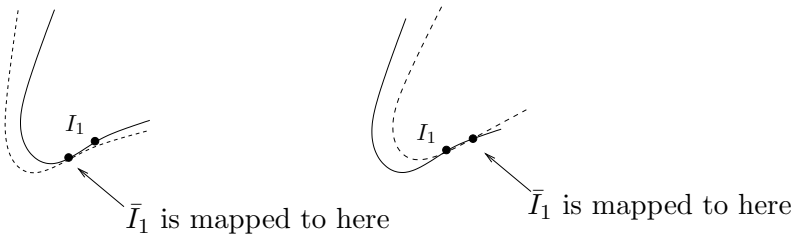

Figure 2.15: $\bar{\mathcal{C}}_1$ overshooting and undershooting $\mathcal{C}_1$ respectively

So if in the beginning I_1 does not exactly match up with $\bar{I}_1$, the difference in the behaviour of the matching shown above can be used to match it correctly. Examples 2 and 3 in this section show that with noise present the above idea can be used to match two curves related by a projective transformation closely.

The convex case is more difficult to handle as the special affine curvature turning points require fourth order derivatives and so many more smoothings are required to locate them. Thus there is a potential for a much larger amount of error to occur. Example 1, though, gives evidence that this case can still be handled by this method.

2.3.1 Example 1

Consider the two equally spaced discretised curves with random noise added, C, and $\overline{C}$ from the first example of section 2.2.3, shown again in figure 2.16.

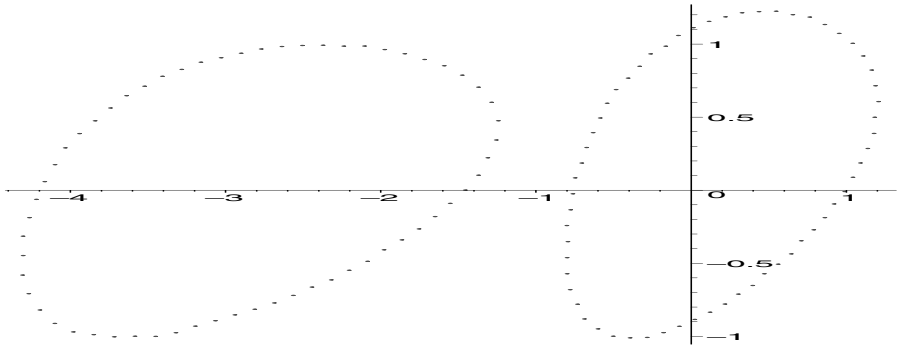

Figure 2.16: Two convex curves related by a projective transformation

Each curve is smoothed a number of times (until the noise is smoothed out) and the discrete special affine curvature is computed for both curves. Both curves have six special affine curvature turning points. These are located on each curve. They are matched up by using the joint-invariants.

The overshooting undershooting method is applied on this convex curve. Four consecutive turning points are chosen in each curve. The first turning point in $\overline{C}$ is shifted in two directions to get an interval where overshooting and undershooting occurs as shown in figure 2.17. The same is done for the second turning point and the combination of points (lying inside these intervals) is found which produces the best local matching, see figure 2.18. The same process is done on the third and fourth turning points, and the best local matching is shown in figure 2.19.

Note: in figures 2.17-2.27, C is denoted by crosses and $\overline{C}$ by circles. Each pair of turning points are denoted by boxes.

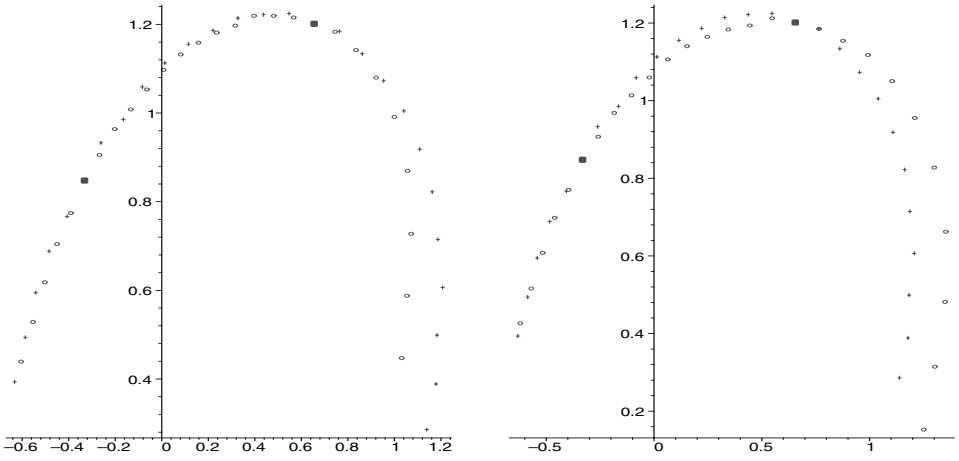

Figure 2.17: First turning point: $\overline{C}$ undershoots and overshoots C respectively

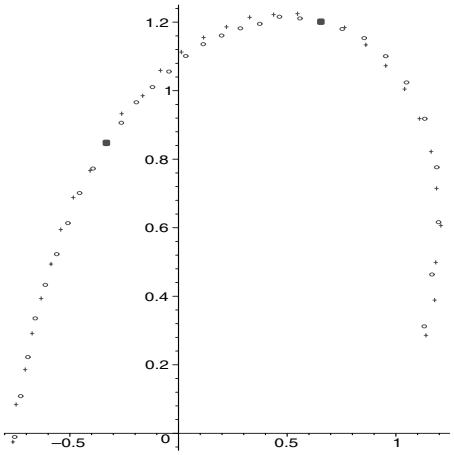

Figure 2.18: Best local matching of first and second turning points

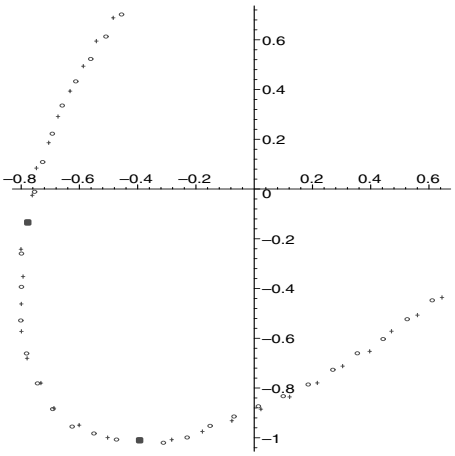

Figure 2.19: Best local matching of third and fourth turning points

The process repeated on the fifth and sixth turning points. But here, fixing the fifth point in its initial position causes C to significantly overshoot $\overline{C}$. This affects the calculation of the interval for the sixth point where overshooting and undershooting occurs in that the interval does not contain the best position for the sixth point. Thus the best local matching of the fifth and sixth turning points (which is shown in figure 2.27) is not obtained. This can be overcome by the following method.

First a limit is fixed on the amount of error allowed in the turning points. If the curves cannot be matched within this tolerance then it is assumed that either the curves are excessively noisy or they are not related by a projective transformation. Note that if the error was too large then the joint-invariants

will not be able to be matched up anyway.

Since it is discrete data that is being worked with, it can be assumed that the initial approximations to the six turning points in $\overline{C}$ are within a certain number of points from a precise matching with the six points in C. This number is essentially arbitrary as the allowable error can be increased or decreased by increasing or decreasing the spacing of the points. This number should not be too high as this would affect the speed of the algorithm.

In order to illustrate the method with the current example, the limit is chosen to be three points. Note that the arguments that follow neglect the contribution of possible errors in the other two special affine curvature turning points used in the local matching. However, for the three examples to follow this did not cause a problem.

Let P_5^{true} and P_6^{true}, be the true positions in $\overline{C}$ for the fifth and sixth turning points respectively (that is they match precisely with the corresponding turning points in C). Let P_5^{init} and P_6^{init} be the initial positions in $\overline{C}$ of the fifth and sixth turning points respectively. Fix the fifth point and move the sixth point in the direction where the curves overshoot, call this direction D_6^+. Denote the other direction where the curves undershoot by D_6^-. Similarly fix the sixth point and move the fifth point and define directions D_5^+, D_5^-. Note that if the fifth point is fixed at P_5^{true} and the sixth point is fixed at two points P_6^- and P_6^+ say where the curves overshoot and undershoot, then $P_6^{\text{true}} \in [P_6^-, P_6^+]$.

If the fifth point was fixed in the direction D_5^- so that the curves undershoot, then to compensate for this so that the curves overshoot again, the sixth point will have to be moved a sufficient amount in the direction D_6^+. Furthermore, the further the fifth point is fixed in the direction D_5^- the further that the sixth point will have to be moved in the direction D_6^+ to compensate.

To illustrate this, consider the smooth versions of the curves C and $\overline{C}$. First the fifth point is fixed at the position $P_{5,1}$ as marked in figure 2.20 so that $\overline{C}$ undershoots C as shown in figure 2.21 (C is the dotted curve, $\overline{C}$ is the solid curve). Then the sixth point is fixed at the position $P_{6,1}$ (with the fifth point still at $P_{5,1}$) so that $\overline{C}$ overshoots C by an amount similar to figure 2.21. The fifth point is then fixed at $P_{5,2}$ and to keep $\overline{C}$ overshooting C by an amount similar to figure 2.22 the sixth point must be fixed at $P_{6,2}$. Similarly for $P_{5,3}$ the sixth point must be fixed at $P_{6,3}$. So that the further the fifth point is fixed so that $\overline{C}$ undershoots C, the further the sixth point has to be fixed to make $\overline{C}$ overshoot C again.

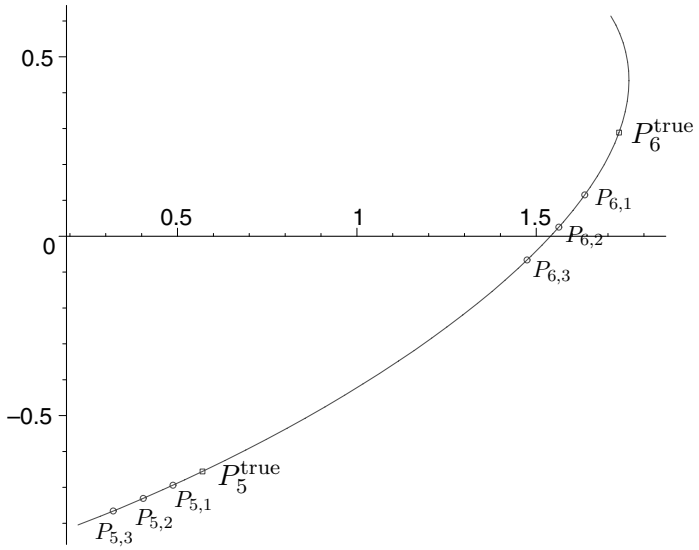

Figure 2.20: Graph of $\overline{C}$ showing the points used to illustrate overshooting and undershooting.

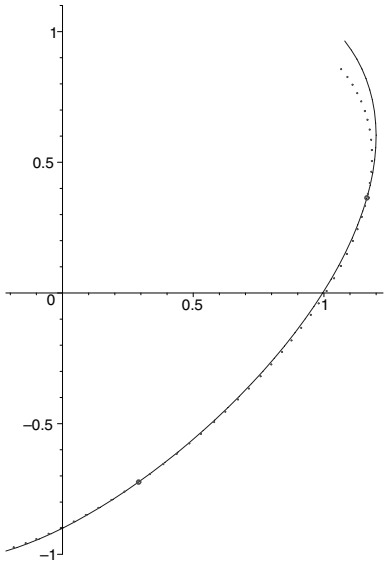

Figure 2.21: $\overline{C}$ undershoots C with $P_{5,1}$

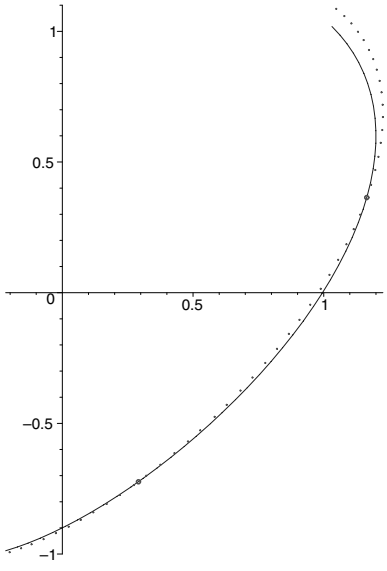

Figure 2.22: $\overline{C}$ overshoots C with $P_{5,1}$ and $P_{6,1}$.

Eventually the fifth point will be fixed a sufficient distance in the direction D_5^- at a point, P_5^{reject} say, such that before the curves overshoot again, the sixth point will have to be moved in excess of the three point limit of P_6^{init}. Thus the two consecutive points P_6^+ and P_6^- which correspond to the curves overshooting and undershooting will lie outside the three point limit of P_6^{init}. This implies $P_6^{\text{true}} \notin [P_6^-, P_6^+]$. Hence the point P_5^{reject} can be rejected as being P_5^{true}. Note that any points fixed further in this direction D_5^- will be rejected as well. Let $P_5^{\text{min}-}$ be the point the closest to P_5^{init} which is rejected. By a similar argument to above the fifth point can be fixed in the direction D_5^+ to find $P_5^{\text{min}+}$. Thus $P_5^{\text{true}} \in [P_5^{\text{min}-}, P_5^{\text{min}+}]$.

Now figure 2.23 shows a point P_5^{reject} denoted by a circle which is rejected as the two points P_6^- and P_6^+ where overshooting and undershooting occurs are outside the three point limit from P_6^{init}, see figures 2.24-2.25.

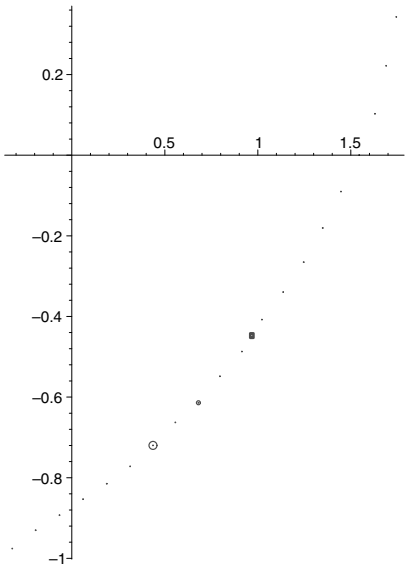

Figure 2.23: Graph showing P_5^{reject} denoted by a circle, P_5^{init} denoted by a black dot and P_5^{true} denoted by a box.

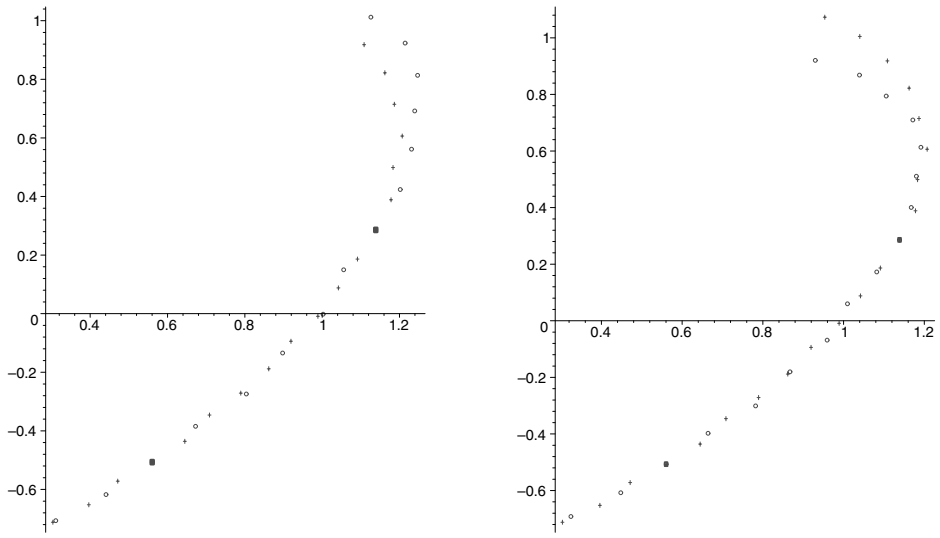

Figure 2.24: $\overline{C}$ overshoots and undershoots C respectively corresponding to the points $P_6^-, P_6^+ \in \overline{C}$.

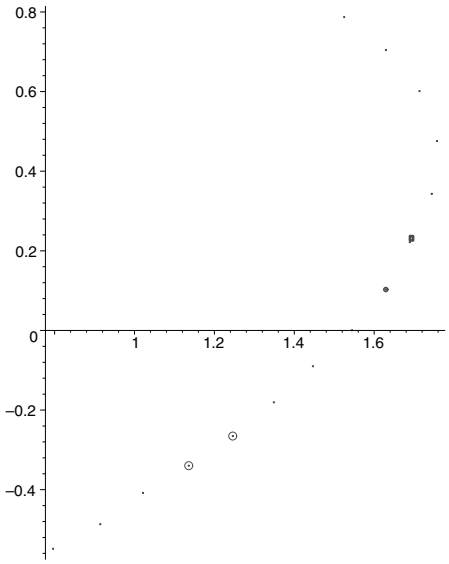

Figure 2.25: Graph showing P_6^- and P_6^+ denoted by a circle, P_6^{init} denoted by a black dot and P_6^{true} denoted by a box.

The method then proceeds as follows. Fix the fifth point at P_5^{init} and say the curves undershoot. Move the sixth point three points both sides of P_6^{init} until the curves overshoot. If no overshooting occurs reject this point and find the position nearby where it is not rejected. Call this point P_0^{accept}. Now find the first two points to the left and right of P_0^{accept} where they are rejected. Call these points P_-^{reject} and P_+^{reject} respectively. These points put a bound around where the true point lies.

Figure 2.26 shows the results of this method applied on the fifth and sixth turning points. The true position for the fifth point in $\overline{C}$ (that which matches up precisely with the fifth point in C), is denoted by a box. P_5^{initial} is denoted by a black dot and P_-^{reject} and P_+^{reject} are circled. Note that here, P_+^{reject} would be rejected anyway as it lies outside the three point limit.

Now let the point closest to the true position of fifth point (between P_-^{reject} and P_+^{reject}) be P_5^{best} and let the point closest to the true position of sixth point be P_6^{best}. For each point between P_-^{reject} and P_+^{reject}, find the two points nearest the initial sixth point where the curves overshoot and undershoot. Eventually P_5^{best} will be fixed, so that the two points where curves overshoot and undershoot will contain P_6^{best}. Hence the best local matching of the fifth and sixth points can be obtained, see figure 2.27.

Note, one could always just check every combination of three points either side of initial points and get the best matching from these, this would take $7^2 = 49$ possibilities to check. The advantage of utilising overshooting and undershooting is that this can significantly decrease the number of possibilities that need to be checked.

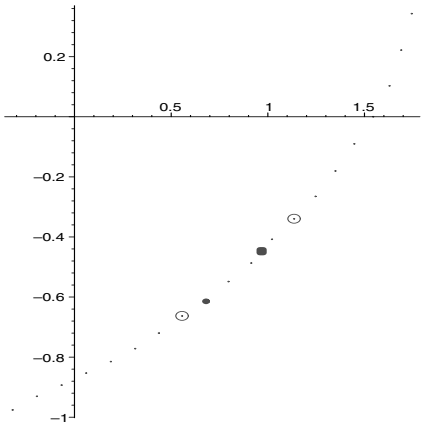

Figure 2.26: Bounds P_-^{reject} and P_+^{reject}, surrounding true fifth point.

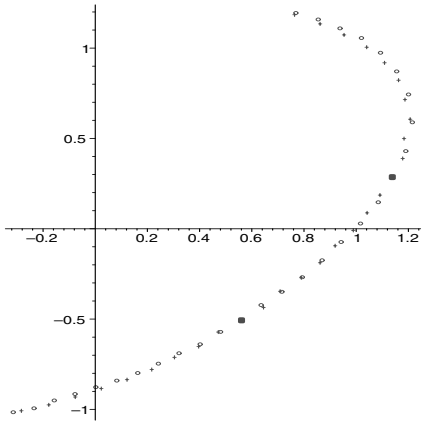

Figure 2.27: Best local matching of fifth and sixth turning points

Finally all the six resulting points are used to map $\overline{C}$ onto C, figure 2.28 shows the curves are matched closely.

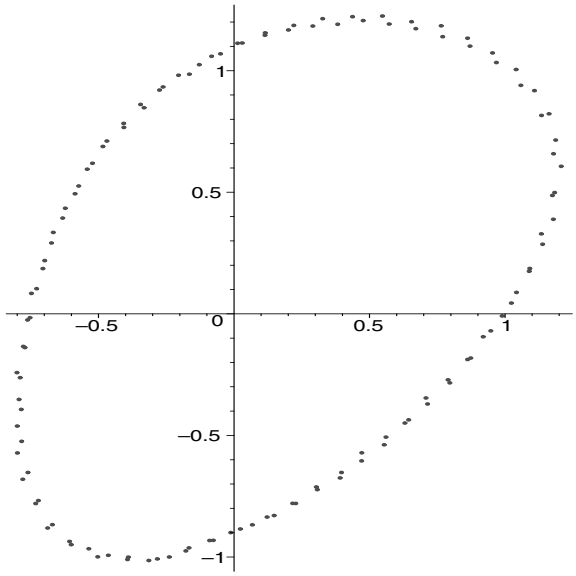

Figure 2.28: Final matching

Note that assuming the curves match, it may be advantageous to map the whole curve back using the initial approximations to the six turning points (by solving a system of 8 equations by least squares) before the overshooting, undershooting method is applied. Then the areas where the two curves deviate the most can be found and the turning points closest to these areas can be located. This will give a good estimate of what turning points have

the greatest amount of error in them.

Also note that when the best local mapping is being found by varying **two** points in $\overline{C}$, the other two points in $\overline{C}$ and the four points in C remain fixed during that whole calculation. The explicit solution to mapping equations (2.17), shows that the $[ijk]$ terms and the majority of the other terms remain fixed throughout, so everytime $a, ..., i$ are recomputed, only a few terms need to be calculated. If the 8 by 8 linear system is solved each time then this makes no use of the fact that six terms are fixed. So using (2.17) reduces the amount of computation involved.

Finally note that the local matching if required could be applied again around the curve as the second time the errors in special affine curvature turning points will have reduced and a better approximation could be obtained. Going around a second time could also avoid the potential problem of error in two other special affine curvature turning points which are fixed during the calculation of the interval where overshooting and undershooting occurs, see comments at the end of this section.

2.3.2 Example 2

Consider the two discretised curves from the second example of section 2.2.3, shown again in figure 2.29.

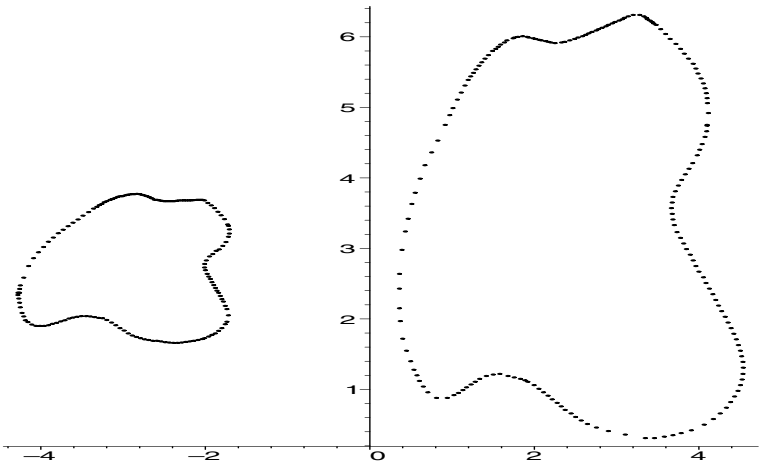

Figure 2.29: Discretised curves

As before, the inflection points are located on each curve. The overshooting, undershooting method is now applied to each concavity.

Note that it is possible that error in the first inflection point could affect the calculation of the correct interval for the second inflection point. That is the point closest to the true second inflection point may not lie inside

this interval (a similar problem to this occurs in example 1 of this section). However for this example and example 3 this problem does not occur.

For the following figures, the first curve is denoted by a cross, the second curve by a circle. Figures 2.30 and 2.31, show the overshooting and undershooting for two inflection points in one of the concavities of the left ventricle. Figure 2.32 shows the best matching of this concavity. Figure 2.33 shows the best matching of the other two concavities.

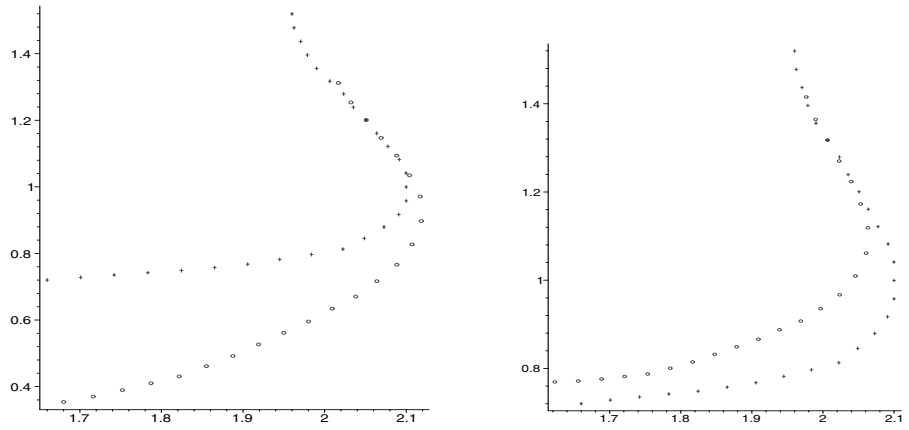

Figure 2.30: First inflection point; first curve **undershoots** and **overshoots** second curve

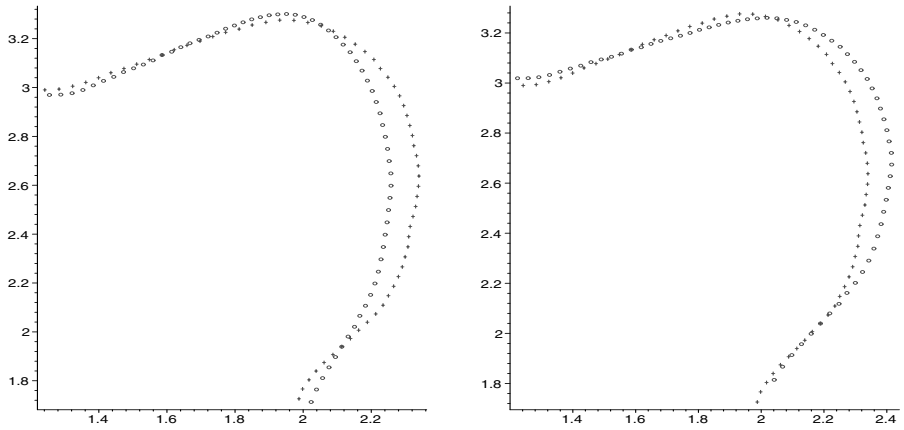

Figure 2.31: Second inflection point; first curve **overshoots** and **undershoots** second curve

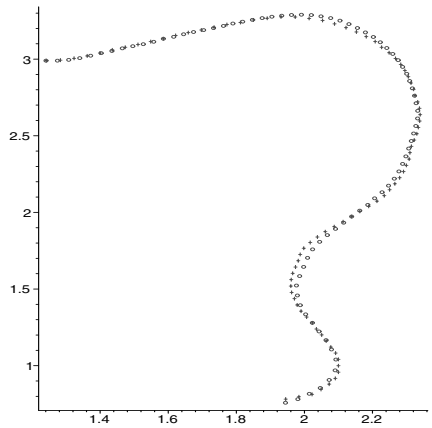

Figure 2.32: Best matching of first concavity

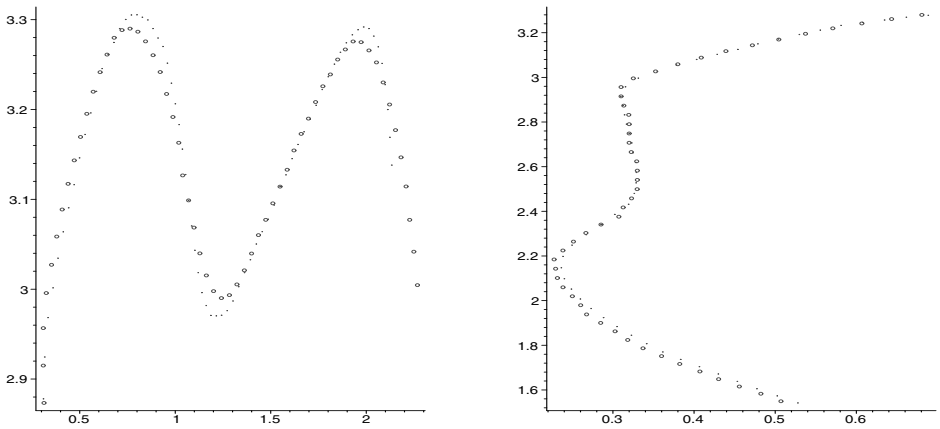

Figure 2.33: Best matching of second and third concavities

Finally, all the resulting six inflection points are used to map the second curve into the first curve. This is done by solving the twelve resulting over-determined equations by least squares. Figure 2.34 shows a close matching.

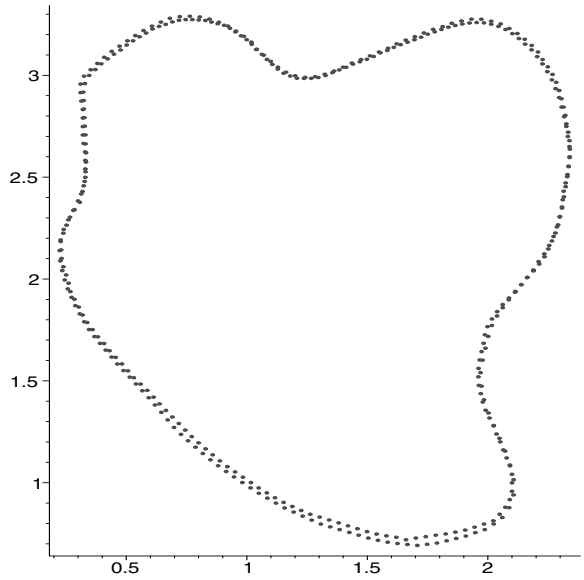

Figure 2.34: Mapping second curve into first curve

Note that the closeness of the matching is dependent on the spacing of the points. Consider the inflection point closest to the bottom right-hand corner of figure 2.34. The second curve overshoots the first curve here showing that this current inflection point is slightly out from the true inflection point. Furthermore, if the point next to this inflection point in

the second curve is used then the second curve undershoots the first curve and so using points in this current discretisation will not correct this error.

However, if the point halfway between these two points where the curve undershoots and overshoots is used, as figure 2.35 shows the matching becomes even closer. This is because the true inflection point lies between the two points above where overshooting and undershooting occurs.

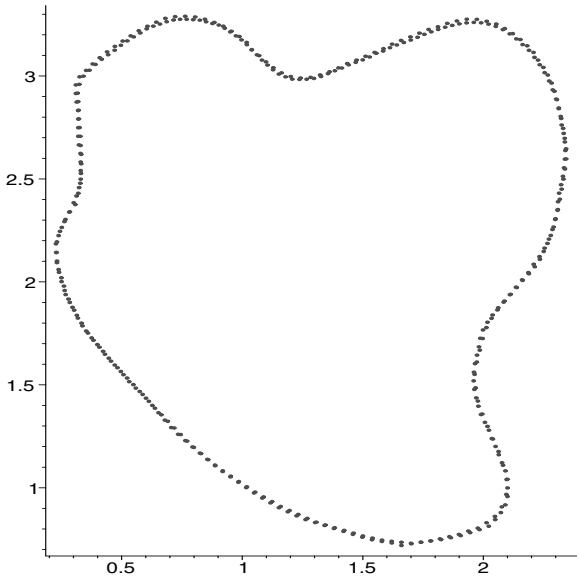

Figure 2.35: Closer matching

2.3.3 Example 3

Consider two **different** curves (not related by a projective transformation) given by $C_1 = \{(X_1(t), U_1(t))\}$, and $C_2 = \{(X_2(t), U_2(t))\}$, where,

$$X_1(t) = \cos(t)$$
$$U_1(t) = \sin(t) + \sin(\frac{1}{2}t)^2\cos(t) + \frac{1}{2}\sin(2t)^2$$

$$X_2(t) = \cos(t)$$
$$U_2(t) = \sin(t) + \sin(\frac{1}{2}t)^2\cos(t) + \frac{2}{3}\sin(2t)^2$$

and a third curve $\overline{C}_1 = \{(\overline{X}_1(t), \overline{U}_1(t))\}$ which is related to C_1 by a projective transformation.

These curves are each discretised using 193 points, random noise is added, and they are equally spaced, see figure 2.36.

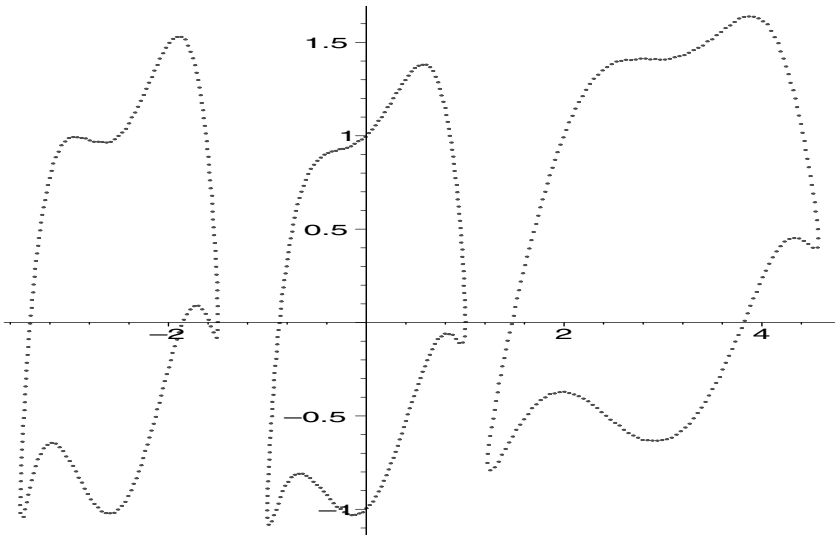

Figure 2.36: Three curves, C_2, C_1 and $\overline{C}_1$ respectively.

Now all three curves are smoothed and their inflection points are calculated. Each curve has **six** inflection points.

The overshooting, undershooting method is applied on C_1 and $\overline{C}_1$. Figures 2.37 and 2.38 show the results for one of the concavities. Figure 2.39

shows the best matching of this concavity. The same is done on the second and third concavities and figure 2.40 shows the best matchings of these. The points of C_1 are denoted by a cross, the points of $\overline{C}_1$ are denoted by a circle.

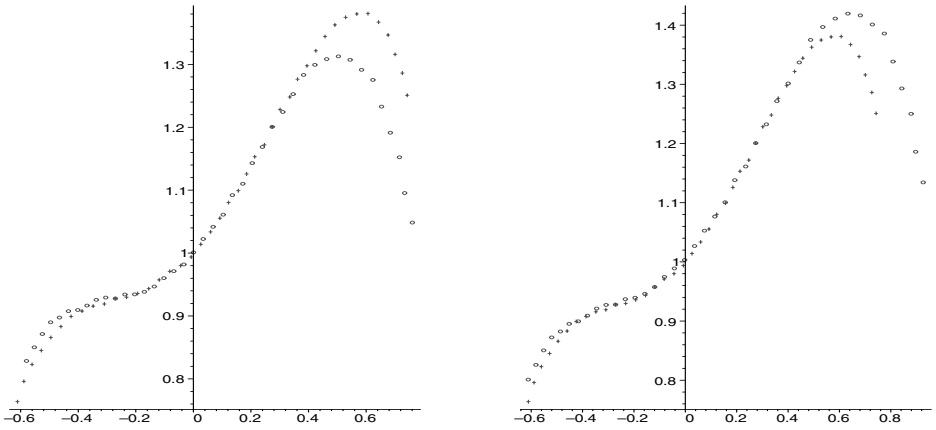

Figure 2.37: First inflection point; C_1 **overshoots** and **undershoots** $\overline{C}_1$

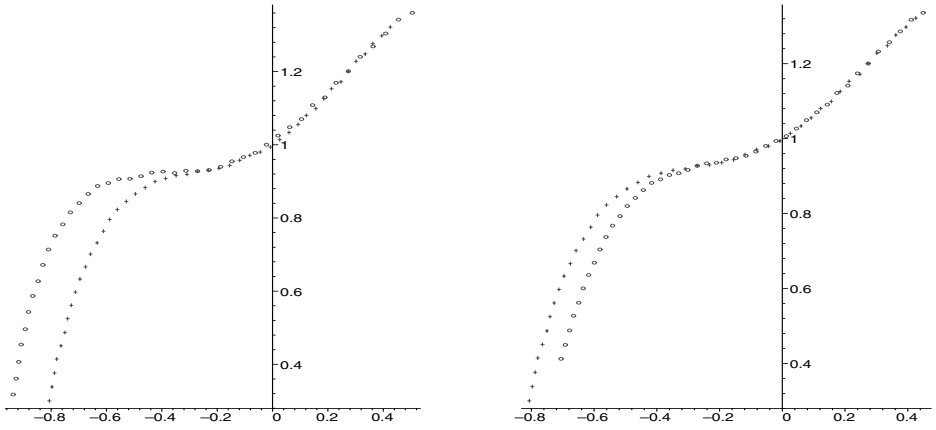

Figure 2.38: Second inflection point; C_1 **undershoots** and **overshoots** $\overline{C}_1$

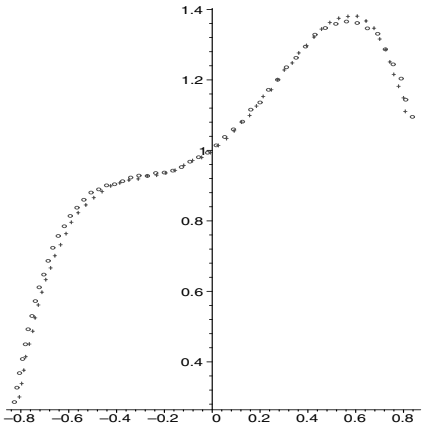

Figure 2.39: Best matching of first concavity

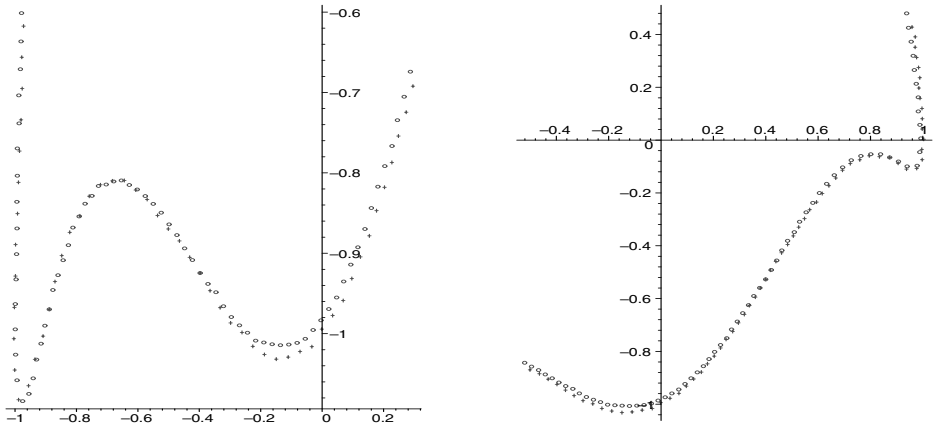

Figure 2.40: Best matching of second and third concavities

Finally, all six corrected inflection points are used to map the whole of curve $\overline{C}_1$ onto C_1. Figure 2.41 shows a close matching.

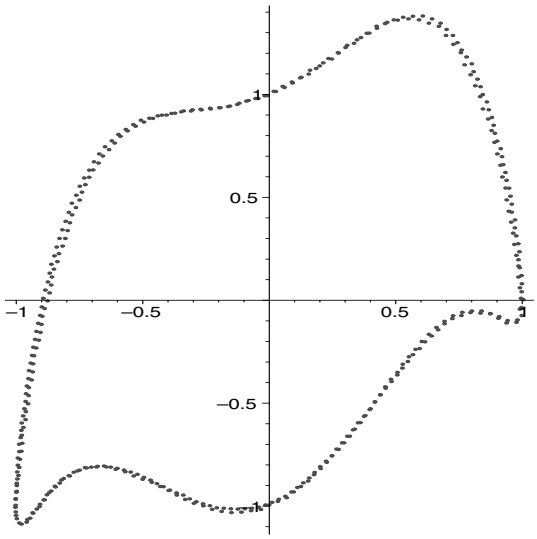

Figure 2.41: Final matching of $\overline{C}_1$ onto C_1

Now the same method is applied on C_1 and C_2. Note that the overshooting and undershooting still occurs as the curves are only a small perturbation of one another. Figure 2.42 shows the best matching of the first and second concavities. The matching of the first concavity is a significantly worse than was the case with C_1 and $\overline{C}_1$, c.f. figure 2.39. Interestingly though, as the second graph in figure 2.42 shows, the best matching of the second concavity is quite good and is comparable to first graph in figure 2.40. But the best matching of the third concavity (see figure 2.43) is significantly worse than second graph of figure 2.40.

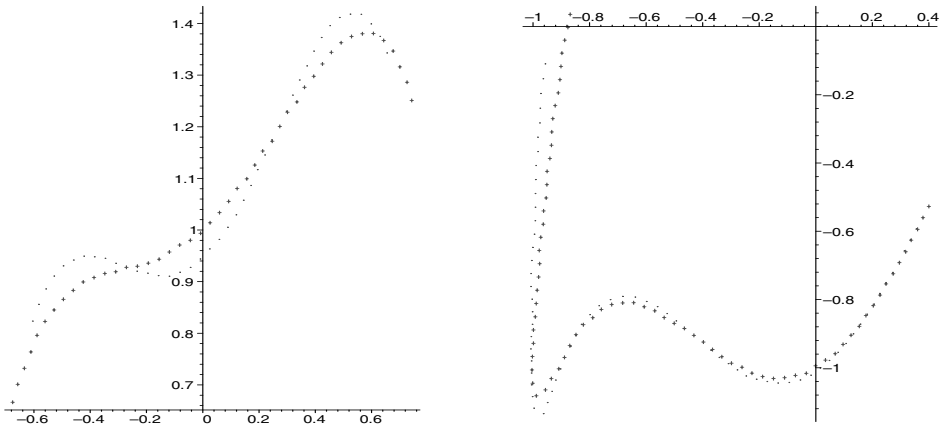

Figure 2.42: Best matching of first and second concavities

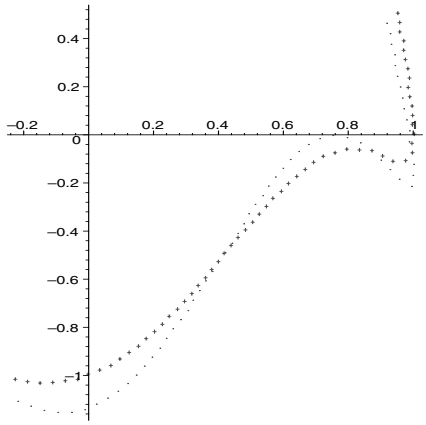

Figure 2.43: Best matching of third concavity

Now using the six corrected inflection points, C_2 is mapped onto C_1, figure 2.44 shows there is a significant difference between the curves.

This result is consistent with the fact that C_1 and C_2 are **different**.

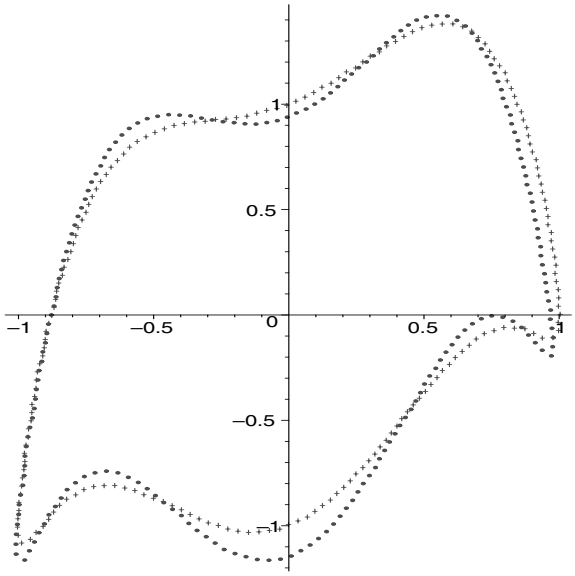

Figure 2.44: Final matching

Comments about overshooting undershooting method

The overshooting undershooting method is a way of correcting the initial error in the matching. It has been assumed in this method that the errors in the two points that are fixed during the calculation of interval where overshooting and undershooting occurs have no effect. In general this may not be the case though, as was mentioned earlier, if the method is applied twice this problem may not occur.

Another problem with this method is that, depending on how much error is needed to be corrected a potentially large number of mappings and local matchings would be required.

However this method provides some insight into the behaviour of projective transformations on curves and led to the canonical form method in chapter 3 which tracks errors to individual parameters of the projective group and can place points where desired on the curves for use in matching.

Chapter 3

Canonical form

3.1 Euclidean canonical form

Consider two curves $u = u(x)$ and $\bar{u} = \bar{u}(\bar{x})$ related by a projective transformation

$$(x, u) \longmapsto (\bar{x}, \bar{u}) = (\frac{ax + bu + c}{gx + hu + i}, \frac{dx + eu + f}{gx + hu + i}), \qquad (3.1)$$
$$\det \begin{pmatrix} a & b & c \\ d & e & f \\ g & h & i \end{pmatrix} = 1.$$

Note that by the chain rule, the derivative u_x transforms by

$$u_x \longmapsto \bar{u}_{\bar{x}} = \frac{dhu + di + eu_x gx + eu_x i - dxhu_x - eug - fg - fhu_x}{ahu + ai + bu_x gx + bu_x i - axhu_x - bug - cg - chu_x} \qquad (3.2)$$

Locate a point common to both curves. This point could be an inflection point, bi-tangent point or special affine curvature turning point as these points are projectively invariant (see chapter 2). A Euclidean transformation is performed on each curve so that this common point satisfies,

$$x = \bar{x} = 0,\ u(0) = \bar{u}(0) = 0,\ u_x(0) = \bar{u}_{\bar{x}}(0) = 0.$$

Note that this Euclidean transformation is unique since there are three parameters in the Euclidean group and the above gives three conditions to solve for these parameters. This form of the curves is called their **Euclidean canonical form**. Then (3.1) and (3.2) implies that $c = 0$, $d = 0$ and $f = 0$.

Now $e \neq 0$ otherwise it is not a projective transformation, so after dividing through every constant by e (this has no effect on the projective

transformation) the two curves are related by

$$(x, u) \longmapsto (\frac{ax + bu}{gx + hu + i}, \frac{u}{gx + hu + i}). \tag{3.3}$$

and therefore

$$\frac{\bar{x}}{\bar{u}} = a\frac{x}{u} + b,$$

Thus the $\frac{x}{u}$ turning points and inflection points are preserved and can be detected in a way which is independent of parametrisation.

3.2 Discussion of the following sections

In the following section (3.3), a method is given which utilises a $\frac{x}{u}$ turning point between two bi-tangents to generate other invariant points which are used to match the curves. Several examples of concave curves with reasonably large concavities are given with random noise added to show the robustness of the use of the Euclidean canonical form. Adaptive spacing is used for accuracy of calculating the bi-tangents and for minimizing the number of points needed in representing the curves for speed of the algorithm.

This method is then adapted to handle convex curves (which have no $\frac{x}{u}$ turning points) utilising an $\frac{x}{u}$ inflection point. A number of examples show the robustness of the use of the Euclidean canonical form.

This is followed by a geometrical interpretation of all the parameters in the projective group (section 3.4).

The method for concave curves in section 3.3 works well for large concavities but in practice a different method will be used (based on the adapted method for convex curves) which can be applied to all curves. This global method (described in section 3.5 using the left-ventricle) can place points used for matching where desired on the curves and enables a way of correcting error in the initial matching. A theoretical formulation of this error correction is given at the end of section 3.5. (An implementation of the error correction is given in chapter 4).

3.3 Utilising the Euclidean canonical form

Suppose two **concave** curves $u = u(x)$ and $\bar{u} = \bar{u}(\bar{x})$ are related by a projective transformation. Suppose an inflection point, bi-tangent or special affine curvature turning point has been identified and that the curves are given in their Euclidean canonical form.

If the canonical point of u is a bi-tangent point then the other bi-tangent point will have $u = 0$. Similarly for $\bar{u}$. Let the other bi-tangent point be $P_1 = (x_1, 0)$. Assume that for x in a neighbourhood of the two bi-tangents P_1 and the canonical point $(0, 0)$, $u(x) > 0$ and $x_1 > 0$ (the case $x_1 < 0$ proceeds similarly). The Taylor series of $u(x)$ for x in a neighbourhood of zero is given by $u(x) = Ax^2 + O(x^3)$, where $A > 0$ and the Taylor series of $u(x)$ for x in a neighbourhood of x_1 is given by $u(x) = A_1(x - x_1)^2 + O((x - x_1)^3)$ where $A_1 > 0$. Thus as $x \to 0^+$, $\frac{x}{u(x)} \to \infty$ and as $x \to x_1^-$ $\frac{x}{u(x)} \to \infty$. Therefore, between $x = 0$ and $x = x_1$, there must be at least one minima of $\frac{x}{u(x)}$. This corresponds to $xu_x - u = 0$. Let $(x_{\text{TP}}, u_{\text{TP}})$ be this point. Note that these points are invariant under rotation, since $xu_x - u$ transforms by

$$\tilde{x}\tilde{u}_{\tilde{x}} - \tilde{u} = \frac{xu_x - u}{\cos(\theta) + u_x \sin(\theta)}.$$

There is a geometric interpretation of the $\frac{x}{u}$ turning points. The line from the canonical point to the $\frac{x}{u}$ turning point is tangent to the curve there, see figure 3.1.

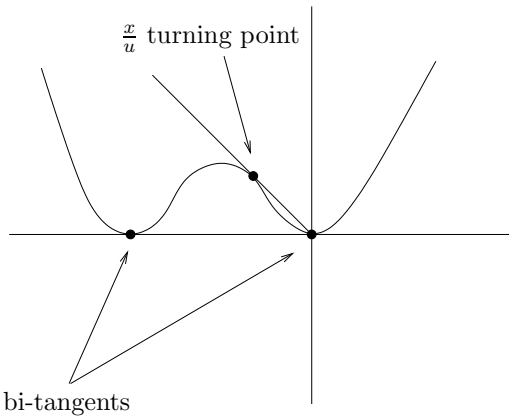

Figure 3.1: Geometric interpretation of the $\frac{x}{u}$ turning point.

Note that there is a proposed object recognition procedure in Rothwell et al., 1995 [7] which uses these bi-tangent points to generate what they call bi-tangent contact points. The $\frac{x}{u}$ turning point corresponds precisely to a

bi-tangent contact point. This method reproduces these points in a more general setting.

Now translate the curve $\frac{x}{u} = \frac{x}{u}(t)$ (for arbitrary parametrisation t) by an amount $b_{\text{TP}}=\frac{x_{\text{TP}}}{u_{\text{TP}}}$ so that the turning point occurs at $x = 0$. This is equivalent to doing the transformation,

$$(x, u) \longmapsto (x - b_{\text{TP}}u, u) \tag{3.4}$$

Do the same for $\frac{\bar{x}}{\bar{u}}$. Thus the resulting curves (using same notation) will satisfy

$$\frac{\bar{x}}{\bar{u}} = a\frac{x}{u}$$

Thus $u = u(x)$ and $\bar{u} = \bar{u}(\bar{x})$ will be related by the following transformation

$$(x, u) \longmapsto (\frac{ax}{gx + hu + i}, \frac{u}{gx + hu + i}) \tag{3.5}$$

Points where $x = 0$ are invariant under this transformation. One of these points is the $\frac{x}{u}$ turning point $(0, u_{\text{TP}})$ with the corresponding point $(0, \bar{u}_{\text{TP}})$ on the curve $\bar{u} = \bar{u}(\bar{x})$. Let another such point where $x = 0$ be $(0, u_2)$, with the corresponding point $(0, \bar{u}_2)$ in the curve $\bar{u} = \bar{u}(\bar{x})$. Geometrically $(0, u_2)$ comes from the point (x_2, u_2) which is the intersection of the tangent line through $(x_{\text{TP}}, u_{\text{TP}})$ and the curve $u = u(x)$, see figure 3.2.

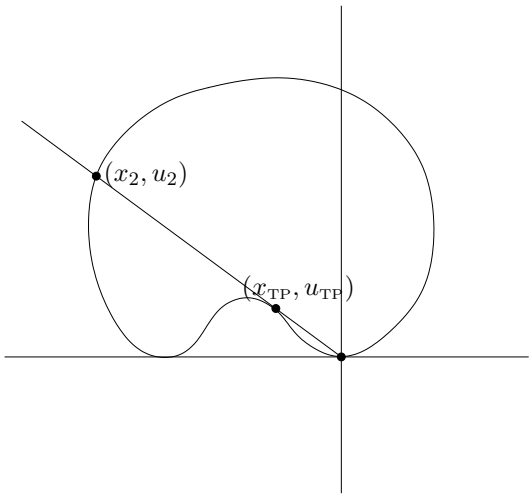

Figure 3.2: Graph showing the points $(x_{\text{TP}}, u_{\text{TP}})$ and (x_2, u_2), which correspond to the points $(0, u_{\text{TP}})$ and $(0, u_2)$ on the curve translated by (3.4).

Using the transformation,

$$(x,u) \longmapsto (\frac{x}{Hu+I}, \frac{u}{Hu+I})$$

where

$$H = \frac{\bar{u}_2 u_{\text{TP}} - u_2 \bar{u}_{\text{TP}}}{\bar{u}_2 \bar{u}_{\text{TP}}(u_{\text{TP}} - u_2)} \qquad I = \frac{u_{\text{TP}} u_2 (\bar{u}_{\text{TP}} - \bar{u}_2)}{\bar{u}_{\text{TP}} \bar{u}_2 (u_{\text{TP}} - u_2)}$$

map $(0, u_{\text{TP}})$ and $(0, u_2)$ onto $(0, \bar{u}_{\text{TP}})$ and $(0, \bar{u}_2)$. Then the new (x, u) and $(\bar{x}, \bar{u})$ are still related by (3.5) but the following equations hold,

$$\frac{\bar{u}_{\text{TP}}}{h\bar{u}_{\text{TP}} + i} = \bar{u}_{\text{TP}} \qquad \frac{\bar{u}_2}{h\bar{u}_2 + i} = \bar{u}_2.$$

So that $h\bar{u}_{\text{TP}} + i = 1 = h\bar{u}_2 + i$ where $\bar{u}_{\text{TP}} \neq \bar{u}_2$ thus $h = 0$ and $i = 1$. That is the curves are now related by,

$$(x,u) \longmapsto (\frac{ax}{gx+1}, \frac{u}{gx+1}) \tag{3.6}$$

Finally, map the other bi-tangent of $u(x)$, call this $(x_0, 0)$, onto the corresponding bi-tangent $(\bar{x}_0, 0)$ of $\bar{u}(\bar{x})$ using the transformation,

$$(x,u) \longmapsto (Ax, u)$$

where

$$A = \frac{\bar{x}_0}{x_0}.$$

Then the new (x, u) and $\bar{x}, \bar{u})$ are still related by (3.6) but now

$$\frac{a\bar{x}_0}{g\bar{x}_0 + 1} = \bar{x}_0 \quad \text{which implies} \quad a = g\bar{x}_0 + 1.$$

The curves are now related by

$$(x,u) \longmapsto (\frac{(g\bar{x}_0 + 1)x}{gx+1}, \frac{u}{gx+1}). \tag{3.7}$$

This transformation forms a group action since

$$g \cdot (h \cdot (x,u)) = (g \cdot h) \cdot (x,u)$$

where,

$$g \cdot h = g(h\bar{x}_0 + 1) + h,$$

The identity is $g_{\mathrm{id}} = 0$ and the inverse of g is

$$g^{-1} = -\frac{g}{g\bar{x}_0 + 1}.$$

Thus (3.7) forms a one parameter subgroup action of the projective group action. Using the method of regularization (see section 1.1.2) the equation

$$\frac{(g\bar{x}_0 + 1)x}{gx + 1} = 0$$

is solved for g and substituted into $\frac{u}{gx+1}$ which gives the curvature,

$$\kappa = -\frac{u\bar{x}_0}{x - \bar{x}_0} \tag{3.8}$$

Thus the curves are related by a projective transformation if and only if κ is the same for both objects (in this final canonical form). Note that by using one invariant point in each curve from (3.8), the two curves can be mapped on top of each other using (3.7). In the examples below, locate approximately the point $(x_{\mathrm{Hpt}}, u_{\mathrm{Hpt}})$ half way (in Euclidean arclength) between the turning point $(x_{\mathrm{TP}}, u_{\mathrm{TP}})$ and the canonical point (x_0, u_0) in the Euclidean canonical form of the first curve by using the distances between the points. Then using κ above find the point in other curve which corresponds to this point. This is the invariant point that will be used. Note that if the nearest turning point of κ to $(x_{\mathrm{Hpt}}, u_{\mathrm{Hpt}})$ is identified in the first curve this can be used to ensure that the corresponding point $(\bar{x}_{\mathrm{Hpt}}, \bar{u}_{\mathrm{Hpt}})$ in the second curve is found uniquely.

Consider the two digital photographs of the canine left ventricle of chapter 2, section 2.2. These are shown again in figures 3.3 and 3.4 below.

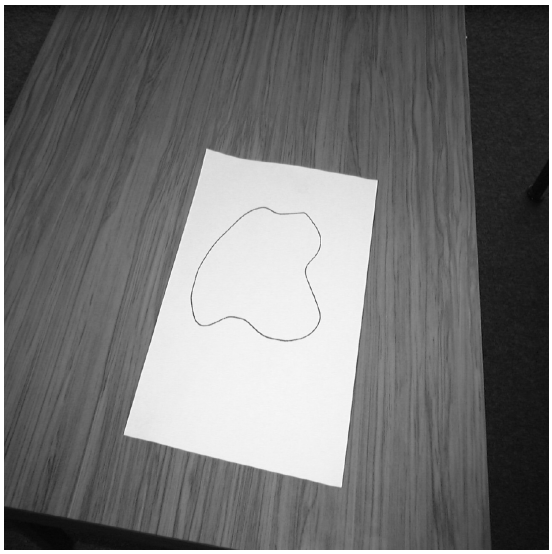

Figure 3.3: First camera angle

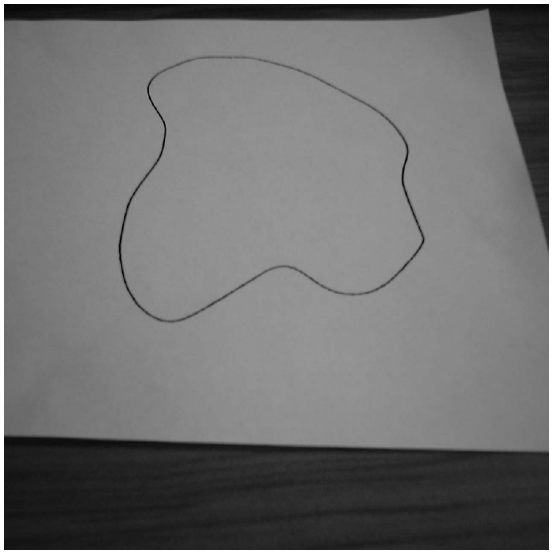

Figure 3.4: Second camera angle

Figure 3.5 shows their discretised curves again.

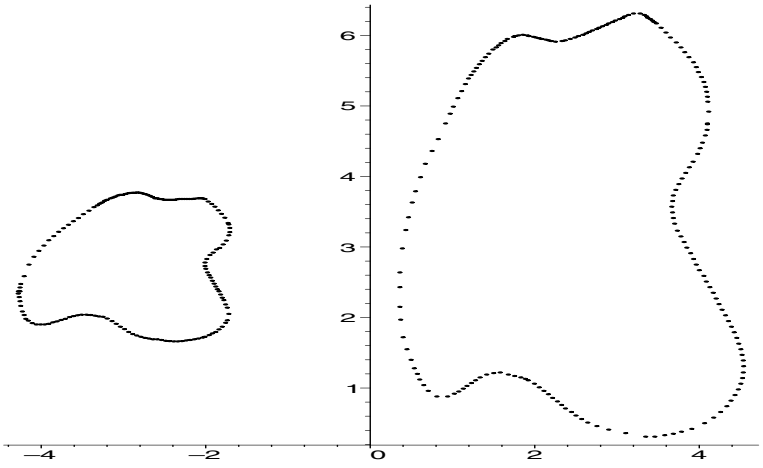

Figure 3.5: Discretised curves

Now 193 points are equally spaced around each curve and the bi-tangents are found for each concavity by first finding the two points in the discretisation that have the closest to the same tangent line, then finding the two points nearby such that the line between these points does not intersect the discretised curve.

There are six bi-tangents in each curve so there are six possible combinations of joint-invariants involving consecutive points. The points are initially ordered by $(x_1, u_1), \ldots, (x_6, u_6)$ in the first curve and $(\bar{x}_1, \bar{u}_1), \ldots, (\bar{x}_6, \bar{u}_6)$ in the second curve. The following table shows the six joint-invariants in each curve plus the corresponding combination of five points. For example [12345] refers to the joint-invariants involving the consecutive points (x_i, u_i), $i = 1, \ldots, 5$ in the first curve ($[\bar{1}\bar{2}\bar{3}\bar{4}\bar{5}]$ refers to the consecutive points $(\bar{x}_i, \bar{u}_i)$, $i = 1, \ldots, 5$ in second curve). Note that the initial ordering of the points in the second curve does not match up with the ordering in the first curve.

Table of joint-invariants

Combination	$[J_1, J_2]$	Combination	$[\bar{J}_1, \bar{J}_2]$
[12345]	[0.6697, 2.2363]	$[\bar{1}\bar{2}\bar{3}\bar{4}\bar{5}]$	[0.5481, 5.2737]
[23456]	[0.7726, 1.6429]	$[\bar{2}\bar{3}\bar{4}\bar{5}\bar{6}]$	[0.8840, 1.2288]
[34561]	[0.5861, 1.8797]	$[\bar{3}\bar{4}\bar{5}\bar{6}\bar{1}]$	[0.5382, 2.4289]
[45612]	[0.5940, 4.9599]	$[\bar{4}\bar{5}\bar{6}\bar{1}\bar{2}]$	[0.6391, 2.4401]
[56123]	[0.8796, 1.2152]	$[\bar{5}\bar{6}\bar{1}\bar{2}\bar{3}]$	[0.7714, 1.6743]
[61234]	[0.5219, 2.6780]	$[\bar{6}\bar{1}\bar{2}\bar{3}\bar{4}]$	[0.6280, 1.7371]

Given a pair of bi-tangents (x_1, u_1), (x_2, u_2) in the first curve these can be matched with the corresponding bi-tangents in the second curve by finding the pair of joint-invariants $(\bar{J}_1, \bar{J}_2)$ which are the closest to (J_1, J_2) for the

combinations [56123] and [61234]. The table of joint-invariants above shows that [56123] and [61234] match with $[\bar{2}\bar{3}\bar{4}\bar{5}\bar{6}]$ and $[\bar{3}\bar{4}\bar{5}\bar{6}\bar{1}]$.

The following table shows the correct order for points in the second curve. Note that even though only crude approximations are used for the bi-tangents the joint-invariants match quite closely.

Table of joint-invariants

Combination	$[J_1, J_2]$	Combination	$[\bar{J}_1, \bar{J}_2]$
[12345]	$[0.6697, 2.2363]$	$[\bar{4}\bar{5}\bar{6}\bar{1}\bar{2}]$	$[0.6391, 2.4401]$
[23456]	$[0.7726, 1.6429]$	$[\bar{5}\bar{6}\bar{1}\bar{2}\bar{3}]$	$[0.7714, 1.6743]$
[34561]	$[0.5861, 1.8797]$	$[\bar{6}\bar{1}\bar{2}\bar{3}\bar{4}]$	$[0.6280, 1.7371]$
[45612]	$[0.5940, 4.9599]$	$[\bar{1}\bar{2}\bar{3}\bar{4}\bar{5}]$	$[0.5481, 5.2737]$
[56123]	$[0.8796, 1.2152]$	$[\bar{2}\bar{3}\bar{4}\bar{5}\bar{6}]$	$[0.8840, 1.2288]$
[61234]	$[0.5219, 2.6780]$	$[\bar{3}\bar{4}\bar{5}\bar{6}\bar{1}]$	$[0.5382, 2.4289]$

The point used for the Euclidean canonical form is the bi-tangent associated with the concavity which has the largest perpendicular distance between the line joining the two bi-tangents and the curve. This point is found in the second curve using joint-invariants. It corresponds to the point (x_2, u_2). The reason for using this point is so that the point arising from the intersection of the tangent line from the canonical point to $(x_{\text{TP}}, u_{\text{TP}})$ (see figure 3.2) is as far as possible away from the other bi-tangent in the concavity.

A least squares cubic fit through nine points around each bi-tangent is used for a better approximation and the curves are mapped to their Euclidean canonical form, see figure 3.6. Figures 3.7-3.11 show the matching of the curves at each step of the above method. Then all the transformations are reversed so that both curves are mapped to the original scale of the second curve. Figure 3.11 shows that this final matching of the curves is close.

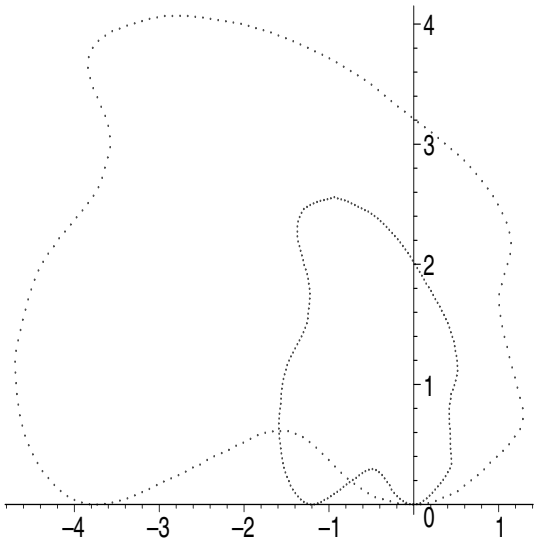

Figure 3.6: Euclidean canonical form.

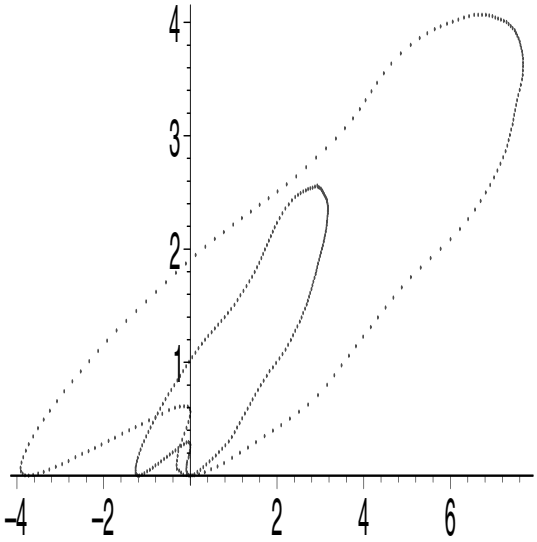

Figure 3.7: Curves related by $(x, u) \longmapsto (\frac{ax}{gx+hu+i}, \frac{u}{gx+hu+i})$.

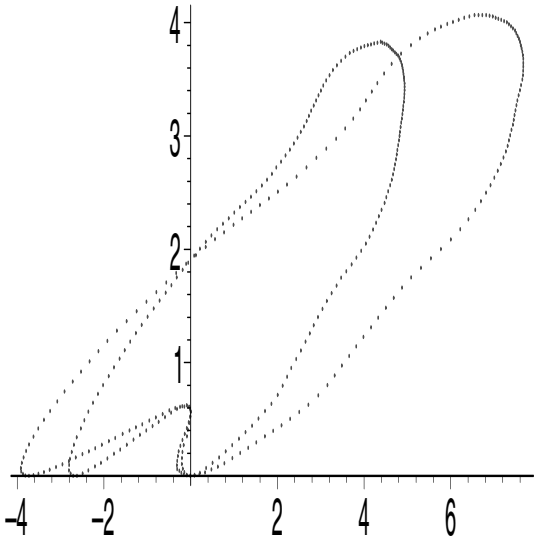

Figure 3.8: Curves related by $(x, u) \longmapsto (\frac{ax}{gx+1}, \frac{u}{gx+1})$.

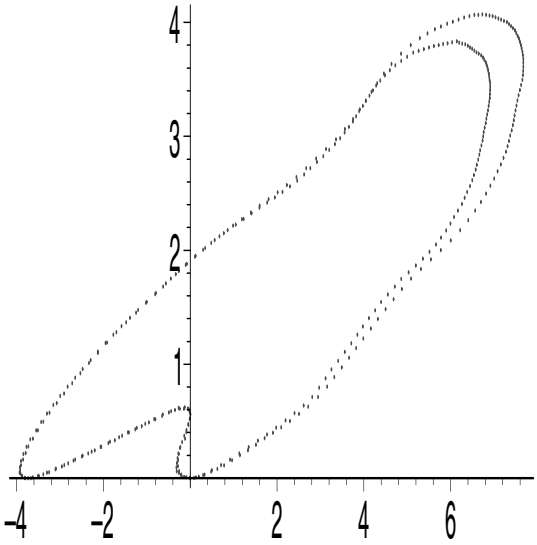

Figure 3.9: Curves related by $(x, u) \longmapsto (\frac{(g\bar{x}_0+1)x}{gx+1}, \frac{u}{gx+1})$.

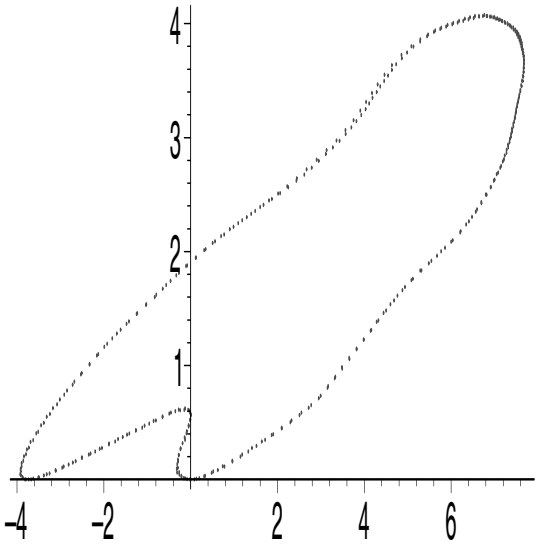

Figure 3.10: Applying the transformation $(x, u) \longmapsto (\frac{(g\bar{x}_0+1)x}{gx+1}, \frac{u}{gx+1})$ (after using (3.8) to identify an invariant point in each curve) to match the curves.

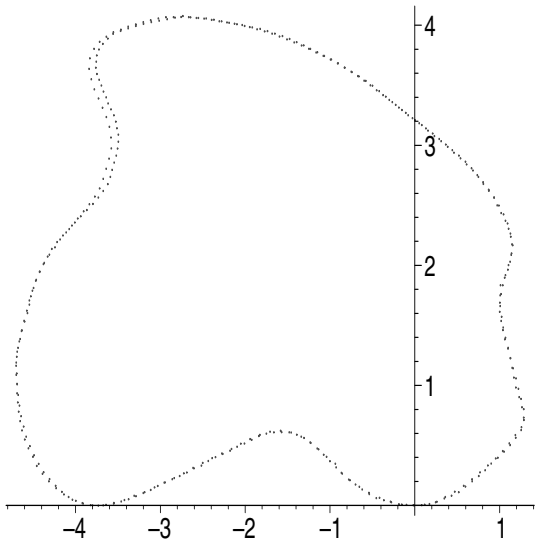

Figure 3.11: Mapping curves back to the original scale of the second curve.

Now the above method is applied on three curves $C_1 = \{(X_1(t), U_1(t))\}$, $\overline{C}_1 = \{(\overline{X}_1(t), \overline{U}_1(t))\}$ and $C_2 = \{(X_2(t), U_2(t))\}$, where,

$$X_1(t) = \cos(t)$$
$$U_1(t) = \sin(t) + \sin(\frac{1}{2}t)^2\cos(t) + \frac{1}{2}\sin(2t)^2$$

$$X_2(t) = \cos(t)$$
$$U_2(t) = \sin(t) + \sin(\frac{1}{2}t)^2\cos(t) + \frac{2}{3}\sin(2t)^2$$

and $\overline{C}_1$ is related to C_1 by a projective transformation.

Initially about 550 points are equally spaced on each curve, and random noise is added. An adaptive spacing is chosen for the curves by plotting more points where the curve has high curvature, and less points where the curve has low curvature.

First the curves are smoothed and then for each curve, start at an arbitary point P_0 on that curve. Consider the two preceeding points P_{-1}, P_{-2} and the vectors v_{-1} from P_{-1} to P_0 and v_{-2} from P_{-2} to P_0.

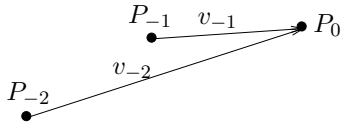

Figure 3.12: Two vectors v_{-1} and v_{-2}.

Let $v_{\text{av}} = \frac{v_{-1}+v_{-2}}{2}$, the find the next point P_1 on curve such that the angle between the vectors v_0 (from P_0 to P_1) and v_{av} is larger than one and a half degrees (this number is essentially arbitrary). Plot this point and continue around the whole curve. Then put this resultant adaptive spacing on the smoothed curves back onto the original non-smoothed curves using the corresponding points.

Now locate two points in the smoothed curve of C_1 which when joined by a straight line, do not intersect the curve in a neighbourhood of each point. Identify the corresponding points in the non-smoothed curve. These will be approximations to the bi-tangents. Using joint-invariants, find the bi-tangents in $\overline{C}_1$ and C_2 which best match up with those bi-tangents in C_1.

This spacing plots too many points around the bi-tangent points. This problem is avoided by the following strategy. Consider one of the bi-tangent

points P_0, a preceeding point P_{-1} and the point P_1 after P_0. Compute the angle θ_0 between the vectors v_{-1} and v_0. If this angle is greater than five degrees, then plot the point P_1. If not then choose the point P_{-2} preceeding P_{-1}, and the point P_2 after P_1. Compute the angle θ_1 between the vectors v_{-2} (from P_{-2} to P_0) and $\tilde{v}_0$ (from P_0 to P_2). If this angle is greater than five degrees, then plot this point P_2, see figure 3.13. If not then continue this process until a point is found where the angle is greater than five degrees.

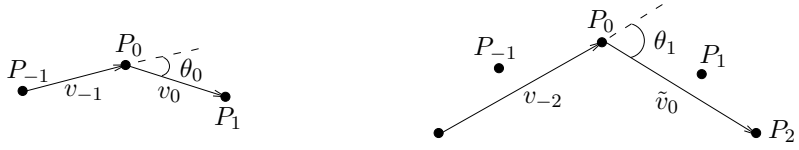

Figure 3.13: Graphs showing the angle θ_0 between v_{-1} and v_0 and the angle θ_1 between v_{-2} and $\tilde{v}_0$.

Note that this method is also used to avoid points in the adaptive spacing suddenly accelerating apart when moving from high curvature to low curvature.

Do this until say five points are plotted and then repeat for five points on the otherside of bi-tangent. The least squares cubic through these 11 points is then computed. This is then repeated for the other bi-tangent.

Now consider the two curves C_1 and $\bar{C}_1$. Map them both to their Euclidean canonical form. The result is shown in figure 3.14.

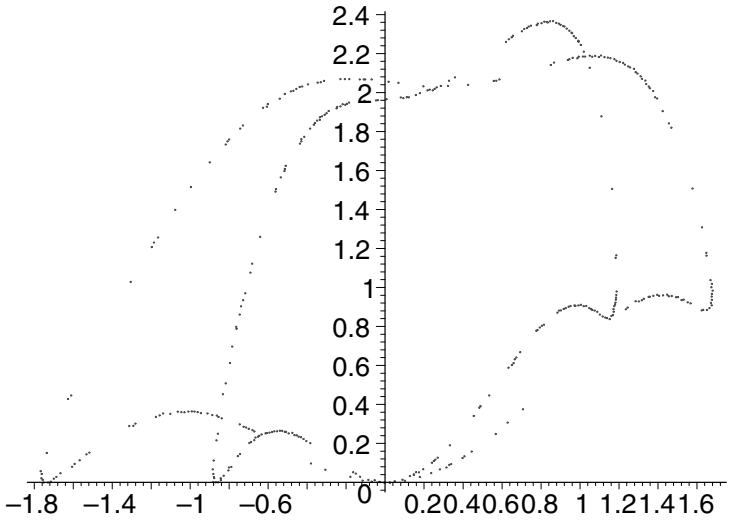

Figure 3.14: Euclidean canonical form of the curves C_1 and $\bar{C}_1$

The $\frac{x}{u}$ and $\frac{\bar{x}}{\bar{u}}$ turning points between the corresponding bi-tangents are computed and the curves are mapped using (3.4) so they are related by

(3.5). The points where each curve passes the u axis are calculated. Note, to get the best approximation to these points, the points in the original discretisation (~ 550 points) are used. The same procedure as the previous example is then applied and both curves are mapped back to the original scale of the second curve. Figure 3.15 shows this final mapping and shows there is error in the turning point. Perturbing the turning point in the second curve (along curve) fixes this error and figure 3.16 shows a close matching.

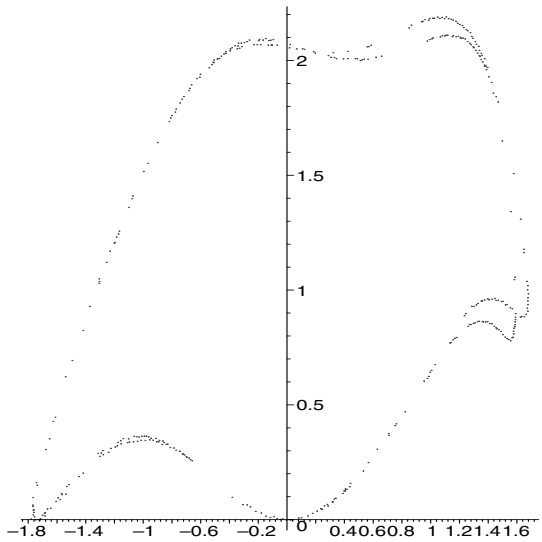

Figure 3.15: Matching curves, with error in turning point.

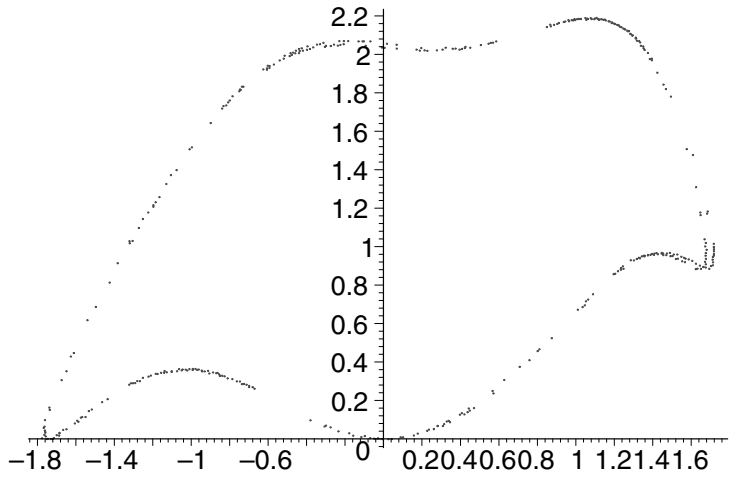

Figure 3.16: Matching curves, after correcting the error in turning point.

Notice that to the right of the canonical point, the second curve slightly overshoots the first curve. This shows there is a slight error in the canonical

point of second curve relative to the first curve. Translating the second curve to the left along x axis fixes this error and gives an even closer matching as shown in figure 3.17.

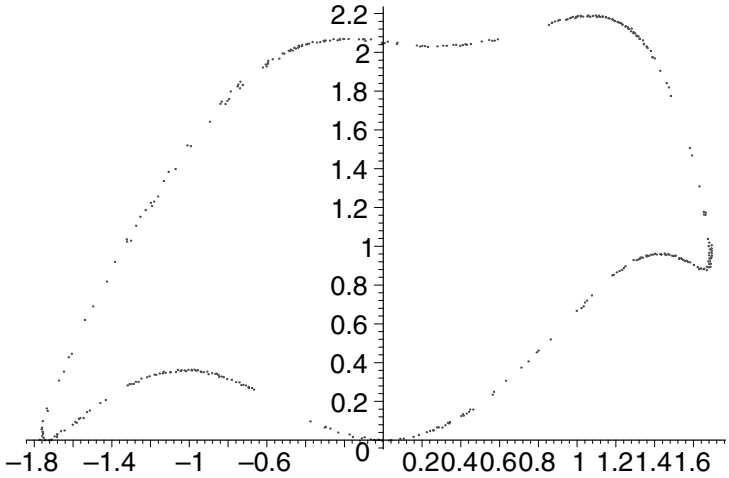

Figure 3.17: Matching curves, after translating second curve slightly to the left along x axis.

The same method is then performed on the curves C_1 and C_2. Figure 3.18 shows the two curves in their Euclidean canonical form and figure 3.19 shows the final matching of the curves. As the figure shows, there is a significant difference between the two curves which is consistent with the fact that C_1 and C_2 are not related by a projective transformation.

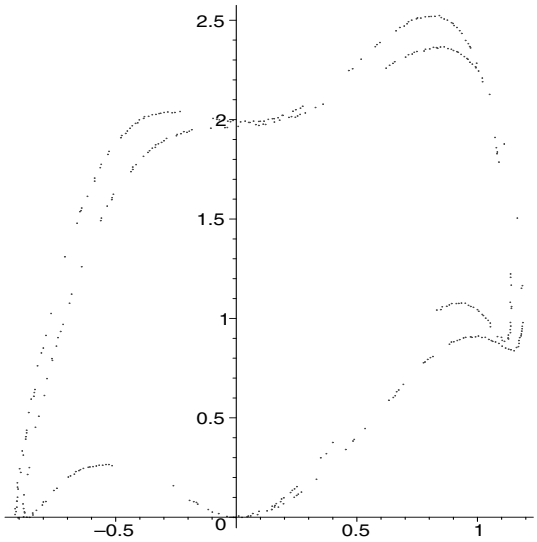

Figure 3.18: Euclidean canonical form of the curves C_1 and C_2

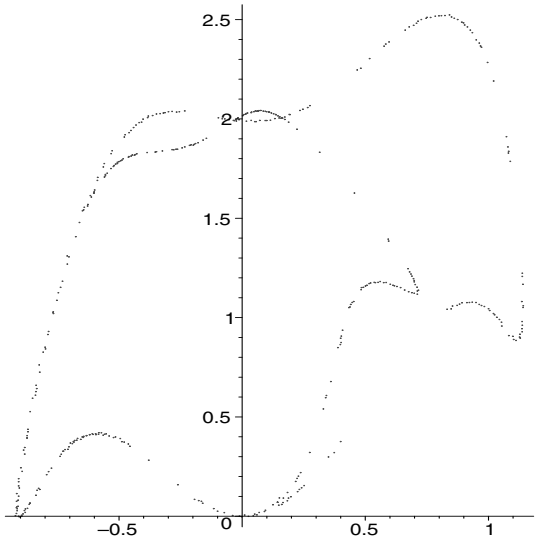

Figure 3.19: Matching the curves

The method is now applied to the curves $C_1 = \{(X_1(t), U_1(t))\}$, and $\overline{C}_1 = \{(\overline{X}_1(t), \overline{U}_1(t))\}$, where,

$$X_1(t) = \cos(t) - \frac{1}{2}\sin(t-1)$$
$$U_1(t) = \sin(t) + \frac{1}{2}\sin(\frac{1}{2}t)^2\cos(t) + \frac{5}{6}\sin(2t)^2 + \frac{1}{5}\cos(2t)^2 + \frac{1}{3}\sin(t)\cos(2t)$$

and $\overline{C}_1$ is a projective transformation of C_1.

They are discretised with random noise added and then they are adaptively spaced and mapped to their Euclidean canonical form, see figure 3.20.

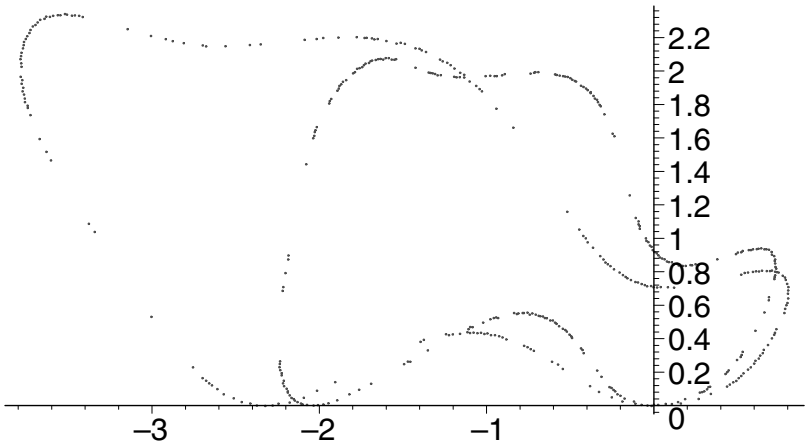

Figure 3.20: Euclidean canonical form of the curves C_1 and $\bar{C}_1$

The method as described in the previous examples is then applied to these curves. Figure 3.21 shows a close matching and also shows that the remaining error is of a similar nature to that in the previous example. Translating the second curve slightly along the x axis corrects this error, and figure 3.22 shows a closer matching.

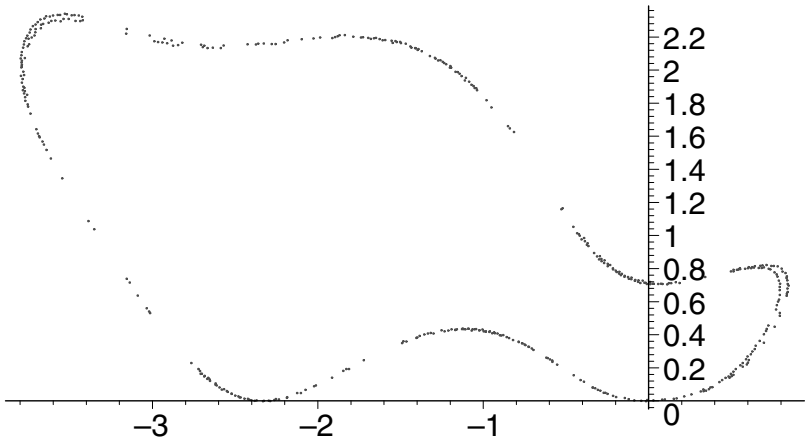

Figure 3.21: Matching curves

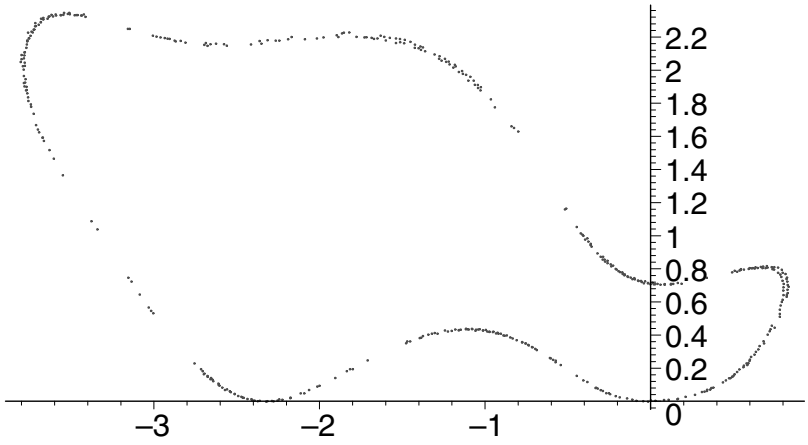

Figure 3.22: Matching curves, after translating second curve slightly to the left along x axis.

If the curves are convex then there are no bi-tangents and so a special affine curvature turning point has to be identified in each curve in order for the curves to be put in their Euclidean canonical form. That is they will be related by the following transformation,

$$(x,u) \longmapsto (\frac{ax+bu}{gx+hu+i}, \frac{u}{gx+hu+i}).$$

Thus

$$\frac{\bar{x}}{\bar{u}} = a\frac{x}{u} + b$$

and so the inflection points and turning points of $\frac{\bar{x}}{\bar{u}}$ correspond to the inflection points and turning points of $\frac{x}{u}$. These can be detected in a way independent of parametrisation as discussed in 3.1.

However, the tangent line at every point does not intersect the curve so there are no $\frac{x}{u}$ turning points (see figure 3.1 for geometric interpretation of a $\frac{x}{u}$ turning point), but because the curves are compact, there must be at least one inflection point in $\frac{x}{u}$. This is because if

$$x \to 0^+ \Longrightarrow \frac{x}{u(x)} = \frac{x}{cx^2+O(x^3)} \to +\infty$$

and if

$$x \to 0^- \Longrightarrow \frac{x}{u(x)} = \frac{x}{cx^2+O(x^3)} \to -\infty$$

where $u(x) = cx^2+O(x^3)$ with $c > 0$ without loss of generality and $u(0) = 0$, $u_x(0) = 0$.

Denote the $\frac{x}{u}$ inflection point on the curve $u = u(x)$ by (x_0, u_0) and the corresponding point on the curve $\bar{u} = \bar{u}(\bar{x})$ by $(\bar{x}_0, \bar{u}_0)$ The transformation

$$(X,U) \longmapsto (X - BU, U)$$

maybe used to map the point (x_0, u_0) with $B = \frac{x_0}{u_0}$ and the point $(\bar{x}_0, \bar{u}_0)$ with $B = \frac{\bar{x}_0}{\bar{u}_0}$ to a point on the u and $\bar{u}$ axes respectively. The curves will now be related by the transformation

$$(x,u) \longmapsto (\frac{ax}{gx+hu+i}, \frac{u}{gx+hu+i}).$$

Now let $(0, u_0)$ and $(0, \bar{u}_0)$ be the corresponding inflection points of $\frac{x}{u}$ and $\frac{\bar{x}}{\bar{u}}$ respectively. Then, using the transformation,

$$(X,U) \longmapsto (\frac{X}{HU+1}, \frac{U}{HU+1})$$

where $H = \frac{u_0 - \bar{u}_0}{u_0 \bar{u}_0}$, $(0, u_0)$ can be mapped to $(0, \bar{u}_0)$. Thus the curves will now be related by

$$(x, u) \longmapsto \left(\frac{ax}{gx + h(u - \bar{u}_0) + 1}, \frac{u}{gx + h(u - \bar{u}_0) + 1}\right).$$

For use later, this form of the curves will be called the **second** canonical form.

If $(x_{\text{TP}}, u_{\text{TP}})$ and $(\bar{x}_{\text{TP}}, \bar{u}_{\text{TP}})$ are two other corresponding special affine curvature turning points then a is given by,

$$a = \frac{\bar{x}_{\text{TP}} u_{\text{TP}}}{\bar{u}_{\text{TP}} x_{\text{TP}}}.$$

Note that in practice $(x_{\text{TP}}, u_{\text{TP}})$ and $(\bar{x}_{\text{TP}}, \bar{u}_{\text{TP}})$ will not be located precisely. An average can be taken of all the a values arising from all the other special affine curvature turning points in the curve or, alternatively, from other $\frac{x}{u}$ turning points and/or inflection points if there are any.

Consider the points (x_1, u_1) and (x_2, u_2) where $\frac{x_2}{u_2} = -\frac{x_1}{u_1}$. These points can be uniquely identified (since there are no $\frac{x}{u}$ turning points) with the corresponding points in $\bar{C}_1$ by finding $(\bar{x}_1, \bar{u}_1)$ and $(\bar{x}_2, \bar{u}_2)$ such that $\frac{\bar{x}_1}{\bar{u}_1} = a\frac{x_1}{u_1}$ and $\frac{\bar{x}_2}{\bar{u}_2} = a\frac{x_2}{u_2}$. This will also imply $\frac{\bar{x}_2}{\bar{u}_2} = -\frac{\bar{x}_1}{\bar{u}_1}$.

These two points in each curve can be used to solve for a, g, h, and thus the curves can be matched. The formulas for a, g, h are

$$a = \frac{\bar{x}_1 u_1}{\bar{u}_1 x_1}$$

$$g = \frac{-u_1 \bar{x}_2 u_2 x_1 + u_1 \bar{x}_2 \bar{u}_0 x_1 + \bar{x}_1 u_1^2 x_2 - u_1 \bar{x}_2 \bar{u}_1 x_1 - \bar{u}_0 \bar{x}_1 u_1 x_2 + \bar{x}_2 u_2 \bar{u}_1 x_1}{\bar{u}_1 x_1 \bar{x}_2 (x_2 u_1 - x_2 \bar{u}_0 - u_2 x_1 + \bar{u}_0 x_1)}$$

$$h = \frac{-\bar{x}_1 u_1 x_2 + \bar{x}_2 x_2 u_1 - \bar{x}_2 x_2 \bar{u}_1 + \bar{x}_2 \bar{u}_1 x_1}{\bar{x}_2 \bar{u}_1 (x_2 u_1 - x_2 \bar{u}_0 - u_2 x_1 + \bar{u}_0 x_1)}$$

This method is now applied on the convex curves $C_1 = \{(X_1(t), U_1(t))\}$ and $\overline{C}_1 = \{(\overline{X}_1(t), \overline{U}_1(t))\}$ where

$$X_1(t) = \cos t + \frac{1}{5}\cos^2 t$$
$$U_1(t) = \frac{1}{2}X_1(t) + \sin t + \frac{1}{10}\sin^2 t$$

and $\overline{C_1}$ is a projective transformation of C_1.

The curves are each discretised with 60 points with random noise added and they are equally spaced. There are six special affine curvature turning points in each curve. These are matched up and one special affine curvature turning point is chosen in each curve so that the curves can be mapped to

their Euclidean canonical form. A least squares cubic (through nine points) is used to estimate the gradients. Figure 3.23 shows the result.

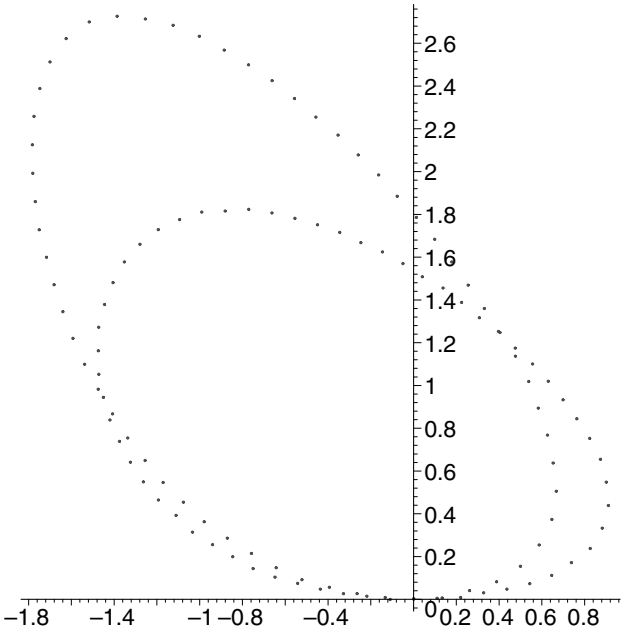

Figure 3.23: Euclidean canonical form for convex curves related by a projective transformation.

There is only one inflection point in $\frac{x}{u}$ and so this and the inflection point in $\frac{\bar{x}}{\bar{u}}$ are located approximately. This is done by smoothing the curve first and then finding the consecutive points where $[ijk]$ changes sign. Here $[ijk]$ is given by

$$[ijk] = \det \begin{pmatrix} i & \frac{x_i}{u_i} & 1 \\ j & \frac{x_j}{u_j} & 1 \\ k & \frac{x_k}{u_k} & 1 \end{pmatrix}.$$

Let (x_0, u_0) and $(\bar{x}_0, \bar{u}_0)$ be the inflection points in $\frac{x}{u}$ and $\frac{\bar{x}}{\bar{u}}$ respectively. The curves are now mapped to their second canonical form. The point (x_1, u_1) halfway (in Euclidean arclength) between (x_0, u_0) and the canonical point in C_1 is located using distances between points and also the point (x_2, u_2) which has $\frac{x_2}{u_2}$ the closest to $-\frac{x_1}{u_1}$ is found. Now using the other five special affine curvature turning points, $a_{\mathrm{TP}} = \frac{\bar{x}_{\mathrm{TP}} u_{\mathrm{TP}}}{\bar{u}_{\mathrm{TP}} x_{\mathrm{TP}}}$ is computed for each one and the average of these five values is used as the approximation to a.

$\overline{C}_1$ is made piecewise linear (by joining a straight line between consecutive pairs of points) and the points $(\bar{x}_1, \bar{u}_1)$ and $(\bar{x}_2, \bar{u}_2)$ are found in $\overline{C}_1$ such that $\frac{\bar{x}_1}{\bar{u}_1} = a\frac{x_1}{u_1}$ and $\frac{\bar{x}_2}{\bar{u}_2} = a\frac{x_2}{u_2}$. The curves are matched using the formulas

for a, g and h.

As figure 3.24 shows they are matched quite closely. The remaining error is due to error in the canonical point (which is about the distance between two points).

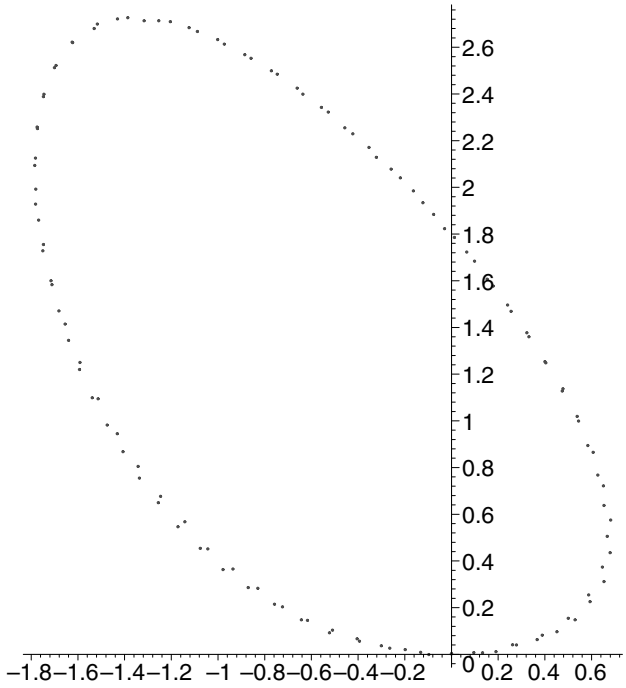

Figure 3.24: Matching the curves with error in the canonical point.

This error is corrected by choosing the point next to the canonical point in the second curve and then repeating the above method. Figure 3.25 shows the resulting matching. Here the error is due to the approximations to the inflection points of $\frac{x}{u}$, and $\frac{\bar{x}}{\bar{u}}$ not matching up. Perturbing the inflection point in $\frac{\bar{x}}{\bar{u}}$ along the curve corrects this error giving a very close matching as shown in figure 3.26.

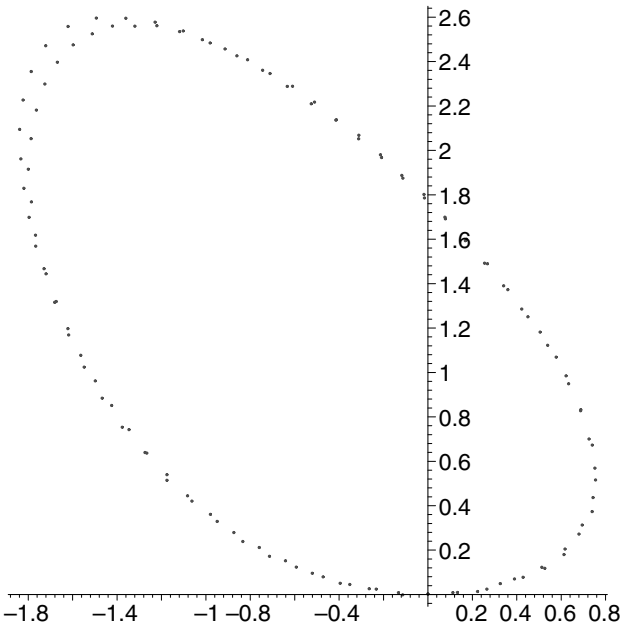

Figure 3.25: Matching the curves with error in the inflection points.

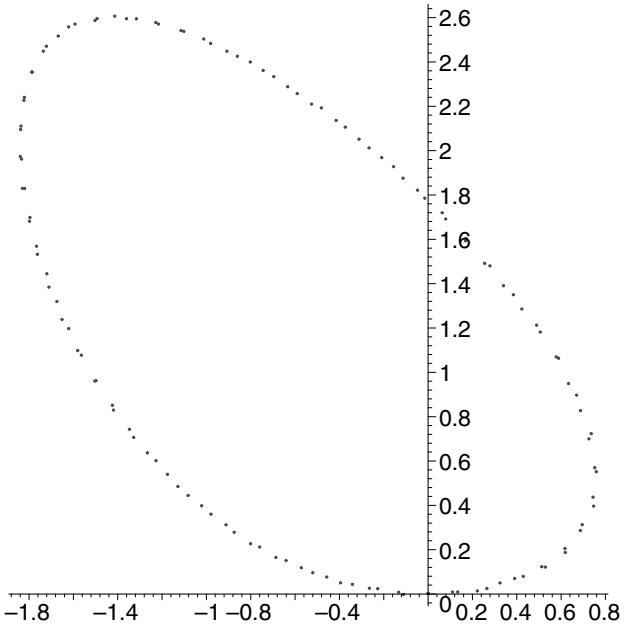

Figure 3.26: Matching the curves after perturbing the inflection point in $\frac{\bar{x}}{\bar{u}}$ along curve)

Now to give further evidence of the robustness of this method, a severe projective transformation is done on the convex curve C_1. Both curves are mapped to their Euclidean canonical form with error placed in their canonical points and gradients, see figure 3.27. Note that the projective transformation is so severe that the curve C_1 cannot be seen on the scale of the figure.

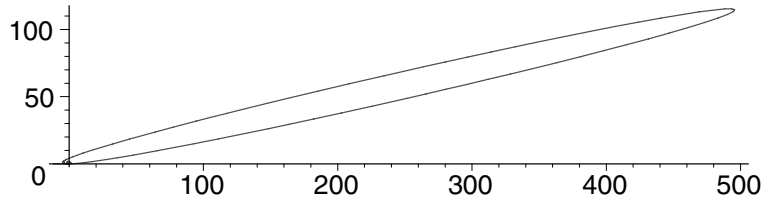

Figure 3.27: Euclidean canonical forms of two convex curves related by a severe projective transformation.

The above method is applied with error put in the inflection points of $\frac{x}{u}$ and $\frac{\bar{x}}{\bar{u}}$. Figure 3.28 shows the final matching of the curves. Now denote the two curves in figure 3.28 by $\tilde{C}_1$ and $\tilde{\bar{C}}_1$ corresponding to the curves C_1 and $\bar{C}_1$ respectively and consider the point $(\tilde{x}_{\max}, \tilde{u}(\tilde{x}_{\max})) \in \tilde{C}_1$ where $\tilde{x}_{\max}$ is the maximum $\tilde{x}$ value of $\tilde{C}_1$ with the corresponding t parameter value of $t = t_{\max}$. This point will be used to demonstrate the effect the severe projective transformation has on the error between the curves. Define the relative error between this point and the corresponding point $(\tilde{\bar{x}}_{\max}, \tilde{\bar{u}}(\tilde{\bar{x}}_{\max})) \in \tilde{\bar{C}}_1$ by

$$\epsilon_{\text{relative}} = \frac{\sqrt{(\tilde{\bar{x}}_{\max} - \tilde{x}_{\max})^2 + (\tilde{\bar{u}}(\tilde{\bar{x}}_{\max}) - \tilde{u}(\tilde{x}_{\max}))^2}}{D_{\max}} = 0.6553$$

where $D_{\max} = \max(\Delta\tilde{x}_{\max}, \Delta\tilde{u}_{\max})$ with $\Delta\tilde{x}_{\max}$ and $\Delta\tilde{u}_{\max}$ being the maximum distances across the curve $\tilde{C}_1$ in the $\tilde{x}$ and $\tilde{u}$ directions. Note that $D_{\max}$ is defined so that the error is given an equal weighting all around the curve. If $D_{\max} = \sqrt{\tilde{x}_{\max}^2 + \tilde{u}(\tilde{x}_{\max})^2}$ was used, then for a fixed absolute error, $\epsilon_{\text{relative}}$ would be smaller for points further away from the origin that for those that are close.

It appears as though there is a significant error in the matchings. However this is due to only a small part of the curve C_1 being blown up by the projective transformation and so any error in this region is also blown up. Mapping the curves back to the scale of C_1 (by reversing the mappings done to C_1), shows that the curves are closely matched, see figure 3.29. The corresponding relative error here is $\epsilon_{\text{relative}} = 0.0292$.

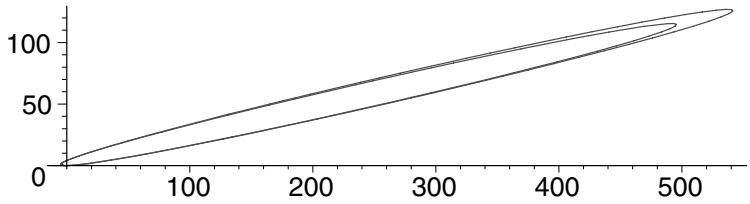

Figure 3.28: Final matching of curves.

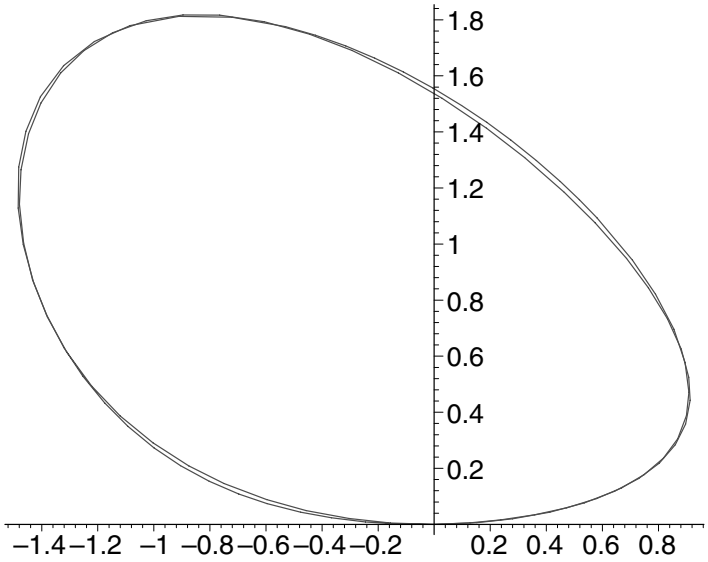

Figure 3.29: Matching of curves to the scale of C_1.

A severe projective transformation is done on another curve $C_2 = \{(X_2(t), U_2(t))\}$ where

$$X_2(t) = \cos(t) + \frac{1}{4}\cos(t)^2$$
$$U_2(t) = \frac{2}{7}\cos(t) + \sin(t) + \frac{1}{10} + \frac{1}{3}\sin(t)^2.$$

C_2 is not a projective transformation of C_1 but has the same number of special affine curvature turning points.

Now both C_1 and C_2 are mapped to their Euclidean canonical form with errors in their canonical points and gradients, see figure 3.30.

The method above is applied and when mapped back to the scale of C_1, figure 3.31 shows they are significantly different. This is consistent with the fact that C_1 and C_2 are not related by a projective transformation.

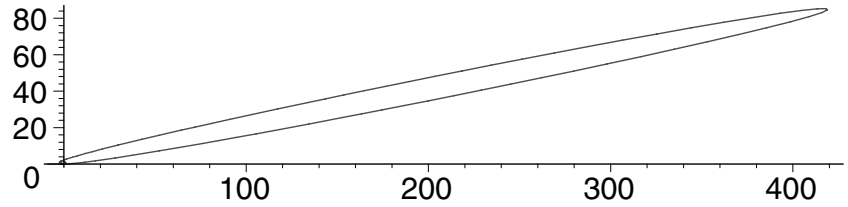

Figure 3.30: Euclidean canonical forms of two convex curves not related by a projective transformation.

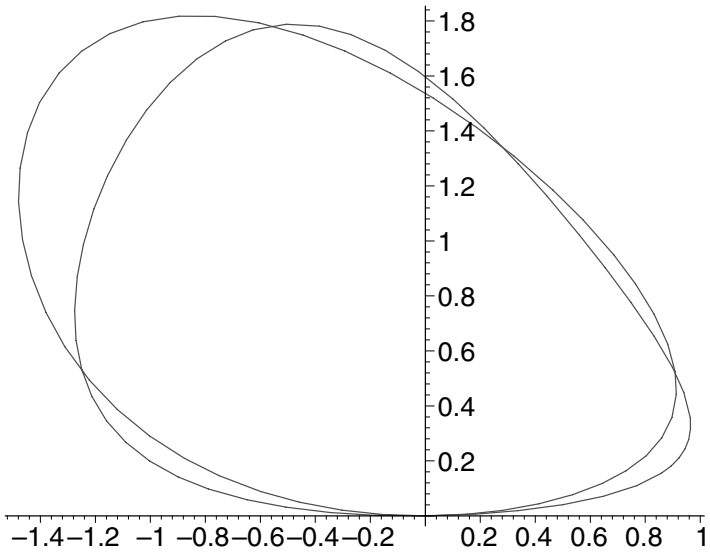

Figure 3.31: Matching curves to the scale of C_1.

3.4 Geometric interpretation.

The projective group action is given by

$$(\bar{x}, \bar{u}) = (\frac{ax + bu + c}{gx + hu + i}, \frac{dx + eu + f}{gx + hu + i}).$$

1. The parameters c and f, allow translation. With $c = 0$ and $f = 0$, the origin of the curve must always remain fixed.

2. With $c = 0$, $f = 0$, the parameter d allows rotation of the curve about the origin. With $d = 0$, the line $u = 0$ must always remain fixed.

3. With $c = 0$, $f = 0$, the parameter b allows any point $(x, u) \neq (0, 0)$ to be mapped onto the u axis. With $b = 0$, the point on curve intersecting the u axis must always remain fixed.

4. With $c = 0$, $f = 0$, $d = 0$, the parameter g can rotate horizontal lines $u = u_0 \neq 0$. With $g = 0$, two points in a horizontal line remain in a horizontal line. Also, substituting $d = 0$ and $u_x = 0$ into the x intercept of the projectively transformed line (2.10) gives $\frac{a}{g}$. That is, with $d = 0$, $g \neq 0$, horizontal lines are mapped to lines each with a common x intercept of $\frac{a}{g}$ independently of the other parameters.

5. With $c = 0$, $f = 0$, $b = 0$, the parameter h can rotate the vertical lines $x = x_0 \neq 0$. With $h = 0$, two points in a vertical line must remain in a vertical line. Also, substituting $b = 0$ and $u_x = \infty$ into the equation (2.12) for $\bar{\alpha}$ gives $\bar{\alpha} = \frac{1}{h}$. That is, with $b = 0$, $h \neq 0$, vertical lines are mapped to lines each with a common u intercept of $\frac{1}{h}$ independently of the other parameters.

6. With the curve in its Euclidean canonical form, that is $c = 0$, $f = 0$, $d = 0$, $e = 1$ and with $g = 0$, $h = 0$, the parameter i scales the u coordinate. Though note that, in the canonical form process, h and i become 0 and 1 simultaneously, see section 3.3.

7. With the curve in its Euclidean canonical form and with $b = 0$, $g = 0$, $h = 0$, $i = 1$, the parameter a scales the x coordinate. It also, with g, h and i arbitrary, rotates lines $u = kx$ through the origin. With $a = 1$, k must remain fixed.

3.5 Global method

The method for concave curves relies on sufficiently large concavities. In the following, a canonical form method will be described which applies to all curves. It utilises the equation

$$\frac{\bar{x}}{\bar{u}} = a\frac{x}{u} + b$$

to place the points used for matching where desired on the curve. Also it enables an error correction method to be formulated (this is implemented in chapter 4).

Consider the two discretised curves of the left-ventricle in their Euclidean canonical form. Now two inflection points of $\frac{x}{u}$ and $\frac{\bar{x}}{\bar{u}}$ are found by detecting when $[ijk]$ changes sign as described in the convex example. Figure 3.32 shows the two curves in their Euclidean canonical form, with the inflection points in each curve denoted by a circle.

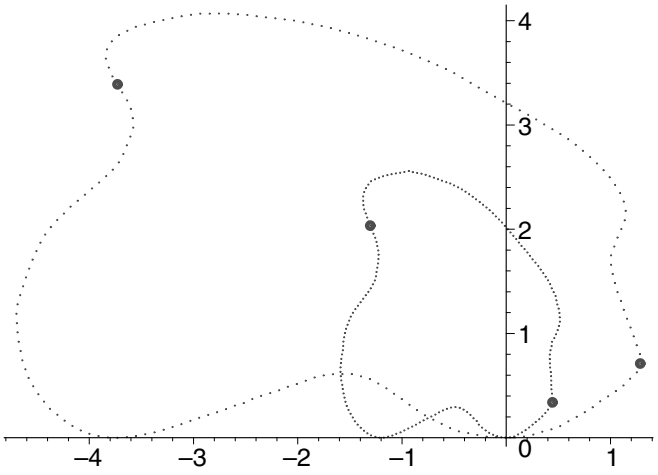

Figure 3.32: Euclidean canonical form of curves with the inflection points of $\frac{x}{u}$ and $\frac{\bar{x}}{\bar{u}}$ denoted by a circle.

The point halfway (in Euclidean arclength) between the bi-tangents on the longer part of curve is found using the distances between the points. Let this point be (x_c, u_c). Let (x_A, u_A), (x_B, u_B) be the two inflection points of $\frac{x}{u}$ and $(\bar{x}_A, \bar{u}_A)$, $(\bar{x}_B, \bar{u}_B)$ be the two inflection points of $\frac{\bar{x}}{\bar{u}}$. Then a and b can be solved to give

$$a = \frac{u_A u_B(\bar{x}_A\bar{u}_B - \bar{x}_B\bar{u}_A)}{\bar{u}_A\bar{u}_B(x_A u_B - x_B u_A)},$$
$$b = \frac{x_A u_B \bar{x}_B\bar{u}_A - \bar{x}_A\bar{u}_B x_B u_A}{\bar{u}_A\bar{u}_B(x_A u_B - x_B u_A)}.$$

Thus the point $(\bar{x}_c, \bar{u}_c)$ which corresponds to (x_c, u_c) satisfies

$$\frac{\bar{x}_c}{\bar{u}_c} = a\frac{x_c}{u_c} + b. \tag{3.9}$$

In general points satisfying (3.9) may not be unique as $\frac{x}{u}$ may have turning points. However if the two $\frac{x}{u}$ turning points P_{TP_1} and P_{TP_2} on each side of (x_c, u_c) are identified with the two $\frac{x}{u}$ turning points $\bar{P}_{\mathrm{TP}_1}$ and $\bar{P}_{\mathrm{TP}_2}$ in $\bar{C}$ then $(\bar{x}_c, \bar{u}_c)$ is the unique point between $\bar{P}_{\mathrm{TP}_1}$ and $\bar{P}_{\mathrm{TP}_2}$ satisfying (3.9). Note the $\frac{x}{u}$ turning points can be identified in each curve by comparing the order in which they appear in the parametrisation from the canonical point.

Note that any two or more inflection points, bi-tangents, special affine curvature turning points, $\frac{x}{u}$ turning points or $\frac{x}{u}$ inflection points could have been used to solve for a and b using least squares.

In this example, the point chosen as an approximation to $(\bar{x}_c, \bar{u}_c)$ is $(\tilde{\bar{x}}_c, \tilde{\bar{u}}_c)$ such that $(\tilde{\bar{x}}_c, \tilde{\bar{u}}_c)$ is the closest to $a\frac{x_c}{u_c} + b$. Also for use below, the points

$$(x_{\mathrm{tmp1}}, u_{\mathrm{tmp1}}) \quad \text{and} \quad (x_{\mathrm{tmp2}}, u_{\mathrm{tmp2}}) \tag{3.10}$$

closest to halfway (in Euclidean arclength) between (x_c, u_c) and the canonical point and (x_c, u_c) and the other bi-tangent respectively are located.

Now using the points (x_c, u_c) and $(\tilde{x}_c, \tilde{u}_c)$, the curves are mapped to their second canonical form so that

$$\frac{\bar{x}}{\bar{u}} = a\frac{x}{u}. \tag{3.11}$$

Let the points corresponding to $(x_{\mathrm{tmp1}}, u_{\mathrm{tmp1}})$ and $(x_{\mathrm{tmp2}}, u_{\mathrm{tmp2}})$ above in the second canonical form of the first curve be (x_1, u_1) and (x_2, u_2). Now an approximation to a, a_{approx} say, is found by taking an average of the values of a determined from the points $\{(x_A, u_A), (x_B, u_B)\}$ and $\{(\bar{x}_A, \bar{u}_A), (\bar{x}_B, \bar{u}_B)\}$, using (3.11). Then after making the second curve piecewise linear, the points $(\bar{x}_1, \bar{u}_1)$ and $(\bar{x}_2, \bar{u}_2)$ are found where $\frac{\bar{x}_1}{\bar{u}_1} = a_{\mathrm{approx}}\frac{x_1}{u_1}$ and $\frac{\bar{x}_2}{\bar{u}_2} = a_{\mathrm{approx}}\frac{x_2}{u_2}$.

Figure 3.33 shows the curves in their second canonical form with the points (x_c, u_c), (x_1, u_1), (x_2, u_2) and their corresponding points in the second curve denoted by a circle. These points are used to match the curves in the same way as was done with the convex curve in the previous section. Figure 3.34 shows a close initial matching.

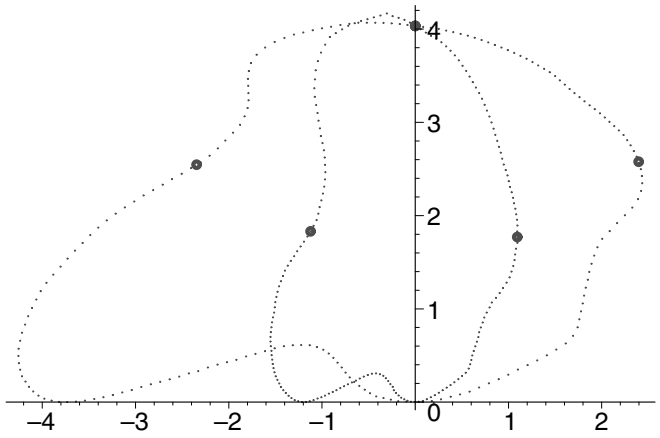

Figure 3.33: Second canonical form of curves with the three points used for matching denoted by a circle

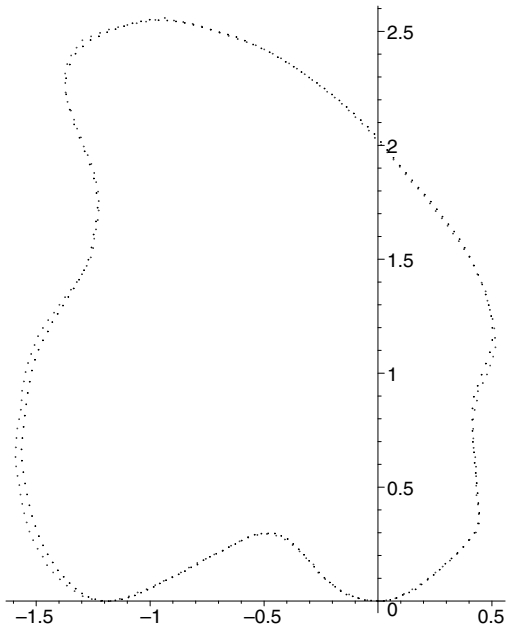

Figure 3.34: Initial matching of the second curve onto the first curve.

Error correction method

In the above method, three points (X_1, U_1), (X_2, U_2), and (X_3, U_3) in the first curve, where (X_3, U_3)=(x_c, u_c), are matched with the corresponding points in the second curve using approximations to the parameters a and b. Thus the error in the initial matching of the second curve onto the first curve (see figure 3.34) only depends on the errors in a and b. Denote the first curve $u = u(x)$ by C_1 and the second curve $\bar{u} = \bar{u}(\bar{x})$ by C_2 where they are both in their Euclidean canonical form.

Let G_{init} be the initial approximation to the projective transformation between C_1 and C_2 and H be the correction factor. That is,

$$C_1 = H \circ G_{\text{init}}(C_2),$$

or equivalently,

$$\tilde{H}(C_1) = G_{\text{init}}(C_2), \tag{3.12}$$

where $\tilde{H} = H^{-1}$. Denote the initial approximations of a and b by $\tilde{a}$ and $\tilde{b}$. G_{init} is found by solving the following set of equations

$$\frac{\alpha\tilde{\bar{X}}_i + \beta\tilde{\bar{U}}_i}{\rho\tilde{\bar{X}}_i + \sigma\tilde{\bar{U}}_i + \tau} = X_i, \quad \frac{\tilde{\bar{U}}_i}{\rho\tilde{\bar{X}}_i + \sigma\tilde{\bar{U}}_i + \tau} = U_i, \quad i = 1, \ldots, 3$$

for α, β, ρ, σ, τ where

$$\frac{\tilde{\bar{X}}_i}{\tilde{\bar{U}}_i} = \tilde{a}\frac{X_i}{U_i} + \tilde{b}. \tag{3.13}$$

This set of equations is equivalent to

$$\alpha\frac{\tilde{\bar{X}}_i}{\tilde{\bar{U}}_i} + \beta = \frac{X_i}{U_i}, \quad \frac{\tilde{\bar{U}}_i}{\rho\tilde{\bar{X}}_i + \sigma\tilde{\bar{U}}_i + \tau} = U_i, \quad i = 1, \ldots, 3.$$

Using (3.13) this can be rewritten as

$$\begin{aligned} \text{eq}_{X_i} &= (\alpha\tilde{a} - 1)\frac{X_i}{U_i} + \alpha\tilde{b} + \beta = 0 \\ \text{eq}_{U_i} &= \frac{\tilde{\bar{U}}_i}{\rho\tilde{\bar{X}}_i + \sigma\tilde{\bar{U}}_i + \tau} - U_i = 0, \quad i = 1, \ldots, 3. \end{aligned} \tag{3.14}$$

However

$$\mathrm{eq}_{X_3} = \frac{\left(\frac{X_3}{U_3} - \frac{X_1}{U_1}\right)}{\left(\frac{X_2}{U_2} - \frac{X_1}{U_1}\right)}(\mathrm{eq}_{X_2} - \mathrm{eq}_{X_1}) + \mathrm{eq}_{X_1}$$

so that eq_{X_3} is redundant. Thus (3.14) is effectively a system of five equations in five unknowns. This is solved for α, β, ρ, σ and τ which gives $\alpha = \frac{1}{\tilde{a}}$, $\beta = -\frac{\tilde{b}}{\tilde{a}}$ and ρ, σ, τ are functions of $\tilde{a}, \tilde{b}, X_i, U_i, \tilde{\tilde{X}}_i, \tilde{\tilde{U}}_i$. Since only the values of α and β are needed below, G_{init} will be denoted by

$$G_{\mathrm{init}} = \left(\frac{1}{\tilde{a}}, -\frac{\tilde{b}}{\tilde{a}}\right).$$

Then the correction factor H will be given by $H = (1+\epsilon, \delta)$ for some small ϵ and δ. Using the same notation, $G_{\mathrm{init}}^{-1} = (\tilde{a}, \tilde{b})$ and $\tilde{H} = H^{-1} = (\frac{1}{1+\epsilon}, -\frac{\delta}{1+\epsilon})$. Thus (3.12) becomes

$$\left(\frac{1}{1+\epsilon}, -\frac{\delta}{1+\epsilon}\right) \cdot C_1 = \left(\frac{1}{\tilde{a}}, -\frac{\tilde{b}}{\tilde{a}}\right) \cdot C_2 \tag{3.15}$$

where $(\frac{1}{1+\epsilon}, -\frac{\delta}{1+\epsilon})$ is the resulting projective transformation which maps the points $(\tilde{X}_i, \tilde{U}_i)$ in C_1 to (X_i, U_i), $i = 1, \ldots, 3$, where

$$\frac{\tilde{X}_i}{\tilde{U}_i} = (1+\epsilon)\frac{X_i}{U_i} + \delta.$$

Note that in this case, C_2 is fixed and C_1 is perturbed, see figure 3.35.

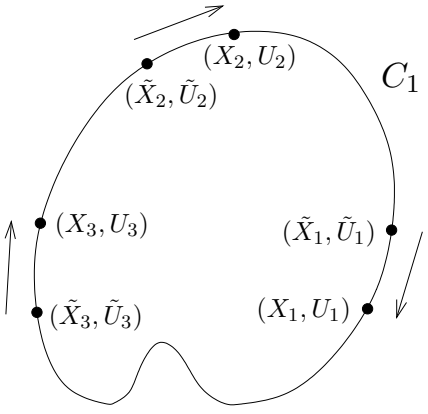

Figure 3.35: Perturbing C_1.

So given $G_{\mathrm{init}}(C_2)$, the error correction method will involve varying ϵ and δ until (3.15) is satisfied. In the following chapter a method for implementing this error correction is presented.

Chapter 4

Error correction

In this chapter it is shown how the error correction method outlined in section 3.5, can be implemented in practice. Section 4.1 demonstrates a method of correcting the error in the initial matching of the left-ventricle (see figure 3.34). Note that this method is more elaborate than it needs to be but it lead to the method in section 4.4 which is much simpler. Also in section 4.1 is an error bound test based on the $\frac{x}{u}$ turning points. This test must be passed before error correction is performed. An example is given where two different curves are distinguished using this $\frac{x}{u}$ turning point test.

In the section 4.2 an analytical error analysis using Taylor series is done which shows how the positions of the points placed on the first curve can significantly affect the error in the matching. The first order terms in Taylor series can be used to ensure this error is minimal. Included in this error analysis is the case when the points chosen in the first curve have the same u coordinate. The reason for this is that the points in this form can be utilised to give an error bound for quickly rejecting curves and this error bound can be applied to convex curves. This is demonstrated in section 4.3 with two examples of convex curves.

Section 4.4 gives an error correction method which is based on the method of section 4.1 but is much simpler.

4.1 Correcting error and rejecting curves

Consider again the formula for error correction given by (3.15). For a given $\tilde{a}$ and $\tilde{b}$ if ϵ and δ are known then

$$\begin{aligned} C_1 &= \left(\frac{1}{1+\epsilon}, -\frac{\delta}{1+\epsilon}\right)^{-1} \cdot \left(\frac{1}{\tilde{a}}, -\frac{\tilde{b}}{\tilde{a}}\right) \cdot C_2 \\ &= \left(\frac{1+\epsilon}{\tilde{a}},\ \delta - \frac{\tilde{b}(1+\epsilon)}{\tilde{a}}\right) \cdot C_2. \end{aligned}$$

This is equivalent to mapping $(\bar{X}_i, \bar{U}_i)$ in C_2 to (X_i, U_i) in C_1 where

$$\frac{\bar{X}_i}{\bar{U}_i} = \frac{\tilde{a}}{1+\epsilon}\frac{X_i}{U_i} + \tilde{b} - \frac{\tilde{a}\delta}{1+\epsilon}.$$

That is given ϵ, δ, $\tilde{a}$ and $\tilde{b}$, the true values of a and b are given by

$$a = \frac{\tilde{a}}{1+\epsilon}, \quad b = \tilde{b} - \frac{\tilde{a}\delta}{1+\epsilon}.$$

Once these are known the error in the initial matching can be corrected for.

Alternatively let $\tilde{C}_2 = (\frac{1}{\tilde{a}}, -\frac{\tilde{b}}{\tilde{a}}) \cdot C_2$. Then

$$C_1 = (1+\epsilon, \delta) \cdot \tilde{C}_2.$$

So $\tilde{C}_2$ can be matched to C_1 by finding the projective transformation that maps $(\tilde{X}_i, \tilde{U}_i) \in \tilde{C}_2$ to $(X_i, U_i) \in C_1$ where

$$\frac{\tilde{X}_i}{\tilde{U}_i} = \frac{1}{1+\epsilon}\frac{\tilde{X}_i}{\tilde{U}_i} - \frac{\delta}{1+\epsilon}, \quad i = 1, \ldots, 3.$$

Thus the error in the initial matching is corrected.

Before the error correction method is applied an error bound test based on the $\frac{x}{u}$ turning points must be passed. Let d_{error} be an estimate of the accuracy of the discretisation of the first curve and (x_T, u_T) be the $\frac{x}{u}$ turning point between the bi-tangents in first curve. Consider the points (x_T^-, u_T^-) and (x_T^+, u_T^+) which are a perpendicular distance of d_{error} from (x_T, u_T) see figure 4.1.

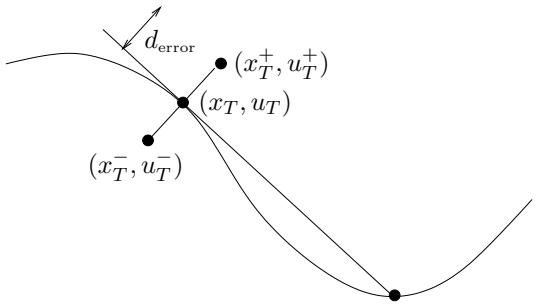

Figure 4.1: Points (x_T^-, u_T^-) and (x_T^+, u_T^+), a perpendicular distance of d_{error} from (x_T, u_T).

For the left ventricle this value was chosen to be 0.01 which was based on the thickness of the boundary of the cluster of points in original .jpg image. Let,

$$\epsilon_{\max} = \max\left(\left|\frac{x_T^-}{u_T^-}\right| , \left|\frac{x_T^+}{u_T^+}\right| \right)$$

be the error bound on the $\frac{x}{u}$ turning point. Let $(\bar{x}_T, \bar{u}_T)$ be the $\frac{\bar{x}}{\bar{u}}$ turning point on the second curve. When the second curve is mapped to the first curve with $(\bar{x}_T, \bar{u}_T) \longmapsto (\tilde{x}_T, \tilde{u}_T)$ say, it is required that

$$\left| \frac{\tilde{x}_T}{\tilde{u}_T} - \frac{x_T}{u_T} \right| < \epsilon_{\max}. \tag{4.1}$$

If for the initial values of b and a (4.1) does not hold, then fix b at the initial value and vary a to try and make (4.1) hold. If no a is found within say ± 0.1 of the initial value of a, repeat this on other values of b in a neighbourhood of the initial b until (4.1) holds. Note that this limit of ± 0.1 only applies if there is only one $\frac{x}{u}$ turning point. If there is two or more $\frac{x}{u}$ turning points then for each b the limits on a where (4.1) hold will be found and these values of a will be tested with the other turning points. See section 4.1.2 for an example of this.

Now consider the points $(\tilde{\bar{X}}_i, \tilde{\bar{U}}_i) \in C_2$ and $(X_i, U_i) \in C_1$ such that

$$\frac{\tilde{\bar{X}}_i}{\tilde{\bar{U}}_i} = \tilde{a}\frac{X_i}{U_i} + \tilde{b} \quad i = 1, \ldots, 3.$$

Without loss of generality $X_2 = 0$ as the transformation $(X, U) \longmapsto (X - \frac{X_2}{U_2}U, U)$ can be applied to C_1 so that $(X_2, U_2) \longmapsto (0, U_2)$. Thus

$$\frac{\tilde{\bar{X}}_2}{\tilde{\bar{U}}_2} = \tilde{b}.$$

Consider the graph $\frac{\bar{x}}{\bar{u}} = \frac{\bar{x}}{\bar{u}}(t)$ (where $\bar{x}(0) = 0 = \bar{u}(0)$), with three values $\tilde{b} - \gamma, \tilde{b}, \tilde{b} + \gamma$ (small $\gamma > 0$) and their corresponding t values t_2^-, t_2, t_2^+, see figure 4.2. These t values will correspond to the points $(\tilde{\bar{X}}_2^-, \tilde{\bar{U}}_2^-), (\tilde{\bar{X}}_2, \tilde{\bar{U}}_2)$, $(\tilde{\bar{X}}_2^+, \tilde{\bar{U}}_2^+)$ as shown in figure 4.3.

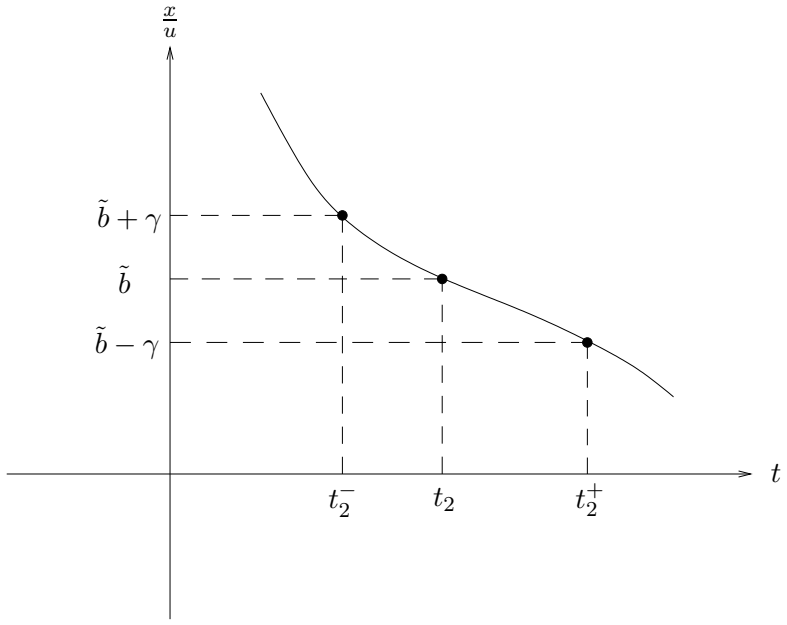

Figure 4.2: Graph of $\frac{\bar{x}}{\bar{u}}$ versus t.

As γ increases t_2^- and t_2^+ will move further away from t_2 thus $(\tilde{\bar{X}}_2^-, \tilde{\bar{U}}_2^-)$ and $(\tilde{\bar{X}}_2^+, \tilde{\bar{U}}_2^+)$ will move further away from $(\tilde{\bar{X}}_2, \tilde{\bar{U}}_2)$.

Alternatively as γ increases the slope of the line from the origin to $(\tilde{\bar{X}}_2^+, \tilde{\bar{U}}_2^+)$ where $\frac{\tilde{\bar{X}}_2^+}{\tilde{\bar{U}}_2^+} = \tilde{b} - \gamma$ will increase (since $\frac{\tilde{\bar{X}}_2^+}{\tilde{\bar{U}}_2^+}$ decreases). Similarly the slope of the line from the origin to $(\tilde{\bar{X}}_2^-, \tilde{\bar{U}}_2^-)$ will decrease as can be seen in figure 4.3.

Thus the effect of varying $\tilde{b}$ from its initial position is to move the point $(\tilde{\bar{X}}_2, \tilde{\bar{U}}_2)$, where $\frac{\tilde{\bar{X}}_2}{\tilde{\bar{U}}_2} = \tilde{b}$ further away from its initial position. Thus a limit can be put on the amount that $\tilde{b}$ can vary by limiting how far the point $(\tilde{\bar{X}}_2, \tilde{\bar{U}}_2)$ can move from its initial position, say five percent of the total arclength of the curve. If the test (4.1) fails for $\tilde{b}$ within this limit the curves are rejected as being different.

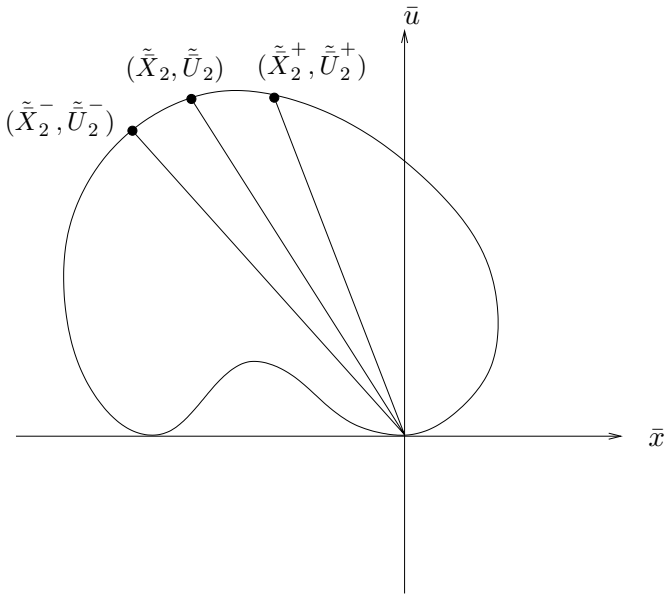

Figure 4.3: Graph of $\bar{u} = \bar{u}(\bar{x})$.

4.1.1 Left-ventricle

For the left-ventricle, the initial values of $\tilde{a}$ and $\tilde{b}$ passed the $\frac{x}{u}$ turning point test (4.1) so error correction is now performed.

Equally space seven points in Euclidean arclength around C_1 between the bi-tangents. These will include the two points (3.10) and (x_c, u_c) which are the points used in section 3.5 to get the initial matching shown in figure 3.34. Denote the points by $p_i = (x_i, u_i)$, $i = 1, \ldots, 9$, where p_1 is the canonical point $(0, 0)$, p_9 is the other bi-tangent. Figure 4.4 shows these nine points on the left-ventricle.

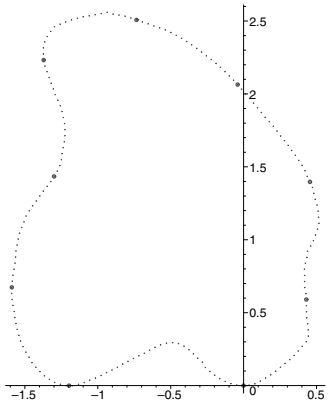

Figure 4.4: Nine points p_i, $i = 1, \ldots, 9$ around the left-ventricle including the canonical point $p_1 = (0, 0)$, the other bi-tangent p_9.

Apply the transformation $(x,u) \longmapsto (x - \frac{x_5}{u_5}u, u)$ to C_1 so that (x_5, u_5) is mapped to $(0, u_5)$. Denote the resulting nine points by $P_i = (X_i, U_i)$, where $X_5 = 0$. For simplicity the same notation C_1 will be used for the resulting curve.

Now using the approximations $\tilde{a} = a_{\text{approx}} = 1.50329$ (calculated in section 3.5) and $\tilde{b} = -0.5795$ to a and b find the points $\bar{P}_i = (\bar{X}_i, \bar{U}_i)$, $i = 2, \ldots, 8$, in the second curve where

$$\frac{\bar{X}_i}{\bar{U}_i} = \tilde{a}\frac{\bar{X}_i}{U_i} + \tilde{b}.$$

Compute the projective joint-invariants $\{J_{1,12345}, J_{2,12345}\}$, $\ldots$, $\{J_{1,56789}, J_{2,56789}\}$. Note that in order to keep a control on the size of the joint-invariant, if any joint-invariant has $J_{n,ijklm} > 1$ then $\frac{1}{J_{n,ijklm}}$ is used.

Compute the corresponding joint-invariants (denote these by $\bar{J}$) in the second curve and define

$$\bar{J}_{\text{L\_sqrs}} = \sqrt{\{(\bar{J}_{1,12345} - J_{1,12345})^2 + (\bar{J}_{2,12345} - J_{2,12345})^2\} + \cdots + \{(\bar{J}_{1,56789} - J_{1,56789})^2 + (\bar{J}_{2,56789} - J_{2,56789})^2\}}$$

Note it was shown in section 2.1.2 that if these nine points in each curve all have the same joint-invariants (this is equivalent to $\bar{J}_{\text{L\_sqrs}} = 0$) then the nine points in each curve must be related by a projective transformation.

Now to represent the error in the matching, $\tilde{b}$ is fixed and a is varied until $\bar{J}_{\text{L\_sqrs}}$ is a minimum, call this value $\bar{J}_{\text{best}}$. The signs of $\Delta\bar{J}_1 = \bar{J}_{1,34567} - J_{1,34567}$ and $\Delta\bar{J}_2 = \bar{J}_{2,34567} - J_{2,34567}$ are then computed. The parameter $\tilde{a}$ was varied in the following way.

First for the values of $a = \tilde{a} = 1.50329$ and $a = \tilde{a} \pm 0.02$, $\bar{J}_{\text{L\_sqrs}}$ was calculated so that the direction of decreasing $\bar{J}_{\text{L\_sqrs}}$ could be found. Then a was varied in steps of 0.02 in this direction until the value of $a = a_{0.02,\text{best}}$ corresponding to the minimum value of $\bar{J}_{\text{L\_sqrs}}$ was found, then was further varied 0.01 each side of $a = a_{0.02,\text{best}}$ to find the minimum value of $\bar{J}_{\text{L\_sqrs}}$. This final minimum value of $\bar{J}_{\text{L\_sqrs}}$ was used as the value for $\bar{J}_{\text{best}}$ corresponding to $b = \tilde{b}$, see above. The following table shows a list of the values of a and the corresponding values of $\bar{J}_{\text{L\_sqrs}}$ for the initial value of $b = \tilde{b} = -0.5795$, the values are to four significant figures. Figure 4.5 shows a plot of these values. The order in which a was varied was, $a - \tilde{a} = 0,\ 0.02,\ -0.02,\ -0.04,\ -0.06,\ -0.05,\ -0.03$.

Table of the values of a and $\bar{J}_{\text{L\_sqrs}}$

$a-\tilde{a}$	$\bar{J}_{\text{L\_sqrs}}$
-0.06	0.06184
-0.05	0.05583
-0.04	0.05155
-0.03	0.05011
-0.02	0.05167
0	0.06294
0.02	0.09288

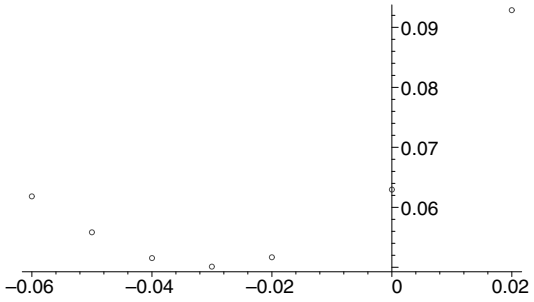

Figure 4.5: A plot of $\bar{J}_{\text{L\_sqrs}}$ versus $a-\tilde{a}$.

In addition, $\bar{J}_{\text{best}} = 0.05011$, $\Delta\bar{J}_1 = 0.01097$ and $\Delta\bar{J}_2 = 0.01990$. The signs of $\Delta\bar{J}_1$ and $\Delta\bar{J}_2$ will characterise what side $\tilde{b}$ is from the true value of b and $\bar{J}_{\text{best}}$ will give the amount that $\tilde{b}$ differs from the true value of b, see below.

From section 3.5 it is now required to find ϵ and δ such that

$$\left(\frac{1}{1+\epsilon}, -\frac{\delta}{1+\epsilon}\right)\cdot C_1 = \left(\frac{1}{\tilde{a}-0.03}, -\frac{\tilde{b}}{\tilde{a}-0.03}\right)\cdot C_2 \tag{4.2}$$

where $\tilde{a}$ is replaced by $\tilde{a}-0.03$ as this corresponds to $\bar{J}_{\text{best}}$ above.

Note that the transformation $(\frac{1}{1+\epsilon}, -\frac{\delta}{1+\epsilon})$ is found from mapping $(\tilde{X}_i, \tilde{U}_i)$ in C_1 to (X_i, U_i) where

$$\frac{\tilde{X}_i}{\tilde{U}_i} = (1+\epsilon)\frac{X_i}{U_i} + \delta \tag{4.3}$$

and $i = 1, \ldots, 3$. Also the transformation $(\frac{1}{\tilde{a}-0.03}, -\frac{\tilde{b}}{\tilde{a}-0.03})$ is found by mapping $(\tilde{\tilde{X}}_i, \tilde{\tilde{U}}_i)$ in C_2 to (X_i, U_i) in C_1 where

$$\frac{\tilde{\tilde{X}}_i}{\tilde{\tilde{U}}_i} = (\tilde{a}-0.03)\frac{X_i}{U_i} + \tilde{b}$$

and $i = 1, \ldots, 3$.

Compute the joint-invariants $\{\tilde{J}_{1,12345}, \tilde{J}_{2,12345}\}$, $\ldots$, $\{\tilde{J}_{1,56789}, \tilde{J}_{2,56789}\}$ corresponding to the points $(\tilde{X}_i, \tilde{U}_i)$, $i = 2, \ldots, 8$ satisfying (4.3) and the bi-tangent points $(\tilde{X}_1, \tilde{U}_1) = (X_1, U_1) = (0, 0)$ and $(\tilde{X}_9, \tilde{U}_9) = (X_9, U_9)$. Define

$$J_{\text{L\_sqrs}} = \sqrt{\{(\tilde{J}_{1,12345} - J_{1,12345})^2 + (\tilde{J}_{2,12345} - J_{2,12345})^2\} + \cdots + \{(\tilde{J}_{1,56789} - J_{1,56789})^2 + (\tilde{J}_{2,56789} - J_{2,56789})^2\}}$$

and $\Delta\tilde{J}_1 = \tilde{J}_{1,34567} - J_{1,34567}$ and $\Delta\tilde{J}_2 = \tilde{J}_{2,34567} - J_{2,34567}$.

The error correction now takes the form of varying ϵ and δ and perturbing points in the first curve (C_2 remains fixed and has no part in this calculation) until the value of $\bar{J}_{\text{best}}$ and the signs of $\Delta\bar{J}_1$ and $\Delta\bar{J}_2$ are reproduced. (This is equivalent to finding the ϵ and δ that satisfy (4.2)). This is achieved in the following way.

For a fixed δ, ϵ is varied and for each ϵ, the points $\tilde{P}_i = (\tilde{X}_i, \tilde{U}_i)$, $i = 2, \ldots, 8$, where

$$\frac{\tilde{X}_i}{\tilde{U}_i} = (1 + \epsilon)\frac{X_i}{U_i} + \delta$$

are found with $\tilde{P}_1 = (\tilde{X}_1, \tilde{U}_1) = (X_1, U_1) = (0, 0)$ and $\tilde{P}_9 = (\tilde{X}_9, \tilde{U}_9) = (X_9, U_9)$. Then the joint-invariants are calculated involving the points P_i and $\tilde{P}_i$, $i = 1, \ldots, 9$ and $J_{\text{L\_sqrs}}$ is calculated.

For each fixed δ, ϵ is varied until $J_{\text{L\_sqrs}}$ is a minimum, call this value $J_{(\delta,\epsilon)\text{best}}$ and the signs of $\Delta\tilde{J}_1 = \tilde{J}_{1,34567} - J_{1,34567}$ and $\Delta\tilde{J}_2 = \tilde{J}_{2,34567} - J_{2,34567}$ are calculated. This is done in the same way as a was varied to get $\bar{J}_{\text{best}}$ above. The values of δ used were based on the discretisation of C_1 surrounding (X_5, U_5) (δ is determined by $\delta = \frac{\tilde{X}_5}{\tilde{U}_5}$ since $X_5 = 0$) and the amount that δ was varied was until $J_{(\delta,\epsilon)\text{best}}$ was twice that of $\bar{J}_{\text{best}}$ to ensure the error in the initial matching of C_2 onto C_1 is covered. This corresponded to four values of δ. The following table shows the results for these values of δ. Also shown using a number in brackets, is the order for how the ϵ was varied, the values are to four significant figures. Figure 4.6 shows a plot of $J_{\text{L\_sqrs}}$ versus ϵ for the case $\delta = -0.01419$.

Table of the values of ϵ and $J_{\text{L\_sqrs}}$ for different values of δ

ϵ	$\delta = -0.02853$	$\delta = -0.01419$	$\delta = 0.01403$	$\delta = 0.02840$
-0.08				0.1557 (6)
-0.07				0.1402 (7)
-0.06				0.1297 (5)
-0.05				0.1351 (8)
-0.04			0.07183 (4)	0.1572 (4)
-0.03			0.05852 (5)	
-0.02	0.09889 (2)	0.07475 (2)	0.05806 (3)	0.2356 (3)
-0.01			0.09095 (6)	
0	0.08792 (1)	0.04896 (1)	0.1399 (1)	0.3743 (1)
0.01	0.08508 (5)	0.04273 (6)		
0.02	0.08397 (3)	0.04471 (3)	0.2542 (2)	0.5517 (2)
0.03	0.08315 (6)	0.05463 (5)		
0.04	0.08572 (4)	0.06973 (4)		

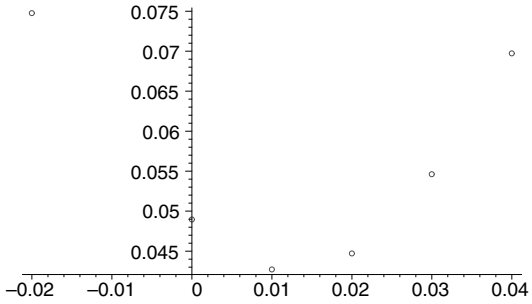

Figure 4.6: A plot of $J_{\text{L\_sqrs}}$ versus ϵ for the case $\delta = -0.01419$.

The following table shows the values of $J_{(\delta,\epsilon)\text{best}}$, $\Delta\tilde{J}_1$ and $\Delta\tilde{J}_2$ for each of the four δ values. Figure 4.7 shows the plot of J_{best} versus δ. The origin has been included in this plot as when $\delta = 0$, $J_{\text{best}} = 0$. This point serves as a reference to the other points. The value of δ must be found which has $J_{(\delta,\epsilon)\text{best}}$ coinciding with $\bar{J}_{\text{best}}$ as well as the signs of $\Delta\tilde{J}_1$ and $\Delta\tilde{J}_2$ coinciding with the signs of $\Delta\bar{J}_1$ and $\Delta\bar{J}_2$.

Table of the values of $J_{(\delta,\epsilon)\text{best}}$, $\Delta\tilde{J}_1$ and $\Delta\tilde{J}_2$ for each δ

δ	$J_{(\delta,\epsilon)\text{best}}$	$[\Delta\tilde{J}_1,\Delta\tilde{J}_2]$
-0.02853	0.08315	[0.01232,0.02217]
-0.01419	0.04273	[0.00491,0.00870]
0	0	[0,0]
0.01403	0.05806	[-0.00910,-0.01628]
0.02840	0.1297	[-0.01171,-0.02088]

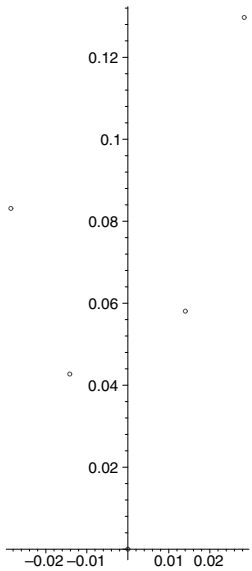

Figure 4.7: A plot of $J_{(\delta,\epsilon)\text{best}}$ versus δ.

Note that these matching corrections are performed on C_1. Thus in practice, a characterisation of the error in the matching corresponding to a number of values of δ could be stored before hand. When this curve is required to be recognised under a viewing transformation, the initial error in the matching will be able to be immediately corrected for.

The signs of $\Delta\bar{J}_1$ and $\Delta\bar{J}_2$ calculated earlier are both positive and the table above shows that positive values of $\Delta\tilde{J}_1$ and $\Delta\tilde{J}_2$ correspond to negative values of δ. Thus $\bar{J}_{\text{best}} = 0.05011$ lies between 0.04273 and 0.08315 and using a linear interpolant gives $\delta = -0.017$. Furthermore, for $J_{(\delta,\epsilon)\text{best}} = 0.04273$, $\epsilon_{\text{best}} = 0.03$ and for $J_{(\delta,\epsilon)\text{best}} = 0.08315$, $\epsilon_{\text{best}} = 0.01$. To find the ϵ corresponding to $J_{(\delta,\epsilon)\text{best}} = \bar{J}_{\text{best}}$ a linear interpolant is also used giving $\epsilon = 0.014$.

The predicted true value of b is given by

$$b_{\text{true}} = \tilde{b} - \frac{(\tilde{a} - 0.03)\delta}{1 + \epsilon}.$$

That is the correction factor for $\tilde{b}$ is

$$-\frac{(\tilde{a} - 0.03)\delta}{1 + \epsilon} = -0.024.$$

So the initial value of $\tilde{b}$ is corrected then $\tilde{a}$ is varied again (in the same way as before) to find the best joint-invariant matching. (This gave $a_{\text{true}} = 1.45$ which coincided with the predicted value of $a_{\text{true}} = \frac{\tilde{a}-0.03}{1+\epsilon} = 1.45$).

Figure 4.8 shows the resulting matching of C_2 onto the original C_1 after this correction is made, which is very close.

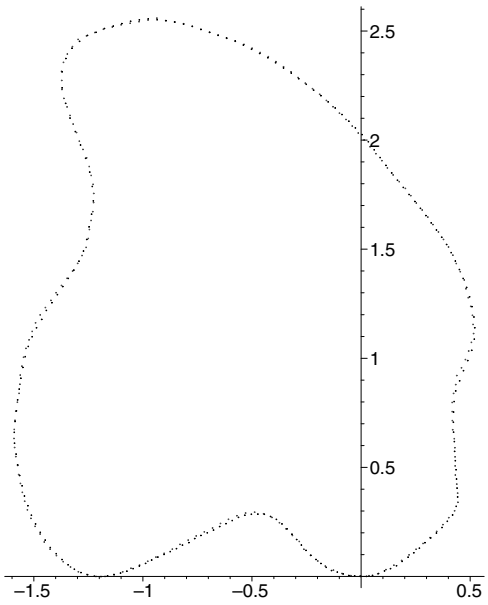

Figure 4.8: Matching after error correction.

Note that it is shown in the section 4.2 that if $\frac{d}{dx}(\frac{x}{u(x)})$ is close to zero at one of the points used for the error correction then small changes in ϵ and δ can cause a large error in the matching. That is $J_{\text{L\_sqrs}}$ would be sensitive to small changes in ϵ and δ making it difficult to locate J_{best} for a fixed δ. However, it is also shown the points can be chosen so that this problem does not occur.

Geometrically this problem can be seen in figure 4.9. Small errors in ϵ and δ which correspond to small changes in the slope $\frac{x}{u}$ cause P_{approx} to move a significant distance away from P_{true}. Thus when P_{approx} is mapped on to P_{true} to match the curves their will be a large error.

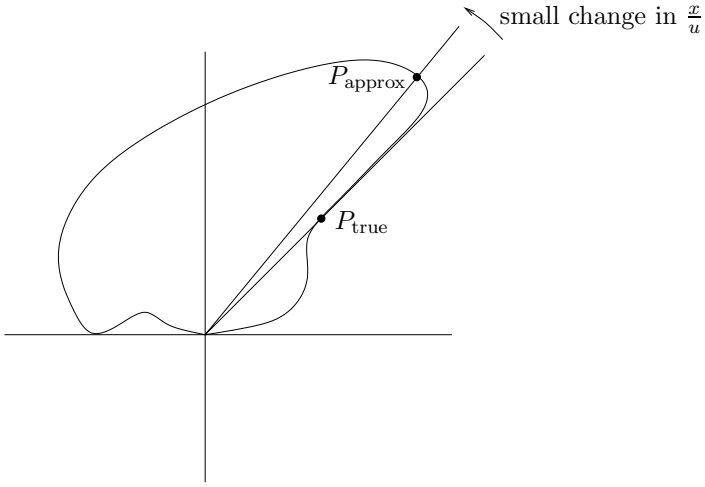

Figure 4.9: Geometrical picture of the situation when $J_{\text{L\_sqrs}}$ is sensitive to small changes in ϵ and δ.

Finally note that although this method worked well in correcting the error in the initial matching of the left-ventricle, the method is much more elaborate than it needs to be. However it lead to a simpler method which is presented in section 4.4.

4.1.2 Different curves

The above method is applied on the two different curves, $C_1 = \{(X_1(t), U_1(t))\}$ and $C_2 = \{(X_2(t), U_2(t))\}$ which were used in the second example of section 3.3

$$X_1(t) = \cos(t)$$
$$U_1(t) = \sin(t) + \sin(\frac{1}{2}t)^2 \cos(t) + \frac{1}{2}\sin(2t)^2$$

$$X_2(t) = \cos(t)$$
$$U_2(t) = \sin(t) + \sin(\frac{1}{2}t)^2 \cos(t) + \frac{2}{3}\sin(2t)^2$$

Three $\frac{x}{u}$ turning points are located in both curves, using their original discretisations ($\sim$ 550 points with random noise added) **before** they are adaptively spaced Figure 4.10 shows the two **adaptively spaced** curves in their Euclidean canonical form, with the $\frac{x}{u}$ turning points in each curve denoted by a circle.

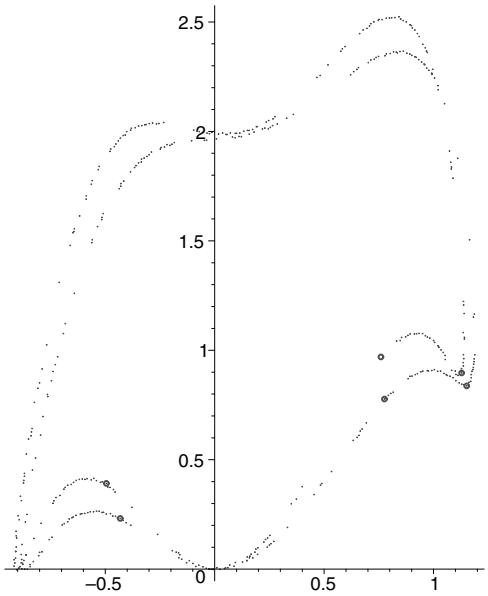

Figure 4.10: Euclidean canonical form of curves with the $\frac{x}{u}$ turning points in each curve denoted by a circle.

The point (x_c, u_c) is chosen in C_1 in the same way as was done for the left-ventricle above and the initial approximations of a and b are obtained from the three $\frac{x}{u}$ turning points by least squares. Also error bounds are put on these $\frac{x}{u}$ turning points based on the discretisation error of the curves. This was approximately 0.01, though the value of d_{error} chosen was 0.015.

Let the three error bounds be $\epsilon_{\max 1}$, $\epsilon_{\max 2}$ and $\epsilon_{\max 3}$, which correspond to the turning point between the two bi-tangents, the minima $\frac{x}{u}$ turning point and the maxima $\frac{x}{u}$ turning point respectively.

The points (x_1, u_1), (x_2, u_2) are chosen in same way as above. But note, that in this case, (x_1, u_1) is very close to an $\frac{x}{u}$ maxima turning point. This restricts how much ϵ and δ can vary in the error characterisation. When finding the point $(\tilde{x}_1, \tilde{u})$ in C_1 where

$$\frac{\tilde{x}_1}{\tilde{u}_1} = (1+\epsilon)\frac{x_1}{u_1} + \delta \tag{4.4}$$

for some ϵ and δ then (4.4) will not have a solution if $(1+\epsilon)\frac{x_1}{u_1} + \delta > \frac{x_{\text{tp}}}{u_{\text{tp}}}$. This can be avoided by choosing a point further away thus allowing more freedom in ϵ and δ. A procedure for doing this is the following. Note that this is for a **maxima** turning point, the procedure for a **minima** turning point is similar.

Let δ^- and δ^+ be the limits placed on how much δ is to be varied in the error characterisation and let $(x_{\text{tp}}, u_{\text{tp}})$ denote the $\frac{x}{u}$ maxima turning point where $\frac{x_{\text{tp}}}{u_{\text{tp}}} > 0$. Choose the point (x_1^0, u_1^0) such that, $\frac{x_1^0}{u_1^0} + \delta^+ = \frac{x_{\text{tp}}}{u_{\text{tp}}}$ and let s_1 be the arclength distance of this point from $(x_{\text{tp}}, u_{\text{tp}})$. Now consider the point (x_1^1, u_1^1) the arclength distance of $2s_1$ from $(x_{\text{tp}}, u_{\text{tp}})$ in the same direction as (x_1^0, u_1^0), see figure 4.11.

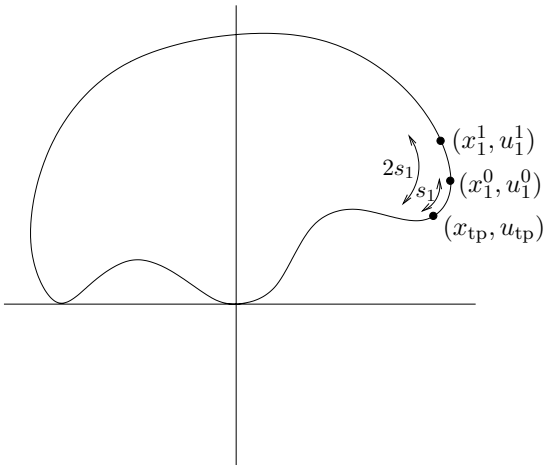

Figure 4.11: Curve showing $\frac{x}{u}$ maxima turning point and points (x_1^0, u_1^0) and (x_1^1, u_1^1).

For this point find $\epsilon_{\text{tp}}^+ > 0$ such that $(1+\epsilon_{\text{tp}}^+)\frac{x_1^1}{u_1^1} + \delta^+ = \frac{x_{\text{tp}}}{u_{\text{tp}}}$. Then compute $J_{\text{L\_sqrs},\epsilon}$ for $\epsilon = \epsilon_{\text{tp}}^+$ and $\epsilon = \epsilon_{\text{tp}}^+ - 0.02$. The value 0.02 is essentially arbitrary but is chosen to test whether J_{best} occurs at a value where $\epsilon < \epsilon_{\text{tp}}^+$ so that $(1+\epsilon_{\text{tp}}^+)\frac{x_1^1}{u_1^1} + \delta^+ < \frac{x_{\text{tp}}}{u_{\text{tp}}}$ and (4.4) will have a solution.

If $J_{\text{L\_sqrs},\epsilon_{\text{tp}}^+ - 0.02} < J^+_{\text{L\_sqrs},\epsilon_{\text{tp}}}$ then this will be the case. If $J_{\text{L\_sqrs},\epsilon_{\text{tp}}^+ - 0.02} > J_{\text{L\_sqrs},\epsilon_{\text{tp}}^+}$ then choose the point (x_1^2, u_1^2) the arclength distance of $3s_1$ from $(x_{\text{tp}}, u_{\text{tp}})$ and continue this process until $J_{\text{L\_sqrs},\epsilon_{\text{tp}}^+ - 0.02} < J^+_{\text{L\_sqrs},\epsilon_{\text{tp}}}$. So that for $\delta = \delta^+$, J_{best} will correspond to a value of ϵ where (4.4) will have a solution.

For $\delta = \delta^-$, find $\epsilon_{\text{tp}}^- > 0$ such that $(1+\epsilon_{\text{tp}}^-)\frac{x_1^2}{u_1^2} + \delta^- = \frac{x_{\text{tp}}}{u_{\text{tp}}}$ and check that $J_{\text{L\_sqrs},\epsilon_{\text{tp}}^- - 0.02} < J^-_{\text{L\_sqrs},\epsilon_{\text{tp}}}$. If this is not true then apply the above process until it is and so for $\delta = \delta^-$, J_{best} will correspond to a value of ϵ where (4.4) will have a solution. Note that this procedure is easily modified for a minima turning point.

The three points in C_2 corresponding to (x_c, u_c), (x_1, u_1) and (x_2, u_2) are found using the initial approximations to a and b. Figure 4.12 shows the curves after they have been mapped to their second canonical form, with the points (x_c, u_c), (x_1, u_1), (x_2, u_2) and their corresponding points in the second curve denoted by a circle. These three points in each curve are used to match the curves. Figure 4.13 shows there is a significant error in the initial matching of the curves, consistent with the fact that the curves are not related by a projective transformation.

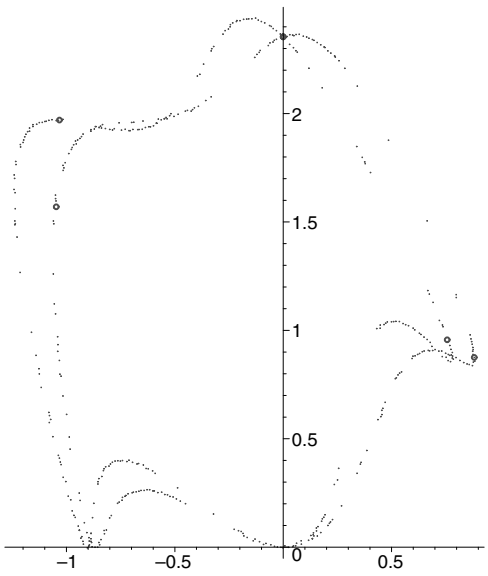

Figure 4.12: Second canonical form of curves with the three points used for matching denoted by a circle.

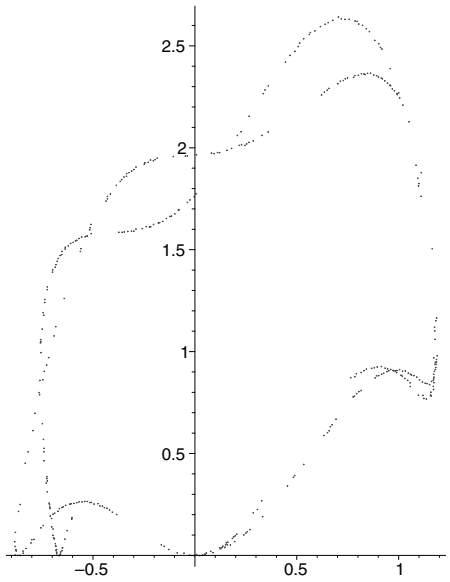

Figure 4.13: Initial matching of curves.

The $\frac{x}{u}$ test is applied on the three $\frac{x}{u}$ turning points with error bounds $\epsilon_{\max 1}$, $\epsilon_{\max 2}$ and $\epsilon_{\max 3}$ from above. First a limit is put on how far b can vary in a neighbourhood of the initial b based on the distance of five percent of the total arclength of the curve C_2. Let this limit correspond to the interval $[b_{\min}, b_{\max}]$.

Now given a and b and the pair of three $\frac{x}{u}$ and $\frac{\bar{x}}{\bar{u}}$ turning points $(x_{\mathrm{tp}_1}, u_{\mathrm{tp}_1})$, $(x_{\mathrm{tp}_2}, u_{\mathrm{tp}_2})$, $(x_{\mathrm{tp}_3}, u_{\mathrm{tp}_3})$ and $(\bar{x}_{\mathrm{tp}_1}, \bar{u}_{\mathrm{tp}_1}), (\bar{x}_{\mathrm{tp}_2}, \bar{u}_{\mathrm{tp}_2}), (\bar{x}_{\mathrm{tp}_3}, \bar{u}_{\mathrm{tp}_3})$ the $\frac{x}{u}$ tests are given by,

$$\left|\frac{1}{a}\left(\frac{\bar{x}_{\mathrm{tp}_1}}{\bar{u}_{\mathrm{tp}_1}} - b\right) - \frac{x_{\mathrm{tp}_1}}{u_{\mathrm{tp}_1}}\right| < \epsilon_{\max 1} \tag{4.5}$$

$$\left|\frac{1}{a}\left(\frac{\bar{x}_{\mathrm{tp}_2}}{\bar{u}_{\mathrm{tp}_2}} - b\right) - \frac{x_{\mathrm{tp}_2}}{u_{\mathrm{tp}_2}}\right| < \epsilon_{\max 2} \tag{4.6}$$

$$\left|\frac{1}{a}\left(\frac{\bar{x}_{\mathrm{tp}_3}}{\bar{u}_{\mathrm{tp}_3}} - b\right) - \frac{x_{\mathrm{tp}_3}}{u_{\mathrm{tp}_3}}\right| < \epsilon_{\max 3} \tag{4.7}$$

Since $\frac{\bar{x}_{\mathrm{tp}_1}}{\bar{u}_{\mathrm{tp}_1}} < 0$, $\frac{x_{\mathrm{tp}_1}}{u_{\mathrm{tp}_1}} < 0$ and $\frac{\bar{x}_{\mathrm{tp}_1}}{\bar{u}_{\mathrm{tp}_1}} - b < 0$ for a given $b \in [b_{\min}, b_{\max}]$, (4.5) is equivalent to

$$\frac{\frac{\bar{x}_{\mathrm{tp}_1}}{\bar{u}_{\mathrm{tp}_1}} - b}{\frac{x_{\mathrm{tp}_1}}{u_{\mathrm{tp}_1}} + \epsilon_{\max 1}} < a < \frac{\frac{\bar{x}_{\mathrm{tp}_1}}{\bar{u}_{\mathrm{tp}_1}} - b}{\frac{x_{\mathrm{tp}_1}}{u_{\mathrm{tp}_1}} - \epsilon_{\max 1}}. \tag{4.8}$$

Now b is equally spaced in increments of 0.02 in $[b_{\min}, b_{\max}]$, and for each b the lower and upper limits of a defined by (4.8) are substituted into (4.6) and (4.7) which in every case fail at least one of these tests. Hence the curves are rejected as different.

4.2 Analytic error analysis

Consider a curve C_1 in its second canonical form, and four points, $(x_1, u_1) = (0, 0)$, (x_2, u_2), $(x_3, u_3) = (0, u_3)$ and (x_4, u_4), see figure 4.14.

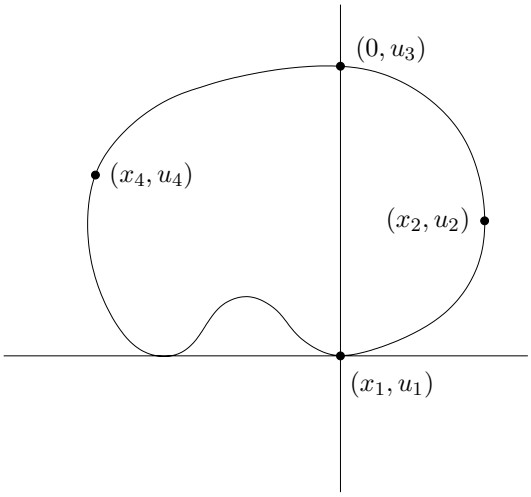

Figure 4.14: Curve C_1 with four points shown.

Denote the derivative at the point $(0, u_3)$ by $u_x^{(3)}$. Consider the transformation

$$(x, u) \longmapsto \left(\frac{x}{gx + 1}, \frac{u}{gx + 1} \right). \tag{4.9}$$

By the chain rule, the derivative $u_x^{(3)}$ transforms by

$$u_x^{(3)} \longmapsto u_x^{(3)} - g u_3.$$

Thus, if the curve is transformed by (4.9) with $g = \frac{u_x^{(3)}}{u_3}$ then $u_x^{(3)}$ will become zero. Thus without loss of generality it can be assumed that $u_x^{(3)} = 0$.

Let (x_c, u_c) be a point with zero gradient. If (x_c, u_c) is mapped to $(0, u_c)$ using the transformation $(x, u) \longmapsto (x - \frac{x_c}{u_c}, u)$ so that C_1 is mapped to its second canonical form then this implies $(0, u_c)$ will have zero gradient.

In a neighbourhood of (x_2, u_2) and (x_4, u_4) represent the curve $u = u(x)$ in the form $x = x(u)$ and in a neighbourhood of (x_3, u_3) keep with the original representation $u = u(x)$. Let h_j, $j = 2, 4$ satisfy

$$\frac{x(u_j + h_j)}{u + h_j} = (1 + \epsilon)\frac{x_j}{u_j} + \delta.$$

for some ϵ and δ. Also let h_3 satisfy,

$$\frac{x_3 + h_3}{u(x_3 + h_3)} = (1+\epsilon)\frac{x_3}{u_3} + \delta = \delta = \frac{h_3}{u(h_3)}$$

since $x_3 = 0$.

The Taylor series of h_2, h_3 and h_4 up to second order derivative terms are given by

$$\begin{aligned}
h_2 &= \frac{U_2}{U_{u_2}}\,\epsilon + \frac{1}{U_{u_2}}\,\delta - \frac{1}{2}\frac{U_2^2 U_{u_2}}{U_{u_2}^3}\,\epsilon^2 - \frac{U_2 U_{uu_2}}{U_{u_2}^3}\,\delta\,\epsilon - \frac{1}{2}\frac{U_{uu_2}}{U_{u_2}^3}\,\delta^2 \\
h_3 &= u_3\,\delta + \frac{1}{2}u_{xx}^{(3)}u_3^2\,\delta^3 \\
h_4 &= \frac{U_4}{U_{u_4}}\,\epsilon + \frac{1}{U_{u_4}}\,\delta - \frac{1}{2}\frac{U_4^2 U_{uu_4}}{U_{u_4}^3}\,\epsilon^2 - \frac{U_4 U_{uu_4}}{U_{u_4}^3}\,\delta\,\epsilon - \frac{1}{2}\frac{U_{uu_4}}{U_{u_4}^3}\,\delta^2
\end{aligned}$$

where

$$U_j = \tfrac{x_j}{u_j}, \quad U_{u_j} = \tfrac{\mathrm{d}}{\mathrm{d}u}\left(\tfrac{x(u)}{u}\right)\Big|_{u=u_j} \text{ and } \quad U_{uu_j} = \tfrac{\mathrm{d}^2}{\mathrm{d}u^2}\left(\tfrac{x(u)}{u}\right)\Big|_{u=u_j}.$$

Also note that

$$U_{u_j} = \frac{x_j U_{x_j}}{(1 - u_j U_{x_j})u_j} \quad j = 2, 4. \tag{4.10}$$

where $U_{x_j} = \tfrac{d}{dx}\left(\tfrac{x}{u(x)}\right)\Big|_{x=x_j}$.

Now using the projective transformation (3.3), the points

$$(\tilde{x}_j, \tilde{u}_j) = (x(u_j + h_j), u + h_j),\ i = 2, 4 \text{ and } (\tilde{x}_3, \tilde{u}_3) = (h_3, u(h_3))$$

are mapped to the points (x_j, u_j), $j = 1, \ldots, 3$ where

$$\frac{\tilde{x}_j}{\tilde{u}_j} = (1+\epsilon)\frac{x}{u} + \delta$$

The parameters of this transformation are given by the solution to the following set of equations

$$\begin{aligned}
\frac{a\tilde{x}_j + b\tilde{u}_j}{g\tilde{x}_j + h\tilde{u}_j + i} - x_j = 0 \\
\frac{\tilde{u}_j}{g\tilde{x}_j + h\tilde{u}_j + i} - u_j = 0
\end{aligned}$$

where $j = 1, \ldots, 3$. This gives

$$a = \frac{1}{1+\epsilon}, \quad b = -\frac{\delta}{1+\epsilon}, \quad g = g(\epsilon, \delta), \quad h = h(\epsilon, \delta), \quad i = i(\epsilon, \delta).$$

The Taylor series of g, h and i up to second order terms are given by

$$
\begin{aligned}
g &= \frac{1}{u_4^2 u_2^2[234]}\left(x_2 u_4^2(u_3-u_4)\hat{\mathrm{U}}_{u_2} - x_4 u_2^2(u_3-u_2)\hat{\mathrm{U}}_{u_4}\right)\epsilon \\
&\quad + \frac{1}{u_4 u_2[234]}\left(u_4(u_3-u_4)\hat{\mathrm{U}}_{u_2} - u_2(u_3-u_2)\hat{\mathrm{U}}_{u_4}\right)\delta \\
&\quad + g_{\epsilon\epsilon}\epsilon^2 + g_{\epsilon\delta}\epsilon\delta + g_{\delta\delta}\delta^2 \\
h &= \frac{1}{u_4^2 u_2^2[234]} x_4 x_2\left(\hat{\mathrm{U}}_{u_2} u_4^2 - u_2^2\hat{\mathrm{U}}_{u_4}\right)\epsilon \\
&\quad + \frac{1}{u_4 u_2[234]}\left(x_4\hat{\mathrm{U}}_{u_2} u_4 - x_2\hat{\mathrm{U}}_{u_4} u_2\right)\delta \\
&\quad + h_{\epsilon\epsilon}\epsilon^2 + h_{\epsilon\delta}\epsilon\delta + h_{\delta\delta}\delta^2 \\
i &= -u_3(h_\epsilon\epsilon + h_\delta\delta) - u_3 h_{\epsilon\epsilon}\epsilon^2 - (u_3 h_{\epsilon\delta} + \delta g_\epsilon) - (u_3 h_{\delta\delta} + \delta g_\delta - \frac{1}{2}u_{xx}^{(3)}\delta^2)\delta^2
\end{aligned}
$$

where $\hat{U}_{u_j} = \frac{1}{U_{u_j}}$ and

$$
\begin{aligned}
g_{\epsilon\epsilon} &= \frac{1}{2u_4^4 u_2^4[234]^2}\Big(- 2(u_4^2 u_2^2[234] + u_3 x_2 x_4(\hat{\mathrm{U}}_{u_2} u_4^2 - u_2^2\hat{\mathrm{U}}_{u_4})) \\
&\quad (x_2 u_4^2(u_3-u_4)\hat{\mathrm{U}}_{u_2} - x_4 u_2^2(u_3-u_2)\hat{\mathrm{U}}_{u_4}) \\
&\quad - x_2^2 u_4^4(u_3-u_4)[234]\hat{\mathrm{U}}_{u_2}^3 x_{uu_2} + x_4^2 u_2^4(u_3-u_2)[234]x_{uu_4}\hat{\mathrm{U}}_{u_4}^3\Big) \\
g_{\epsilon\delta} &= \frac{1}{u_4^3 u_2^3[234]^2}\Big(u_3(x_2u_4 + x_4u_2)u_2u_4(2x_2(u_3-u_4) - [234])\hat{\mathrm{U}}_{u_2}\hat{\mathrm{U}}_{u_4} \\
&\quad - u_4^3 u_2^2(u_3-u_4)[234]\hat{\mathrm{U}}_{u_2} - 2x_2u_3u_2^3x_4(u_3-u_2)\hat{\mathrm{U}}_{u_4}^2 \\
&\quad - 2x_2u_3x_4u_4^3(u_3-u_4)\hat{\mathrm{U}}_{u_2}^2 + u_4^2u_2^3(u_3-u_2)[234]\hat{\mathrm{U}}_{u_4} \\
&\quad - [234]\hat{\mathrm{U}}_{u_2}^3 x_2u_4^3(u_3-u_4)x_{uu_2} + [234]x_4\hat{\mathrm{U}}_{u_4}^3 u_2^3(u_3-u_2)x_{uu_4}\Big) \\
g_{\delta\delta} &= \frac{1}{2u_4^2 u_2^2[234]^2}\Big(- 2u_3(u_4(u_3-u_4)\hat{\mathrm{U}}_{u_2} - u_2(u_3-u_2)\hat{\mathrm{U}}_{u_4}) \\
&\quad (x_4\hat{\mathrm{U}}_{u_2}u_4 - x_2\hat{\mathrm{U}}_{u_4}u_2) - \hat{\mathrm{U}}_{u_2}^3 u_4^2(u_3-u_4)[234]x_{uu_2} \\
&\quad + \hat{\mathrm{U}}_{u_4}^3 u_2^2(u_3-u_2)[234]x_{uu_4} + (u_4-u_2)u_3u_4^2u_2^2[234]u_{xx}^{(3)}\Big) \\
h_{\epsilon\epsilon} &= \frac{1}{2u_4^4 u_2^4[234]^2}\Big(- 2x_2^2x_4^2u_3(\hat{\mathrm{U}}_{u_2}u_4^2 \\
&\quad - u_2^2\hat{\mathrm{U}}_{u_4})^2 - x_2(-x_4x_{uu_4}u_2^4\hat{\mathrm{U}}_{u_4}^3 + x2x_{uu_2}u_4^4\hat{\mathrm{U}}_{u_2}^3)x_4[234]\Big) \\
h_{\epsilon\delta} &= \frac{1}{u_4^3 u_2^3[234]^2}\Big(- x_2u_4^3u_2(u_3-u_4)[234]\hat{\mathrm{U}}_{u_2} + x_4u_2^3u_4(u_3-u_2)[234]\hat{\mathrm{U}}_{u_4} \\
&\quad - 2x_2(\hat{\mathrm{U}}_{u_2}u_4^2 - u_2^2\hat{\mathrm{U}}_{u_4})x_4u_3(x_4\hat{\mathrm{U}}_{u_2}u_4 - x_2\hat{\mathrm{U}}_{u_4}u_2) \\
&\quad - x_2(-x_{uu4}u_2^3\hat{\mathrm{U}}_{u_4}^3 + x_{uu2}u_4^3\hat{\mathrm{U}}_{u_2}^3)x_4[234]\Big)
\end{aligned}
$$

$$
\begin{aligned}
h_{\delta\delta} &= \frac{1}{2u_4^2 u_2^2[234]^2}\Big(- 2u_2u_4^2(u_3-u_4)[234]\hat{\mathrm{U}}_{u_2} + 2u_2^2u_4(u_3-u_2)[234]\hat{\mathrm{U}}_{u_4} \\
&\quad - 2u_3(x_4\hat{\mathrm{U}}_{u_2}u_4 - x_2\hat{\mathrm{U}}_{u_4}u_2)^2 - (x_4x_{uu_2}u_4^2\hat{\mathrm{U}}_{u_2}^3 - x_2x_{uu_4}\hat{\mathrm{U}}_{u_4}^3u_2^2)[234] \\
&\quad + u_3u_4^2u_2^2(x_2-x_4)[234]u_{xx}^{(3)}\Big)
\end{aligned}
$$

Thus points where U_{u_j} are close to zero will result in the coefficients of the Taylor series blowing up. This will cause g, h and i to be very sensitive to small changes in ϵ and δ. Note the problem discussed in the second example of section 3.5 where a point is chosen close to an $\frac{x}{u}$ turning point reappears here since at an $\frac{x}{u}$ turning point, $U_{u_j} = 0$. This is because by (4.10), $U_{u_j} = 0$ if and only if $U_{x_j} = 0$. The Taylor series is undefined at these points. The other possibility for when U_{u_j} is close to zero is when a point is near an inflection point of $\frac{x}{u}$.

Also points where [234] and x_2, x_4 are close to zero will result in the coefficients blowing up. This corresponds to the points (x_2, u_2) and (x_4, u_4) being close to each other.

A way to avoid choosing those points above and to ensure the error is minimal would be to choose points which minimize the first order terms of g and h. This can be done by the following. For each pair of points compute

$$gh_{\text{l\_sqrs}} = \sqrt{(|g_\epsilon| + |g_\delta|)^2 + (|h_\epsilon| + |h_\delta|)^2}$$

say, where g_ϵ, g_δ, h_ϵ and h_δ are the first order terms of g and h then varying the points until $gh_{\text{l\_sqrs}}$ is a minimum. The first order term of i is a constant multiple of the first order term of h and so i does not need to be included.

Now consider the points (x_2, u_2), (x_4, u_4) where $u_4 = u_2$. Putting $u_4 = u_2$ gives a significant simplification to the above Taylor series given by

$$\begin{aligned}
g = &\frac{1}{u_2^2[234]}\Big((u_3 - u_2)(\hat{\mathrm{U}}_{u_2}x_2 - \hat{\mathrm{U}}_{u_4}x_4)\Big)\epsilon \\
&+ \frac{1}{u_2[234]}\Big((u_3 - u_2)(\hat{\mathrm{U}}_{u_2} - \hat{\mathrm{U}}_{u_4})\Big)\delta \\
&+ g_{\epsilon\epsilon}\epsilon^2 + g_{\epsilon\delta}\epsilon\delta + g_{\delta\delta}\delta^2 \\
h = &\frac{1}{u_4^2u_2^2[234]}x_4x_2\left(\hat{\mathrm{U}}_{u_2}u_4^2 - u_2^2\hat{\mathrm{U}}_{u_4}\right)\epsilon \\
&+ \frac{1}{u_4u_2[234]}\left(x_4\hat{\mathrm{U}}_{u_2}u_4 - x_2\hat{\mathrm{U}}_{u_4}u_2\right)\delta \\
&+ h_{\epsilon\epsilon}\epsilon^2 + h_{\epsilon\delta}\epsilon\delta + h_{\delta\delta}\delta^2
\end{aligned}$$

where,

$$
\begin{aligned}
g_{\epsilon\epsilon} &= \frac{1}{2u_2^3[124][234]}\Big((-2(x_2\hat{\mathrm{U}}_{u_2} - x_4\hat{\mathrm{U}}_{u_4})(u_2^2[234] + x_2x_4u_3(\hat{\mathrm{U}}_{u_2} - \hat{\mathrm{U}}_{u_4})) \\
&\quad - [234](x_2^2\hat{\mathrm{U}}^3_{u_2}x_{uu_2} - x_4^2x_{uu_4}\hat{\mathrm{U}}^3_{u_4}))\Big) \\
g_{\epsilon\delta} &= \frac{1}{u_2^2[234][124]}\Big((-(\hat{\mathrm{U}}_{u_2} - \hat{\mathrm{U}}_{u_4})[234]u_2^2 \\
&\quad - [234](\hat{\mathrm{U}}^3_{u_2}x_2x_{uu_2} - \hat{\mathrm{U}}^3_{u_4}x_{uu_4}x_4) \\
&\quad - 2x_2u_3x_4(\hat{\mathrm{U}}^2_{u_2} + \hat{\mathrm{U}}^2_{u_4}) + u_3(x_4 + x_2)^2\hat{\mathrm{U}}_{u_2}\hat{\mathrm{U}}_{u_4})\Big) \\
g_{\delta\delta} &= \frac{1}{2u_2^3[234][124]}\Big((-[234]u_2^2(x_{uu_2}\hat{\mathrm{U}}^3_{u_2} - x_{uu_4}\hat{\mathrm{U}}^3_{u_4}) \\
&\quad - 2u_3u_2^2(\hat{\mathrm{U}}_{u_2} - \hat{\mathrm{U}}_{u_4})(\hat{\mathrm{U}}_{u_2}x_4 - x_2\hat{\mathrm{U}}_{u_4}))\Big)
\end{aligned}
$$

$$
\begin{aligned}
h_{\epsilon\epsilon} &= \frac{1}{2u_2^4[234]^2}\Big((-2x_2^2x_4^2u_3(\hat{\mathrm{U}}_{u_2} - \hat{\mathrm{U}}_{u_4})^2 \\
&\quad - [234]x_2x_4(\hat{\mathrm{U}}^3_{u_2}x_2x_{uu_2} - \hat{\mathrm{U}}^3_{u_4}x_{uu_4}x_4))\Big) \\
h_{\epsilon\delta} &= \frac{1}{u_2^3[234]^2}\Big((-[234]u_2(u_3 - u_2)(\hat{\mathrm{U}}_{u_2}x_2 - \hat{\mathrm{U}}_{u_4}x_4) \\
&\quad - 2x_2(\hat{\mathrm{U}}_{u_2} - \hat{\mathrm{U}}_{u_4})x_4u_3(\hat{\mathrm{U}}_{u_2}x_4 - x_2\hat{\mathrm{U}}_{u_4}) \\
&\quad - x_2(x_{uu_2}\hat{\mathrm{U}}^3_{u_2} - x_{uu_4}\hat{\mathrm{U}}^3_{u_4})x_4[234])\Big) \\
h_{\delta\delta} &= \frac{1}{2u_2^2[234]^2}\Big((-2[234]u_2(u_3 - u_2)(\hat{\mathrm{U}}_{u_2} - \hat{\mathrm{U}}_{u_4}) \\
&\quad - 2u_3(\hat{\mathrm{U}}_{u_2}x_4 - x_2\hat{\mathrm{U}}_{u_4})^2 - (x_4x_{uu_2}\hat{\mathrm{U}}^3_{u_2} - x_2x_{uu_4}\hat{\mathrm{U}}^3_{u_4})[234] \\
&\quad + u_3u_2^2(x_2 - x_4)[234]u^{(3)}_{xx})\Big)
\end{aligned}
$$

Notice that if the two points are chosen where,

$$x_2\hat{\mathrm{U}}_{u_2} - x_4\hat{\mathrm{U}}_{u_4} = u_2(\hat{\mathrm{U}}_{x_2} - \hat{\mathrm{U}}_{x_4}) = 0$$

then g will become second order. Also when $b = 0$ and $g = 0$, $\hat{\mathrm{U}}_{x_2} - \hat{\mathrm{U}}_{x_4}$ transforms by,

$$\overline{\hat{\mathrm{U}}}_{\bar{x}_2} - \overline{\hat{\mathrm{U}}}_{x_4} = \frac{i}{hu_3 + i}(\hat{\mathrm{U}}_{x_2} - \hat{\mathrm{U}}_{x_4}).$$

Thus,

$$\hat{\mathrm{U}}_{x_2} - \hat{\mathrm{U}}_{x_4} = 0$$

is invariant, (that is $x_2u_{x_2} - x_4u_{x_4} = 0$ is invariant).

4.3 Error bound for rejecting curves

Consider two curves $u = u(x)$ and $\bar{u} = \bar{u}(\bar{x})$ where,

$$(\bar{x}, \bar{u}) = \left(\frac{ax}{gx + hu + i}, \frac{u}{gx + hu + i} \right).$$

Assuming $x = 0$, $u(0) = u_0 \neq 0$, and $u_x(0) = 0$ implies

$$\bar{u}_{\bar{x}}(0) = \frac{-gu_0}{a(hu_0 + i)} = \frac{-g}{a}\bar{u}_0.$$

Therefore if a transformation of the form (4.9) is performed on $(\bar{x}, \bar{u})$ that puts $\bar{u}_{\bar{x}}(0) = 0$, then $g = 0$. Thus the two curves are now related by

$$(\bar{x}, \bar{u}) = \left(\frac{ax}{hu + i}, \frac{u}{hu + i} \right).$$

Thus horizontal lines $u_x = 0$ are mapped to horizontal lines $\bar{u}_{\bar{x}} = 0$. This form of the curves will called their **third canonical form**.

Let $|\bar{u}_{\bar{x}}(0)| = \bar{\epsilon}$. Any horizontal line $u_x = 0$ is mapped to $\bar{u}_{\bar{x}} = \frac{-g}{a}\bar{u}$. So for all horizontal lines $u_x = 0$ that pass through $(0, u)$ where u chosen such that $\bar{u} < \bar{u}_0$,

$$|\bar{u}_{\bar{x}}| < \bar{\epsilon},$$

which will serve as a bound for accepting and rejecting curves. The value $\bar{\epsilon}$ will be based on an estimate of the error in the gradient due to noise at the point $(0, \bar{u}_0)$.

Consider the two convex curves $C_1 = \{(X_1(t), U_1(t))\}$ and $\bar{C}_1 = \{(\overline{X}_1(t), \overline{U}_1(t))\}$ where

$$X_1(t) = \cos t + \frac{1}{5}\cos^2 t$$
$$U_1(t) = \frac{1}{2}X_1(t) + \sin t + \frac{1}{10}\sin^2 t$$

and $\bar{C}_1$ is a projective transformation of C_1. These two curves are identical to those used in section 3.3. Both of these curves are mapped to their Euclidean canonical form and C_1 is mapped to its third canonical form by using the point $(x_c, u_c) \in C_1$ with zero gradient. $\bar{C}_1$ is mapped to its third canonical form but an error of $t = -0.2$ is placed in the point $(\bar{x}_c, \bar{u}_c) \in \bar{C}_1$ which corresponds to (x_c, u_c). This error is equivalent to $b = -0.072138$. Also an error of one degree is placed in the gradient. This corresponds to a slope of $\tan^{-1}(\theta) \sim \theta$ where $\theta = \frac{\pi}{180}$. The value chosen for the bound $\bar{\epsilon}$ on the gradient was two degrees.

Three pairs of points $\{P_{a_i} = (x_{a_i}, u_i), P_{b_i} = (x_{b_i}, u_i)\}$, $i = 1, \ldots, 3$ with the same u coordinate are chosen in the first curve where $x_{a_i} > 0$, $x_{b_i} > 0$, $i = 1, \ldots, 3$. The point P_{a_2} was chosen to be the point with vertical gradient with the corresponding point P_{b_2} having a gradient close to vertical. The reason these points were chosen is explained further below.

The points P_{a_1} and P_{a_3} were chosen in the following way. Let $P_{A_1}^{\text{Euc}}$, $P_{A_2}^{\text{Euc}}$, $P_{A_3}^{\text{Euc}}$ and $P_{A_0}^{\text{Euc}}$ in the Euclidean canonical form of C_1 denote the corresponding points to P_{a_1}, P_{a_2}, P_{a_3} and $P_0 = (0, u(0) \neq 0)$. The points P_{a_1} and P_{a_3} are chosen such that $P_{A_1}^{\text{Euc}}$ and $P_{A_3}^{\text{Euc}}$ are halfway in Euclidean arclength between $(0,0)$ and $P_{A_2}^{\text{Euc}}$ and $P_{A_2}^{\text{Euc}}$ and P_0^{Euc}. Figure 4.15 shows C_1 in its third canonical form with the six points $\{P_{a_i}, P_{b_i}\}$, $i = 1, \ldots, 3$ denoted by circles.

The points $(\bar{x}_{a_i}, \bar{u}_{a_i})$ and $(\bar{x}_{b_i}, \bar{u}_{b_i})$ in $\bar{C}_1$ are found using,

$$\frac{\bar{x}}{\bar{u}} = \tilde{a}\frac{x}{u}.$$

Note that these points can be found uniquely since there are no $\frac{x}{u}$ inflection points in a convex curve. Here error is put into $\tilde{a}$ by falsely identifying two points, (x_*, u_*) in C_1 and $(\tilde{\bar{x}}_*, \tilde{\bar{u}}_*)$ in $\bar{C}_1$. That is, a point (x_*, u_*) is chosen in C_1 with a parameter value of $t = 1$ and a point $(\tilde{\bar{x}}_*, \tilde{\bar{u}}_*)$ in chosen in $\bar{C}_1$ with a parameter value of $t = 1.1$. Then

$$\tilde{a} = \frac{\tilde{\bar{x}}_* u_*}{\tilde{\bar{u}}_* x_*}$$

is calculated. Note that, for each value b, $\tilde{a}$ could be calculated by using an

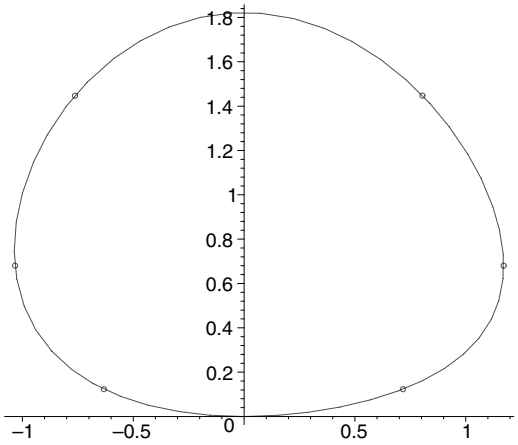

Figure 4.15: Choosing points in first curve.

average of a number of invariant points.

Next

$$m_i = \frac{\bar{u}_{a_i} - \bar{u}_{b_i}}{\bar{x}_{a_i} - \bar{x}_{b_i}}, \quad i = 1, \ldots, 3$$

is calculated. Let $I = [b_{\min}, b_{\max}]$ be the interval that restricts where b can be varied in (see the example of left-ventricle earlier). It is required that for some $b \in I$,

$$|m_i| < \bar{\epsilon}, \quad i = 1, \ldots, 3.$$

Figure 4.16 shows the value of $b = \tilde{b} = -0.072138$ where two of the slopes are greater than two degrees. Thus this value of b is rejected.

The reason for the choice of the points (x_{a_2}, u_2) and (x_{b_2}, u_2) is so that errors in $(\bar{x}_{a_2}, \bar{x}_{a_2})$, $(\bar{x}_{b_2}, \bar{x}_{b_2})$ will show up as much as possible in $|m_2|$. This can be seen in figure 4.16 by comparing this slope to the other the slopes. Notice that the first slope is still essentially horizontal. Figure 4.17 shows the matching of the curves using this rejected b. Note the points (x_{a_2}, u_2) and (x_{b_2}, u_2) are used to match the curves since these points correspond to a value of $gh_{\text{l\_sqrs}}$ close to the minimum value.

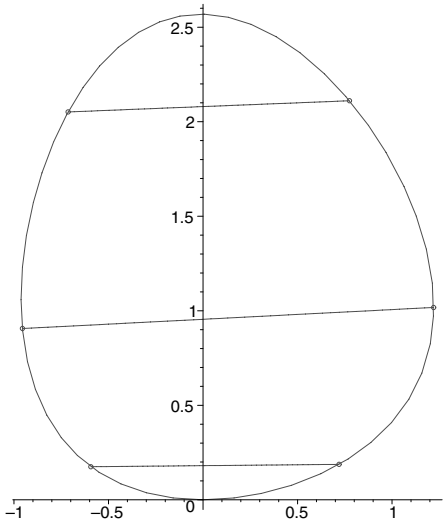

Figure 4.16: Slopes m_i, $i = 1, \ldots, 3$ where the gradient test fails.

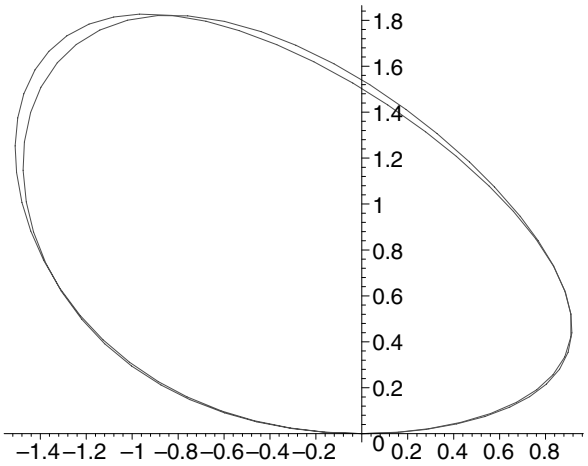

Figure 4.17: Matching of the curves for value of b which is rejected.

The parameter b is varied in steps of 0.01 until the slopes are all less than two degrees. Call this value $b_{<2^\circ}$. Note that for two points (X_1, u_1) and (X_2, U_1) where $\text{sign}(X_1) = -\text{sign}(X_2)$, the effect of varying b is to increase (or decrease) $|\frac{X_1}{U_1}|$ and decrease (or increase) $|\frac{X_2}{U_2}|$. That is the points will move in opposite directions so that the direction of b where the slopes all decrease can be determined by testing 0.01 each side of $\tilde{b}$. Also one further test is done.

The distances d_{ij} between all the points above are computed after the curves are matched. Let $D_{\max} = \max(\Delta x_{\max}, \Delta u_{\max})$ where $\Delta x_{\max}$ and $\Delta u_{\max}$ are the maximum distances across curve in x and u directions. It is then required that for some $b \in I$

$$\frac{d_{ij}}{D_{\max}} < 0.1. \tag{4.11}$$

If one or both of the tests fails, the curves are rejected as being different. An example where both tests fail is demonstrated in the second example below.

For this example, the value of $b_{<2^\circ}$ satisfied (4.11) and figure 4.18 shows the resulting matching. Then b is varied in steps of 0.01 until the m_i are all less than one degree. Figure 4.19 shows an even closer matching.

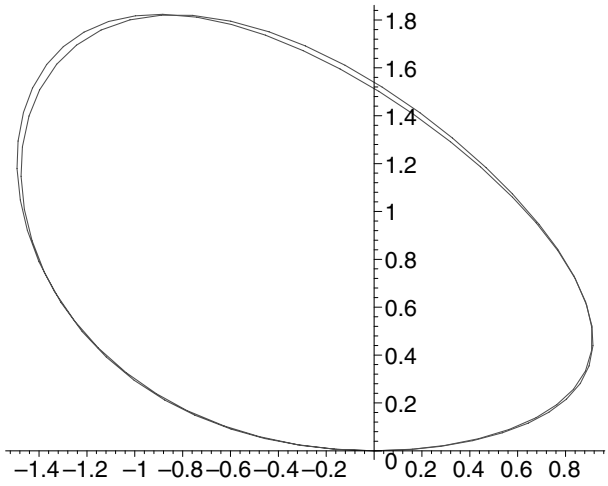

Figure 4.18: Matching of curves when gradient test passes.

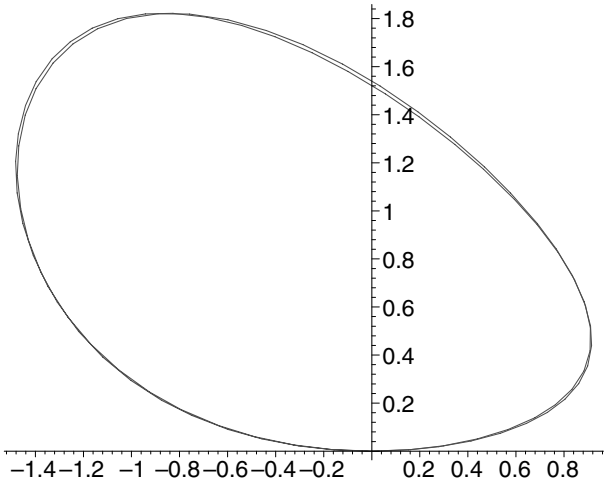

Figure 4.19: Matching of curves when b is varied in steps of 0.01 to give all slopes less than one degree.

This method is now applied to two different convex curves. The initial value of b used was that which corresponded to the points (x_c, u_c) and $(\bar{x}_c, \bar{u}_c)$ in each curve having the same t parameter value. Figure 4.20 shows the slopes m_i, $i = 1, \ldots, 3$, two of which are significantly greater than two degrees. The distance test also failed for this initial b. Figure 4.21 shows the matching for this failed b. Then b is varied in steps of 0.02 in the interval $I = [b_{\min}, b_{\max}]$ starting from $b_{\min}$ and for each b at least one of the two tests failed. Thus the curves are rejected as being different.

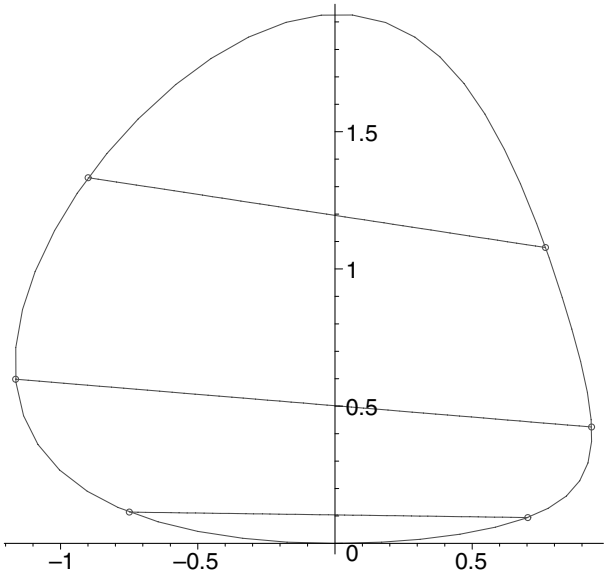

Figure 4.20: Gradients of points in second different curve.

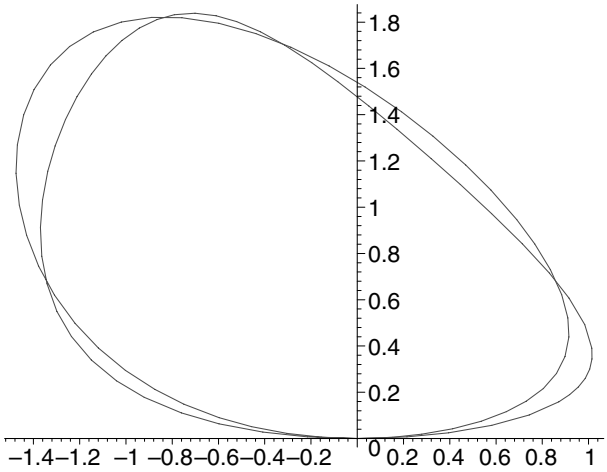

Figure 4.21: Matching of curves with this initial b which fails both gradient and distance tests.

Note that this method will not be used in practice for error correction but gives further understanding of how geometric properties can be used to describe and correct error.

4.4 Simpler method for error correction

Consider the following two curves related by a projective transformation where they are both in their Euclidean canonical forms as shown in figure 4.22.

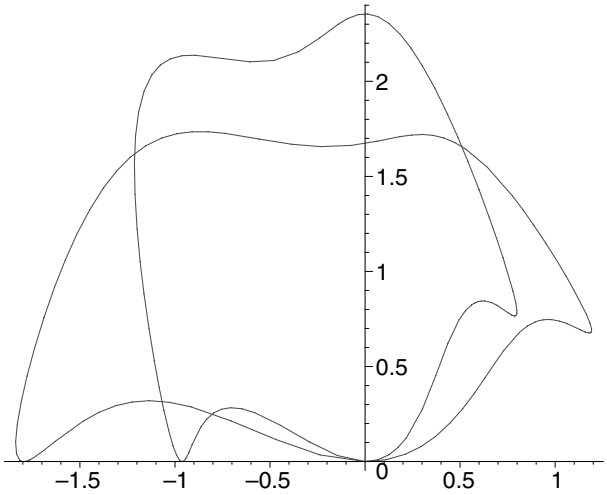

Figure 4.22: Two curves related by a projective transformation, both in their Euclidean canonical forms.

Nine points $P_i = (X_i, U_i),\ i = 1, \ldots, 9$ are placed around the first curve including the canonical point, the other bi-tangent point and the point (X_5, U_5) which has $X_5 = 0$, see figure 4.23.

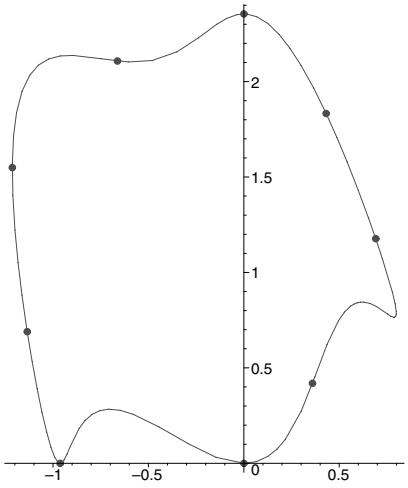

Figure 4.23: First curve with nine points denoted by circles.

Denote this first curve by C_1 and the second curve by C_2. An error of -0.12 is put into the a parameter of the projective transformation and an

error of 0.1 is put into the b parameter. Then the points $\bar{P}_i = (\bar{X}_i, \bar{U}_i) \in C_2,\ i = 2, \ldots, 8$ are found such that

$$\frac{\bar{X}_i}{\bar{U}_i} = \tilde{a}\frac{X_i}{U_i} + \tilde{b}$$

where $\tilde{a} = a - 0.12$ and $\tilde{b} = b + 0.1$. $\bar{P}_1 = (0, 0)$ and $\bar{P}_9$ (the other bi-tangent) remain fixed independent of $\tilde{a}$ and $\tilde{b}$.

The projective transformation that maps the points $\bar{P}_3$, $\bar{P}_5$ and $\bar{P}_7$ to P_3, P_5 and P_7 is then applied to C_2 producing figure 4.24. This represents the initial matching of the curves.

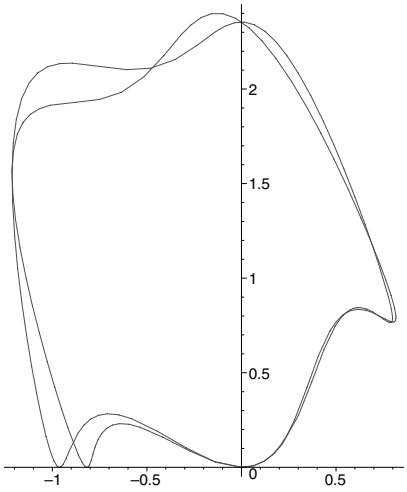

Figure 4.24: Initial matching of C_2 onto C_1.

Let $\tilde{C}_2$ be the resulting curve. Then

$$C_1 = (1 + \epsilon, \delta) \cdot \tilde{C}_2 \tag{4.12}$$

for some small ϵ and δ. Note that $(1 + \epsilon, \delta)$ represents a projective transformation, see section 3.5 for this terminology. The projective transformation $(1 + \epsilon, \delta)$ is the transformation that maps $(\tilde{X}_i^{C_2}, \tilde{U}_i^{C_2}) \in \tilde{C}_2$ to $(X_i, U_i) \in C_1$ where

$$\frac{\tilde{X}_i^{C_2}}{\tilde{U}_i^{C_2}} = \frac{1}{1+\epsilon}\frac{X_i}{U_i} - \frac{\delta}{1+\epsilon}, \quad i = 3, 5, 7. \tag{4.13}$$

The formula (4.12) can be rewritten as

$$\left(\frac{1}{1+\epsilon}, -\frac{\delta}{1+\epsilon}\right) \cdot C_1 = \tilde{C}_2 \tag{4.14}$$

Thus to correct the error in the initial matching given by figure 4.24 it is required to find ϵ and δ such that (4.14) holds.

The joint-invariants $\{\bar{J}_{1,12345}, \bar{J}_{2,12345}\}, \ldots, \{\bar{J}_{1,56789}, \bar{J}_{2,56789}\}$ corresponding to the points $(\bar{X}_i, \bar{U}_i)$, $i = 1, \ldots, 9$ are now computed. For a given ϵ and δ let $\{\tilde{J}_{1,12345}(\epsilon,\delta), \tilde{J}_{2,12345}(\epsilon,\delta)\}$, $\ldots$, $\{\tilde{J}_{1,56789}(\epsilon,\delta), \tilde{J}_{2,56789}(\epsilon,\delta)\}$ be the joint-invariants associated with the points $(\tilde{X}_i, \tilde{U}_i)$, $i = 1, \ldots, 9$ where

$$\frac{\tilde{X}_i}{\tilde{U}_i} = (1+\epsilon)\frac{X_i}{U_i} + \delta, \quad i = 2, \ldots, 8 \tag{4.15}$$

and $(\tilde{X}_1, \tilde{U}_1) = (X_1, U_1) = (0, 0)$, $(\tilde{X}_9, \tilde{U}_9) = (X_9, U_9)$.

Finding ϵ and δ that satisfy (4.14) is equivalent to solving the following system of equations

$$\begin{aligned} \tilde{J}_{1,12345}(\epsilon,\delta) &= \bar{J}_{1,12345}, \quad \ldots \quad \tilde{J}_{1,56789}(\epsilon,\delta) = \bar{J}_{1,56789} \\ \tilde{J}_{2,12345}(\epsilon,\delta) &= \bar{J}_{2,12345}, \quad \ldots \quad \tilde{J}_{2,56789}(\epsilon,\delta) = \bar{J}_{2,56789} \end{aligned}$$

for ϵ and δ. This is an overdetermined system of 10 equations in two unknowns where the analytic expressions for $\tilde{J}_{1,12345}(\epsilon,\delta), \ldots, \tilde{J}_{1,56789}(\epsilon,\delta)$ and $\tilde{J}_{2,12345}(\epsilon,\delta), \ldots, \tilde{J}_{2,56789}(\epsilon,\delta)$ are unknown. However for any given ϵ and δ the numerical value for these joint-invariants can be found by recomputing the points $(\tilde{X}_i, \tilde{U}_i)$, $i = 1, \ldots, 9$ each time that satisfy (4.15) then computing the joint-invariants. Thus the equations can be solved by an iterative scheme using least squares. An initial starting point for the iterative process will be $\epsilon = 0$, $\delta = 0$. Define

$$\begin{aligned} J_1(\epsilon,\delta) &= (\tilde{J}_{1,12345}(\epsilon,\delta) - \bar{J}_{1,12345})^2 + \ldots + (\tilde{J}_{1,56789}(\epsilon,\delta) - \bar{J}_{1,56789})^2 \\ J_2(\epsilon,\delta) &= (\tilde{J}_{2,12345}(\epsilon,\delta) - \bar{J}_{2,12345})^2 + \ldots + (\tilde{J}_{2,56789}(\epsilon,\delta) - \bar{J}_{2,56789})^2 \end{aligned} \tag{4.16}$$

Let

$$J(\epsilon,\delta) = \max\{J_1(\epsilon,\delta), J_2(\epsilon,\delta)\}$$

The parameter ϵ is now fixed at 0 and δ is varied in steps of 0.02 in a depth first search to find the minimum value of $J(\epsilon,\delta)$. Then δ is varied in steps of 0.01 to further minimize $J(\epsilon,\delta)$. This gave $\delta = 0.08$ (see results below) which is the first iteration. Then δ is fixed at 0.08 and ϵ is first varied in steps of 0.02 and then 0.01 in a depth first search to find the minimum of $J(\epsilon,\delta)$. This gave $\epsilon = 0.09$ which is the second iteration. This process is continued until no further improvement to $J(\epsilon,\delta)$ is obtained using the step

size of 0.01 for both ϵ and δ. The table below shows the results.

Iterative scheme with joint-invariants

	ϵ	δ	$J(\epsilon, \delta)$
Starting point:	0	0	0.3272
First iteration:	0	0.08	0.04903
Second iteration:	-0.09	0.08	0.0006745
Third iteration:	-0.09	0.07	0.0004983
Fourth iteration:	-0.08	0.07	0.00005950

This gives $\epsilon = -0.08$ and $\delta = 0.07$ as the solution to (4.16). These values for ϵ and δ also satisfy (4.14) and (4.12).

The projective transformation $(1 + \epsilon, \delta)$ which maps $(\tilde{X}_i^{C_2}, \tilde{U}_i^{C_2}) \in \tilde{C}_2$ (satisfying (4.13)) to $(X_i, U_i) \in C_1$ is then applied to the curve $\tilde{C}_2$. Thus the error in the initial matching (see figure 4.24) is corrected. The result is shown in figure 4.25 which shows a very close matching.

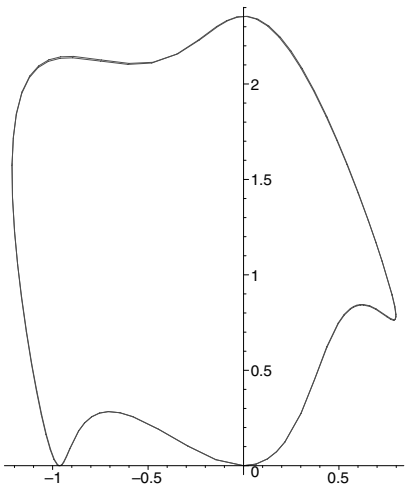

Figure 4.25: Correcting the error in the initial matching.

The above method is now applied on two curves in their Euclidean canonical form which appear that they might be related by a projective transformation but are in fact different, see figure 4.26. The second curve is created by adding extra terms with small coefficients to the formula for the first curve, mapping it to its Euclidean canonical form, then applying the same projective transformation as that in figure 4.22.

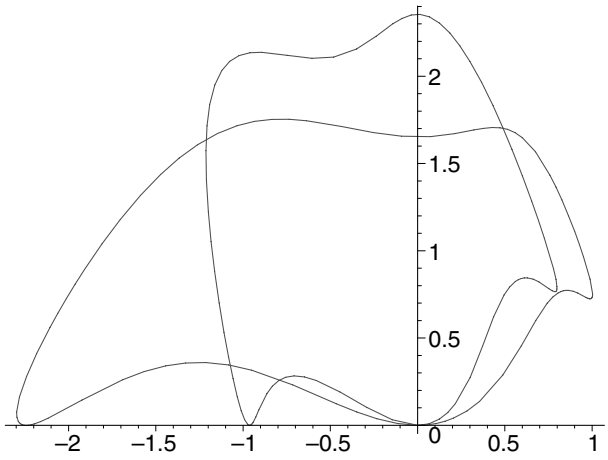

Figure 4.26: Two different curves not related by a projective transformation.

Denote this second curve by C_2. In the same way as before, an error of -0.12 is put into the a parameter of the projective transformation and an error of 0.1 is put into the b parameter. Then the points $\bar{P}_i = (\bar{X}_i, \bar{U}_i) \in C_2,\ i = 2, \ldots, 8$ are found such that

$$\frac{\bar{X}_i}{\bar{U}_i} = \tilde{a}\frac{X_i}{U_i} + \tilde{b}$$

where $\tilde{a} = a - 0.12$ and $\tilde{b} = b + 0.1$. $\bar{P}_1 = (0, 0)$ and $\bar{P}_9$ (the other bi-tangent) remain fixed independent of $\tilde{a}$ and $\tilde{b}$.

The projective transformation that maps the points $\bar{P}_3$, $\bar{P}_5$ and $\bar{P}_7$ to P_3, P_5 and P_7 is then applied to C_2 producing figure 4.27. This represents the initial matching of the curves.

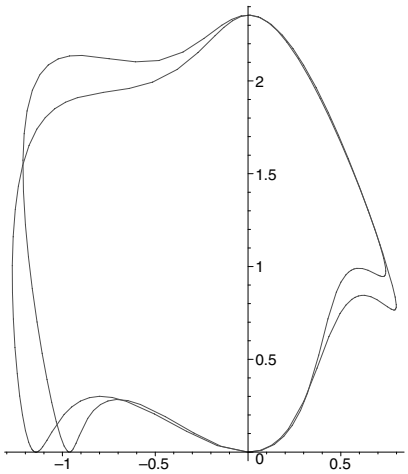

Figure 4.27: Initial matching of C_2 onto C_1.

The same iterative process of the joint-invariants is then applied as before. The following table shows the results.

Iterative scheme with joint-invariants

	ϵ	δ	$J(\epsilon, \delta)$
Starting point:	0	0	0.3333
First iteration:	0	0.06	0.09811114107
Second iteration:	-0.1	0.06	0.01648496408

No further improvement (in steps of 0.01 for ϵ and δ) is found so the values of $\epsilon = -0.1$ and $\delta = 0.06$ are used to correct the error in the initial matching of figure 4.27. Figure 4.28 shows that there is still a significant error in the matching. This is consistent with the fact that the curves are not related by a projective transformation.

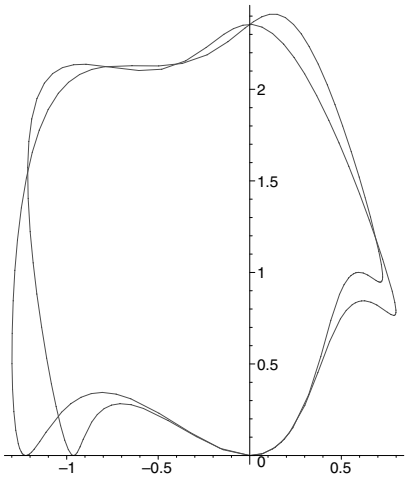

Figure 4.28: Correcting the error in the initial matching.

In summary this method gives a simple iterative scheme using the joint-invariants for correcting the error in the initial matching of two curves related by a projective transformation. Note that in practice the stopping criteria for the iterations will either be a lower tolerance placed on $J(\epsilon, \delta)$ or a tolerance based on a Euclidean measure of the distance between the curves (for example the maximum of the distances between $P_i \in C_1$ and $\tilde{P}_i \in (1+\epsilon, \delta) \cdot C_2$ (see earlier)). If the curves fail to reach this tolerance they will be rejected as being different.

Also the iterative scheme could be adapted to include error in the canonical point parameter, call this α say. The same procedure will then follow except $J(\epsilon, \delta)$ will become $J(\epsilon, \delta, \alpha)$.

Finally note that a range of values of $\{\tilde{J}_{1,12345}(\epsilon,\delta), \tilde{J}_{2,12345}(\epsilon,\delta)\}$, ..., $\{\tilde{J}_{1,56789}(\epsilon,\delta), \tilde{J}_{2,56789}(\epsilon,\delta)\}$ could be stored before hand in a library. Thus when this curve is required to be recognised under a viewing transformation the initial error in the matching will be able to be very quickly corrected by applying the iterative scheme using the previously stored values.

4.5 Curves that are close to symmetric

This case is special because a curve that is symmetric can be mapped onto itself by more than one projective map. Thus if it is close to symmetric, the wrong projective map could be chosen.

Consider the following curve C, which is an ellipse with a small convex bump added, shown in figure 4.29.

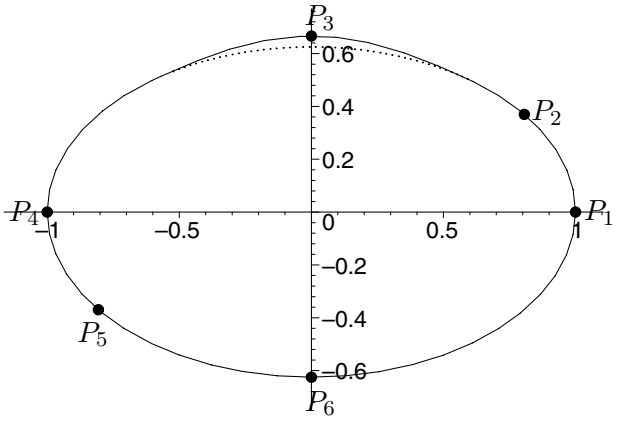

Figure 4.29: Curve C which is an ellipse with a small convex bump. C is denoted by a solid line, the ellipse is denoted by a dotted line.

Six points $P_1, \ldots, P_6$ are placed on the curve such that a rotation of 180 degrees maps the points P_1, P_2 and P_3 very closely to the points P_4, P_5 and P_6. The six consecutive pairs of joint-invariants to four decimal places are shown in the following table.

Table of joint-invariants for the curve C

Combination	$[J_1, J_2]$
[12345]	$[0.8470, 0.2887]$
[23456]	$[0.4782, 1.6707]$
[34561]	$[0.6828, 1.8823]$
[45612]	$[0.8341, 0.3276]$
[56123]	$[0.4857, 1.5459]$
[61234]	$[0.6724, 2.1750]$

Notice that the joint-invariants [12345], [23456] and [34561] correspond closely to the joint-invariants [45612], [56123] and [61234]. This indicates that the curve is almost invariant under a non-trivial transformation.

Suppose that the point P_6 was chosen to be the canonical point to map C to its Euclidean Canonical form and let $\overline{C}$ be a curve which is a projective transformation of C with corresponding points $\bar{P}_1, \ldots, \bar{P}_6$. In practice there will be error in the points $\bar{P}_1, \ldots, \bar{P}_6$, so it is possible that the best joint-invariant matching of the six combinations in $\overline{C}$ onto $[12345], \ldots, [61234]$ is $[\bar{4}\bar{5}\bar{6}\bar{1}\bar{2}], \ldots, [\bar{3}\bar{4}\bar{5}\bar{6}\bar{1}]$ which is in the wrong order. That is a false identification of the point $\bar{P}_3$ would be made with the canonical point P_6. In this case the error correction method will not be able to correct the error in the matching. However, because the correct order $[\bar{1}\bar{2}\bar{3}\bar{4}\bar{5}], \ldots, [\bar{6}\bar{1}\bar{2}\bar{3}\bar{4}]$ will also have a close joint-invariant matching with $[12345], \ldots, [61234]$, if the error correction method is also applied using the point $\bar{P}_6$ it will correct the error in the matching.

So given a canonical point in one curve, if the joint-invariants show up two or more possible points that correspond to this canonical point, the canonical form method will be applied for each of these points thus avoiding a false identification.

Chapter 5

Integral invariants and projective curvature

5.1 Integral Invariants

Consider the full affine group action on $\mathbf{R}^2$ given by,

$$(x,u) \longmapsto (ax+bu+c, dx+eu+f), \quad \det \begin{pmatrix} a & b \\ d & e \end{pmatrix} \neq 0.$$

This action is represented by the matrix

$$G = \begin{pmatrix} a & b & c \\ d & e & f \\ 0 & 0 & 1 \end{pmatrix}. \tag{5.1}$$

Now define new coordinates z, v and w by

$$z_x = u, \qquad v_x = xu, \qquad w_x = u^2$$

That is, z, v and w are potentials. Consider the transformation given by

$$\begin{aligned} \bar{z} = (ea-db)z + \frac{1}{2}da(x^2-x_0^2) + db(xu - x_0u_0) \\ + \frac{1}{2}eb(u^2-u_0^2) + fa(x-x_0) + fb(u-u_0), \end{aligned}$$

$$\begin{aligned}\bar{v} &= c(ae-bd)z + a(ae-bd)v + \frac{1}{2}b(ae-bd)w \\ &+ \frac{1}{2}b(bf+ec)(u^2-u_0^2) + \frac{1}{2}a(dc+af)(x^2-x_0^2) + \frac{1}{3}b^2e(u^3-u_0^3) \\ &+ bcd(xu-x_0u_0) + bcf(u-u_0) + \frac{1}{2}abe(xu^2-x_0u_0^2) \\ &+ abf(xu-x_0u_0) + acf(x-x_0) + \frac{1}{3}a^2d(x^3-x_0^3) \\ &+ abd(x^2u-x_0^2u_0) + \frac{1}{2}b^2d(xu^2-x_0u_0^2),\end{aligned}$$

$$\begin{aligned}\bar{w} &= 2f(ae-bd)z + 2d(ae-bd)v + e(ae-bd)w + bfe(u^2-u_0^2) \\ &+ afd(x^2-x_0^2) + bd^2(x^2u-x_0^2u_0) + bde(xu^2-x_0u_0^2) \\ &+ 2bfd(xu-x_0u_0) + af^2(x-x_0) + \frac{1}{3}be^2(u^3-u_0^3) \\ &+ \frac{1}{3}ad^2(x^3-x_0^3) + bf^2(u-u_0),\end{aligned}$$

where $u_0 = u(x_0)$. This gives

$$\bar{z}_{\bar{x}} = \bar{u}, \qquad \bar{v}_{\bar{x}} = \bar{x}\bar{u}, \qquad \bar{w}_{\bar{x}} = \bar{u}^2$$

That is there is an induced action,

$$\bar{z} = G \cdot z, \qquad \bar{v} = G \cdot v, \qquad \bar{w} = G \cdot w$$

on the coordinates z, v and w where G is given by (5.1).

Now for any other full affine transformation H,

$$G \cdot (H \cdot (z,v,w)) = (G \cdot H) \cdot (z,v,w),$$

$$G \cdot (G^{-1} \cdot (z,v,w)) = (z,v,w)$$

and

$$G^{-1} \cdot (G \cdot (z,v,w)) = (z,v,w).$$

Also

$$I \cdot (z,v,w) = (z,v,w)$$

where I is the identity.

Thus the affine group has an action on $(x, u, x_0, u_0, z, v, w)$. This action can be extended to arbitrarily high order using,

$$Z_x = xu^2, \quad V_x = x^2u, \quad W_x = u^3, \quad \cdots .$$

Hence for the full affine group there is an induced group action on the potentials analogous to the induced action on the derivatives of u.

Note that the infinitesimal generators of this group action are given by

$$\begin{aligned}
\mathbf{V}_1 &= x\partial_x + z\partial_z + 2v\partial_v + w\partial_w + x_0\partial_{x_0} \\
\mathbf{V}_2 &= u\partial_x + \frac{1}{2}(u^2 - u_0^2)\partial_z + \frac{1}{2}(w + xu^2 - x_0u_0^2)\partial_v + \frac{1}{3}(u^3 - u_0^3)\partial_w + u_0\partial_{x_0} \\
\mathbf{V}_3 &= \partial_x + z\partial_v + \partial_{x_0} \\
\mathbf{V}_4 &= x\partial_u + \frac{1}{2}(x^2 - x_0^2)\partial_z + \frac{1}{3}(x^3 - x_0^3)\partial_v + 2v\partial_w + x_0\partial_{u_0} \\
\mathbf{V}_5 &= u\partial_u + z\partial_z + v\partial_v + 2w\partial_w + u_0\partial_{u_0} \\
\mathbf{V}_6 &= \partial_u + (x - x_0)\partial_z + \frac{1}{2}(x^2 - x_0^2)\partial_v + 2z\partial_w + \partial_{u_0}
\end{aligned}$$

The regularization approach allows the parameters a, b, c, d, e and f to be normalized by setting

$$(\bar{x}, \bar{u}, \bar{z}, \bar{v}, \bar{x}_0, \bar{u}_0) = (0, 0, 0, 0, 1, 1).$$

They can be substituted into $\bar{w}$ to give the curvature

$$\kappa = \frac{1}{3}\frac{-3(x-x_0)w + 6(u-u_0)v + 4z^2 - 2(2xu - 2x_0u_0 + ux_0 - xu_0)z + uu_0(x-x_0)^2}{((x-x_0)(u+u_0) - 2z)^2}.$$

Using the theory of Cartan, this curvature characterises all curves up to a full affine transformation. In practice this curvature can be evaluated for each point x by using

$$z = \int_{x_0}^{x} u\,dx, \quad v = \int_{x_0}^{x} xu\,dx, \quad w = \int_{x_0}^{x} u^2\,dx$$

Note that this integral invariant is different from the traditional moment invariants, see [4] and [10] for example, as the moment invariants are global invariants where this invariant is semi-local as by varying (x_0, u_0) it can be defined on any segment of the curve. Also another type of integral invariant has been looked at in [8] but this involves integrating with respect to the invariant special affine arclength.

The numerator and denominator of the integral curvature κ above trans-

form by

$$\begin{aligned}\text{numer}(\kappa) &\longmapsto (ae-bd)^2\text{numer}(\kappa)\\ \text{denom}(\kappa) &\longmapsto (ae-bd)^2\text{denom}(\kappa)\end{aligned}$$

Thus, in the case of the special affine group where $ae - bd = 1$, the numerator and denominator of κ are separately invariant.

Note that, for each point $(x, u(x))$, $\kappa(x)$ is a two point invariant between (x_0, u_0) and (x, u).

Consider the prolonged full affine group action up to third order **derivatives** given by

$$\begin{aligned}\bar{u}_{\bar{x}} &= \frac{d+eu_x}{a+bu_x}, \quad \bar{u}_{\bar{x}\bar{x}} = \frac{(ae-bi)u_{xx}}{(a+bu_x)^3},\\ \bar{u}_{\bar{x}\bar{x}\bar{x}} &= \frac{(ae-bi)(au_{xxx}+bu_{xxx}u_x-3bu_{xx}^2)}{(a+bu_x)^5}\end{aligned}$$

The integral invariant $\kappa(x)$ is analogous to the two point **differential** invariant

$$\kappa^A_{\text{derivative}} = \frac{(u-u_0-xu_x+x_0u_x)^{\frac{1}{3}}u_{xx}}{(-3xu_{xx}^2+3x_0u_{xx}^2-uu_{xxx}+u_{xxx}u_0+xu_xu_{xxx}-x_0u_xu_{xxx})^{\frac{2}{3}}}$$

which is derived by normalizing the parameters using

$$(\bar{x}, \bar{u}, \bar{x}_0, \bar{u}_0, \bar{u}_{\bar{x}}, \bar{u}_{\bar{x}}, \bar{u}_{\bar{x}\bar{x}\bar{x}}) = (0, 1, 0, 0, 0, 1)$$

and substituting them into $\bar{u}_{\bar{x}\bar{x}}$. They are both two point invariants but $\kappa(x)$ is in terms of **potentials** and $\kappa^A_{\text{derivative}}$ is in terms of **derivatives**.

If the transformation is special affine the two point differential invariant is given by,

$$\kappa^{SA}_{\text{derivative}} = \frac{u_{xx}}{(u-u_0-xu_x+x_0u_x)^3}$$

Example

Two convex curves related by a full affine transformation which are parametrised by t from 0 to 2π are each translated by mapping a common point in each curve to the origin so that $c = 0$ and $f = 0$. They are then equally spaced in Euclidean arclength using 99 points, see figure 5.1. Note that the value

of $t = 2\pi$ which corresponds to going around the curve once is arbitrary.

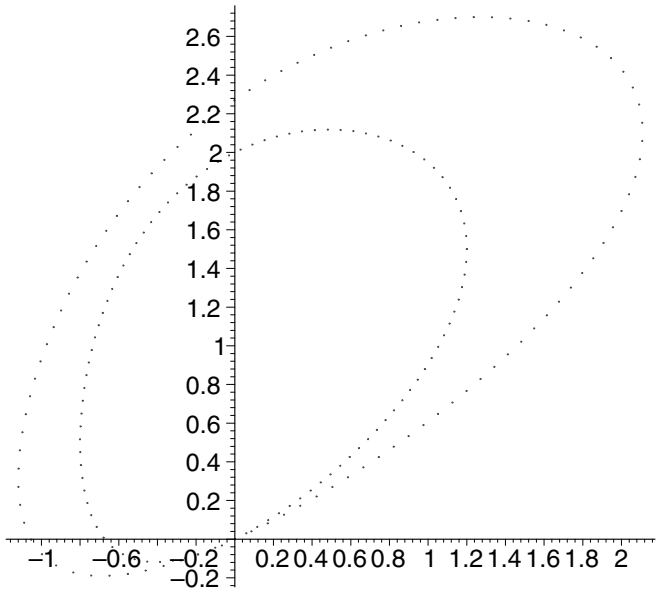

Figure 5.1: Discretised curves.

Since $(x_0, u_0) = (\bar{x}_0, \bar{u}_0) = (0, 0)$ the above curvature takes the simpler form

$$\kappa = \frac{-3xw + 6uv + 4z^2 - 4xuz}{(xu - 2z)^2}$$

Here the fraction $\frac{1}{3}$ has been omitted.

Consider

$$\kappa_1 = xu - 2z.$$

and so

$$\kappa_1(2\pi) = -2 \int_0^{2\pi} u(t)x'(t)\, dt$$

in parametrised form, where $x(0) = 0$ and $u(0) = 0$. Note that if the translation is performed on $x(t)$ and $u(t)$

$$\tilde{x}(t) = x(t) + c$$
$$\tilde{u}(t) = u(t) + f$$

then for arbitrary t_0,

$$\begin{aligned}\int_{t_0}^{t_0+2\pi} \tilde{u}(t)\tilde{x}'(t)\,dt &= \int_{t_0}^{t_0+2\pi} (u(t)+f)x'(t)\,dt \\ &= \int_{t_0}^{t_0+2\pi} u(t)x'(t)\,dt + f\int_{t_0}^{t_0+2\pi} x'(t)\,dt \\ &= \int_{0}^{2\pi} u(t)x'(t)\,dt.\end{aligned}$$

Hence the value of $\kappa_1(2\pi)$ is independent of translation of the curve. Since, under a general affine transformation, $\bar{\kappa}_1(2\pi) = (ae-bd)\kappa_1(2\pi)$, the values of $\bar{\kappa}_1(2\pi)$ and $\kappa_1(2\pi)$ can be used to determine $(ae-bd)$ independent of translation along the curve thus the full affine transformation will become special affine. The integrals can be found by making the discretised curves piecewise linear and summing up the areas of the trapeziums around the curve.

For the curves in figure 5.1, the factor $(ae-bd)$ is found by the above method and κ_1 and $\frac{1}{ae-bd}\bar{\kappa}_1$ are both plotted against the parameter t associated with each point on the discretised curve on the same axis. Figure 5.2 shows that the two graphs are very close and figure 5.3 shows a blow up of a region in figure 5.2 where the points in each curve are denoted by a circle and cross respectively.

Note in practice the parametrisations are not known but κ_1 can be used to generate as many invariant points as desired to match the curves.

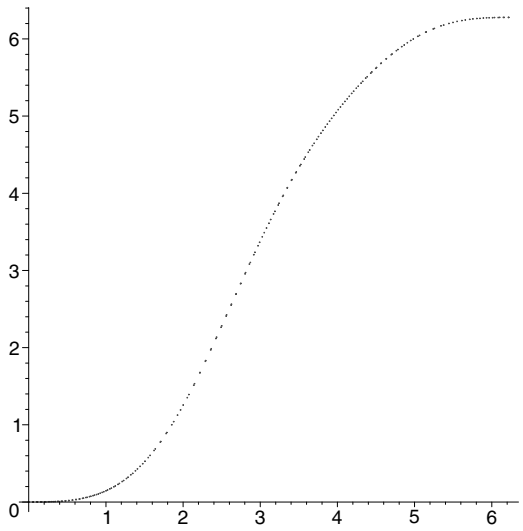

Figure 5.2: Plotting κ_1 and $\frac{1}{ae-bd}\bar{\kappa}_1$ vs t.

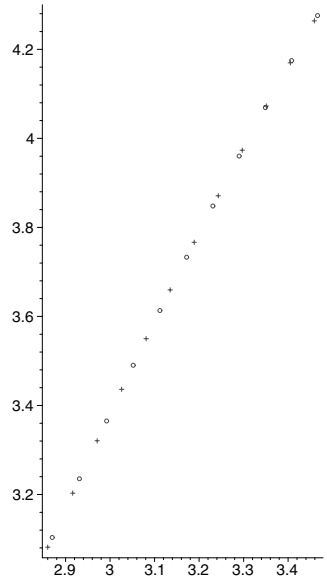

Figure 5.3: A blow up of a region in figure 5.2.

The integral curvature κ is next plotted against t for both curves and also the true integral curvature is plotted on the same axis. Figure 5.4 shows that for the region $0 \leq t \leq 1.5$, the approximate integral curvatures differ from the true. This is because here both numerator and denominator are close to zero so that round off error occurs. For $t > 1.5$ the integral curvature is very close to the true integral curvature.

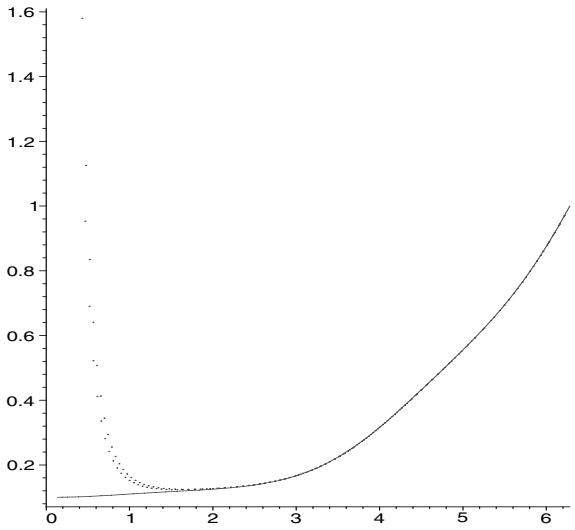

Figure 5.4: The integral curvature κ vs t.

Note that an alternative way to find $(ae - bd)$ would be to locate a point common to both curves using the integral curvature then to calculate $\frac{\bar{\kappa}_1}{\kappa_1}$ for this common point.

An integral invariant is now derived for another subgroup of the projective group. Consider the subgroup action on $\mathbf{R}^2$ given by

$$(x,u) \longmapsto (\bar{x},\bar{u}) = \left(\frac{ax+bu}{gx+hu+i}, \frac{u}{gx+hu+i}\right) \tag{5.2}$$

This is the Euclidean canonical form.

New coordinates v and w can be defined by,

$$v_x = \frac{1}{u^2}, \qquad w_x = \frac{x}{u^3}$$

Consider

$$\begin{aligned}
\bar{v} &= aiv + (ah-bg)\frac{x}{u} - bi\frac{1}{u} - (ah-bg)\frac{x_0}{u_0} + bi\frac{1}{u_0} \\
\bar{w} &= a^2 iw + \frac{3}{2}abiv - \frac{1}{2}abi\frac{x}{u^2} + b((ah-bg)\frac{x}{u} - bi\frac{1}{u}) - \frac{1}{2}a(ah-bg)\frac{x_0^2}{u_0^2} \\
&\quad + \frac{1}{2}abi\frac{x_0}{u_0^2} - b(ah-bg)\frac{x_0}{u_0} + b^2 i\frac{1}{u_0} + \frac{1}{2}a(ah-bg)\frac{x^2}{u^2}
\end{aligned}$$

where $u(x_0) \neq 0$. This gives,

$$\bar{v}_{\bar{x}} = \frac{1}{\bar{u}^2}, \qquad \bar{w}_{\bar{x}} = \frac{\bar{x}}{\bar{u}^3}$$

and so there is an induced action,

$$\bar{v} = G \cdot v, \qquad \bar{w} = G \cdot w$$

on the coordinates v and w where

$$G = \begin{pmatrix} a & b & 0 \\ 0 & 1 & 0 \\ g & h & i \end{pmatrix}.$$

It can be shown by a similar method to the above that this integral prolongation forms a group action and this can be extended to arbitrarily high order using,

$$V_x = \frac{1}{u^2}, \qquad W_x = \frac{x}{u^3}, \quad \cdots .$$

Note that the infinitesimal generators of this group action are given by

$$\mathbf{V}_1 = x\partial_x + v\partial_v + 2w\partial_w + x_0\partial_{x_0}$$

$$\mathbf{V}_2 = u\partial_x + \left(\frac{1}{u_0} - \frac{1}{u}\right)\partial_v + \frac{1}{2}\left(\frac{x_0}{u_0^2} - \frac{x}{u^2} + 3v\right)\partial_w + u_0\partial_{x_0}$$
$$\mathbf{V}_3 = x^2\partial_x + xu\partial_u + x_0^2\partial_{x_0} + x_0u_0\partial_{u_0}$$
$$\mathbf{V}_4 = xu\partial_x + u^2\partial_u + \left(\frac{x}{u} - \frac{x_0}{u_0}\right)\partial_v + \frac{1}{2}\left(\frac{x^2}{u^2} - \frac{x_0^2}{u_0^2}\right)\partial_w + x_0u_0\partial_{x_0} + u_0^2\partial_{u_0}$$
$$\mathbf{V}_5 = x\partial_x + u\partial_u - v\partial_v - w\partial_w + x_0\partial_{x_0} + u_0\partial_{u_0}$$

Now using the regularization approach the parameters a, b, g, h and i can be normalized by setting

$$(\bar{x}, \bar{u}, \bar{v}, \bar{x}_0, \bar{u}_0) = (0, 1, 0, 1, 1)$$

and then they can be substituted into $\bar{w}$ to give the integral curvature

$$\kappa = -\frac{1}{2}\frac{u_0(x_0u^2v - 2u_0u^2w + 2u_0xuv + x_0x - x^2)}{(u_0uv + x_0 - x)(x_0u - xu_0)}.$$

Using the theory of Cartan, this integral curvature characterises all curves up to the transformation (5.2). Similarly to the full affine group above, this integral curvature can be evaluated at each point x by using,

$$v = \int_{x_0}^{x} \frac{1}{u^2}\,dx, \quad w = \int_{x_0}^{x} \frac{x}{u^3}\,dx.$$

Now consider the full projective transformation,

$$(x,u)\longmapsto\left(\frac{ax+bu+c}{gx+hu+i},\frac{dx+eu+f}{gx+hu+i}\right),\quad \det\begin{pmatrix}a&b&c\\d&e&f\\g&h&i\end{pmatrix}=1$$

New coordinates I, I_x, I_u, I_{xx}, I_{xu}, I_{uu}, can be defined by,

$$\frac{d}{ds_{\mathbf{SA}}}I=\kappa_s^{\mathbf{SA}},\quad \frac{d}{ds_{\mathbf{SA}}}I_x=x\kappa_s^{\mathbf{SA}},\quad \frac{d}{ds_{\mathbf{SA}}}I_u=u\kappa_s^{\mathbf{SA}},$$
$$\frac{d}{ds_{\mathbf{SA}}}I_{xx}=x^2\kappa_s^{\mathbf{SA}},\quad \frac{d}{ds_{\mathbf{SA}}}I_{xu}=xu\kappa_s^{\mathbf{SA}},\quad \frac{d}{ds_{\mathbf{SA}}}I_{uu}=u^2\kappa_s^{\mathbf{SA}}$$

Consider

$$\begin{aligned}
\bar{I}&=g^2I_{xx}+2ghI_{xu}+h^2I_{uu}+2giI_x+2hiI_u+i^2I\\
\bar{I}_{\bar{x}}&=agI_{xx}+(ah+bg)I_{xu}+bhI_{uu}+(ai+gc)I_x+(bi+hc)I_u+ciI\\
\bar{I}_{\bar{u}}&=dgI_{xx}+(dh+ge)I_{xu}+ehI_{uu}+(di+gf)I_x+(ei+hf)I_u+fiI\\
\bar{I}_{\bar{x}\bar{x}}&=a^2I_{xx}+2abI_{xu}+b^2I_{uu}+2acI_x+2bcI_u+c^2I\\
\bar{I}_{\bar{x}\bar{u}}&=adI_{xx}+(ea+bd)I_{xu}+beI_{uu}+(fa+dc)I_x+(fb+ec)I_u+cfI\\
\bar{I}_{\bar{u}\bar{u}}&=d^2I_{xx}+2deI_{xu}+e^2I_{uu}+2dfI_x+2efI_u+f^2I
\end{aligned}$$

This gives,

$$\frac{d}{d\bar{s}_{\mathbf{SA}}}\bar{I}=\bar{\kappa}_{\bar{s}}^{\mathbf{SA}}\quad \frac{d}{d\bar{s}_{\mathbf{SA}}}\bar{I}_{\bar{x}}=\bar{x}\bar{\kappa}_{\bar{s}}^{\mathbf{SA}},\quad \frac{d}{d\bar{s}_{\mathbf{SA}}}\bar{I}_{\bar{u}}=\bar{u}\bar{\kappa}_{\bar{s}}^{\mathbf{SA}},$$
$$\frac{d}{d\bar{s}_{\mathbf{SA}}}\bar{I}_{\bar{x}\bar{x}}=\bar{x}^2\bar{\kappa}_{\bar{s}}^{\mathbf{SA}},\quad \frac{d}{d\bar{s}_{\mathbf{SA}}}\bar{I}_{\bar{x}\bar{u}}=\bar{x}\bar{u}\bar{\kappa}_{\bar{s}}^{\mathbf{SA}},\quad \frac{d}{d\bar{s}_{\mathbf{SA}}}\bar{I}_{\bar{u}\bar{u}}=\bar{u}^2\bar{\kappa}_{\bar{s}}^{\mathbf{SA}}$$

and so there is an induced action

$$\bar{I}=G\cdot I,\qquad \bar{I}_{\bar{x}}=G\cdot I_x,\qquad \bar{I}_{\bar{u}}=G\cdot I_u,\qquad \bar{I}_{\bar{x}\bar{x}}=G\cdot I_{xx},$$
$$\bar{I}_{\bar{x}\bar{u}}=G\cdot I_{xu},\qquad \bar{I}_{\bar{u}\bar{u}}=G\cdot I_{uu}$$

on the coordinates I, I_x, I_u, I_{xx}, I_{xu}, I_{uu}, where G is an element of the projective group.

Using a similar method to the above this can be shown to be a group action. The parameters may be normalized by setting

$$(\bar{x},\bar{u},\bar{I},\bar{I}_{\bar{x}},\bar{I}_{\bar{u}},\bar{I}_{\bar{x}\bar{u}},\bar{x}_0,\bar{u}_0)=(0,0,1,0,0,0,0,1)$$

and substituting into $\bar{I}_{\bar{x}\bar{x}} \cdot \bar{I}_{\bar{u}\bar{u}}$ gives the invariant

$$\kappa_I^{\text{proj}} = -I_{xx}I_u^2 + I_{xx}I_{uu}I + 2I_{xu}I_xI_u - I_{uu}I_x^2 - I_{xu}^2 I.$$

This invariant can be evaluated by using,

$$I = \int_0^s \kappa_s^{\mathbf{SA}} ds_{\mathbf{SA}}, \quad I_x = \int_0^s x\kappa_s^{\mathbf{SA}} ds_{\mathbf{SA}}, \quad I_u = \int_0^s u\kappa_s^{\mathbf{SA}} ds_{\mathbf{SA}},$$
$$I_{xx} = \int_0^s x^2\kappa_s^{\mathbf{SA}} ds_{\mathbf{SA}}, \quad I_{xu} = \int_0^s xu\kappa_s^{\mathbf{SA}} ds_{\mathbf{SA}}, \quad I_{uu} = \int_0^s u^2\kappa_s^{\mathbf{SA}} ds_{\mathbf{SA}}$$

where in each integral $s_{\mathbf{SA}}$ varies from a common starting position which is designated to be $s_{\mathbf{SA}} = 0$ corresponding to some point (x_0, u_0). Note that using integration by parts the coordinates can be written in the following form,

$$I = \kappa^{\mathbf{SA}} - \kappa_0^{\mathbf{SA}}, \quad I_x = x\kappa^{\mathbf{SA}} - x_0\kappa_0^{\mathbf{SA}} - \int_{x_0}^x \kappa^{\mathbf{SA}}\, dx,$$
$$I_u = u\kappa^{\mathbf{SA}} - u_0\kappa_0^{\mathbf{SA}} - \int_{u_0}^u \kappa^{\mathbf{SA}}\, du, \quad I_{xx} = x^2\kappa^{\mathbf{SA}} - x_0^2\kappa_0^{\mathbf{SA}} - 2\int_{x_0}^x x\kappa^{\mathbf{SA}}\, dx,$$
$$I_{xu} = xu\kappa^{\mathbf{SA}} - x_0u_0\kappa_0^{\mathbf{SA}} - \int_{x_0}^x u\kappa^{\mathbf{SA}}\, dx - \int_{u_0}^u x\kappa^{\mathbf{SA}}\, du,$$
$$I_{uu} = u^2\kappa^{\mathbf{SA}} - u_0^2\kappa_0^{\mathbf{SA}} - 2\int_{u_0}^u u\kappa^{\mathbf{SA}}\, du$$

Also since

$$\kappa^{\mathbf{SA}} = \frac{d^2}{dx^2}(u_{xx}^{-\frac{2}{3}}) = \frac{d^2}{du^2}(x_{uu}^{-\frac{2}{3}}),$$

κ_I^{proj} can be written in terms of $\kappa^{\mathbf{SA}}$, $\int_0^s ds_{\mathbf{SA}}$ and up to third order derivatives of u.

The theory of Cartan guarantees that κ_I^{proj} characterises all curves up to a projective transformation.

5.2 Alternative derivation of projective curvature

5.2.1 First approach

Under the projective group, the special affine arclength,

$$ds_{\mathbf{SA}} = u_{xx}^{\frac{1}{3}} dx$$

transforms by

$$d\bar{s}_{\mathbf{SA}} = \frac{ds_{\mathbf{SA}}}{gx + hu + i}.$$

Also $\kappa^{\mathbf{SA}}$ transforms by

$$\begin{aligned}\bar{\kappa}^{\mathbf{SA}} = (gx + hu + i)^2 \kappa^{\mathbf{SA}} + 18h(gx + hu + i)u_{xx}^{\frac{1}{3}} - 9\frac{(g + hu_x)^2}{u_{xx}^{\frac{2}{3}}} \\ - 6\frac{(gx + hu + i)(g + hu_x)u_{xxx}}{u_{xx}^{\frac{5}{3}}}.\end{aligned}$$

and $\bar{\kappa}_{\bar{s}}^{\mathbf{SA}}$ is given by

$$\begin{aligned}\bar{\kappa}_{\bar{s}}^{\mathbf{SA}} &= (gx + hu + i)\frac{d}{d\bar{s}_{\mathbf{SA}}}(\kappa^{\mathbf{SA}}) \\ &= (gx + hu + i)^3 \kappa_s^{\mathbf{SA}}.\end{aligned}$$

Similarly, $\bar{\kappa}_{\bar{s}\bar{s}}^{\mathbf{SA}}$ and $\bar{\kappa}_{\bar{s}\bar{s}\bar{s}}^{\mathbf{SA}}$ can be found giving

$$\bar{\kappa}_{\bar{s}\bar{s}}^{\mathbf{SA}} = (gx + hu + i)^4 \kappa_{ss}^{\mathbf{SA}} + 3\frac{(gx + hu + i)^3(g + hu_x)}{u_{xx}^{\frac{1}{3}}}\kappa_s^{\mathbf{SA}}$$

$$\begin{aligned}\bar{\kappa}_{\bar{s}\bar{s}\bar{s}}^{\mathbf{SA}} = (gx + hu + i)^3\Big((gx + hu + i)^2\kappa_{sss}^{\mathbf{SA}} + 7\frac{(gx + hu + i)(g + hu_x)}{u_{xx}^{\frac{1}{3}}}\kappa_{ss}^{\mathbf{SA}} \\ + \frac{3h(gx + hu + i)u_{xx}^2 + 9(g + hu_x)^2 u_{xx} - (gx + hu + i)(g + hu_x)u_{xxx}}{u_{xx}^{\frac{5}{3}}}\kappa_s^{\mathbf{SA}}\Big)\end{aligned}$$

Thus the projective group gives an action on $(\kappa_s^{\mathbf{SA}}, \kappa_{ss}^{\mathbf{SA}}, \kappa_{sss}^{\mathbf{SA}})$ and by setting

$$(\bar{\kappa}_{\bar{s}}^{\mathbf{SA}}, \bar{\kappa}_{\bar{s}\bar{s}}^{\mathbf{SA}}, \bar{\kappa}_{\bar{s}\bar{s}\bar{s}}^{\mathbf{SA}}) = (1, 0, 0),$$

the parameters can be normalized and substituted into $\bar{\kappa}^{\mathbf{SA}}$ to give,

$$\kappa^{\text{proj}} = \frac{-6\kappa_s^{\mathbf{SA}}\kappa_{sss}^{\mathbf{SA}} + 7(\kappa_{ss}^{\mathbf{SA}})^2 + \kappa^{\mathbf{SA}}(\kappa_s^{\mathbf{SA}})^2}{\kappa_s^{\mathbf{SA}\frac{8}{3}}}.$$

This coincides with the projective curvature from section 2.1.1.

Note that this method is an example of the general concept of using the

simpler equivalence problem based on a subgroup to aid the solution to the more complicated equivalence problem with the larger group. This general concept is mentioned in chapter 10 of Equivalence, Invariants and Symmetry by Peter J Olver [6] using Cartan's equivalence method.

5.2.2 Second approach

The infinitesimal generators of the projective group are,

$$\mathbf{V}_1 = x\partial_x, \quad \mathbf{V}_2 = u\partial_x, \quad \mathbf{V}_3 = \partial_x, \quad \mathbf{V}_4 = x\partial_u, \quad \mathbf{V}_5 = -x\partial_x + u\partial_u,$$
$$\mathbf{V}_6 = \partial_u, \quad \mathbf{V}_7 = x^2\partial_x + xu\partial_u, \quad \mathbf{V}_8 = xu\partial_x + u^2\partial_u.$$

Using the coordinates $(x, u_x, u_{xx}, u_{xxx}, \kappa^{\mathbf{SA}}, \kappa^{\mathbf{SA}}_s, \kappa^{\mathbf{SA}}_{ss}, \kappa^{\mathbf{SA}}_{sss})$, each vector field

$$\mathbf{V} = \xi(x,u)\partial_x + \eta(x,u)\partial_u$$

can be prolonged by,

$$\begin{aligned}\mathbf{V} = {} & \xi(x,u)\partial_x + \eta(x,u)\partial_u + \eta^{(1)}(x,u,u_x)\partial_{u_x} + \eta^{(2)}(x,u,u_x,u_{xx})\partial_{u_xx} \\ & + \eta^{(3)}(x,u,u_x,u_{xx},u_{xxx})\partial_{u_{xxx}} + \eta^{(4)}(x,u,u_x,u_{xx},u_{xxx},\kappa^{\mathbf{SA}})\partial_{\kappa^{\mathbf{SA}}} \\ & + \eta^{(5)}(x,u,u_x,u_{xx},u_{xxx},\kappa^{\mathbf{SA}},\kappa^{\mathbf{SA}}_s)\partial_{\kappa^{\mathbf{SA}}_s} \\ & + \eta^{(6)}(x,u,u_x,u_{xx},u_{xxx},\kappa^{\mathbf{SA}},\kappa^{\mathbf{SA}}_s,\kappa^{\mathbf{SA}}_{ss})\partial_{\kappa^{\mathbf{SA}}_{ss}} \\ & + \eta^{(7)}(x,u,u_x,u_{xx},u_{xxx},\kappa^{\mathbf{SA}},\kappa^{\mathbf{SA}}_s,\kappa^{\mathbf{SA}}_{ss},\kappa^{\mathbf{SA}}_{sss})\partial_{\kappa^{\mathbf{SA}}_{sss}}\end{aligned}$$

For $n = 1, \ldots, 3$ the action of the one parameter group determined by $\mathbf{V}$ acts on the derivatives of u by

$$\tilde{u}^{(n)} = u^{(n)} + \epsilon\,\eta^{(n)}(x,u,u',\ldots,u^{(n)}) + \cdots = x + \epsilon\,\mathbf{V}(u^{(n)}) + \cdots$$

where the $\eta^{(n)}$ are defined by

$$\eta^{(n)} = \left.\frac{\partial\tilde{u}^{(n)}}{\partial\epsilon}\right|_{\epsilon=0}.$$

This gives

$$\begin{aligned}\tilde{u}^{(n)} = u^{(n)} + \epsilon\,\eta^{(n)} + \cdots = \frac{d\tilde{u}^{(n-1)}}{d\tilde{x}} &= \frac{d\tilde{u}}{dx}\Big/\frac{d\tilde{x}}{dx} \\ = \frac{u^{(n)} + \epsilon\,(\frac{d\eta^{(n-1)}}{dx}) + \cdots}{1 + \epsilon\,(\frac{d\xi}{dx}) + \cdots} &= u^{(n)} + \epsilon\left(\frac{d\eta^{(n-1)}}{dx} - u^{(n)}\frac{d\xi}{dx}\right) + \cdots.\end{aligned}$$

Thus

$$\eta^{(n)} = \frac{d\eta^{(n-1)}}{dx} - u^{(n)}\frac{d\xi}{dx}, \quad n = 1, \dots, 3.$$

For $\eta^{(i)},\ i = 4, \dots, 7$, a similar process can be done. That is put,

$$\tilde{\kappa}^{\mathbf{SA}} = \kappa^{\mathbf{SA}} + \epsilon\eta^{(4)} + \cdots, \quad \tilde{\kappa}^{\mathbf{SA}}_{\tilde{s}} = \kappa^{\mathbf{SA}}_{s} + \epsilon\eta^{(5)} + \cdots,$$
$$\tilde{\kappa}^{\mathbf{SA}}_{\tilde{s}\tilde{s}} = \kappa^{\mathbf{SA}}_{ss} + \epsilon\eta^{(5)} + \cdots, \quad \tilde{\kappa}^{\mathbf{SA}}_{\tilde{s}\tilde{s}\tilde{s}} = \kappa^{\mathbf{SA}}_{sss} + \epsilon\eta^{(6)} + \cdots,$$

then

$$\tilde{\kappa}^{\mathbf{SA}} = \kappa^{\mathbf{SA}} + \epsilon\,\eta^{(4)} + \cdots = \frac{3\tilde{u}^{(2)}\tilde{u}^{(4)} - 5(\tilde{u}^{(3)})^2}{(\tilde{u}^{(2)})^{\frac{8}{3}}},$$
$$\tilde{\kappa}^{\mathbf{SA}}_{\tilde{s}} = \kappa^{\mathbf{SA}}_{s} + \epsilon\,\eta^{(5)} + \cdots = \frac{d\tilde{\kappa}^{\mathbf{SA}}}{d\tilde{s}} = \frac{d\kappa^{\mathbf{SA}} + \epsilon\,d\eta^4 + \cdots}{(\tilde{u}^{(2)})^{\frac{1}{3}}(dx + \epsilon\,d\xi + \cdots)}$$

and similarly for $\tilde{\kappa}^{\mathbf{SA}}_{\tilde{s}\tilde{s}}$ and $\tilde{\kappa}^{\mathbf{SA}}_{\tilde{s}\tilde{s}\tilde{s}}$. This gives

$$\eta^{(4)} = \frac{1}{3}\kappa^{\mathbf{SA}}\Big(2\frac{d\xi}{dx} - \frac{5}{u_{xx}}\frac{d\eta^{(1)}}{dx}\Big) + \frac{1}{u_{xx}^{\frac{11}{3}}}\Big(5u_{xxx}^2\frac{d\eta^{(1)}}{dx} - 10u_{xx}u_{xxx}\frac{d\eta^{(2)}}{dx} + 3u_{xx}^2\frac{d\eta^{(3)}}{dx}\Big)$$
$$\eta^{(5)} = -\frac{1}{3}\kappa^{\mathbf{SA}}_{s}\Big(2\frac{d\xi}{dx} + \frac{1}{u_{xx}}\frac{d\eta^{(1)}}{dx}\Big) + \frac{1}{u_{xx}^{\frac{1}{3}}}\frac{d\eta^{(4)}}{dx}$$
$$\eta^{(6)} = -\frac{1}{3}\kappa^{\mathbf{SA}}_{ss}\Big(2\frac{d\xi}{dx} + \frac{1}{u_{xx}}\frac{d\eta^{(1)}}{dx}\Big) + \frac{1}{u_{xx}^{\frac{1}{3}}}\frac{d\eta^{(5)}}{dx}$$
$$\eta^{(7)} = -\frac{1}{3}\kappa^{\mathbf{SA}}_{sss}\Big(2\frac{d\xi}{dx} + \frac{1}{u_{xx}}\frac{d\eta^{(1)}}{dx}\Big) + \frac{1}{u_{xx}^{\frac{1}{3}}}\frac{d\eta^{(6)}}{dx}.$$

Using these formulas the prolonged infinitesimal generators of the projective group are,

$$\mathbf{V}_1 = x\partial_x - u_x\partial_{u_x} - 2u_{xx}\partial_{u_{xx}} - 3u_{xxx}\partial_{u_{xxx}} - \frac{2}{3}\kappa^{\mathbf{SA}}\partial_{\kappa^{\mathbf{SA}}} - \kappa^{\mathbf{SA}}_{s}\partial_{\kappa^{\mathbf{SA}}_{s}} - \frac{4}{3}\kappa^{\mathbf{SA}}_{ss}\partial_{\kappa^{\mathbf{SA}}_{ss}} - \frac{5}{3}\kappa^{\mathbf{SA}}_{sss}\partial_{\kappa^{\mathbf{SA}}_{sss}}$$
$$\mathbf{V}_2 = u\partial_x - u_x^2\partial_{u_x} - 3u_xu_{xx}\partial_{u_{xx}} - (3u_{xx}^2 + 4u_xu_{xxx})\partial_{u_{xxx}}$$
$$\mathbf{V}_3 = \partial_x$$
$$\mathbf{V}_4 = x\partial_u + \partial_{u_x}$$
$$\mathbf{V}_5 = -x\partial_x + u\partial_u + 2u_x\partial_{u_x} + 3u_{xx}\partial_{u_{xx}} + 4u_{xxx}\partial_{u_{xxx}}$$
$$\mathbf{V}_6 = \partial_u$$

$$\begin{aligned}
\mathbf{V}_7 &= x^2\partial_x + xu\partial_u + (u - xu_x)\partial_{u_x} - 3xu_{xx}\partial_{u_{xx}} - (3u_{xx} + 5xu_{xxx})\partial_{u_{xxx}} \\
&\quad + (6\frac{u_{xxx}}{u_{xx}^{\frac{5}{3}}} - 2x\frac{2}{3}\kappa^{\mathbf{SA}})\partial_{\kappa^{\mathbf{SA}}} - 3x\kappa_s^{\mathbf{SA}}\partial_{\kappa_s^{\mathbf{SA}}} - (3\frac{\kappa_s^{\mathbf{SA}}}{u_{xx}^{\frac{1}{3}}} + 4x\kappa_{ss}^{\mathbf{SA}})\partial_{\kappa_{ss}^{\mathbf{SA}}} \\
&\quad + (\frac{u_{xxx}\kappa_s^{\mathbf{SA}}}{u_{xx}^{\frac{5}{3}}} - 7\frac{\kappa_{ss}^{\mathbf{SA}}}{u_{xx}^{\frac{1}{3}}} - 5x\kappa_{sss}^{\mathbf{SA}})\partial_{\kappa_{sss}^{\mathbf{SA}}} \\
\mathbf{V}_8 &= xu\partial_x + u^2\partial_u + u_x(u - xu_x)\partial_{u_x} - 3xu_xu_{xx}\partial_{u_{xx}} \\
&\quad + (-3u_xu_{xx} - 3xu_{xx}^2 - 4xu_xu_{xxx} - uu_{xxx})\partial_{u_{xxx}} \\
&\quad + (6\frac{u_xu_{xxx}}{u_{xx}^{\frac{5}{3}}} - 18u_{xx}^{\frac{1}{3}} - 2u\kappa^{\mathbf{SA}})\partial_{\kappa^{\mathbf{SA}}} - 3u\kappa_s^{\mathbf{SA}}\partial_{\kappa_s^{\mathbf{SA}}} \\
&\quad - (3\frac{u_x\kappa_s^{\mathbf{SA}}}{u_{xx}^{\frac{1}{3}}} + 4u\kappa_{ss}^{\mathbf{SA}})\partial_{\kappa_{ss}^{\mathbf{SA}}} \\
&\quad + (\kappa_s^{\mathbf{SA}}(\frac{u_xu_{xxx}}{u_{xx}^{\frac{5}{3}}} - 3u_{xx}^{\frac{1}{3}}) - 7\frac{u_x\kappa_{ss}^{\mathbf{SA}}}{u_{xx}^{\frac{1}{3}}} - 5u\kappa_{sss}^{\mathbf{SA}})\partial_{\kappa_{sss}^{\mathbf{SA}}}
\end{aligned}$$

The curvature for the projective group $\kappa^{\mathbf{proj}}$ can be written as

$$\kappa^{\mathbf{proj}} = \kappa^{\mathbf{proj}}(x, u, u_x, u_{xx}, u_{xxx}, \kappa^{\mathbf{SA}}, \kappa_s^{\mathbf{SA}}, \kappa_{ss}^{\mathbf{SA}}, \kappa_{sss}^{\mathbf{SA}})$$

which can be determined from

$$\mathbf{V}_i(\kappa^{\mathbf{proj}}) = 0, \quad i = 1, \dots, 8.$$

Note that only three of the generators have $\partial_{\kappa^{\mathbf{SA}}}$, $\partial_{\kappa_s^{\mathbf{SA}}}$, $\partial_{\kappa_{ss}^{\mathbf{SA}}}$ and $\partial_{\kappa_{sss}^{\mathbf{SA}}}$ terms and so the conditions $\mathbf{V}_i(\kappa^{\mathbf{proj}}) = 0,\ i = 2, \dots, 6$ give

$$\kappa^{\mathbf{proj}} = \kappa^{\mathbf{proj}}(\kappa^{\mathbf{SA}}, \kappa_s^{\mathbf{SA}}, \kappa_{ss}^{\mathbf{SA}}, \kappa_{sss}^{\mathbf{SA}}).$$

That is $\kappa^{\mathbf{proj}}$ can be written as a function of $\kappa^{\mathbf{SA}}$ and its arclength derivatives.

Now the condition $\mathbf{V}_1(\kappa^{\mathbf{proj}}) = 0$ gives,

$$\kappa^{\mathbf{proj}} = \phi\left(\frac{\kappa_s^{\mathbf{SA}}}{(\kappa^{\mathbf{SA}})^{\frac{3}{2}}}, \frac{\kappa_{ss}^{\mathbf{SA}}}{(\kappa^{\mathbf{SA}})^2}, \frac{\kappa_{sss}^{\mathbf{SA}}}{(\kappa^{\mathbf{SA}})^{\frac{5}{2}}}\right)$$

for an arbitrary function $\phi \in C^\infty$.

The infinitesimal generators $\mathbf{V}_1, \dots, \mathbf{V}_6$ generate the full affine group, so if $\mathbf{V}_1, \dots, \mathbf{V}_6$ are prolonged only up to $\partial_{\kappa^{\mathbf{SA}}}$, this implies the full affine invariant $\kappa^{\mathbf{A}}$ is given by any function of

$$\kappa^{\mathbf{A}} = \frac{\kappa_s^{\mathbf{SA}}}{(\kappa^{\mathbf{SA}})^{\frac{3}{2}}},$$

which reproduces the formula given in section 2.1.1.

If $\mathbf{V}_1, \ldots, \mathbf{V}_6$ are prolonged up to $\partial_{\kappa_s^{\mathbf{SA}}}$ and $\partial_{\kappa_{ss}^{\mathbf{SA}}}$ this gives the higher order differential invariants of the full affine curvature. These must be functions of $\kappa^{\mathbf{A}}$ and its arclength derivatives and are given by

$$\frac{\kappa_{ss}^{\mathbf{SA}}}{(\kappa^{\mathbf{SA}})^2} = \kappa_{\tilde{s}}^{\mathbf{A}} + (\kappa^{\mathbf{A}})^2,$$
$$\frac{\kappa_{sss}^{\mathbf{SA}}}{(\kappa^{\mathbf{SA}})^{\frac{5}{2}}} = \kappa_{\tilde{s}\tilde{s}}^{\mathbf{A}} + 3(\kappa^{\mathbf{A}})^3.$$

where $\tilde{s} = s_{\mathbf{A}}$.

The condition $\mathbf{V}_7(\kappa^{\mathbf{proj}}) = 0$, gives the projective curvature $\kappa^{\mathbf{proj}}$ as any function of

$$\kappa^{\mathbf{proj}} = \frac{-6\kappa_{ss}^{\mathbf{SA}}\kappa_{sss}^{\mathbf{SA}} + 7(\kappa_{ss}^{\mathbf{SA}})^2 + \kappa^{\mathbf{SA}}(\kappa_s^{\mathbf{SA}})^2}{\kappa_s^{\mathbf{SA}\,\frac{8}{3}}},$$

this gives $\mathbf{V}_8(\kappa^{\mathbf{proj}}) = 0$.

Bibliography

[1] E. Calabi, P. J. Olver, C. Shakiban, A. Tannenbaum, and S. Haker. Differential and numerically invariant signature curves applied to object recognition. *International Journal of Computer Vision*, 26:107–135, 1998.

[2] M. Fels and P. J. Olver. Moving coframes. I. A practical algorithm. *Acta Appl. Math.*, 51:161–213, 1998.

[3] M. Fels and P. J. Olver. Moving coframes. II. Regularization and Theoretical Foundations. *Acta Appl. Math.*, 55:127–208, 1999.

[4] B.-C. Li and J. Shen. Fast computation of moment invariants. *Pattern Recognition*, 24(8):807–813, 1991.

[5] P. J. Olver. *Applications of Lie Groups to Differential Equations.* Springer, New York, 1993.

[6] P. J. Olver. *Equivalence, Invariants, and Symmetry.* Cambridge University Press, Cambridge, 1995.

[7] C. A. Rothwell, A. Zisserman, D. A. Forsyth, and J. L. Mundy. Planar object recognition using projective shape representation. *International Journal of Computer Vision*, 16:57–99, 1995.

[8] J. Sato and R. Cipolla. Affine integral invariants for extracting symmetry axes. *Image and Vision Computing*, 15:627–635, 1997.

[9] B. Sturmfels. *Algorithms in Invariant Theory.* Springer-Verlag, New York, 1993.

[10] D. M. Zhao and J. Chen. Affine curve moment invariants for shape recognition. *Pattern Recognition*, 30(6):895–901, 1997.

[11] **MAPLE**. http://www.maplesoft.com.

[12] **MATLAB**. http://www.mathworks.com.

Appendix A

Error correction and strategy

In section 4.1.1 an error correction method is given by fixing one parameter δ and varying ϵ to minimize the error in the matching. This error was stored using joint-invariants.

The following is an example of using the Taylor series approximations for g, h and i in section 4.2 to generate an error characterisation using **distance** as a measure of error. It is compared with the error characterisation using the true values of g, h and i. This gives evidence that the Taylor series for g, h and i could be used to assist with error correction. This is followed by a method for varying ϵ and δ with potentially very fast convergence. Finally a general strategy for planar object recognition is outlined.

A.1 Example compared with Taylor series

Consider the curve given in figure A.1.

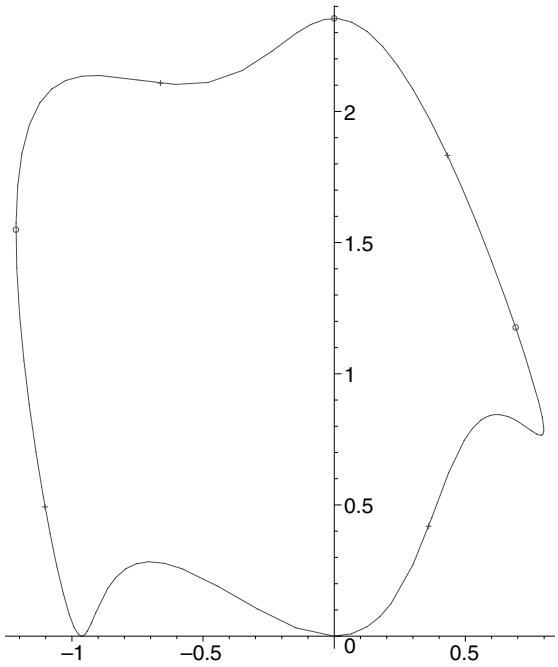

Figure A.1: Initial curve with points used to match the curve denoted by a circle and points used to get a measure of the error denoted by a cross.

The three points denoted by a circle are used to match the curve onto itself by putting errors in ϵ and δ and the four other points denoted by a cross are used to get a measure of the error in the matching. This is done in the following way.

First $\{(\bar{x}_2, \bar{u}_2), (\bar{x}_4, \bar{u}_4), (\bar{x}_3, \bar{u}_3)\}$ are mapped onto $\{(x_2, u_2), (x_4, u_4), (0, u_3)\}$ where

$$\frac{\bar{x}_j}{\bar{u}_j} = (1+\epsilon)\frac{x_j}{u_j} + \delta, \quad i = 2, 4 \quad \text{and}$$
$$\frac{\bar{x}_3}{\bar{u}_3} = \delta$$

for some ϵ and δ. This gives $a = \frac{1}{1+\epsilon}$, $b = \frac{-\delta}{1+\epsilon}$, $g = g(\epsilon, \delta)$, $h = h(\epsilon, \delta)$ and $i = i(\epsilon, \delta)$. Now using the other four points (X_j, U_j), $j = 1, \ldots, 4$, (crosses in figure A.1) the distance

$$\text{dist} = \sqrt{\sum_{j=1}^{4} \left((\bar{X}_j - X_j)^2 + (\bar{U}_j - U_j)^2 \right)}$$

is computed where,

$$(\bar{X}_j, \bar{U}_j) = \left(\frac{aX_j + bU_j}{gX_j + hU_j + i}, \frac{U_j}{gX_j + hU_j + i} \right), \quad j = 1, \ldots, 4.$$

For 10 equally spaced values of δ in the interval $[-0.1, 0.1]$, ϵ is varied in steps of 0.02, then in steps of 0.01 until the value ϵ_{best} corresponding to the minimum value of dist is found. Let this value be $\text{dist}_{\epsilon_{\text{best}}}$.

The values of $\text{dist}_{\epsilon_{\text{best}}}$ for each δ are predicted using the Taylor series approximations to g, h and i. This is done by substituting $g = g(\epsilon, \delta)$, $h = h(\epsilon, \delta)$ and $i = i(\epsilon, \delta)$ into dist^2 and then taking a Taylor series of dist^2 with respect to ϵ to get ϵ_{best}. This value ϵ_{best} is then substituted ϵ_{best} into dist. The Taylor series for g, h and i (to four decimal places) are

$$\begin{aligned}
g(\epsilon, \delta) &= 0.3338\,\epsilon - 1.1899\,\delta - 0.7162\,\epsilon^2 + 2.4802\,\epsilon\,\delta - 0.4901\,\delta^2 \\
h(\epsilon, \delta) &= 0.7324\,\epsilon + 0.2150\,\delta - 1.1148\,\epsilon^2 - 1.3043\,\epsilon\,\delta - 5.7371\,\delta^2 \\
i(\epsilon, \delta) &= 1 - 1.7246\,\epsilon - 0.5062\,\delta + 2.6250\,\epsilon^2 + 3.0711\,\epsilon\,\delta + 11.5583\,\delta^2.
\end{aligned}$$

Figure A.2 shows the comparison between the true values and the approximated values which is very close.

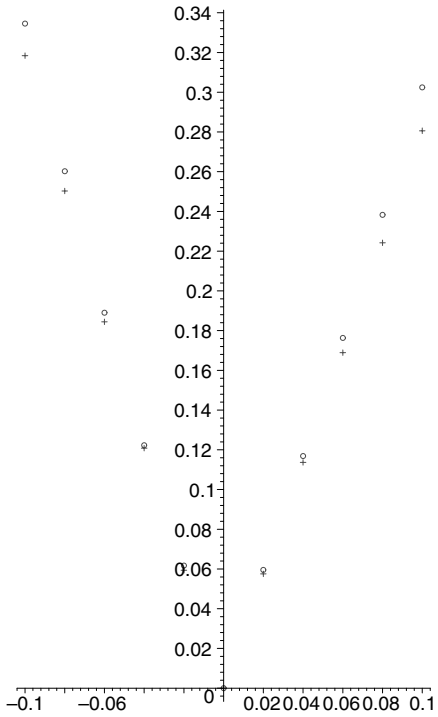

Figure A.2: Comparing true dist vs δ graph with the Taylor series approximation. The true values are denoted by a circle, the approximated values by a cross.

A.2 Potentially fast convergent method

A very large error of $\delta = 0.1$, $\epsilon = -0.1$ is applied to the curve in figure A.1, see figure A.3.

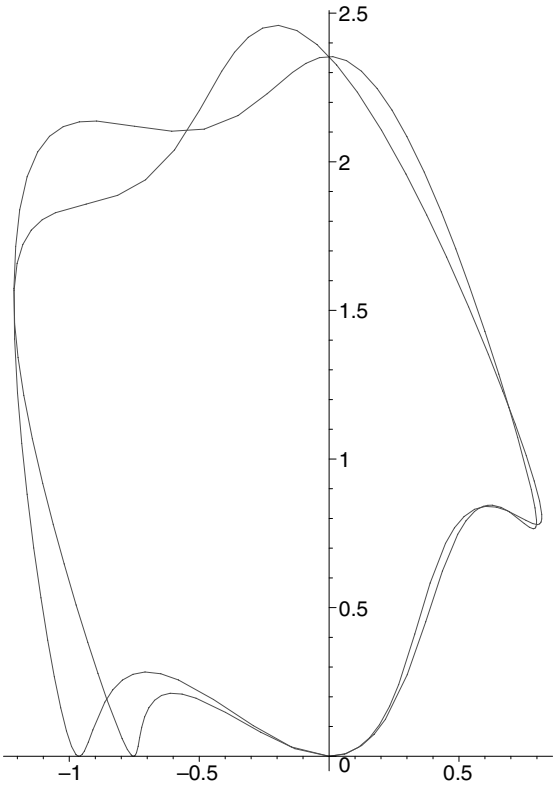

Figure A.3: Initial matching of curves.

The parameter ϵ is fixed and δ is varied initially in steps of 0.04, then in steps of 0.02 and finally in steps of 0.01 until the best matching of dist is obtained, let this value of δ be δ^1_{best}. Then δ^1_{best} is fixed and ϵ is varied in a similar way to get ϵ^1_{best}. This process is continued until the graphs are matched. Figures A.4 and A.5 show the first two iterations which converge very rapidly. Notice that a significant amount of the error has been reduced just by varying δ with ϵ fixed at a large error of $\epsilon = -0.1$. The reason for this is due to dist being much more sensitive to changes in δ than in ϵ as shown by the following Taylor series for dist^2,

$$\text{dist}^2 = 2.859052113\epsilon^2 - 3.112656824\epsilon\delta + 9.3834163 29\delta^2.$$

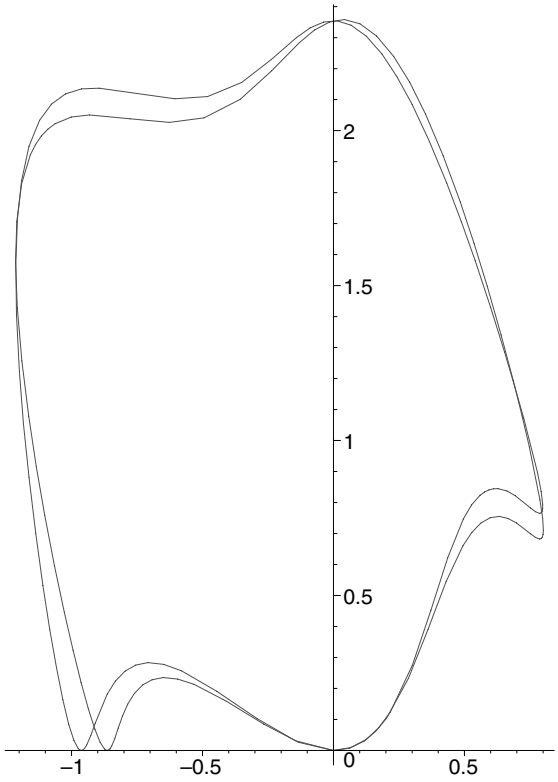

Figure A.4: First iteration.

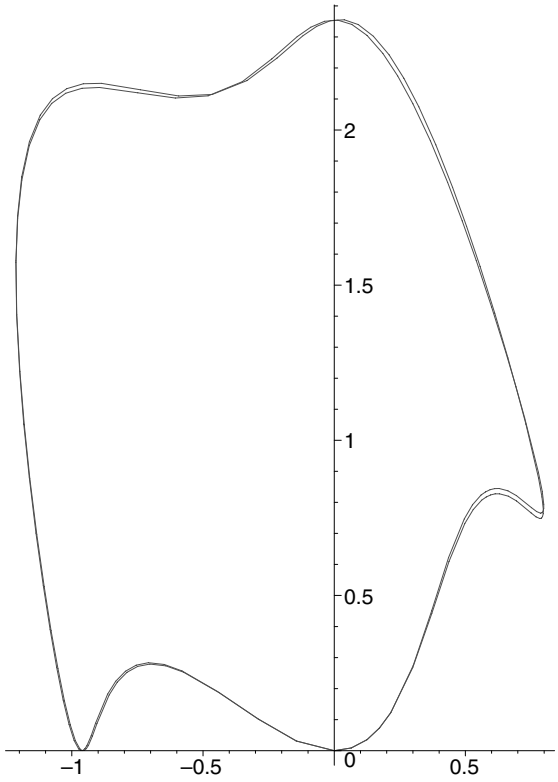

Figure A.5: Second iteration.

Note, error in the canonical point could also be included in this error correction. Let this error be α. Then for the initial α, apply the above method until the changes in ϵ and δ result in changes in the matching error to be less than some specified value. Then fix ϵ and δ and vary α until the best matching is found. Then repeat the above procedure until the improvement in the matching is less than some specified value. If this final error in the matching is sufficiently small, accept curves as being the same, otherwise reject them as different.

In the general strategy of planar object recognition to follow, this method is used as the error correction method and the error correction method of the section 4.4 is presented as optional.

A.3 General strategy of planar object recognition